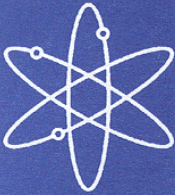




Parametric Study of the Effect of Burnable Poison Rods for PWR Burnup Credit



Prepared by
J. C. Wagner and C. V. Parks, ORNL



Oak Ridge National Laboratory



U.S. Nuclear Regulatory Commission
Office of Nuclear Regulatory Research
Washington, DC 20555-0001



AVAILABILITY OF REFERENCE MATERIALS IN NRC PUBLICATIONS

NRC Reference Material

As of November 1999, you may electronically access NUREG-series publications and other NRC records at NRC's Public Electronic Reading Room at www.nrc.gov/NRC/ADAMS/index.html.

Publicly released records include, to name a few, NUREG-series publications; *Federal Register* notices; applicant, licensee, and vendor documents and correspondence; NRC correspondence and internal memoranda; bulletins and information notices; inspection and investigative reports; licensee event reports; and Commission papers and their attachments.

NRC publications in the NUREG series, NRC regulations, and *Title 10, Energy*, of the Code of *Federal Regulations*, may also be purchased from one of these two sources:

1. The Superintendent of Documents
U.S. Government Printing Office
Mail Stop SSOP
Washington, DC 20402-0001
Internet: bookstore/gpo.gov
Telephone: 202-512-1800
Facsimile: 202-512-2250
2. The National Technical Information Service
Springfield, VA 22161-0002
www.ntis.gov
1-800-553-6847 or, locally, 703-605-6000

A single copy of each NRC draft report for comment is available free, to the extent of supply, upon written request as follows:

Address: Office of the Chief Information Officer,
Reproduction and Distribution
Services Section
U.S. Nuclear Regulatory Commission
Washington, DC 20555-0001

E-mail: DISTRIBUTION@nrc.gov
Facsimile: 301-415-2289

Some publications in the NUREG series that are posted at NRC's Web site address www.nrc.gov/NRC/NUREGS/indexnum.html are updated periodically and may differ from the last printed version. Although references to material found on a Web site bear the date the material was accessed, the material available on the date cited may subsequently be removed from the site.

Non-NRC Reference Material

Documents available from public and special technical libraries include all open literature items, such as books, journal articles, and transactions, *Federal Register* notices, Federal and State legislation, and congressional reports. Such documents as theses, dissertations, foreign reports and translations, and non-NRC conference proceedings may be purchased from their sponsoring organization.

Copies of industry codes and standards used in a substantive manner in the NRC regulatory process are maintained at:

The NRC Technical Library
Two White Flint North
11545 Rockville Pike
Rockville, MD 20852-2738

These standards are available in the library for reference use by the public. Codes and standards are usually copyrighted and may be purchased from the originating organization or, if they are American National Standards, from—

American National Standards Institute
11 West 42nd Street
New York, NY 10036-8002
www.ansi.org
212-642-4900

Legally binding regulatory requirements are stated only in laws; NRC regulations; licenses, including technical specifications; or orders, not in NUREG-series publications. The views expressed in contractor-prepared publications in this series are not necessarily those of the NRC.

The NUREG series comprises (1) technical and administrative reports and books prepared by the staff (NUREG-XXXX) or agency contractors (NUREG/CR-XXXX), (2) proceedings of conferences (NUREG/CP-XXXX), (3) reports resulting from international agreements (NUREG/IA-XXXX), (4) brochures (NUREG/BR-XXXX), and (5) compilations of legal decisions and orders of the Commission and Atomic and Safety Licensing Boards and of Directors' decisions under Section 2.206 of NRC's regulations (NUREG-0750).

DISCLAIMER: This report was prepared as an account of work sponsored by an agency of the U.S. Government. Neither the U.S. Government nor any agency thereof, nor any employee, makes any warranty, expressed or implied, or assumes any legal liability or responsibility for any third party's use, or the results of such use, of any information, apparatus, product, or process disclosed in this publication, or represents that its use by such third party would not infringe privately owned rights.

Parametric Study of the Effect of Burnable Poison Rods for PWR Burnup Credit

Manuscript Completed: September 2001
Date Published: March 2002

Prepared by
J. C. Wagner and C. V. Parks, ORNL

Oak Ridge National Laboratory
Managed by UT-Battelle, LLC
Oak Ridge, TN 37831-6370

R. Y. Lee, NRC Project Manager

Prepared for
Division of Systems Analysis and Regulatory Effectiveness
Office of Nuclear Regulatory Research
U.S. Nuclear Regulatory Commission
Washington, DC 20555-0001
NRC Job Code W6479



ABSTRACT

The Interim Staff Guidance on burnup credit (ISG-8) issued by the United States Nuclear Regulatory Commission's (U.S. NRC) Spent Fuel Project Office recommends restricting the use of burnup credit to assemblies that have not used burnable absorbers. This recommended restriction eliminates a large portion of the currently discharged spent fuel assemblies from cask loading, and thus severely limits the practical usefulness of burnup credit. In the absence of readily available information on burnable poison rod (BPR) design specifications and usage in U.S. pressurized-water-reactors (PWRs), and the subsequent reactivity effect of BPR exposure on discharged spent nuclear fuel (SNF), NRC staff has indicated a need for additional information in these areas. In response, this report presents a parametric study of the effect of BPR exposure on the reactivity of SNF for various BPR designs, fuel enrichments, and exposure conditions, and documents BPR design specifications. Trends in the reactivity effects of BPRs are established with infinite pin-cell and assembly array calculations with the SCALE and HELIOS code packages, respectively. Subsequently, the reactivity effects of BPRs for typical initial enrichment and burnup combinations are quantified based on three-dimensional (3-D) KENO V.a Monte Carlo calculations with a realistic rail-type cask designed for burnup credit. The calculations demonstrate that the positive reactivity effect due to BPR exposure increases nearly linearly with burnup and is dependent on the number, poison loading, and design of the BPRs and the initial fuel enrichment. Expected typical reactivity increases, based on one-cycle BPR exposure, were found to be less than 1% Δk . Based on the presented analysis, guidance is offered on an appropriate approach for calculating bounding SNF isotopic data for assemblies exposed to BPRs. Although the analyses do not address the issue of validation of depletion methods for assembly designs with BPRs, they do demonstrate that the effect of BPRs is generally well behaved and that independent codes and cross-section libraries predict similar results. The report concludes with a discussion of the issues for consideration and recommendations for inclusion of SNF assemblies exposed to BPRs in criticality safety analyses using burnup credit for dry cask storage and transport.

CONTENTS

	<u>Page</u>
ABSTRACT	iii
LIST OF FIGURES.....	vii
LIST OF TABLES	xi
FOREWORD	xiii
ACKNOWLEDGEMENTS.....	xv
1 INTRODUCTION.....	1
2 REVIEW OF BURNABLE POISON ROD DESIGNS AND OPERATIONAL PRACTICES.....	3
2.1 BURNABLE POISON ROD DESIGNS CONSIDERED	3
2.2 BURNABLE POISON ROD ASSEMBLY OPERATIONAL PRACTICES.....	3
3 INPUT DATA.....	5
3.1 WESTINGHOUSE ASSEMBLY AND BURNABLE POISON ROD DESIGN SPECIFICATIONS	5
3.2 B&W ASSEMBLY AND BURNABLE POISON ROD DESIGN SPECIFICATIONS	5
3.3 DEPLETION ENVIRONMENT.....	5
3.4 CASK SPECIFICATIONS	5
4 COMPUTATIONAL METHODS AND MODELS	11
4.1 HELIOS CODE PACKAGE.....	11
4.2 SCALE CODE PACKAGE	13
4.2.1 Codes Used	13
4.2.2 SAS2H Modeling for BPRs.....	13
4.2.3 Nuclide Sets Used in SCALE Criticality Calculations	15
5 REACTIVITY EFFECT OF BURNABLE POISON RODS.....	17
5.1 INTRODUCTION AND BACKGROUND.....	17
5.2 INFINITE ASSEMBLY ARRAY CALCULATIONS WITH HELIOS	18
5.2.1 Westinghouse BPR Designs	18
5.2.1.1 Wet Annular Burnable Absorber (WABA) BPRs	18
5.2.1.1.1 Effect of initial fuel enrichment	18
5.2.1.1.2 Effect of variations in the number of BPRs present	23
5.2.1.1.3 Absorber (¹⁰ B) depletion.....	32
5.2.1.1.4 Effect of cooling time	32
5.2.1.2 Pyrex Burnable Absorber Assembly (BAA) BPRs	32
5.2.2 B&W BPR Designs.....	39
5.2.2.1 Effect of Variations in the BPR Poison (B ₄ C) Loading	39
5.3 INFINITE PIN-CELL CALCULATIONS WITH SAS2H-CSAS1X	46
5.3.1 Comparison of SAS2H and HELIOS Results	53
5.4 BURNUP CREDIT CASK CALCULATIONS	57
5.4.1 Effect of BPRs with Uniform Axial Burnup	57
5.4.1.1 Effect of Cooling Time	58
5.4.2 Effect of BPRs with Consideration of the Axial Burnup Distribution.....	58
5.4.3 Consideration of Risk-Based Approaches.....	59

6	DISCUSSION AND IMPLICATIONS	71
7	RECOMMENDATIONS.....	73
8	REFERENCES	75
	APPENDIX A: SELECTED HELIOS INPUT FILES.....	79
	APPENDIX B: SELECTED SAS2H INPUT FILES.....	107

LIST OF FIGURES

<u>Figures</u>	<u>Page</u>
1 Pyrex BAA and WABA BPR loading patterns used for analysis	7
2 B&W BPR loading patterns used for analysis	9
3 Illustration of assembly lattice with WABA BPRs as modeled with HELIOS	12
4 Radial cross-section of one quadrant of the KENO V.a model of the GBC-32 cask.....	14
5 k_{inf} values as a function of burnup for various WABA exposures. The results correspond to fuel with 4.0 wt % ^{235}U initial enrichment that has been exposed to Westinghouse WABA rods (3 cycles of 15 GWd/MTU per cycle were assumed).	19
6 Δk values as a function of burnup for Westinghouse 17×17 fuel with 3.0 wt % ^{235}U initial enrichment that has been exposed to Westinghouse WABA rods (3 cycles of 15 GWd/MTU per cycle were assumed)	20
7 Δk values as a function of burnup for Westinghouse 17×17 fuel with 4.0 wt % ^{235}U initial enrichment that has been exposed to Westinghouse WABA rods (3 cycles of 15 GWd/MTU per cycle were assumed)	21
8 Δk values as a function of burnup for Westinghouse 17×17 fuel with 5.0 wt % ^{235}U initial enrichment that has been exposed to Westinghouse WABA rods (3 cycles of 15 GWd/MTU per cycle were assumed)	22
9 Δk values as a function of burnup for Westinghouse 17×17 fuel assemblies with various initial enrichments that have been exposed to 24 Westinghouse WABA rods for the first 15 GWd/MTU of burnup.	24
10 Δk values as a function of burnup for Westinghouse 17×17 fuel with various initial enrichments that have been exposed to 24 Westinghouse WABA rods for the first 30 GWd/MTU of burnup.....	25
11 Differences in ^{235}U atom densities, ΔN values, as a function of burnup for Westinghouse 17×17 fuel with various initial enrichments that have been exposed to 24 Westinghouse WABA rods for the first 15 GWd/MTU of burnup.....	26
12 Differences in ^{239}Pu atom densities, ΔN values, as a function of burnup for Westinghouse 17×17 fuel with various initial enrichments that have been exposed to 24 Westinghouse WABA rods for the first 15 GWd/MTU of burnup.....	27
13 Δk values as a function of burnup (for extended burnup) for Westinghouse 17×17 fuel with various initial enrichments that have been exposed to 24 Westinghouse WABA rods for the first 30 GWd/MTU of burnup.....	28
14 Δk values as a function of burnup for Westinghouse 17×17 fuel with 4.0 wt % ^{235}U initial enrichment that has been exposed to various numbers of Westinghouse WABA rods for the first 15 GWd/MTU of burnup.....	29

LIST OF FIGURES (continued)

<u>Figure</u>	<u>Page</u>
15	Δk values as a function of burnup for Westinghouse 17×17 fuel with 4.0 wt % ^{235}U initial enrichment that has been exposed to various numbers of Westinghouse WABA rods during the entire depletion. 30
16	Δk values for Westinghouse 17×17 fuel with 4.0 wt % ^{235}U initial enrichment and a total burnup of 45 GWd/MTU that has been exposed to various numbers of Westinghouse WABA rods for various burnup exposures..... 31
17	^{10}B atom density as a function of burnup for various cases of initial fuel enrichment. The results correspond to 24 Westinghouse WABA rods inserted into Westinghouse 17×17 fuel with various initial enrichments during the entire depletion. 33
18	Δk values as a function of burnup for various cooling times with Westinghouse 17×17 fuel assemblies that have been exposed to 24 WABA rods for the first 15 GWd/MTU of burnup34
19	Δk values as a function of burnup for various cooling times with Westinghouse 17×17 fuel assemblies that have been exposed to 24 WABA rods during the entire depletion (3 cycles).....35
20	Δk values as a function of burnup for Westinghouse 17×17 fuel with 3.0 wt % ^{235}U initial enrichment that has been exposed to Westinghouse Pyrex BAA rods (3 cycles of 15 GWd/MTU per cycle were assumed).....36
21	Δk values as a function of burnup for Westinghouse 17×17 fuel with 4.0 wt % ^{235}U initial enrichment that has been exposed to Westinghouse Pyrex BAA rods (3 cycles of 15 GWd/MTU per cycle were assumed)..... 37
22	Δk values as a function of burnup for Westinghouse 17×17 fuel with 5.0 wt % ^{235}U initial enrichment that has been exposed to Westinghouse Pyrex BAA rods (3 cycles of 15 GWd/MTU per cycle were assumed)..... 38
23	Δk values as a function of burnup for B&W 15×15 fuel with 3.0 wt % ^{235}U initial enrichment that has been exposed to B&W (2.0 wt % B_4C) BPRs (3 cycles of 15 GWd/MTU per cycle were assumed) 40
24	Δk values as a function of burnup for B&W 15×15 fuel with 4.0 wt % ^{235}U initial enrichment that has been exposed to B&W (2.0 wt % B_4C) BPRs (3 cycles of 15 GWd/MTU per cycle were assumed)..... 41
25	Δk values as a function of burnup for B&W 15×15 fuel with 5.0 wt % ^{235}U initial enrichment that has been exposed to B&W (2.0 wt % B_4C) BPRs (3 cycles of 15 GWd/MTU per cycle were assumed)..... 42

LIST OF FIGURES (continued)

<u>Figure</u>	<u>Page</u>
26	Δk values as a function of burnup for B&W 15×15 fuel with 4.0 wt % ^{235}U initial enrichment that has been exposed to B&W BPRs with varying B_4C weight percents for the first 15 GWd/MTU of burnup (3 cycles of 15 GWd/MTU per cycle were assumed). 43
27	Δk values as a function of burnup for B&W 15×15 fuel with 4.0 wt % ^{235}U initial enrichment that has been exposed to B&W BPRs with varying B_4C weight percents for the first 30 GWd/MTU of burnup (3 cycles of 15 GWd/MTU per cycle were assumed). 44
28	Δk values for B&W 15×15 fuel with 4.0 wt % ^{235}U initial enrichment and a total burnup of 45 GWd/MTU that has been exposed to BPRs with varying poison loading and burnup exposures 45
29	Δk values as a function of burnup for Westinghouse 17×17 fuel with 4.0 wt % ^{235}U initial enrichment that has been exposed to Westinghouse WABA rods (3 cycles of 15 GWd/MTU per cycle were assumed). The results are based on SAS2H-depletion and CSAS1X-criticality calculations with “actinide + fission product” nuclides 47
30	Δk values as a function of burnup for Westinghouse 17×17 fuel with 4.0 wt % ^{235}U initial enrichment that has been exposed to Westinghouse WABA rods (3 cycles of 15 GWd/MTU per cycle were assumed). The results are based on SAS2H-depletion and CSAS1X-criticality calculations with “actinide-only” nuclides 48
31	Δk values as a function of burnup for Westinghouse 17×17 fuel with 4.0 wt % ^{235}U initial enrichment that has been exposed to Westinghouse BAA rods (3 cycles of 15 GWd/MTU per cycle were assumed). The results are based on SAS2H-depletion and CSAS1X-criticality calculations with “actinide + fission product” nuclides 49
32	Δk values as a function of burnup for Westinghouse 17×17 fuel with 4.0 wt % ^{235}U initial enrichment that has been exposed to Westinghouse BAA rods (3 cycles of 15 GWd/MTU per cycle were assumed). The results are based on SAS2H-depletion and CSAS1X-criticality calculations with “actinide-only” nuclides 50
33	Δk values as a function of burnup for B&W 15×15 fuel with 4.0 wt % ^{235}U initial enrichment that has been exposed to B&W (2.0 wt % B_4C) BPRs (3 cycles of 15 GWd/MTU per cycle were assumed). The results are based on SAS2H-depletion and CSAS1X-criticality calculations with “actinide + fission product” nuclides 51
34	Δk values as a function of burnup for B&W 15×15 fuel with 4.0 wt % ^{235}U initial enrichment that has been exposed to B&W (2.0 wt % B_4C) BPRs (3 cycles of 15 GWd/MTU per cycle were assumed). The results are based on SAS2H-depletion and CSAS1X-criticality calculations with “actinide-only” nuclides 52

LIST OF FIGURES (continued)

<u>Figure</u>	<u>Page</u>
35	Comparison of reactivity differences (Δk values relative to the no BPR condition) as calculated with CSAS1X based on isotopics calculated with SAS2H and HELIOS for actinide-only burnup credit. The results correspond to fuel with 4.0 wt % ^{235}U initial enrichment that has been exposed to either 12 or 24 WABAs..... 54
36	Comparison of reactivity differences (Δk values relative to the no BPR condition) as calculated with CSAS1X based on isotopics calculated with SAS2H and HELIOS for actinide-only burnup credit. The results correspond to fuel with 4.0 wt % ^{235}U initial enrichment that has been exposed to either 12 or 24 BAAs..... 55
37	Comparison of reactivity differences (Δk values relative to the no BPR condition) as calculated with CSAS1X based on isotopics calculated with SAS2H and HELIOS for actinide-only burnup credit. The results correspond to B&W 15 \times 15 fuel with 4.0 wt % ^{235}U initial enrichment that has been exposed to 16 B&W BPRs. 56
38	Comparison of reactivity differences (Δk values relative to the no BPR condition) in the GBC-32 cask (45 GWd/MTU, 5-year cooling) as calculated with KENO V.a for actinide-only (AO) and actinide + fission product (A + FP) burnup credit, based on isotopic compositions from SAS2H and HELIOS depletion calculations. The results correspond to fuel with 4.0 wt % ^{235}U initial enrichment that has been exposed to 24 WABA BPRs for various burnups..... 62
39	Comparison of reactivity differences (Δk values relative to the no BPR condition) in the GBC-32 cask (45 GWd/MTU, 5-year cooling) as calculated with KENO V.a for actinide-only (AO) and actinide + fission product (A + FP) burnup credit, based on isotopic compositions from SAS2H and HELIOS depletion calculations. The results correspond to fuel with 4.0 wt % ^{235}U initial enrichment that has been exposed to 24 BAA BPRs for various burnups..... 64
40	Comparison of reactivity differences (Δk values relative to the no BPR condition) in the GBC-32 cask (45 GWd/MTU, 5-year cooling) as calculated with KENO V.a for actinide-only (AO) and actinide + fission product (A + FP) burnup credit, based on isotopic compositions from SAS2H and HELIOS depletion calculations. The results correspond to fuel with 4.0 wt % ^{235}U initial enrichment that has been exposed to 24 B&W (2 wt % B_4C) BPRs for various burnups..... 66
41	Increase in k_{eff} due to loading assemblies with 3-cycle BPR exposure into a GBC-32 cask in which the remaining assemblies have 1-cycle BPR exposure. The results correspond to Westinghouse 17 \times 17 fuel with 4.0 wt % ^{235}U , Westinghouse WABA rods, actinide-only nuclides, and spent-fuel isotopic compositions from SAS2H depletion calculations. 69

LIST OF TABLES

<u>Table</u>	<u>Page</u>
1 Westinghouse 17 × 17 OFA fuel assembly specifications	6
2 Westinghouse BAA and WABA BPR design specifications	6
3 Westinghouse BAA and WABA fresh burnable poison (BP) material compositions	8
4 B&W 15 × 15 fuel assembly specifications	8
5 B&W BPR design specifications	9
6 B&W BPR fresh burnable poison (BP) material compositions used for analysis	9
7 Summary of parameters used for the depletion calculations	10
8 Nuclides associated with the classifications of burnup credit used for analysis.....	15
9 Reactivity effect of various BPR exposures for actinide-only burnup credit (See Table 8 for specific nuclides) in the GBC-32 cask using isotopic compositions from SAS2H depletion calculations (45 GWd/MTU, 5-year cooling). The results correspond to Westinghouse 17 × 17 fuel with 4.0 wt % ²³⁵ U exposed to Westinghouse WABA rods.....	60
10 Reactivity effect of various BPR exposures for actinide + fission product burnup credit (See Table 8 for specific nuclides) in the GBC-32 cask using isotopic compositions from SAS2H depletion calculations (45 GWd/MTU, 5-year cooling). The results correspond to Westinghouse 17 × 17 fuel with 4.0 wt % ²³⁵ U exposed to Westinghouse WABA rods.....	60
11 Reactivity effect of various BPR exposures for actinide-only burnup credit (See Table 8 for specific nuclides) in an infinite pin-cell array using isotopic compositions from SAS2H depletion calculations (45 GWd/MTU, 5-year cooling). The results correspond to Westinghouse 17 × 17 fuel with 4.0 wt % ²³⁵ U exposed to Westinghouse WABA rods.....	61
12 Reactivity effect of various BPR exposures for actinide + fission product burnup credit (See Table 8 for specific nuclides) in an infinite pin-cell array using isotopic compositions from SAS2H depletion calculations (45 GWd/MTU, 5-year cooling). The results correspond to Westinghouse 17 × 17 fuel with 4.0 wt % ²³⁵ U exposed to Westinghouse WABA rods.....	61
13 Reactivity effect of various BPR exposures for actinide-only burnup credit (See Table 8 for specific nuclides) in the GBC-32 cask using isotopic compositions from SAS2H depletion calculations (45 GWd/MTU, 5-year cooling). The results correspond to Westinghouse 17 × 17 fuel with 4.0 wt % ²³⁵ U exposed to Westinghouse BAA rods.	63
14 Reactivity effect of various BPR exposures for actinide + fission product burnup credit (See Table 8 for specific nuclides) in the GBC-32 cask using isotopic compositions from SAS2H depletion calculations (45 GWd/MTU, 5-year cooling). The results correspond to Westinghouse 17 × 17 fuel with 4.0 wt % ²³⁵ U exposed to Westinghouse BAA rods.....	63

LIST OF TABLES (continued)

<u>Table</u>	<u>Page</u>
15	Reactivity effect of various BPR exposures for actinide-only burnup credit (See Table 8 for specific nuclides) in the GBC-32 cask using isotopic compositions from SAS2H depletion calculations (45 GWd/MTU, 5-year cooling). The results correspond to B&W 15 × 15 fuel with 4.0 wt % ²³⁵ U exposed to B&W BPRs (2.0 wt % B ₄ C)..... 65
16	Reactivity effect of various BPR exposures for actinide + fission product burnup credit (See Table 8 for specific nuclides) in the GBC-32 cask using isotopic compositions from SAS2H depletion calculations (45 GWd/MTU, 5-year cooling). The results correspond to B&W 15 × 15 fuel with 4.0 wt % ²³⁵ U exposed to B&W BPRs (2.0 wt % B ₄ C)..... 65
17	Δk values as a function of cooling time for actinide-only burnup credit (See Table 8 for specific nuclides) in the GBC-32 cask using isotopic compositions from SAS2H depletion calculations. The results correspond to Westinghouse 17 × 17 fuel with 4.0 wt % burned to 45 GWd/MTU..... 67
18	Δk values as a function of cooling time for actinide + fission product burnup credit (See Table 8 for specific nuclides) in the GBC-32 cask using isotopic compositions from SAS2H depletion calculations. The results correspond to Westinghouse 17 × 17 fuel with 4.0 wt % burned to 45 GWd/MTU..... 67
19	Reactivity effect of various BPR exposures in the GBC-32 cask with the axial burnup distribution included, using isotopic compositions from SAS2H depletion calculations (45 GWd/MTU, 5-year cooling). The results correspond to Westinghouse 17 × 17 fuel with 4.0 wt % ²³⁵ U exposed to Westinghouse WABA rods. 68

FOREWORD

In 1999 the United States Nuclear Regulatory Commission (NRC) issued initial recommended guidance for using reactivity credit due to fuel irradiation (i.e., burnup credit) in the criticality safety analysis of spent pressurized-water-reactor (PWR) fuel in storage and transportation packages. This guidance was issued by the NRC Spent Fuel Project Office (SFPO) as Revision 1 to Interim Staff Guidance 8 (ISG8R1) and published in the *Standard Review Plan for Transportation Packages for Spent Nuclear Fuel*, NUREG-1617 (March 2000). With this initial guidance as a basis, the NRC Office of Nuclear Regulatory Research initiated a program to provide the SFPO with technical information that would:

- enable realistic estimates of the subcritical margin for systems with spent nuclear fuel (SNF) and an increased understanding of the phenomena and parameters that impact the margin, and
- support the development of technical bases and recommendations for effective implementation of burnup credit and provide realistic SNF acceptance criteria while maintaining an adequate margin of safety.

One restriction recommended by the ISG8R1 is to preclude assemblies irradiated with burnable absorbers from being used in a cask that implements burnup credit (BUC). Since a large portion (perhaps 50% or more) of the discharged SNF inventory has been exposed to burnable absorbers, this restriction was identified as a potentially unnecessary and costly restriction that could be removed with improved understanding of the impact of burnable absorbers on SNF reactivity in transportation and storage environments. Burnable absorbers used in PWR fuel designs can be classed into two categories: burnable poison rods (BPRs) that can be separated from an assembly and integral burnable absorbers that are a fixed part of the assembly. This report presents a parametric study that quantifies the changes in the SNF neutron multiplication factor due to the presence of BPRs during fuel irradiation and discusses the behavior that causes the changes. Based on this study and discussion, the report proposes recommendations for modifying ISG8R1 to allow loading of burnup credit casks with assemblies exposed to BPRs. The use of BUC results in fewer casks needing to be transported, thereby reducing regulatory burden on licensee while maintaining safety for transporting SNF.



Farouk Eltawila, Director
Division of Systems Analysis and Regulatory Effectiveness

ACKNOWLEDGEMENTS

This work was supported by the Office of Nuclear Regulatory Research, U.S. Nuclear Regulatory Commission (NRC), under Project JCN W6479, Development and Applicability of Criticality Safety Software for Licensing Review. The authors acknowledge review and useful comments by Carl J. Withee of the Spent Fuel Project Office. The careful review of the manuscript and constructive comments by M. D. DeHart, J. C. Gehin, R. T. Primm, III, and C. E. Sanders are very much appreciated. Finally, the authors are thankful to W. C. Carter for her preparation of the final report.

1 INTRODUCTION

The concept of taking credit for the reduction in reactivity due to fuel burnup is commonly referred to as *burnup credit*. The reduction in reactivity that occurs with fuel burnup is due to the change in concentration (net reduction) of fissile nuclides and the production of actinide and fission-product neutron absorbers. The change in the concentration of these nuclides with fuel burnup, and consequently the reduction in reactivity, is dependent upon the depletion environment (e.g., the neutron spectrum). Therefore, the utilization of credit for fuel burnup necessitates consideration of variations in fuel designs and operating conditions, including exposure to burnable absorbers.

The presence of burnable absorbers during depletion hardens the neutron spectrum, resulting in lower ^{235}U depletion and higher production of fissile plutonium isotopes. The simultaneous increase in plutonium production and decrease in fission of ^{235}U may increase the reactivity of the fuel at discharge and beyond. Consequently, an assembly exposed to burnable absorbers may have a higher reactivity for a given burnup than an assembly that has not been exposed to burnable absorbers.

Burnable absorbers may be classified into two distinct categories: (1) burnable poison rods (BPRs) and (2) integral burnable absorbers (IBAs). BPRs are rods containing neutron absorbing material that are inserted into the guide tubes of a pressurized water reactor (PWR) assembly during normal operation and are commonly used for reactivity control and enhanced fuel utilization. In contrast to BPRs, IBAs refer to burnable poisons that are a nonremovable or integral part of the fuel assembly once it is manufactured. An example of an IBA is the Westinghouse Integral Fuel Burnable Absorber (IFBA) rod, which has a coating of zirconium diboride (ZrB_2) on a select number of the fuel pellets. IBAs are also used for reactivity control and enhanced fuel utilization. Although IBAs are also common in current PWR fuel designs, this report will focus only on the effect of BPRs. The effect of IBAs on PWR burnup-credit criticality safety analyses for dry cask storage and transportation is investigated in Ref. 1.

Control rods are similar to BPRs in that they also contain neutron-absorbing material and may be inserted into the guide tubes of a PWR assembly. However, with the exception of axial power shaping rods (APSRs), control rods are primarily used during reactor startup and shutdown and are not inserted (to a significant extent) into the guide tubes during normal full-power operation. Depending on plant-specific fuel management strategies, control rods may be either completely withdrawn or partially inserted during normal full-power operations. Due to their composition and limited exposure, control rods are not considered *burnable*. Therefore, control rods are not classified herein as *burnable absorbers* and are not addressed in this report. The effect of control rods, including APSRs, on PWR burnup-credit criticality safety analyses for dry cask storage and transportation is investigated in Ref. 2.

The Interim Staff Guidance on burnup credit (ISG-8)³ issued by the U.S. Nuclear Regulatory Commission's (NRC) Spent Fuel Project Office recommends restricting the use of burnup credit to assemblies that have not used burnable absorbers. This recommended restriction eliminates a large portion of the currently discharged spent fuel assemblies from cask loading, and thus severely limits the practical usefulness of burnup credit. In the absence of readily available information on BPR design specifications and usage in U.S. PWRs, and the subsequent reactivity effect of BPR exposure on discharged spent nuclear fuel (SNF), NRC staff has indicated a need for additional information in these areas.⁴ In response, this report presents parametric studies of the effect of BPR exposure on the reactivity of SNF for various BPR designs, fuel enrichments, and exposure conditions, and documents BPR design specifications.

When used, burnable poison rod assemblies (BPRAs) are typically (but not always) employed during the first third (approximately) of an assembly life (first cycle) and may have varying numbers of BPRs or varying poison loading. It should be noted that not all PWR SNF assemblies have been exposed to BPRs and that

trends in PWR fuel management have shifted away from the use of BPRs and towards the use of IBAs. The effect of BPRs on reactivity is dependent upon the assembly exposure to BPRs during depletion, the subsequent accumulated burnup, the BPR design, and the initial fuel-assembly enrichment. Although BPR exposures are typically limited to one cycle, exceptions to this practice exist. Therefore, parametric analyses were performed for a variety of exposure scenarios to establish an increased understanding and quantify the effect of BPR exposure on the reactivity of discharged SNF. Variations in BPR exposure, BPR design characteristics, and initial fuel-assembly enrichment are considered for all BPR designs that have been widely used in U.S. commercial PWRs. Trends in the reactivity effects of BPRs are established with infinite pin-cell and assembly array calculations with the SCALE (Ref. 5) and HELIOS (Ref. 6) code packages, respectively. Additionally, the reactivity effects of BPRs for typical initial enrichment and burnup combinations are quantified based on three-dimensional (3-D) KENO V.a (Ref. 7) Monte Carlo calculations with a realistic rail-type cask designed for burnup credit. Based on the presented analyses, recommended guidance is provided for an appropriate approach for calculating bounding SNF isotopic compositions for assemblies exposed to BPRs. The report concludes with a discussion on the issues for consideration and preliminary recommendations for inclusion of SNF assemblies exposed to BPRs in criticality safety analyses using burnup credit for dry cask storage and transportation.

The remainder of this report is organized as follows: Section 2 describes the BPR designs considered in this study and reviews typical BPR operating practices in U.S. PWRs. Section 3 documents the input data used for this study, including detailed fuel assembly and BPR design specifications. The computational methods and models are described in Section 4. The actual analyses for the reactivity effects of BPRs are given in Section 5. Finally, summary discussions and recommendations are provided in Sections 6 and 7, respectively.

2 REVIEW OF BURNABLE POISON ROD DESIGNS AND OPERATIONAL PRACTICES

Several different BPR designs have been used in U.S. commercial nuclear PWRs. However, all BPR designs are similar in that they contain thermal neutron absorbing material (boron) in rods sized to fit within the fuel assembly guide tubes. Burnable poison rod assemblies (BPRAs) consist of a finite number and configuration of BPRs to be inserted into a single PWR fuel assembly. The BPR characteristics (e.g., BPR number, configuration, and poison loading) may be varied in combination with the fuel assembly initial enrichment and core location to achieve core operating and fuel management objectives. All BPR designs that have been widely used in U.S. commercial PWRs are included in this evaluation. For clarity, each of the BPR designs considered in this report is described below. The BPR design specifications required for this analysis were assembled from multiple nonproprietary sources and are documented in Section 3 of this report.

Note that some Combustion Engineering (CE) fuel assembly designs use $\text{Al}_2\text{O}_3\text{-B}_4\text{C}$ rods that are referred to as BPRs. However, because the CE $\text{Al}_2\text{O}_3\text{-B}_4\text{C}$ rods may not be separated (withdrawn) from the assembly, they are treated as IBAs and their impact on burnup credit analyses is discussed in Ref. 1.

2.1 BURNABLE POISON ROD DESIGNS CONSIDERED

Westinghouse has manufactured two main types of BPRs:^{8,9} (1) Pyrex Burnable Absorber Assemblies (BAAs) and (2) Wet Annular Burnable Absorbers (WABAs). The BAA BPRs utilize borosilicate glass ($\text{B}_2\text{O}_3\text{-SiO}_2$ with 12.5 wt % B_2O_3) in the form of Pyrex tubing as a neutron absorber with a void central region.¹⁰ The Pyrex BAA BPRs are clad in 304 stainless steel. The WABA BPRs are similar to BAA BPRs, but use annular pellets of $\text{Al}_2\text{O}_3\text{-B}_4\text{C}$ (14.0 wt % B_4C) as the neutron absorber and have a wet (water-filled) central region.¹¹ The WABA BPRs are clad in Zircaloy. Configurations of BAA and WABA BPRs have been identified with varying numbers of rods (4 to 24).^{8,9}

The B&W BPR design^{8,9} consists of solid rods containing $\text{Al}_2\text{O}_3\text{-B}_4\text{C}$ clad in Zircaloy. Unlike the Westinghouse designs, the number of BPRs per assembly is fixed, and the weight percent of B_4C in the BPRs is variable. Actual plant data in Ref. 12 show variations in B_4C loading from 0.0 to 2.1 wt %.

Detailed design specifications for each of the BPR designs are given in Section 3.

2.2 BURNABLE POISON ROD ASSEMBLY OPERATIONAL PRACTICES

Because the effect of BPRs on reactivity is dependent on the duration of BPR exposure, the BPR characteristics, and the burnup without BPRs present, it is important to understand typical operating practices. In U.S. PWR operations, BPRAs have typically been inserted into the fuel assemblies during their first cycle in the reactor core. Depending on the vendor, the number of BPRs within a BPR (Westinghouse) or the poison loading in the BPRs within a BPR (B&W) is variable, typically less than the maximum possible. Based on limited Westinghouse plant operational data,^{10,11,13-15} the average number of Westinghouse BPRs in a BPR is typically much less than the maximum possible (dictated by the number of guide tubes in the assembly). For example, review of operational data^{10,13,14} shows the number of BPRs per BPR, averaged over a core, is approximately 65% of the maximum possible. In other words, for an assembly with 24 guide tubes, the average number of BPRs per BPR, averaged over a core, is approximately 16. Similarly, based on limited B&W plant operational data,¹² the average poison loading (wt % B_4C) in the BPRs is typically much less than the design maximum.

Due to the depletion of the neutron absorbing material (boron), BPRAs are typically (but not always) discarded after a one-cycle residence in the core.^{10,11,13-15} However, documented examples of the use of depleted BPRs in an assembly's second cycle are available.^{13,14}

3 INPUT DATA

3.1 WESTINGHOUSE ASSEMBLY AND BURNABLE POISON ROD DESIGN SPECIFICATIONS

The fuel assembly design used for analysis of the Westinghouse BPR designs is the Westinghouse 17×17 optimized fuel assembly (OFA). The fuel assembly specifications are listed in Table 1. The Westinghouse BPRAs utilized for this analysis consist of two types: Pyrex BAA (Burnable Absorber Assembly) and WABA (Wet Annular Burnable Absorber). The Pyrex BAA BPRs use $B_2O_3-SiO_2$ as the absorber material, while the WABA BPRs use $Al_2O_3-B_4C$ as the absorber material. Both the BAA and WABA BPRs are annular in design. However, the BAA BPR has a dry annular gap, while the WABA BPR has a wet annular gap. Specifications for both the BAA and WABA BPRs are summarized in Table 2. As mentioned, the Westinghouse BPRAs are composed of various numbers of either Pyrex BAA or WABA BPRs arranged in specific geometric patterns. Although numerous patterns are known to exist,¹¹ including asymmetric arrangements, Figure 1 shows the different (symmetric) assembly lattices considered in this analysis. The burnable poison (BP) in each BPRa is depleted during reactor operation. The fresh (unburned) BP material compositions for both the Pyrex BAA and WABA BPRs are provided in Table 3.

3.2 B&W ASSEMBLY AND BURNABLE POISON ROD DESIGN SPECIFICATIONS

The B&W 15×15 fuel assembly design was used for analysis of the B&W BPR design. The fuel assembly specifications are listed in Table 4. The B&W BPR design consists of solid rods containing $Al_2O_3-B_4C$ clad in Zircaloy. The specifications for the B&W BPRs are summarized in Table 5. Unlike the Westinghouse designs, the number of BPRs per assembly is fixed, and the weight percent of B_4C in the BPRs is variable. Each of the BPRAs contains sixteen BPRs, each being inserted into a guide tube. The burnable poison (BP) in each BPRa is depleted during reactor operation. The fresh (unburned) BP material compositions for the various weight percents of B_4C considered in this analysis are provided in Table 6. Figure 2 shows the assembly lattices¹⁶ used for this analysis.

3.3 DEPLETION ENVIRONMENT

All depletion calculations were performed using the properties and parameters given in Table 7. The sensitivity of k_{eff} to variations in these parameters is discussed in Ref. 17.

3.4 CASK SPECIFICATIONS

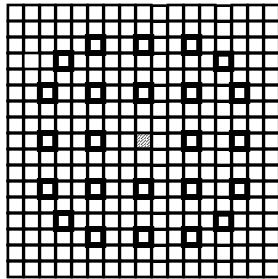
The generic 32 PWR-assembly burnup credit (GBC-32) cask was used for calculations to quantify the reactivity effect of BPRs within a realistic high-capacity rail-type cask. The GBC-32 design was developed to provide a reference cask configuration that is representative of typical high-capacity rail casks being considered by industry. The boron loading in the Boral panels in the GBC-32 cask is $0.0225 \text{ g }^{10}\text{B}/\text{cm}^2$; detailed specifications for the GBC-32 cask are provided in Ref. 18.

Table 1 Westinghouse 17 × 17 OFA fuel assembly specifications

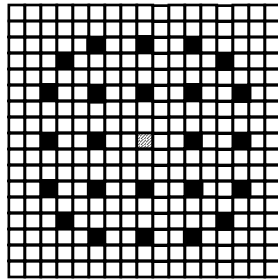
Parameter	inches	cm
Fuel pellet outside diameter	0.3088	0.7844
Cladding inside diameter	0.3150	0.8001
Cladding outside diameter	0.3600	0.9144
Cladding radial thickness	0.0225	0.0572
Rod pitch	0.4960	1.2598
Guide tube/thimble inside diameter	0.4420	1.1227
Guide tube/thimble outside diameter	0.4740	1.2040
Thimble radial thickness	0.0160	0.0406
Instrument tube inside diameter	0.4420	1.1227
Instrument tube outside diameter	0.4740	1.2040
Instrument tube radial thickness	0.0160	0.0406
Active fuel length	144	365.76
Array size	17 × 17	
Number of fuel rods	264	
Number of guide tubes/thimbles	24	
Number of instrument tubes	1	

Table 2 Westinghouse BAA and WABA BPR design specifications (Source: Ref. 11)

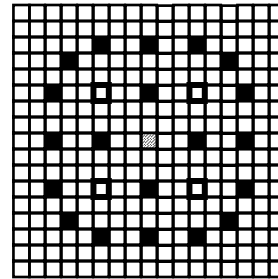
Description	BAA	WABA
BP material	B ₂ O ₃ -SiO ₂	Al ₂ O ₃ -B ₄ C
Boron loading	12.5 wt % B ₂ O ₃ 0.00624 g B-10/cm	14.0 wt % Al ₂ O ₃ 0.006165 g B-10/cm
BP density (g/cm ³)	2.299	2.593
BP outer diameter (OD) (cm)	0.85344	0.8077
BP inner diameter (ID) (cm)	0.48260	0.7061
BPR clad material	Stainless Steel (Type 304)	Zircaloy-4
BPR outer clad OD (cm)	0.96774	0.96774
BPR outer clad ID (cm)	0.87376	0.83570
BPR inner clad OD (cm)	0.46101	0.67820
BPR inner clad ID (cm)	0.42799	0.57150



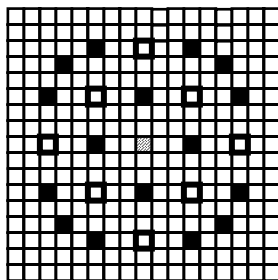
24 Guide Tubes and
1 Instrument Tube



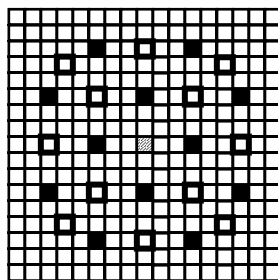
24 Burnable Poison Rods



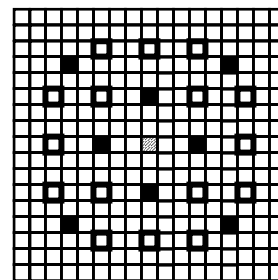
20 Burnable Poison Rods



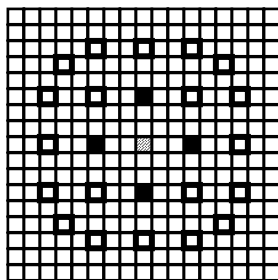
16 Burnable Poison Rods



12 Burnable Poison Rods



8 Burnable Poison Rods



4 Burnable Poison Rods

- ▨ Instrument Tube
- ◻ Guide Tube
- Burnable Poison Rod
- Fuel Rod

Figure 1 Pyrex BAA and WABA BPR loading patterns used for analysis (Source: Ref. 11)

Table 3 Westinghouse BAA and WABA fresh burnable poison (BP) material compositions

Element/Isotope	Wt % of element/Isotope in material composition	
	Pyrex BP (B_2O_3 - SiO_2)	WABA BP (Al_2O_3 - B_4C)
Boron-10	0.699	1.968
Boron-11	3.207	8.992
Carbon	---	3.040
Oxygen	53.902	40.479
Aluminum	1.167	45.521
Silicon	37.856	---
Potassium	0.332	---
Sodium	2.837	---

Table 4 B&W 15 × 15 fuel assembly specifications

Parameter	inches	cm
Fuel pellet outside diameter	0.3742	0.9505
Cladding inside diameter	0.3820	0.9703
Cladding outside diameter	0.4280	1.0871
Cladding radial thickness	0.0230	0.0584
Rod pitch	0.5680	1.4427
Guide tube/thimble inside diameter	0.5000	1.2700
Guide tube/thimble outside diameter	0.5280	1.3411
Thimble radial thickness	0.0140	0.0356
Instrument tube inside diameter	0.5000	1.2700
Instrument tube outside diameter	0.5280	1.3411
Instrument tube radial thickness	0.0140	0.0356
Active fuel length	144	365.76
Array size	15 × 15	
Number of fuel rods	208	
Number of guide tubes/thimbles	16	
Number of instrument tubes	1	

Table 5 B&W BPR design specifications (Source: Ref. 12)

BP material	Al ₂ O ₃ -B ₄ C
BP density (g/cm ³)	3.7
BP diameter (cm)	0.8636
BPR clad material	Zircaloy-4
BPR clad OD (cm)	1.0922
BPR clad ID (cm)	0.9144

Table 6 B&W BPR fresh burnable poison (BP) material compositions used for analysis

Element/ Isotope	Wt % of element/Isotope in material composition			
	0.00 wt % B ₄ C	1.00 wt % B ₄ C	2.000 wt % B ₄ C	3.000 wt % B ₄ C
Boron-10	0.00000	0.14087	0.28174	0.42262
Boron-11	0.00000	0.64175	1.28350	1.92525
Carbon	0.00000	0.21738	0.43475	0.65213
Oxygen	47.07493	46.60418	46.13343	45.66268
Aluminum	52.92507	52.39582	51.86657	51.33732

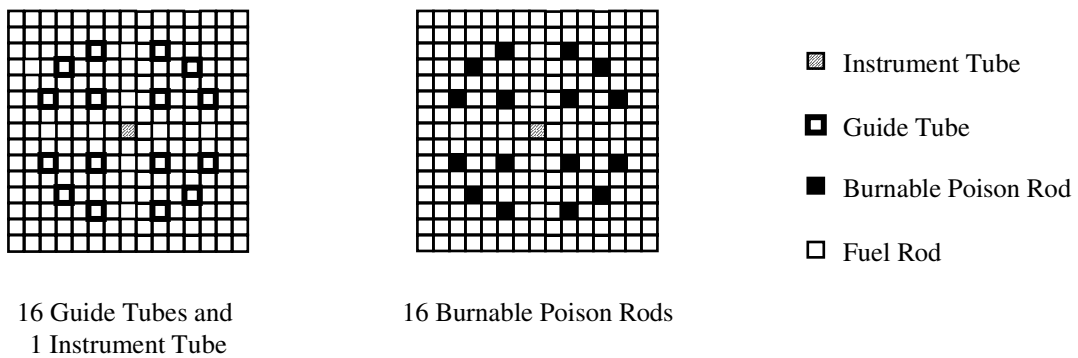


Figure 2 B&W BPR loading patterns used for analysis (Source: Ref. 16)

Table 7 Summary of parameters used for the depletion calculations[†]

Parameter	Value used in analysis
Moderator temperature (K)	600
Fuel temperature (K)	1000
Fuel density (g/cm ³)	10.5216 (UO ₂)
Clad temperature (K)	620
Clad density (g/cm ³)	6.56 (Zr)
Power density (MW/MTU)	60
Moderator boron concentration (ppm)	650

[†] All values are held constant during depletion.

4 COMPUTATIONAL METHODS AND MODELS

The computational methods necessary for this analysis include codes for depletion and criticality simulation. As mentioned, there is a great deal of variety in BPR designs, and possibly in their use during operations. A thorough investigation of the effect of BPRs on the reactivity of SNF requires calculations to examine the impact of variations in BPR design, BPR exposure, and initial fuel enrichment. Performing such a spectrum of analyses using Monte Carlo calculations of a loaded cask is not computationally practical or necessary to establish the reactivity behavior. Therefore, infinite pin-cell and assembly array calculations were performed to establish trends in the reactivity effects of BPRs. Independent code packages were employed and selected results were compared to gain confidence in the results and assess accuracy. Once the trends with the relevant/important parameters were established, the reactivity effects of BPRs were quantified based on 3-D KENO V.a Monte Carlo calculations with a realistic rail-type cask designed for burnup credit. The code packages used for the analyses are described in the following subsections.

4.1 HELIOS CODE PACKAGE

The HELIOS-1.6 code package⁶ primarily consists of three programs: AURORA, HELIOS, and ZENITH. HELIOS is a two-dimensional (2-D) transport theory code based on the method of collision probabilities with current coupling. AURORA, the input processor, is used to define the geometry, materials, and calculational parameters. ZENITH, the output processor, reads the HELIOS results and outputs the results in a user-defined format. The HELIOS code system also contains the ORION program for viewing and checking model geometries and materials. The various structures within the computational models were coupled using angular current discretization (interface currents).

For this analysis, the HELIOS code was used for 2-D depletion calculations as well as 2-D criticality calculations for an infinite radial array of fuel assemblies. The HELIOS depletion calculations were performed using the cycle-averaged operational parameters listed in Table 7. Using the isotopic compositions from the depletion calculations, branch or restart calculations were performed with HELIOS to determine the infinite neutron-multiplication factor, k_{inf} , as a function of burnup for out-of-reactor conditions (i.e., unborated water at 20°C). All HELIOS depletion and criticality calculations are for an infinite radial array of fuel assemblies, utilize the 45-group neutron cross-section library based on ENDF/B-VI, and include all of the actinide and fission product nuclides available in the cross-section library. HELIOS input files for selected cases are provided in Appendix A.

An illustration of the HELIOS model of the Westinghouse 17×17 assembly lattice with WABA BPRs present, as generated by ORION, is shown in Figure 3. The HELIOS model with Westinghouse BAA BPRs looks very similar, with the notable exception that the BAA BPR has a dry annular gap, while the WABA BPR has a wet annular gap. All of the HELIOS models represent one quadrant of an assembly and utilize reflective boundary conditions to simulate an infinite radial array of assemblies. The assembly and BPR specifications are provided in the previous section.

In the evolution of this study, HELIOS was initially employed to assess/verify isotopics calculated with the SAS2H sequence¹⁹ of SCALE.⁵ HELIOS was employed for this purpose because of its capability to explicitly model the relatively complicated, heterogeneous assembly lattices associated with BPRs. However, once the effort of HELIOS model development was expended, it became simpler and more efficient to perform the majority of the analysis variations with HELIOS. The simplicity is associated with the fact that the depletion in in-reactor conditions and criticality in out-of-reactor conditions may be done in a single calculation.

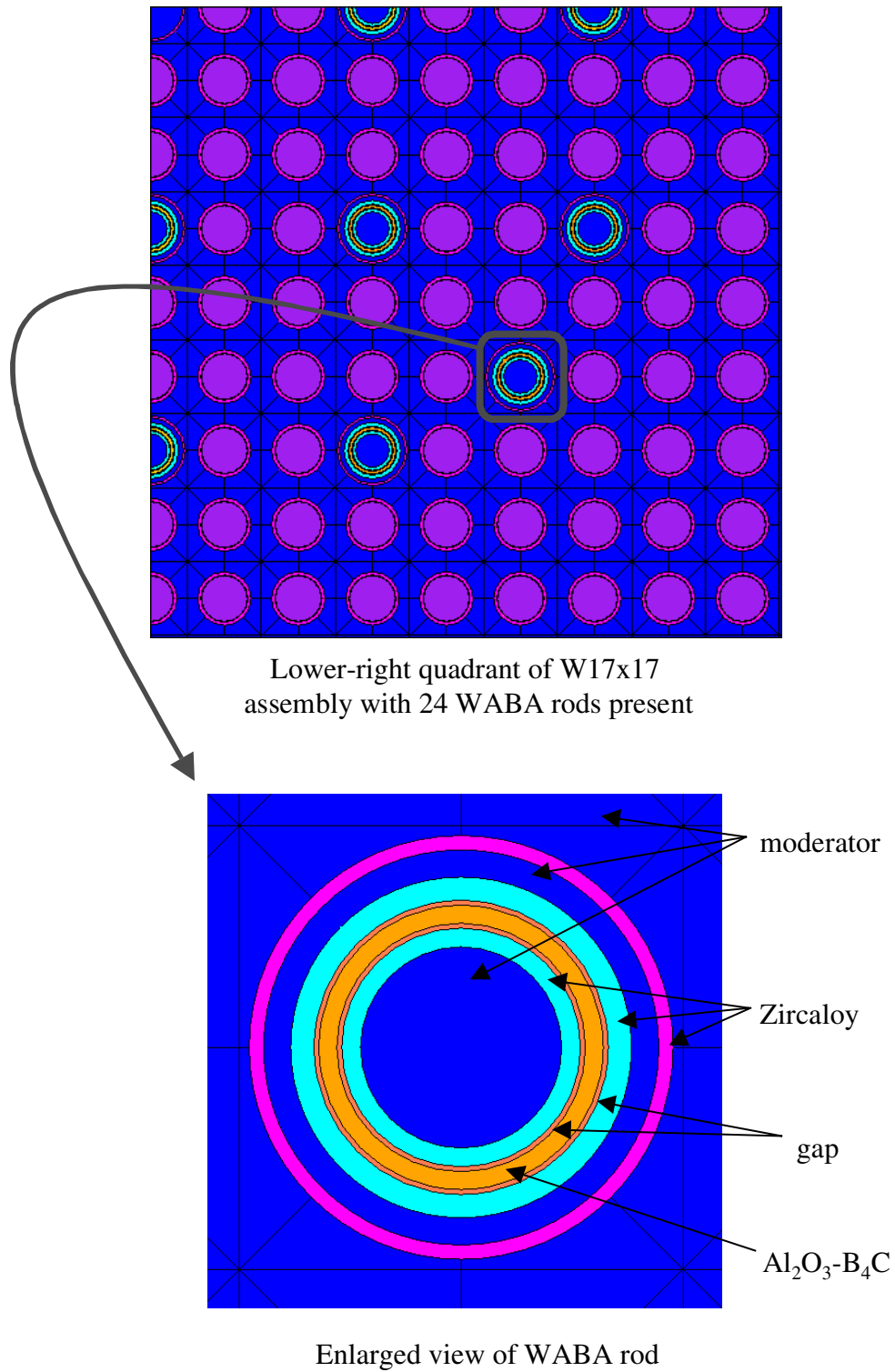


Figure 3 Illustration of assembly lattice with WABA BPRs as modeled with HELIOS

4.2 SCALE CODE PACKAGE

4.2.1 Codes Used

The SCALE code sequences used for this analysis include SAS2H, CSAS1X, and CSAS25.

The SCALE depletion sequence, SAS2H, has been extensively used (e.g., Refs. 17, 18, 20-22) and validated (e.g., Refs. 23-25) in studies of the burnup credit phenomenon. Therefore, fuel depletion calculations were performed with the SAS2H sequence,¹⁹ which uses ORIGEN-S for depletion. All SAS2H calculations utilized the SCALE 44-group library (primarily based on ENDF/B-V data) and were performed using the depletion parameters listed in Table 7. Isotopics for each burnup of interest were extracted from SAS2H output for use in the criticality calculations.

For scoping analyses, criticality calculations were performed to calculate k_{inf} values for an infinite array of fuel pin-cells with the CSAS1X sequence of SCALE, which uses the XSDRNPM one-dimensional (1-D) discrete ordinates code. The calculations used the SCALE 44-group cross-section library. The actual calculational model is a 1-D fuel pin cell in out-of-reactor conditions (i.e., unborated water at 20°C).

To quantify the effect of assembly exposure to BPRs on the effective neutron multiplication factor, k_{eff} , for a realistic high-capacity rail-type cask, criticality calculations were also performed with the CSAS25 sequence of SCALE, which uses the 3-D KENO V.a Monte Carlo code. The CSAS25 calculations used the SCALE 238-group cross-section library, which is primarily based on ENDF/B-V data. A cross-sectional view of one quadrant of the computational model of the GBC-32 cask, as generated by KENO V.a, is shown in Figure 4. Note that in this study the reactivity effect of BPRs is determined based on their effect on the depletion isotopics, and thus the BPRAs are not included in the KENO V.a criticality model.

4.2.2 SAS2H Modeling for BPRs

A SAS2H model of a fuel assembly is limited to a 1-D radial model with a single smeared fuel region. Geometric modeling approximations are made in an effort to achieve a reasonable assembly-averaged neutron energy spectrum during the depletion process. The SAS2H approach utilizes two distinct geometric models. The first model, referred to as the Path-A model, is a pin-cell model with white boundary conditions, which represents an infinite lattice of fuel pins. Cross-sections are processed with this model using a resonance self-shielding calculation followed by a 1-D discrete-ordinates transport calculation (XSDRNPM) for the neutron flux. The cell-weighted cross-sections produced with the pin-cell model are then applied to the fuel region of the Path-B model, which is a larger unit-cell model used to represent part or all of a fuel assembly. The concept of using cell-weighted data in the 1-D transport analysis of the Path-B model is an approximate method for including the 2-D assembly effects. The Path-B model is used by SAS2H to calculate an “assembly-averaged” fuel region flux that includes the effects of the Path-A model and the overall assembly characteristics (e.g., guide tubes, burnable poison rods, etc.).

The Path-B model is intended to represent a larger unit cell within an infinite lattice. The SAS2H manual¹⁹ provides examples and/or guidelines for describing PWR fuel assemblies with BPRs within the SAS2H geometric modeling capabilities/limitations. These guidelines were employed in the construction of the SAS2H models for this analysis. Because it is not possible to explicitly represent the spatially distributed BPRs with SAS2H, some approximate representation must be developed. The SAS2H approach for this type of configuration assumes a single BPR in the center, surrounded by smeared fuel that represents part of the assembly fuel volume, bounded by a corresponding volume of moderator material to represent the moderator between assemblies. In order to preserve the fuel-to-BP ratio, the assembly fuel volume, as well as the corresponding volume of the assembly moderator, is reduced by the inverse of the number of BPRs.

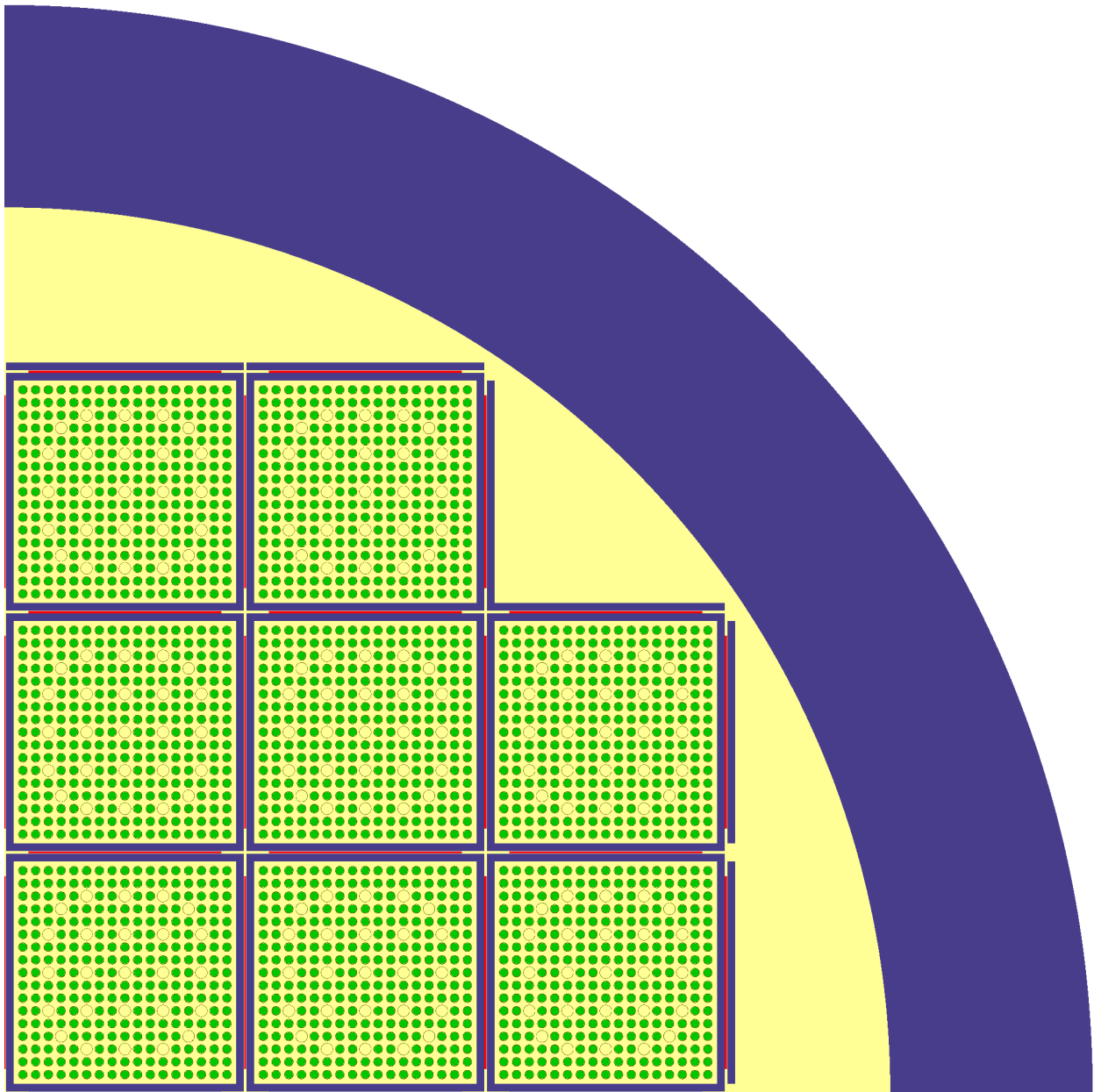


Figure 4 Radial cross-section of one quadrant of the KENO V.a model of the GBC-32 cask

For SAS2H models of fuel assemblies in which BPRs are not present in all guide tubes, the BP rod diameters are reduced in the SAS2H model to account for their absence in the unoccupied guide tube positions. The method for determining the effective cell dimensions was based on conservation of the material masses, and details for calculating the effective cell dimensions for the SAS2H models are given in Ref. 10. SAS2H input files for selected cases are provided in Appendix B.

4.2.3 Nuclide Sets Used in SCALE Criticality Calculations

Unlike the HELIOS criticality calculations, which include all of the actinide and fission product nuclides available in the HELIOS cross-section library, the criticality calculations with the SCALE sequences were performed with subsets of the available nuclides. Consequently, in this subsection the subsets of nuclides considered in the analyses are defined. The use of a subset of possible actinides in burnup credit calculations is referred to as “actinide-only” burnup credit. The nuclides used here for actinide-only calculations are consistent with those specified in a DOE Topical Report on burnup credit,²⁰ with the exception that ²³⁶U and ²³⁷Np are also included. While not consistently defined in the literature, the use of a subset of possible actinides and fission products will be referred to herein as “actinide + fission product” burnup credit. The fission product nuclides used here for actinide + fission product calculations are consistent with those identified in Table 2 of Ref. 26 as being the most important for criticality calculations. Table 8 lists the nuclides included for the two classifications of burnup credit. These “classes” of burnup credit and the nuclides included within each are defined here for the purposes of analysis and discussion; other terminology and specific sets of nuclides have been defined and used by others studying burnup credit phenomena.

Table 8 Nuclides associated with the classifications of burnup credit used for analysis

Actinide-only burnup credit nuclides (12 total)									
U-234	U-235	U-236	U-238	Pu-238	Pu-239	Pu-240	Pu-241	Pu-242	Np-237
Am-241	O [†]								
Actinide + fission product burnup credit nuclides (28 total)									
U-234	U-235	U-236	U-238	Pu-238	Pu-239	Pu-240	Pu-241	Pu-242	Np-237
Am-241	Mo-95	Tc-99	Ru-101	Rh-103	Ag-109	Cs-133	Sm-147	Sm-149	Sm-150
Sm-151	Sm-152	Nd-143	Nd-145	Eu-151	Eu-153	Gd-155	O [†]		

[†]Oxygen is neither an actinide nor a fission product, but is included in this list because it is included in the fuel specifications of the calculations.

5 REACTIVITY EFFECT OF BURNABLE POISON RODS

5.1 INTRODUCTION AND BACKGROUND

The presence of BPRs during depletion hardens the neutron spectrum due to removal of thermal neutrons by capture and by displacement of moderator, resulting in enhanced production of fissile plutonium isotopes and diminished ^{235}U depletion. Consequently, an assembly exposed to BPRs may have a higher reactivity for a given burnup than an assembly that has not been exposed to BPRs. The net effect of BPRs is similar to that of soluble boron,¹⁷ since the same mechanism applies: preferential removal of thermal neutrons.

BPRAs are typically employed during an assembly's first cycle¹⁵ and may have varying numbers of BPRs or varying poison loading. The effect on reactivity is dependent upon the assembly exposure to BPRs during depletion, the subsequent accumulated burnup, BPR design, and the initial fuel enrichment. Studies to assess the significance of BPRs are minimal, but early work,¹⁵ which compared a depletion case (4.2 wt % ^{235}U , 36 Wd/MTU, 5-year cooled) with 20 BPRs in an assembly to a depletion case with no BPRs, found an increase of 0.6% in a storage cask k_{eff} value when the cask was fully loaded with assemblies. Indications from this study are that insertion of a maximum BPR loading in all depletion analyses would be a simple, yet not overly conservative approach to facilitate allowance for assemblies that have been exposed to BPRs.

As mentioned, there is a great deal of variety in BPR designs, and possibly in their use during operations. Addressing the effect of BPRs requires calculations to examine how BPR design and exposure impact SNF reactivity. Therefore parametric analyses were performed for a variety of exposure scenarios to establish an increased understanding of the effect of BPR exposure on the reactivity of discharged SNF. Although many of the scenarios considered are not realistic (e.g., 3-cycle BPR exposure), it should be possible to estimate the reactivity effect of actual BPR exposure conditions based on inspection of the presented results and trends.

The analyses were performed from an out-of-reactor criticality safety perspective, which is concerned with the determination and usage of limiting configurations and conditions. For each fuel assembly/BPR design variation considered, a depletion calculation was performed for (1) the un-poisoned assembly condition (i.e., no BPRs present) and (2) the conditions in which the BPRs were assumed to be present for various periods of burnup. The calculated isotopic compositions from these conditions were subsequently used in criticality calculations for an out-of-reactor environment. Throughout the following sections, the Δk values between these two conditions are reported to assess the effect of the BPRs on the reactivity of SNF. Note that in all cases the reactivity effect of BPR exposure is determined based on their effect on the depletion isotopic compositions (i.e., the BPRs are not included in the criticality models).

The study is performed in two parts. In the first part, 2-D calculations are performed with the HELIOS code package for an infinite radial array of assemblies and 1-D calculations are performed with the SCALE code package for an infinite pin-cell array. Calculations are performed for each BPR design and a variety of exposure conditions and assembly initial enrichments. These calculations quantify the effect of BPR exposure and enable comparisons of the reactivity effect of the various BPR designs. The 1-D calculations are performed with and without fission products present to investigate the reactivity effect of BPRs within the limitations of actinide-only burnup credit. Finally, results from HELIOS and SAS2H are compared to assess the adequacy of the SAS2H modeling and the agreement between independent codes/methods. In the second part, 3-D KENO V.a calculations are performed to determine the reactivity effect of BPRs, with and without fission products present, in a high-capacity rail-type cask designed for burnup credit. The 3-D calculations are performed with and without consideration of the axial burnup distribution. Finally, because it may be difficult (or even impossible) to assure/verify that the SNF assemblies to be loaded into a cask comply with the calculational assumption for BPR exposure in a safety evaluation, 3-D cask calculations are

performed to quantify the impact (on k_{eff}) of loading SNF assemblies that experienced more significant BPR exposure (i.e., 3-cycle) than what is assumed for the remaining assemblies (1-cycle) residing in the cask.

5.2 INFINITE ASSEMBLY ARRAY CALCULATIONS WITH HELIOS

In this section, results of 2-D HELIOS calculations for infinite radial arrays of assemblies are presented. Calculations were performed for each BPR design and a variety of exposure conditions and initial enrichments. Using the isotopic compositions from the depletion calculations (all nuclides available in the cross-section library), branch or restart calculations were performed to determine the infinite neutron multiplication factor, k_{inf} , as a function of burnup for out-of-reactor conditions (i.e., 20°C, no soluble boron present, and no BPRs present). Unless explicitly stated otherwise, all HELIOS criticality calculations correspond to zero cooling time. Where exceptions are made to study the effect of cooling time, they are clearly stated. For each case considered, a calculation was performed for (1) the reference assembly condition (i.e., no BPR exposure) and (2) conditions including BPR exposure. Throughout the following sections, the Δk values between these two conditions are reported to assess the effect of each of the BPR designs on the reactivity of SNF in out-of-reactor conditions.

5.2.1 Westinghouse BPR Designs

For both of the Westinghouse BPR designs, calculations were performed assuming the maximum possible number of BPRs present (i.e., 24). Calculations were also performed for fewer BPRs present to assess the effect as a function of the number of BPRs present. In general, calculations were performed assuming the BPRs were present during (1) the first cycle of irradiation, (2) the first two cycles of irradiation, and (3) the entire irradiation period (i.e., all three cycles). For the purpose of the depletion calculations, 3 cycles of 15 GWd/MTU per cycle were assumed. For comparison purposes, reference calculations were performed assuming no BPRs present. The various calculations are compared to determine the reactivity effect of each BPR design as a function of burnup.

5.2.1.1 Wet Annular Burnable Absorber (WABA) BPRs

Figure 5 shows k_{inf} values as a function of burnup for an infinite radial array of Westinghouse 17×17 OFA assemblies with 4.0 wt % ^{235}U initial enrichment and various WABA exposures. The k_{inf} values are calculated for out-of-reactor conditions at burnup steps of 1 GWd/MTU and zero cooling time. While Figure 5 shows the existence of differences between the cases, the magnitude and behavior of the difference is not readily discernable. Therefore, Figures 6–8 plot the Δk values (relative to the no BPR condition) as a function of burnup for initial fuel enrichments of 3.0, 4.0, and 5.0 wt % ^{235}U , respectively. It is evident from the figures that the reactivity effect of BPRs increases with increasing BPR exposure, and thus it would be conservative (maximize k_{inf}) to assume that the BPRs are present throughout the irradiation.

5.2.1.1.1 Effect of initial fuel enrichment

Figures 6–8 also demonstrate a decrease in the reactivity effect of BPRs with increasing initial fuel enrichment (for a fixed burnup). For initial enrichments of 3.0, 4.0, and 5.0 wt % ^{235}U , Δk values for continuous BPR exposure up to a burnup of 45 GWd/MTU are 0.0194, 0.0155, and 0.0109, respectively. Note that fuel assemblies with initial enrichments of 3.0 wt % ^{235}U do not typically achieve a burnup as high as 45 GWd/MTU. In practice, discharge burnups decrease with decreasing initial enrichment. Therefore, examination of a typical burnup and enrichment combination provides a reasonable representation of the reactivity effect for other typical discharge burnup and enrichment combinations. As an example, compare

the Δk values for 4.0 wt % ^{235}U fuel burned to 45 GWd/MTU (0.0155 Δk from Figure 7) and 3.0 wt % ^{235}U fuel burned to 30 GWd/MTU (0.0149 Δk from Figure 6).

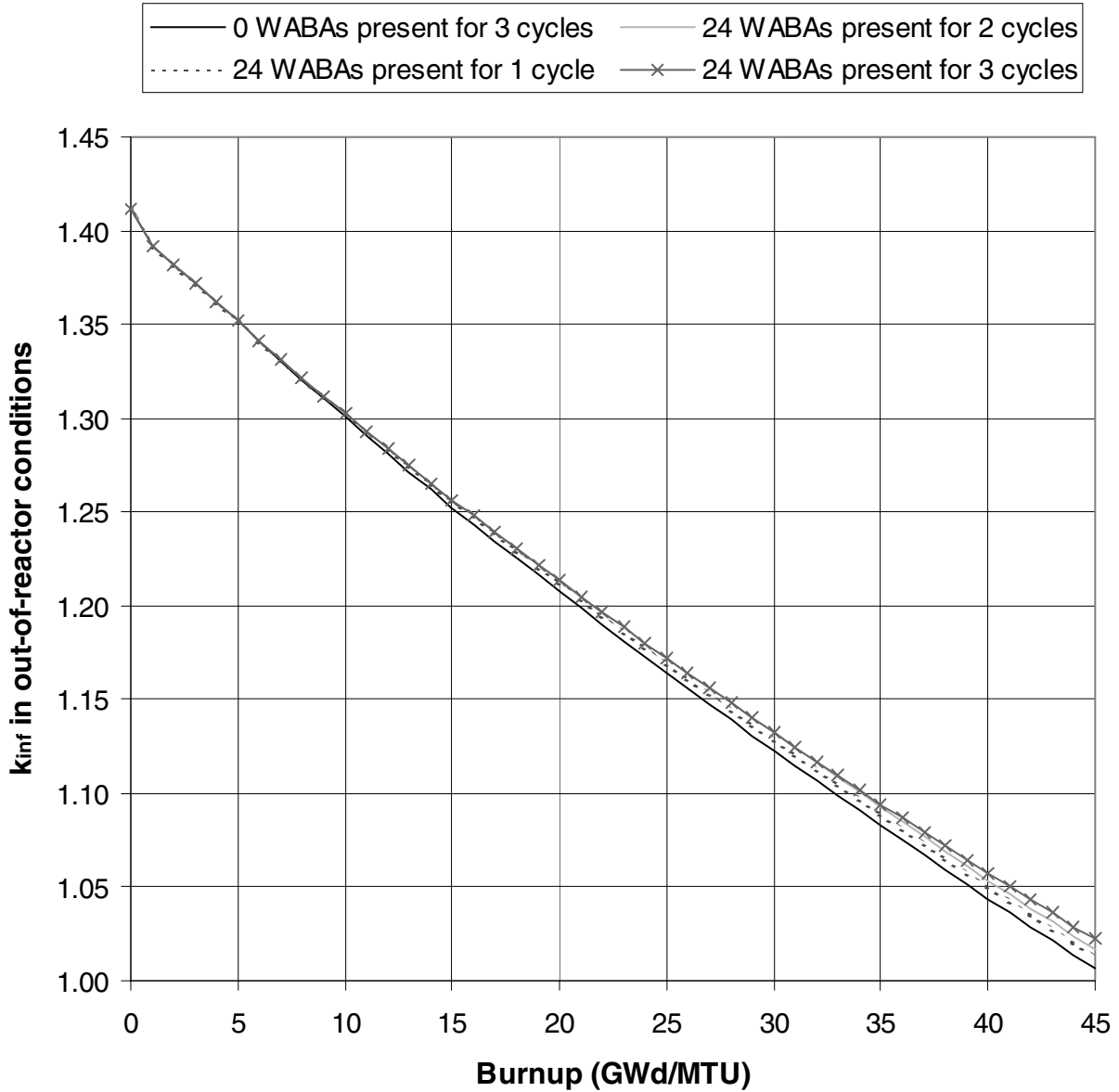


Figure 5 k_{inf} values as a function of burnup for various WABA exposures. The results correspond to fuel with 4.0 wt % ^{235}U initial enrichment that has been exposed to Westinghouse WABA rods (3 cycles of 15 GWd/MTU per cycle were assumed).

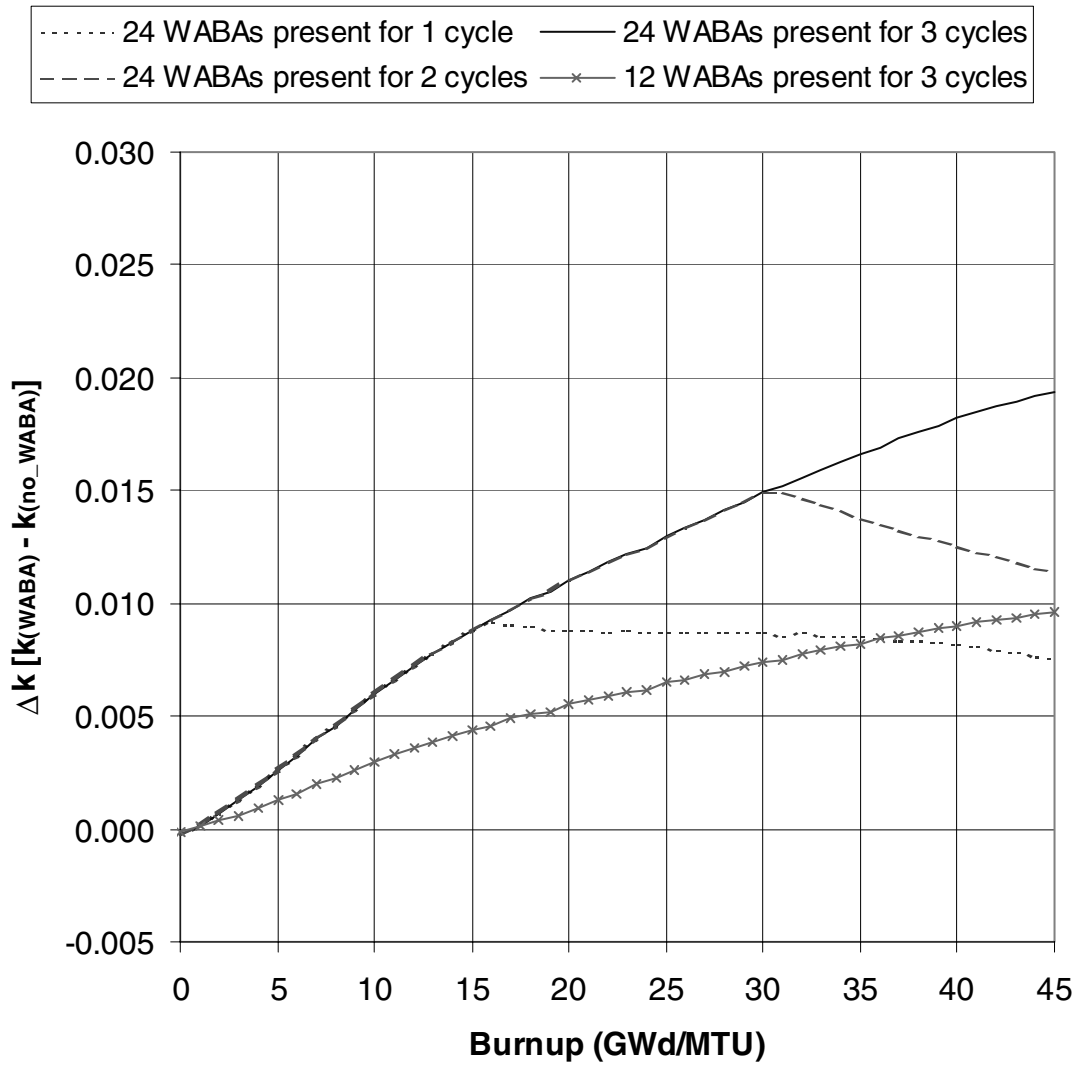


Figure 6 Δk values as a function of burnup for Westinghouse 17×17 fuel with 3.0 wt % ^{235}U initial enrichment that has been exposed to Westinghouse WABA rods (3 cycles of 15 GWd/MTU per cycle were assumed)

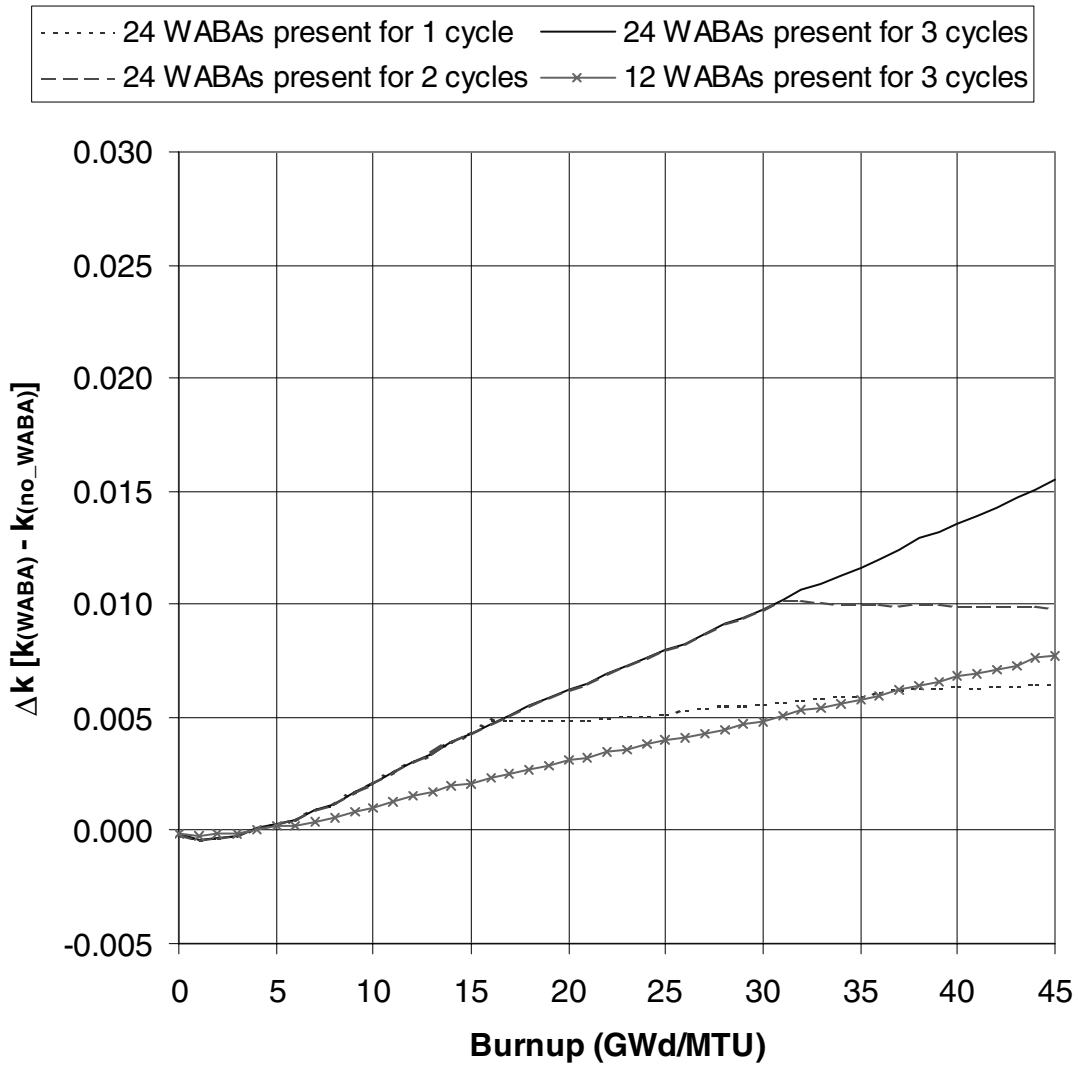


Figure 7 Δk values as a function of burnup for Westinghouse 17×17 fuel with 4.0 wt % ^{235}U initial enrichment that has been exposed to Westinghouse WABA rods (3 cycles of 15 GWd/MTU per cycle were assumed)

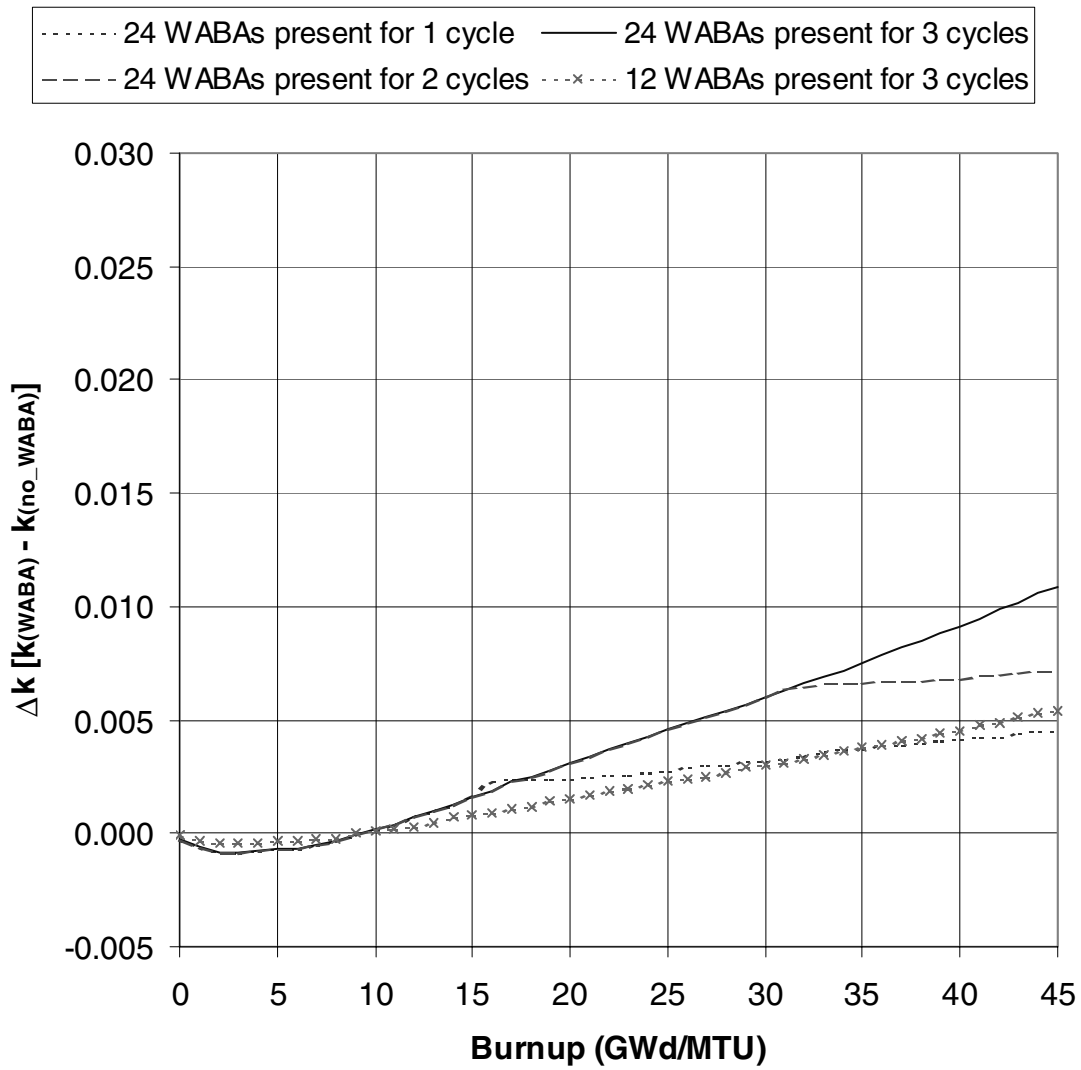


Figure 8 Δk values as a function of burnup for Westinghouse 17×17 fuel with 5.0 wt % ^{235}U initial enrichment that has been exposed to Westinghouse WABA rods (3 cycles of 15 GWd/MTU per cycle were assumed)

Figures 6–8 show the results of parametric analyses for a variety of exposure scenarios to establish an increased understanding of the effect of BPR exposure on the reactivity of discharged SNF; they do not all represent realistic scenarios. Based on the authors' research of BPR usage in U.S. PWRs, BPRAs have been typically inserted into a fuel assembly during its first exposure cycle, which generally corresponds to slightly more than one-third of its ultimate three-cycle burnup. In less frequent instances, BPRAs have also been used in fuel assemblies during their second exposure cycle, either cumulative two-cycle exposure or isolated second-cycle exposure (i.e., no first-cycle exposure).^{11,13,14,15} To highlight the effect of initial fuel enrichment on these possible exposure conditions, Figures 9 and 10 show the reactivity effect of WABA BPRs with various initial fuel enrichments for one- and two-cycle exposures, respectively.

Careful examination of Figure 9 reveals that the Δk values increase after the BPRs are withdrawn for the cases with 4.0 and 5.0 wt % ^{235}U enrichment, but decrease for the 3 wt % ^{235}U enrichment case. While the BPRs are present in the assembly lattice, they displace moderator and absorb thermal neutrons, significantly hardening the neutron spectrum. The hardened neutron spectrum results in reduced rate of ^{235}U depletion, higher production of fissile plutonium isotopes and increased plutonium fission. Examination of the atom densities of ^{239}Pu and ^{235}U as a function of burnup reveals that the lower the initial ^{235}U enrichment, the greater the ^{239}Pu fission while the BPRs are present. Therefore, lower initial ^{235}U enrichments have less net buildup of ^{239}Pu while the BPRs are present (as compared to higher initial ^{235}U enrichments), because they have an increased rate of plutonium fission during this period. To illustrate these points, the differences in the ^{235}U and ^{239}Pu atom densities, ΔN , for cases with and without BPRs present for the first cycle (i.e., the cases considered in Figure 9) are shown in Figures 11 and 12, respectively.

When the BPRs are removed, the neutron spectrum softens due to the replacement of the thermal neutron absorber with moderator. Consequently, the reactivity worth and fission rate of ^{235}U increase. However, the higher initial ^{235}U enrichment cases have more fissile plutonium built in, as compared to cases without BPRs present. The increased quantity of fissile plutonium and subsequent increased plutonium fission result in a continued decrease in the ^{235}U depletion rate, as compared to cases without BPRs present (see Figure 11) and a small degree of conversion, and thus there is an increase in Δk after the BPRs are removed for the 4.0 and 5.0 wt % ^{235}U cases. Note, however, that this increase in Δk does not continue indefinitely. Extension of the calculations to longer burnups reveals that the Δk reaches a maximum and then begins decreasing. The Δk values for the 3 wt % ^{235}U enriched case do not increase because, due to the lower initial ^{235}U enrichment, a significant portion of the ^{239}Pu is being depleted while the BPRs are still present; resulting in less net buildup of fissile plutonium. The behavior is illustrated in Figure 13, which shows the Δk values at extended burnups (out to 70 GWd/MTU) for Westinghouse 17×17 fuel with the various initial fuel enrichments that have been exposed to WABA rods for the first 30 GWd/MTU of burnup.

5.2.1.1.2 Effect of variations in the number of BPRs present

As mentioned, the Westinghouse BPRAs are composed of various numbers of BPRs arranged in specific geometric patterns. Although numerous patterns are known to exist,¹¹ including asymmetric arrangements, Figure 1 shows the different symmetric assembly lattices considered in this analysis. To demonstrate the effect of variations in the number of BPRs per assembly, Figures 14 and 15 show the Δk values (relative to the no BPR condition) as a function of burnup for an initial fuel enrichment of 4.0 wt % ^{235}U for one- and three-cycle exposures, respectively. Note that the results shown in Figure 14 for one-cycle exposure are expected to be more representative of actual operations than the three-cycle results in Figure 15. The reactivity effect increases linearly with the number of BPRs present, as is more clearly shown in Figure 16, which plots the Δk values at 45 GWd/MTU as a function of the number of BPRs present.

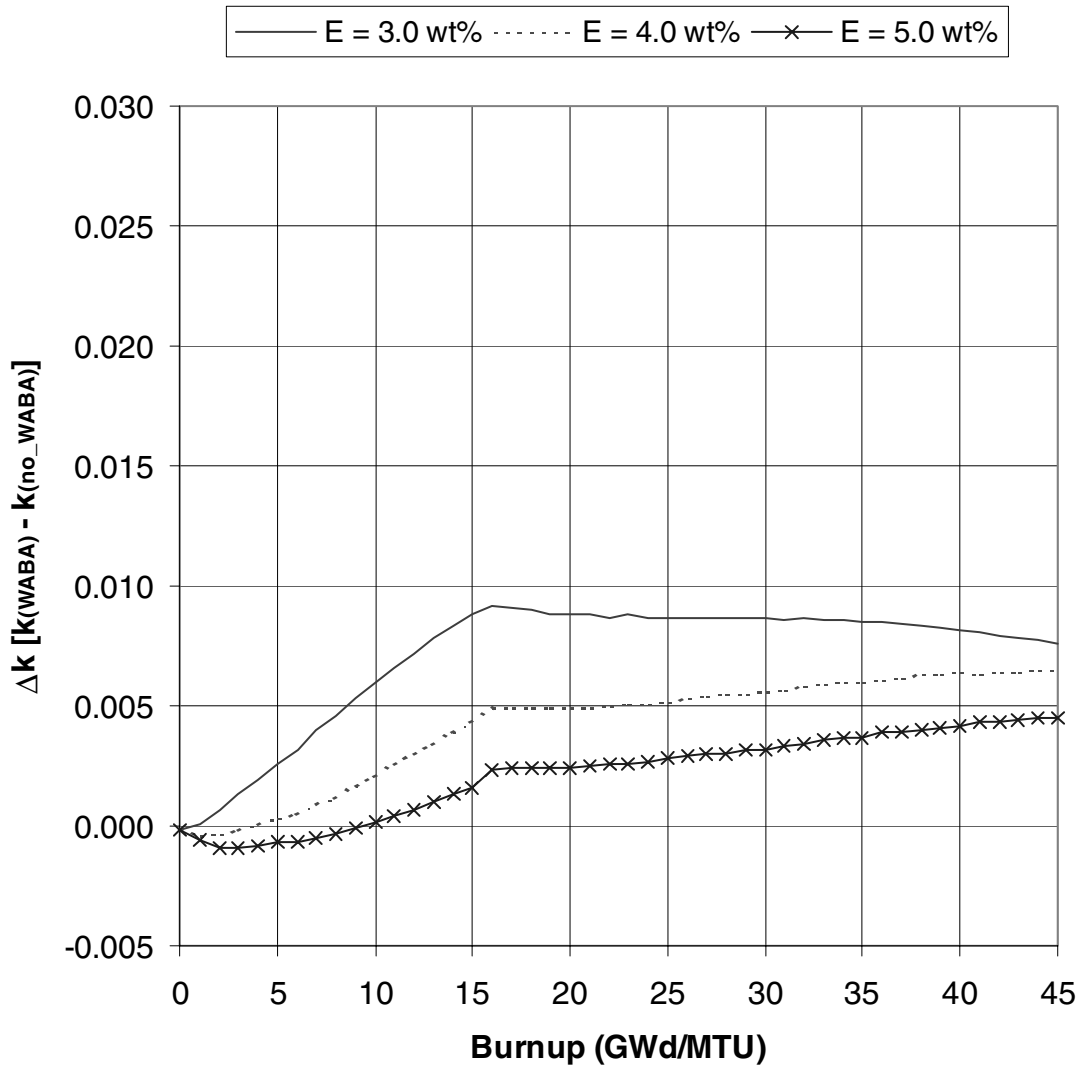


Figure 9 Δk values as a function of burnup for Westinghouse 17×17 fuel assemblies with various initial enrichments that have been exposed to 24 Westinghouse WABA rods for the first 15 GWd/MTU of burnup

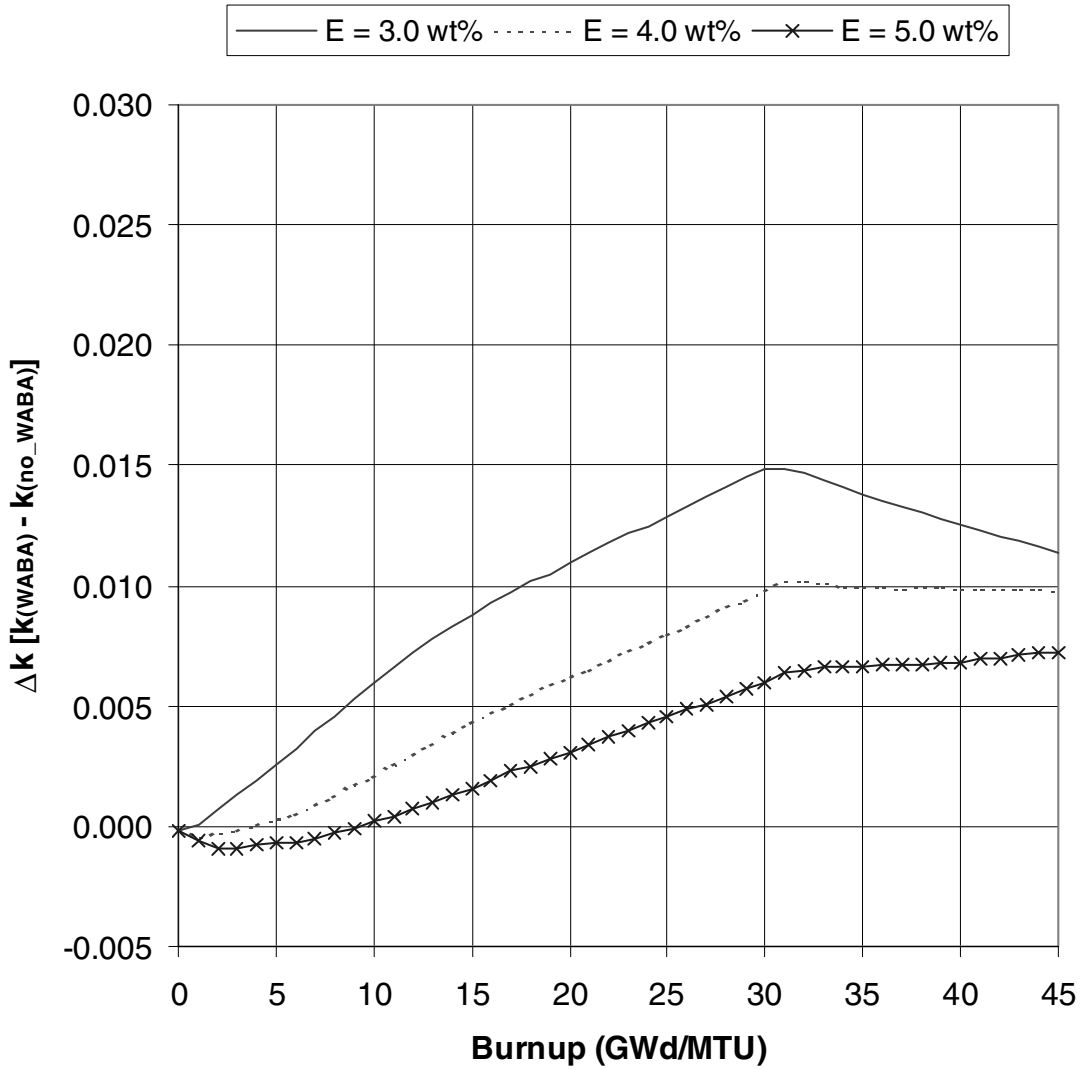


Figure 10 Δk values as a function of burnup for Westinghouse 17×17 fuel with various initial enrichments that have been exposed to 24 Westinghouse WABA rods for the first 30 GWd/MTU of burnup

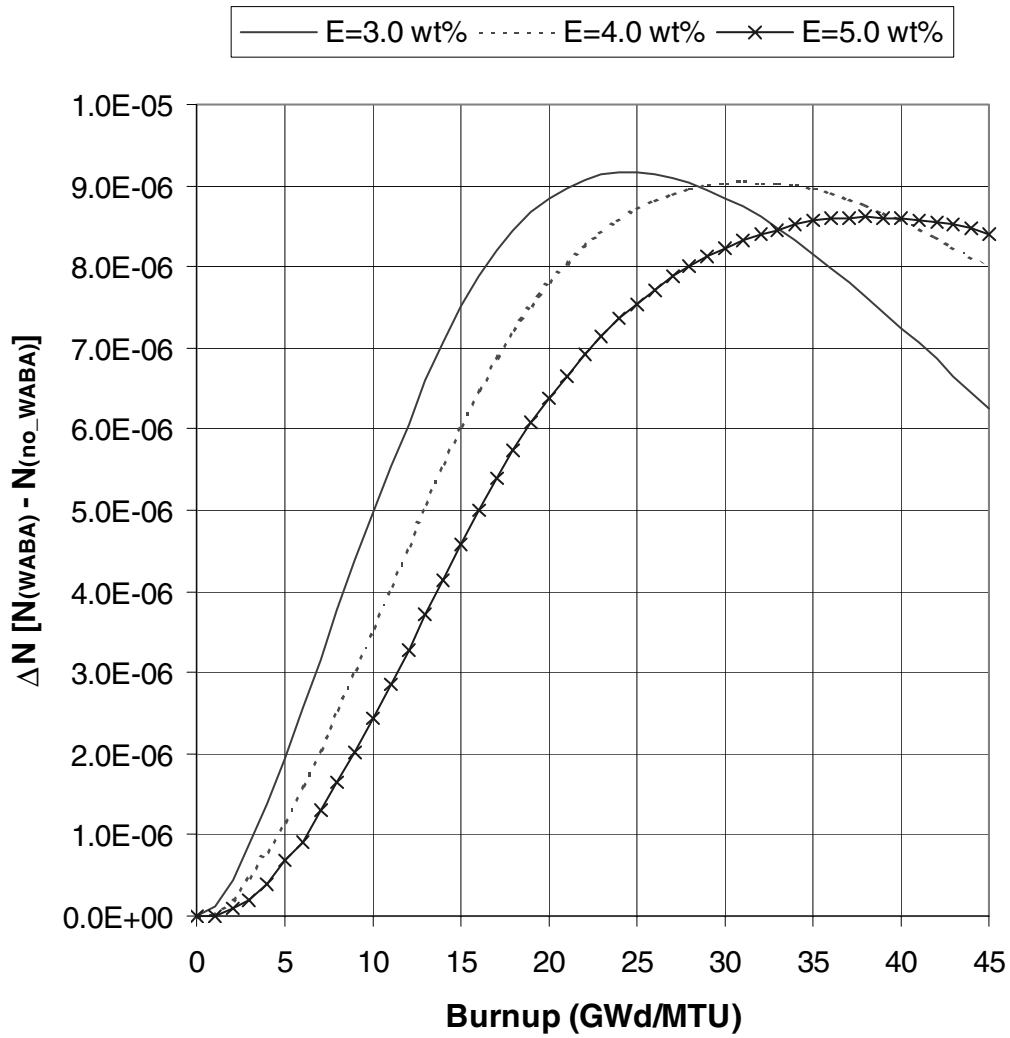


Figure 11 Differences in ²³⁵U atom densities, ΔN values, as a function of burnup for Westinghouse 17 × 17 fuel with various initial enrichments that have been exposed to 24 Westinghouse WABA rods for the first 15 GWd/MTU of burnup

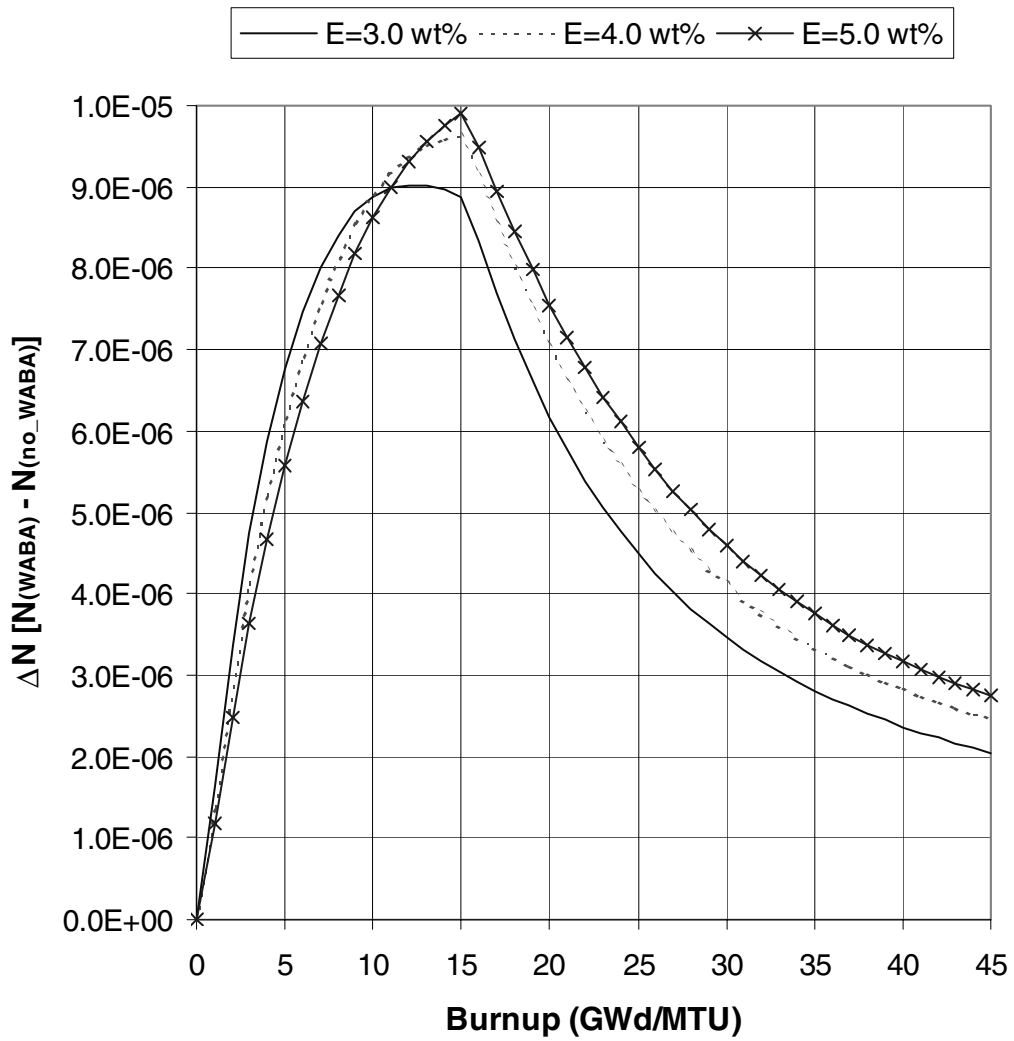


Figure 12 Differences in ²³⁹Pu atom densities, ΔN values, as a function of burnup for Westinghouse 17 × 17 fuel with various initial enrichments that have been exposed to 24 Westinghouse WABA rods for the first 15 GWd/MTU of burnup

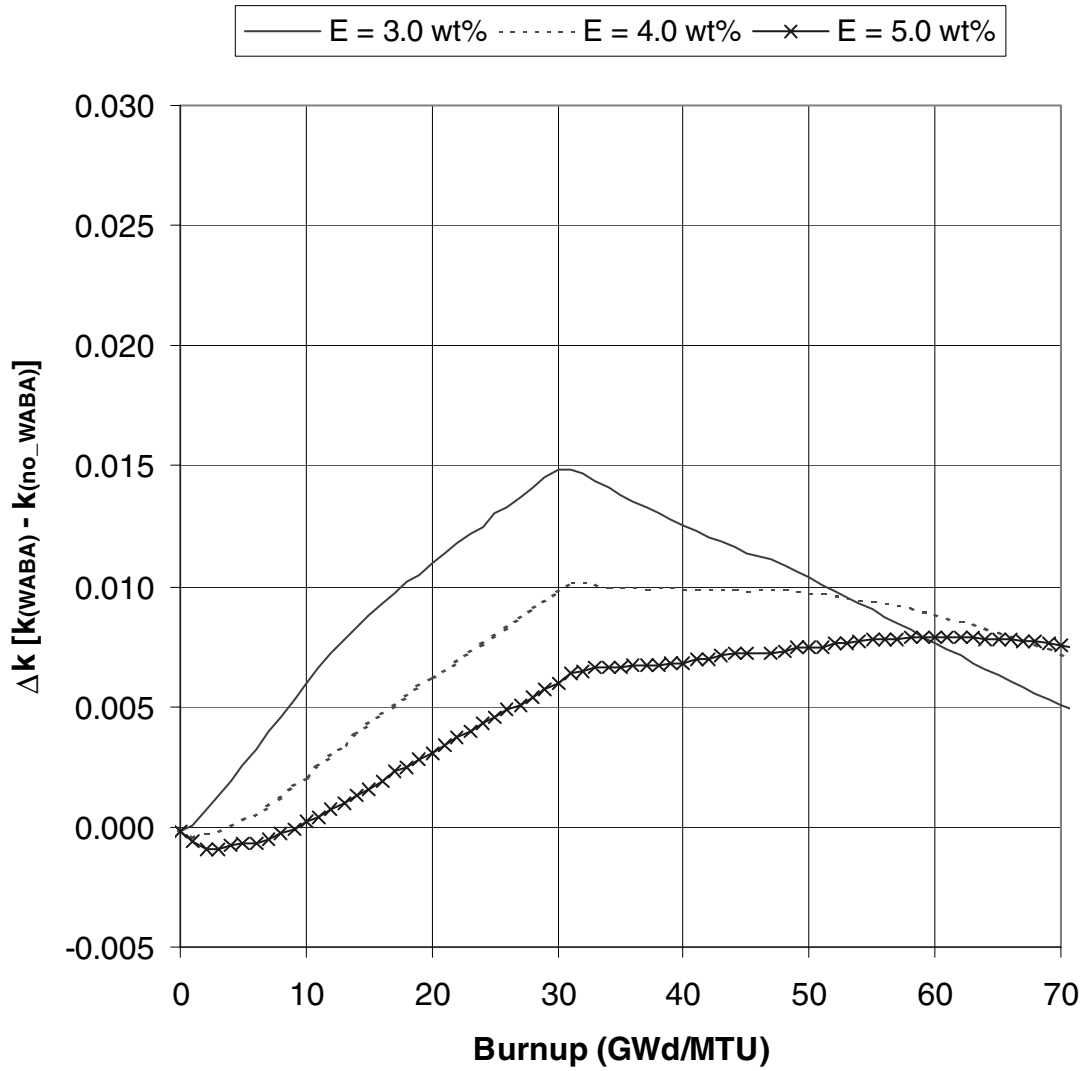


Figure 13 Δk values as a function of burnup (for extended burnup) for Westinghouse 17×17 fuel with various initial enrichments that have been exposed to 24 Westinghouse WABA rods for the first 30 GWd/MTU of burnup

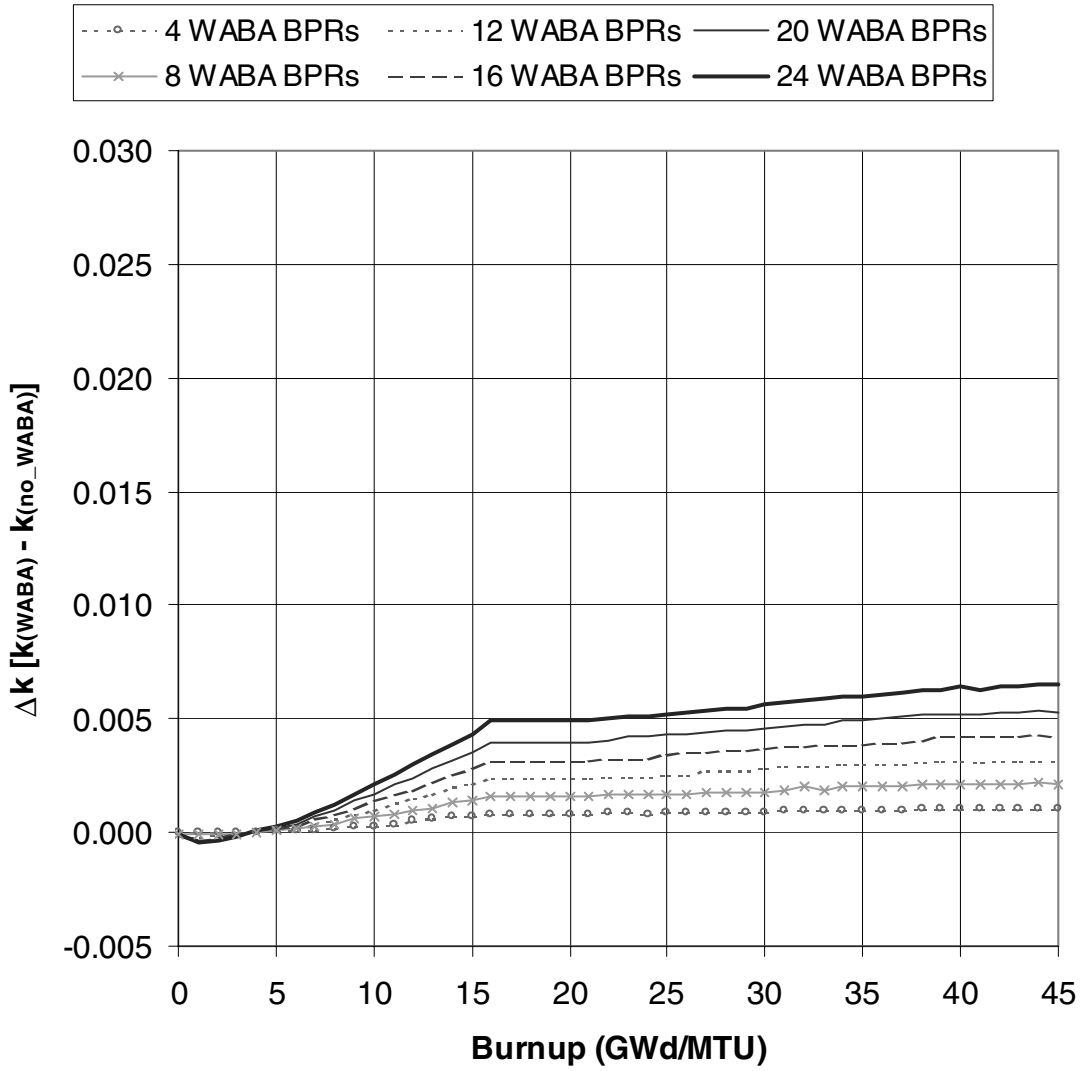


Figure 14 Δk values as a function of burnup for Westinghouse 17×17 fuel with 4.0 wt % ^{235}U initial enrichment that has been exposed to various numbers of Westinghouse WABA rods for the first 15 GWd/MTU of burnup

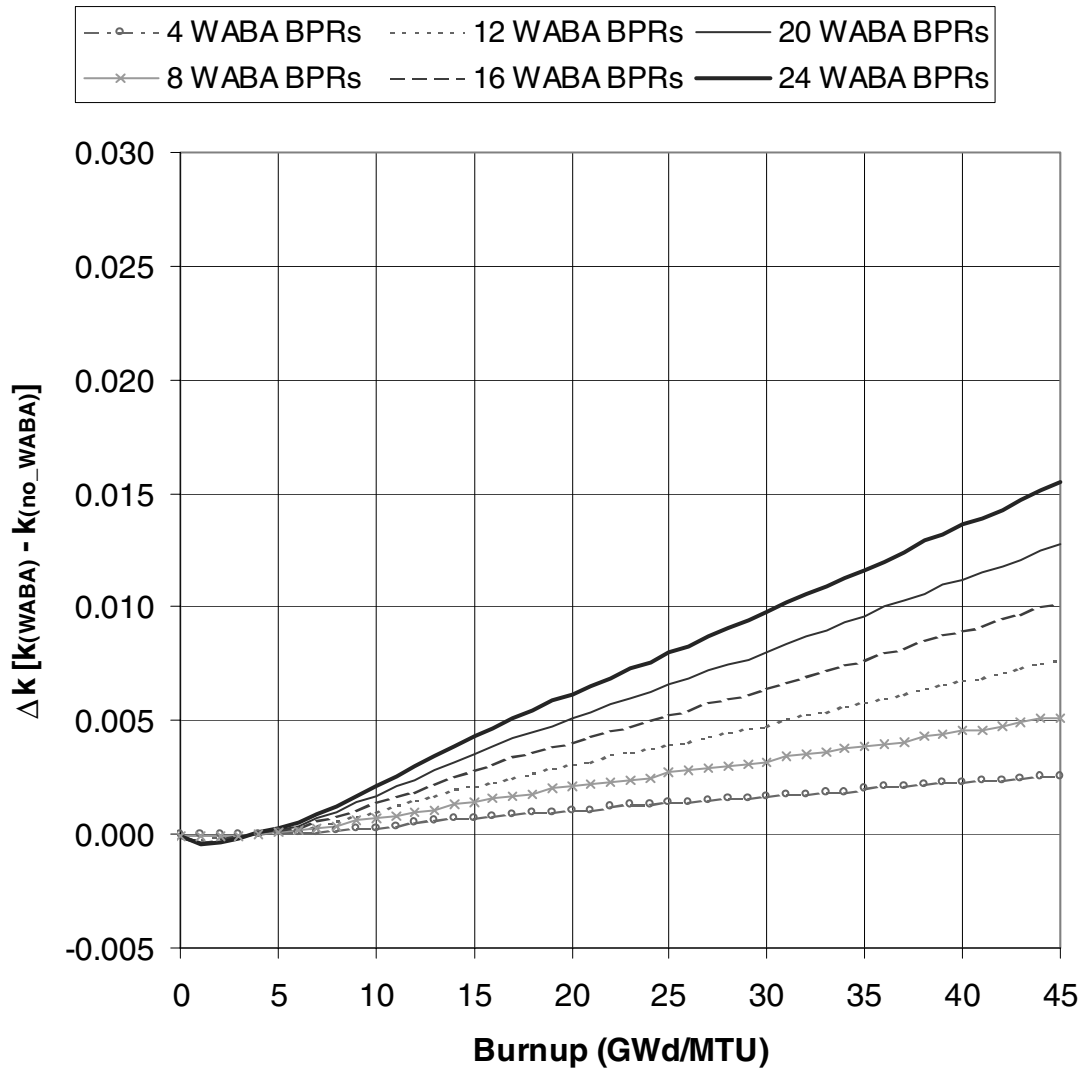


Figure 15 Δk values as a function of burnup for Westinghouse 17×17 fuel with 4.0 wt % ^{235}U initial enrichment that has been exposed to various numbers of Westinghouse WABA rods during the entire depletion

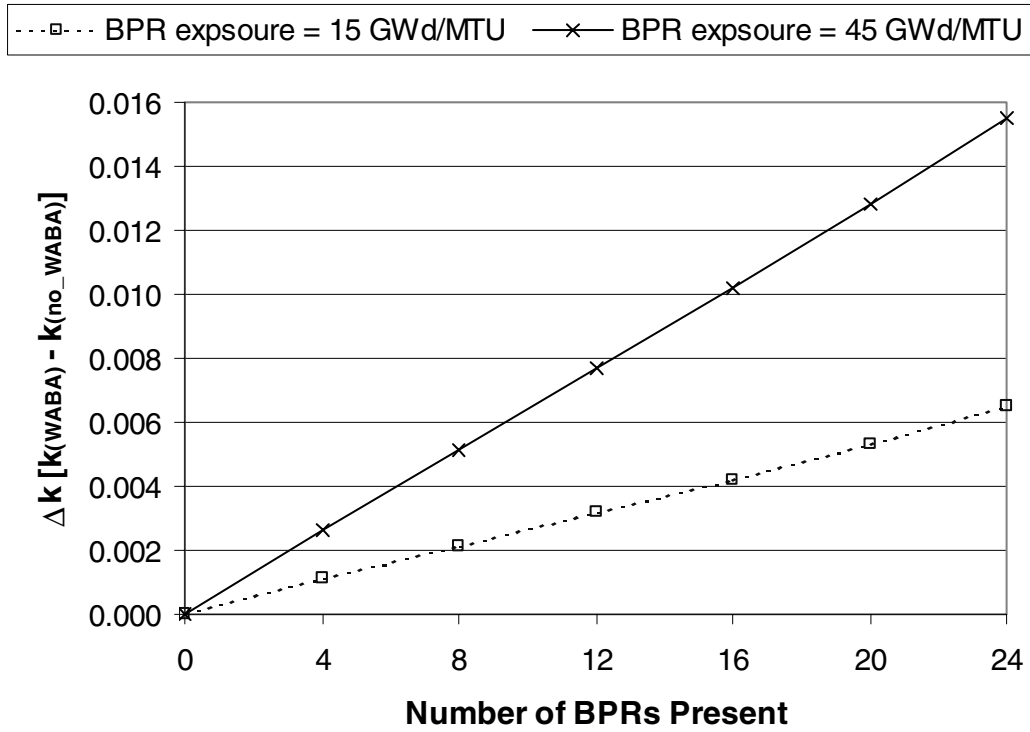


Figure 16 Δk values for Westinghouse 17×17 fuel with 4.0 wt % ^{235}U initial enrichment and a total burnup of 45 GWd/MTU that has been exposed to various numbers of Westinghouse WABA rods for various burnup exposures

5.2.1.1.3 Absorber (^{10}B) depletion

As has been noted, the presence of the BPRs within the assembly guide tubes hardens the neutron spectrum due to removal of thermal neutrons by capture in ^{10}B and displacement of moderator. Thus, the BPRs continue to harden the neutron spectrum even after the neutron absorber material has been essentially depleted. To assist in understanding the depletion of ^{10}B in BPRs, Figure 17 plots the ^{10}B atom density as a function of burnup for the various initial fuel enrichment cases considered, and demonstrates the increased rate of depletion with decreasing initial fuel enrichment. The reason for this behavior is that to maintain constant fission power, lower ^{235}U enrichment requires higher fuel flux, which leads to greater capture in ^{10}B . The differences in the rate of ^{10}B depletion with variations in initial fuel enrichment are also evident by comparing the slope of the Δk values in Figures 6–8.

5.2.1.1.4 Effect of cooling time

It has been shown in numerous studies (e.g., Ref. 27) that SNF discharged from a reactor will increase in reactivity for approximately 100 hours after discharge due to the decrease in neutron absorption caused by the decay of very short-lived fission products. The decrease in reactivity from 100 hours to 100 years is driven by the decay of the ^{241}Pu fissile nuclide ($t_{1/2} = 14.4$ years) and the buildup of the neutron absorbers ^{241}Am (from decay of ^{241}Pu) and ^{155}Gd (from ^{155}Eu which decays with $t_{1/2} = 4.7$ years). After about 50 years the ^{155}Gd buildup is complete and the ^{241}Pu has decayed out by approximately 100 years. After this time the reactivity begins to increase, governed primarily by the decay of two major neutron absorbers – ^{241}Am ($t_{1/2} = 432.7$ years) and ^{240}Pu ($t_{1/2} = 6,560$ years) – and mitigated somewhat by a decrease in the fissile inventory as ^{239}Pu ($t_{1/2} = 24,100$ years) decays and causes an increase in ^{235}U . After approximately 30,000 years, the ^{240}Pu and ^{241}Am decay is complete and the reactivity again begins to decrease as the decay of ^{239}Pu dominates the process. Consequently, cooling time is an important parameter in a burnup credit evaluation.

For simplicity, the HELIOS analyses presented in the previous subsections all correspond to zero cooling time. To evaluate the effect of cooling time, a number of the calculations were repeated for cooling times that are more consistent with cask storage and transportation (i.e., 5–40 years). Figures 18 and 19 show Δk values (relative to the no BPR condition) as a function of burnup for various cooling times (within the 0–40 year timeframe) for 1- and 3-cycle BPR exposure, respectively. These results show that the Δk values between cases with and without BPRs are fairly insensitive to cooling time, with a minor trend toward lower Δk values for cooling times greater than 5 years. However, at the final burnup (i.e., 45 GWd/MTU) the differences with cooling time are very small. Therefore, the results at zero cooling time are expected to be representative of other cooling times within the timeframe of storage and transportation.

5.2.1.2 Pyrex Burnable Absorber Assembly (BAA) BPRs

As noted previously, the primary difference between the Westinghouse WABA and BAA BPRs is that the central annular gap is dry in the BAA BPRs, while it is wet in the WABA BPRs. Thus, the BAA BPRs displace a greater volume of water and hence result in a larger effect on reactivity. Figures 20–22 plot the Δk values (relative to the no BPR condition) associated with various exposures to BAA BPRs as a function of burnup for initial fuel enrichments of 3.0, 4.0, and 5.0 wt % ^{235}U , respectively. The same trends identified with the WABA BPRs are also observed with the BAA BPRs; namely that the reactivity effect increases with increasing BPR exposure and decreasing initial fuel enrichment. However, as expected, the BAA BPRs have a larger effect on reactivity. For initial enrichments of 3.0, 4.0, and 5.0 wt % ^{235}U , maximum Δk values for continuous BAA BPR exposure up to a burnup of 45 GWd/MTU are 0.0302, 0.0231, and 0.0159, respectively, as compared to 0.0194, 0.0155, and 0.0109, respectively, for the WABA BPRs.

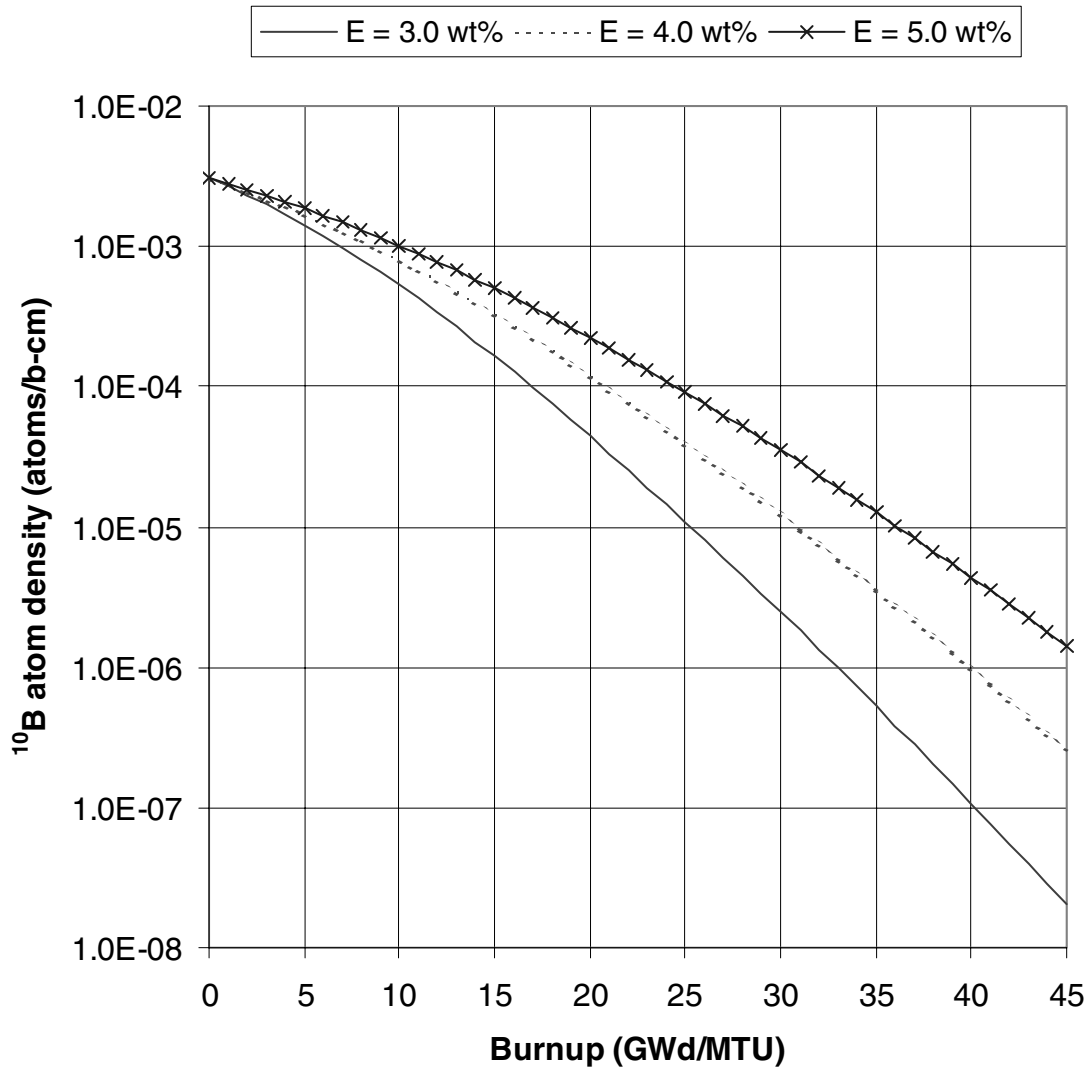


Figure 17 ¹⁰B atom density as a function of burnup for various cases of initial fuel enrichment. The results correspond to 24 Westinghouse WABA rods inserted into Westinghouse 17 × 17 fuel with various initial enrichments during the entire depletion.

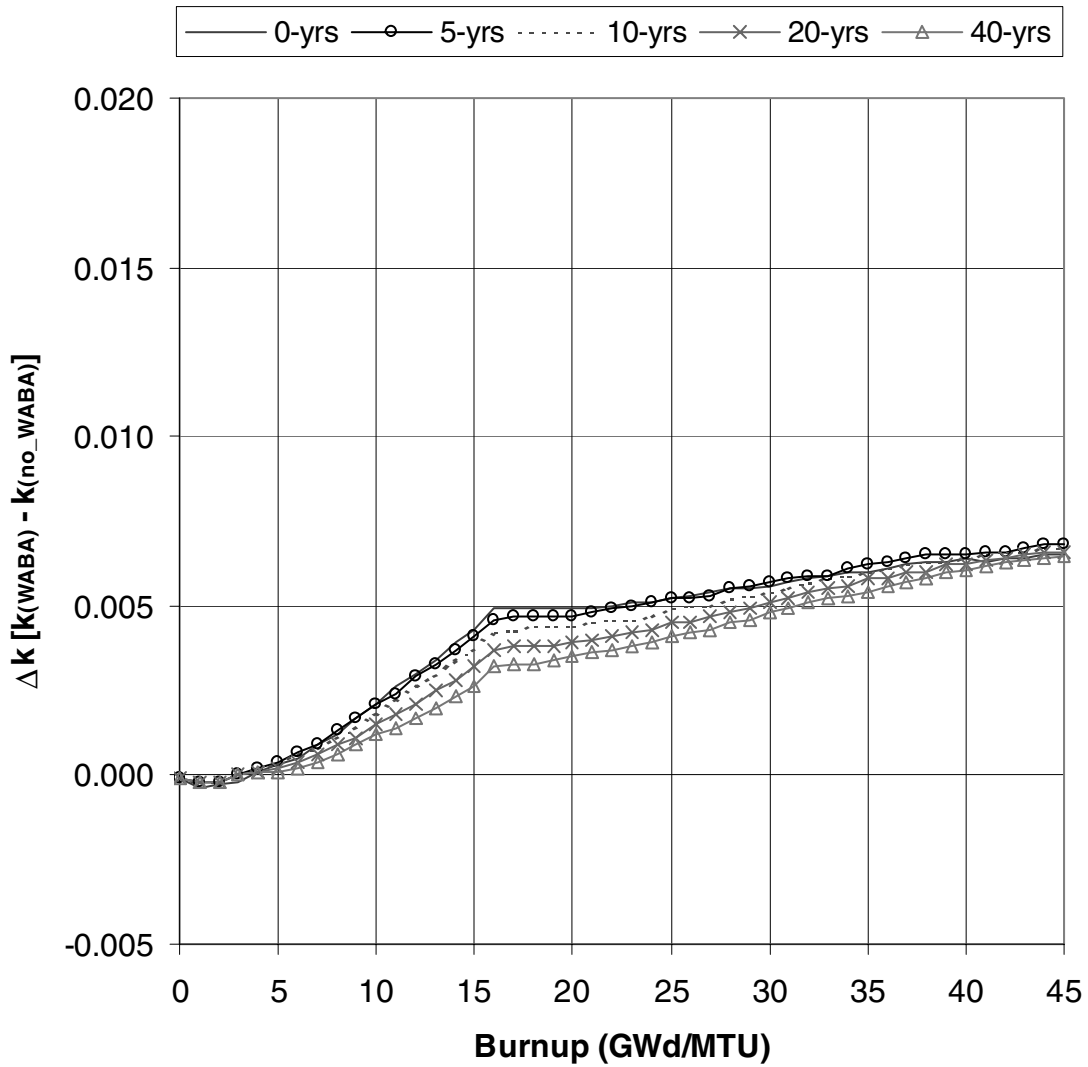


Figure 18 Δk values as a function of burnup for various cooling times with Westinghouse 17×17 fuel assemblies that have been exposed to 24 WABA rods for the first 15 GWd/MTU of burnup

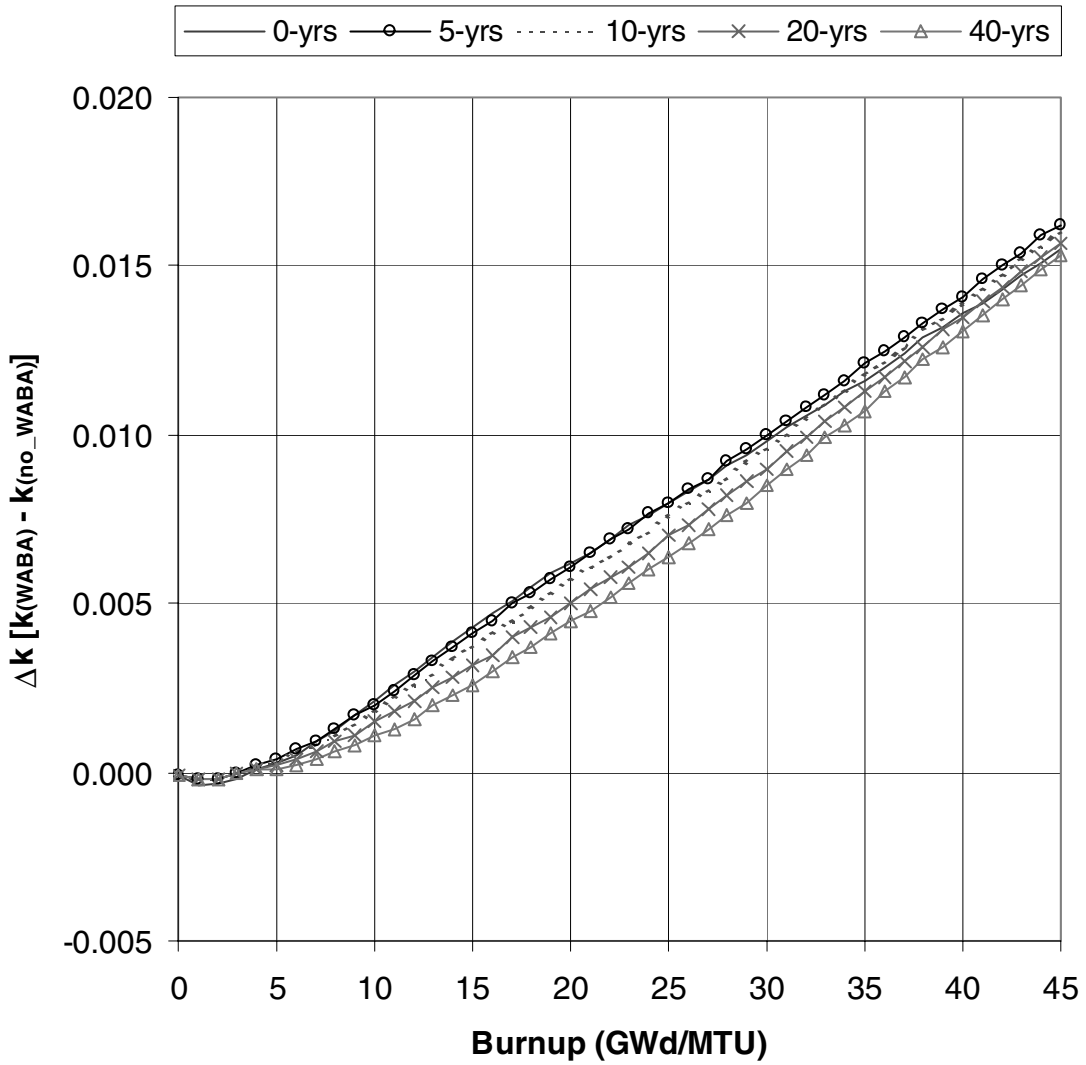


Figure 19 Δk values as a function of burnup for various cooling times with Westinghouse 17×17 fuel assemblies that have been exposed to 24 WABA rods during the entire depletion (3 cycles)

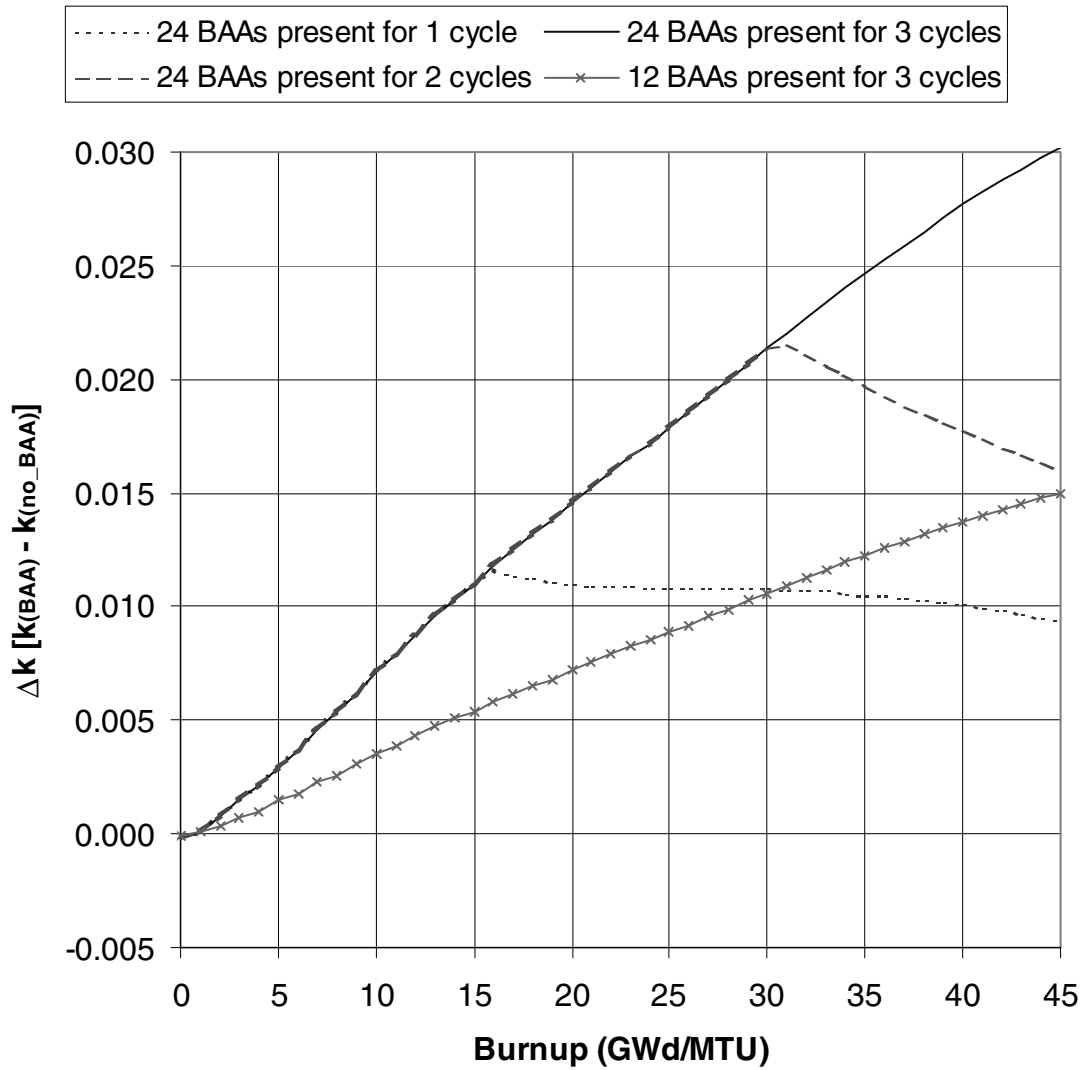


Figure 20 Δk values as a function of burnup for Westinghouse 17×17 fuel with 3.0 wt % ^{235}U initial enrichment that has been exposed to Westinghouse Pyrex BAA rods (3 cycles of 15 GWd/MTU per cycle were assumed)

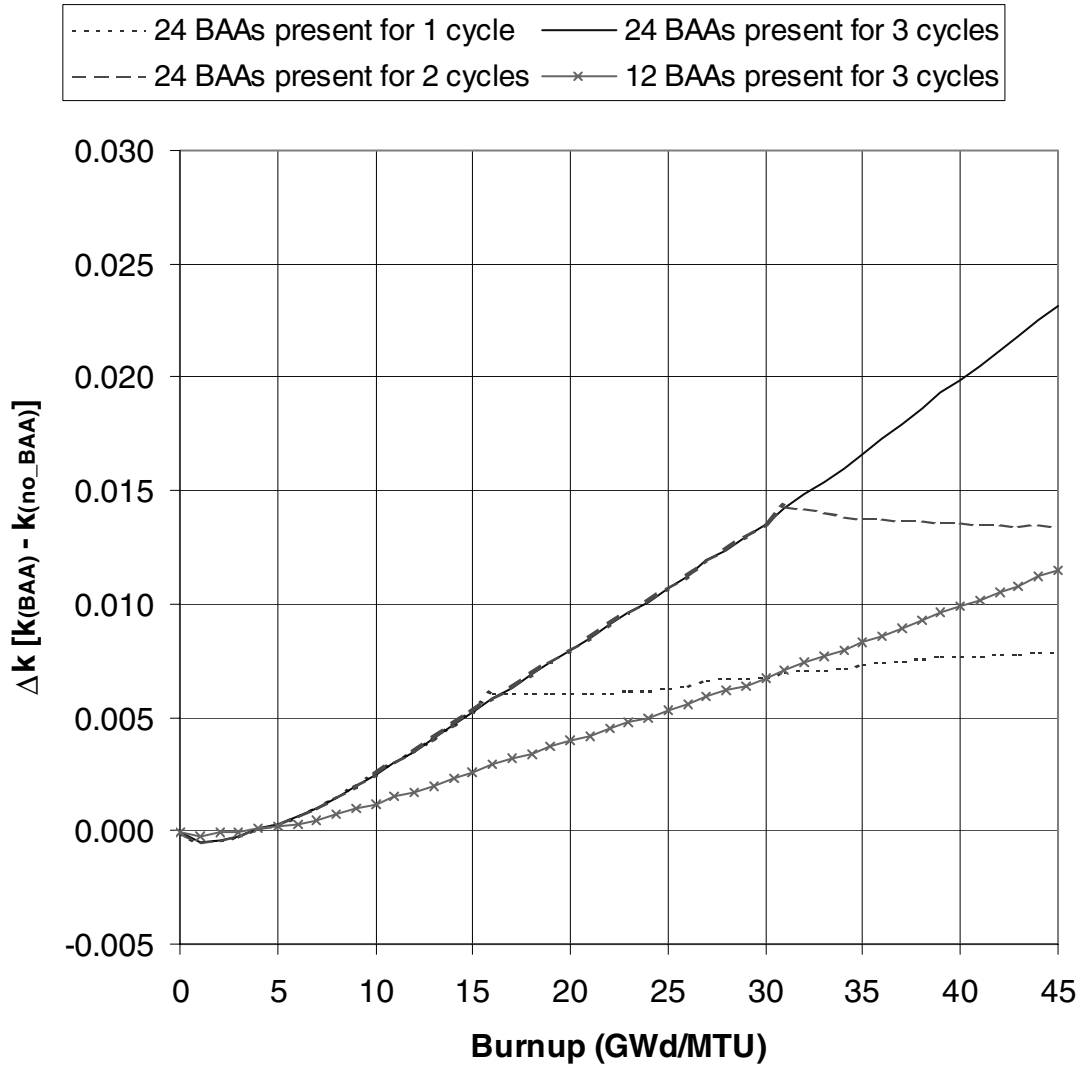


Figure 21 Δk values as a function of burnup for Westinghouse 17×17 fuel with 4.0 wt % ^{235}U initial enrichment that has been exposed to Westinghouse Pyrex BAA rods (3 cycles of 15 GWd/MTU per cycle were assumed)

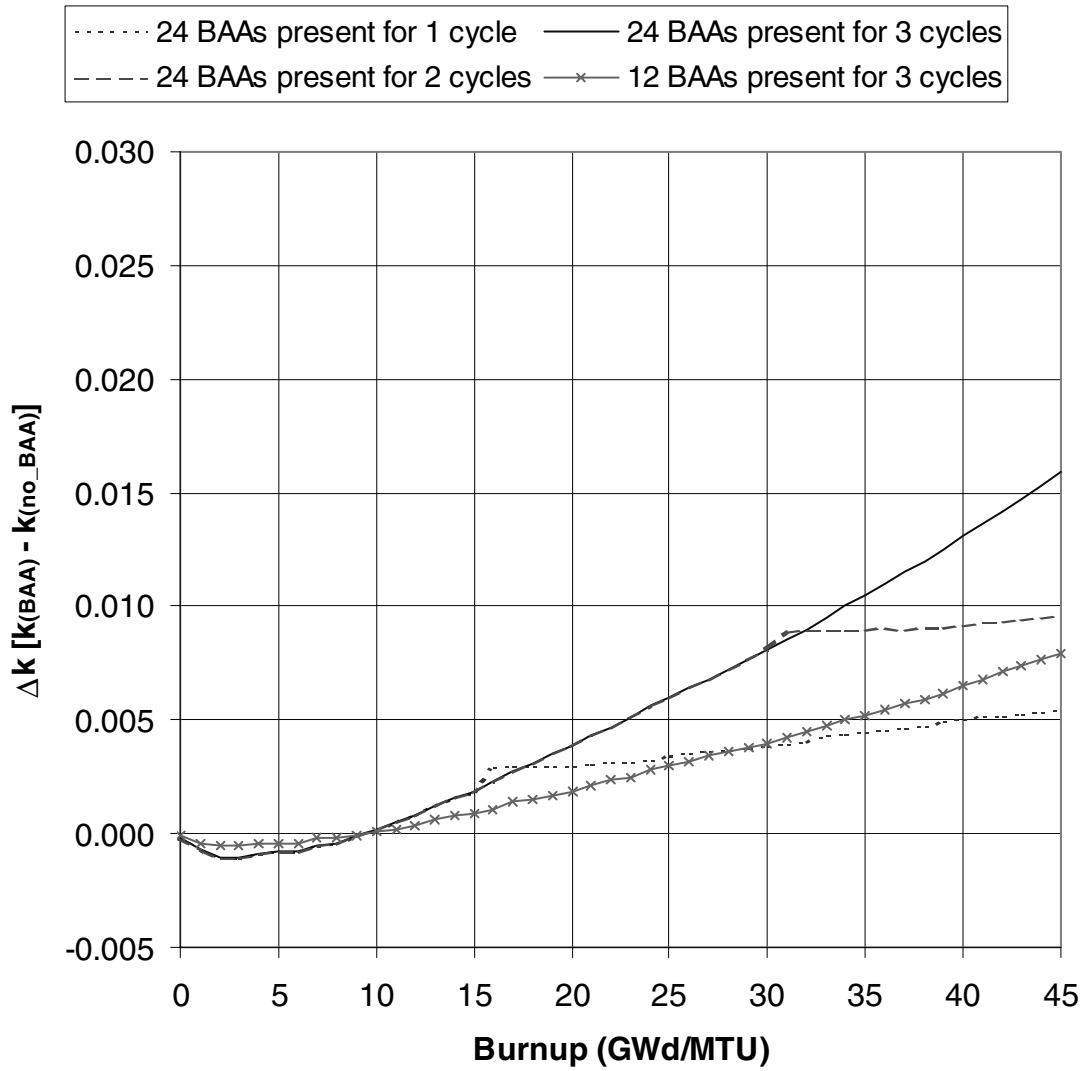


Figure 22 Δk values as a function of burnup for Westinghouse 17×17 fuel with 5.0 wt % ^{235}U initial enrichment that has been exposed to Westinghouse Pyrex BAA rods (3 cycles of 15 GWd/MTU per cycle were assumed)

The majority of results shown in Figures 20–22 correspond to the maximum possible number of BPRs (24) per BPRA, while selected results are shown for half of the maximum number (12). Based on limited Westinghouse plant operational data,^{10,11,13–15} the average number of Westinghouse BPRs in a BPRA is typically much less than the maximum possible (dictated by the number of guide tubes in the assembly). For example, review of operational data in Refs. 10, 13, and 14, shows the number BPRs per BPRA, averaged over a core, is approximately 65% of the maximum possible. In other words, for an assembly with 24 guide tubes, the average number of BPRs per BPRA, averaged over a core, is approximately 16.

5.2.2 B&W BPR Designs

For the B&W BPR designs, the number of BPRs per BPRA is fixed, and thus the calculations were performed for a fixed number of BPRs present (i.e., 16 BPRs in a 15×15 fuel assembly). Consistent with the analyses for the Westinghouse BPRs, calculations were performed assuming the BPRs were present during (1) the first cycle of irradiation, (2) the first two cycles of irradiation, and (3) the entire irradiation period (i.e., all three cycles). For comparison purposes, reference calculations were performed assuming no BPRs present and the various calculations are compared to determine the reactivity effect as a function of burnup.

The primary differences between the B&W BPR design and the Westinghouse BPR designs are that the B&W BPRs are solid, have a fixed number of BPRs per BPRA, and may have varying poison (B_4C) loading, as opposed to the Westinghouse designs which are annular, have varying numbers of BPRs per BPRA, and have fixed poison loadings. As noted in Section 2.1, actual plant data in Ref. 12 shows variations in B_4C loading from 0.0 to 2.1 wt %. Since 2.0 wt % B_4C is approximately the maximum poison loading found in available plant data, the initial parametric calculations for the B&W BPRs used 2.0 wt % B_4C for the poison loading. Figures 23–25 plot the Δk values (relative to the no BPR condition) associated with various exposures to B&W BPRs as a function of burnup for initial fuel enrichments of 3.0, 4.0, and 5.0 wt % ^{235}U , respectively. The same trends identified with the Westinghouse BPRs are also observed with the B&W BPRs; namely that the Δk values increase with increasing BPR exposure and decreasing initial fuel enrichment. The B&W BPRs with 2.0 wt % B_4C are shown to have a comparable effect to the Westinghouse WABA BPRs. For initial enrichments of 3.0, 4.0, and 5.0 wt % ^{235}U , Δk values for continuous B&W BPR exposure up to a burnup of 45 GWd/MTU are 0.0204, 0.0155, and 0.0106, respectively. When considering these (and the previous) quoted “maximum Δk values”, the reader should be mindful that they are based on calculational assumptions selected for bounding the reactivity effect (e.g., BPR exposure during all three cycles of burnup, maximum number of BPRs per BPRA in the case of Westinghouse BPRs, near maximum poison loading in the case of the B&W BPRs), not realism of operations.

5.2.2.1 Effect of Variations in the BPR Poison (B_4C) Loading

Since the B_4C weight percent is known to vary in the B&W BPRs, calculations were also performed for arbitrary variations in the B_4C poison loading from 0 to 3 wt % B_4C . Note that actual plant data¹² shows variations in B_4C loading up to 2.1 wt %, and thus 3 wt % is notably higher than any known poison loading; 3 wt % was simply chosen as an upper bound for this parametric study. Figures 26 and 27 show the reactivity differences (Δk values relative to the no BPR condition) as a function of burnup for an initial fuel enrichment of 4.0 wt % ^{235}U for one- and two-cycle exposures, respectively. The significance of the moderator displacement is apparent in the case with 0 wt % B_4C , in which case the BPR is composed of Al_2O_3 . Note that the one-cycle results shown in Figure 26 are expected to be more representative of actual plant operations than the two-cycle result in Figure 27. The reactivity effect increases linearly with the poison loading, as is more clearly shown in Figure 28, which plots the Δk values at 45 GWd/MTU as a function of poison loading.

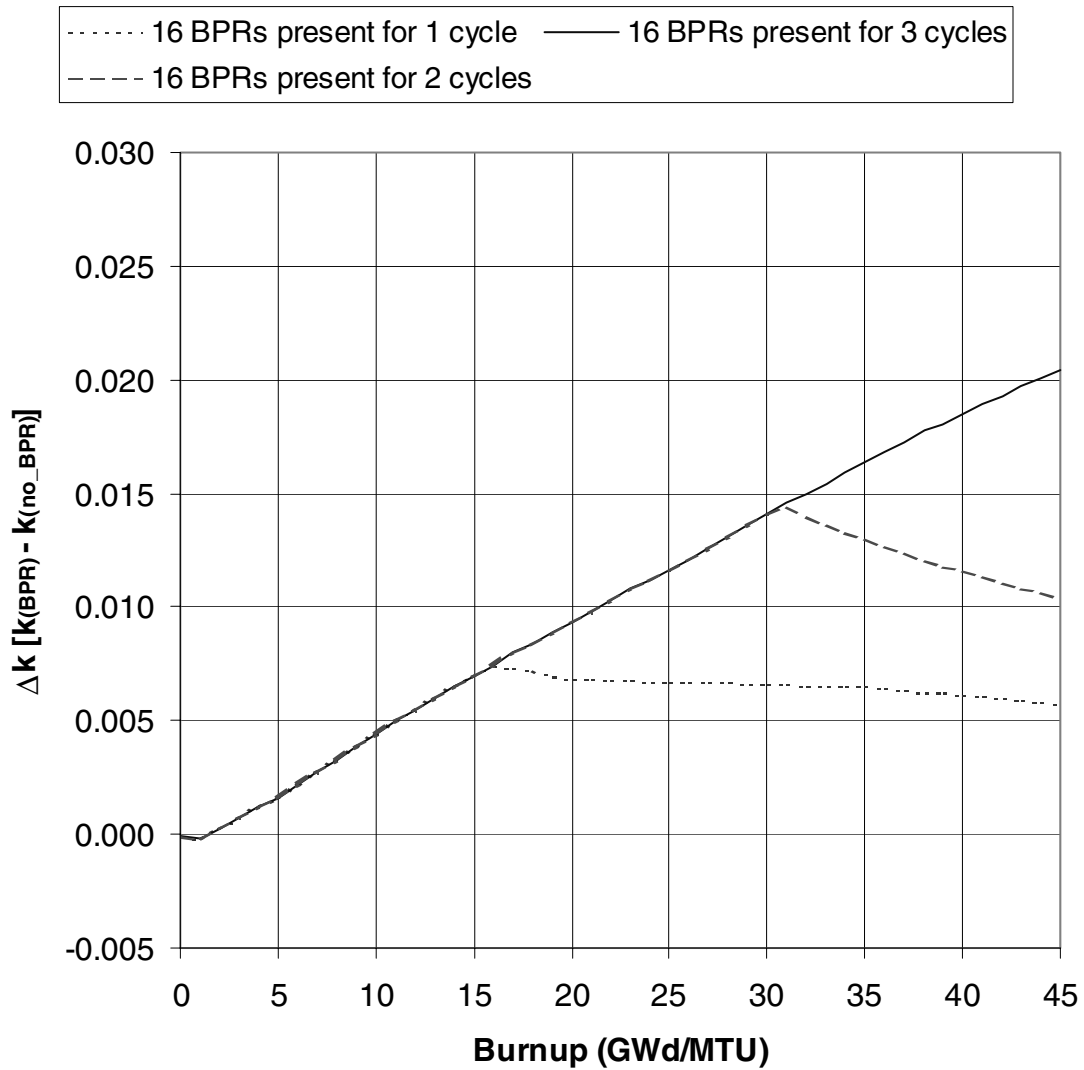


Figure 23 Δk values as a function of burnup for B&W 15×15 fuel with 3.0 wt % ^{235}U initial enrichment that has been exposed to B&W (2.0 wt % B_4C) BPRs (3 cycles of 15 GWd/MTU per cycle were assumed)

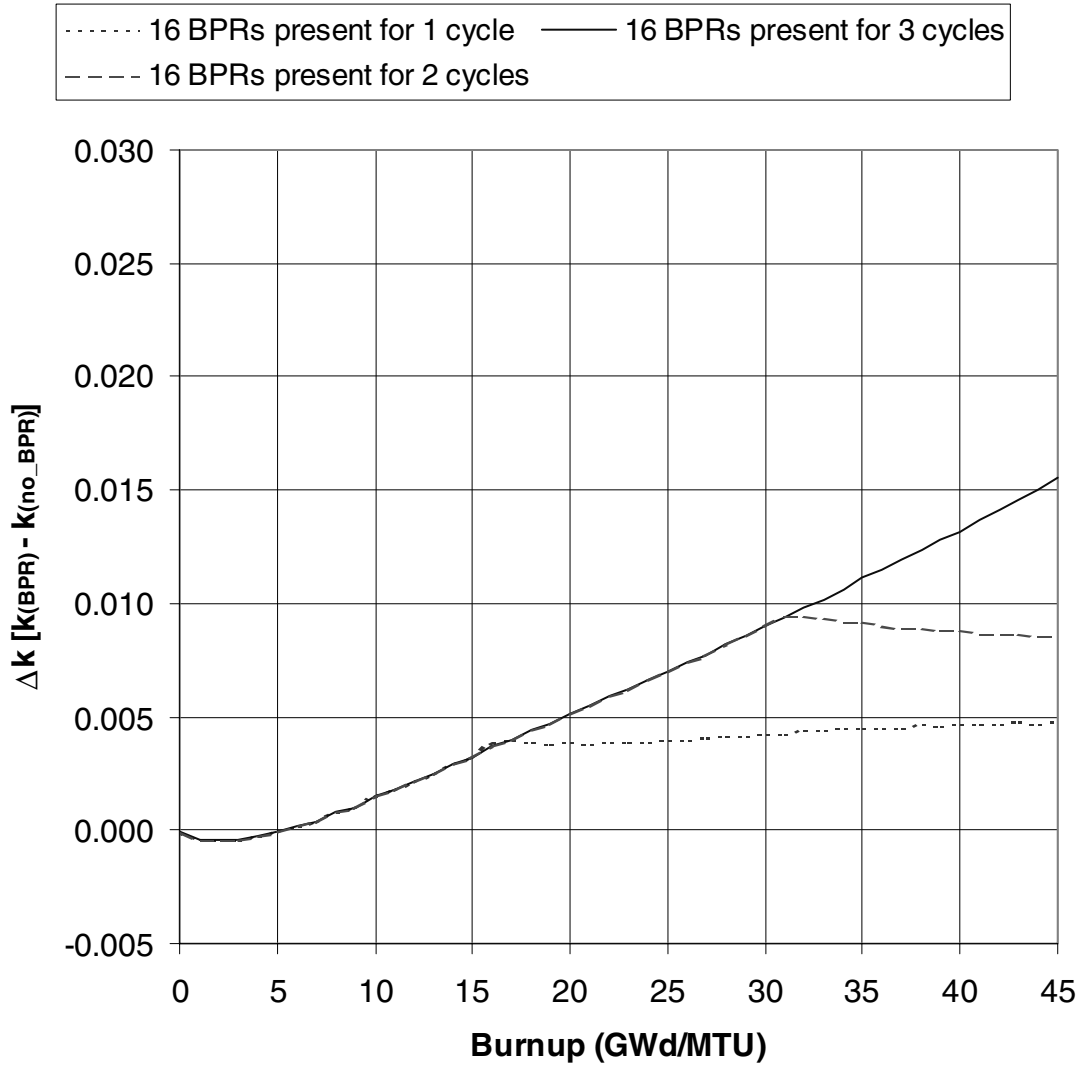


Figure 24 Δk values as a function of burnup for B&W 15×15 fuel with 4.0 wt % ^{235}U initial enrichment that has been exposed to B&W (2.0 wt % B_4C) BPRs (3 cycles of 15 GWd/MTU per cycle were assumed)

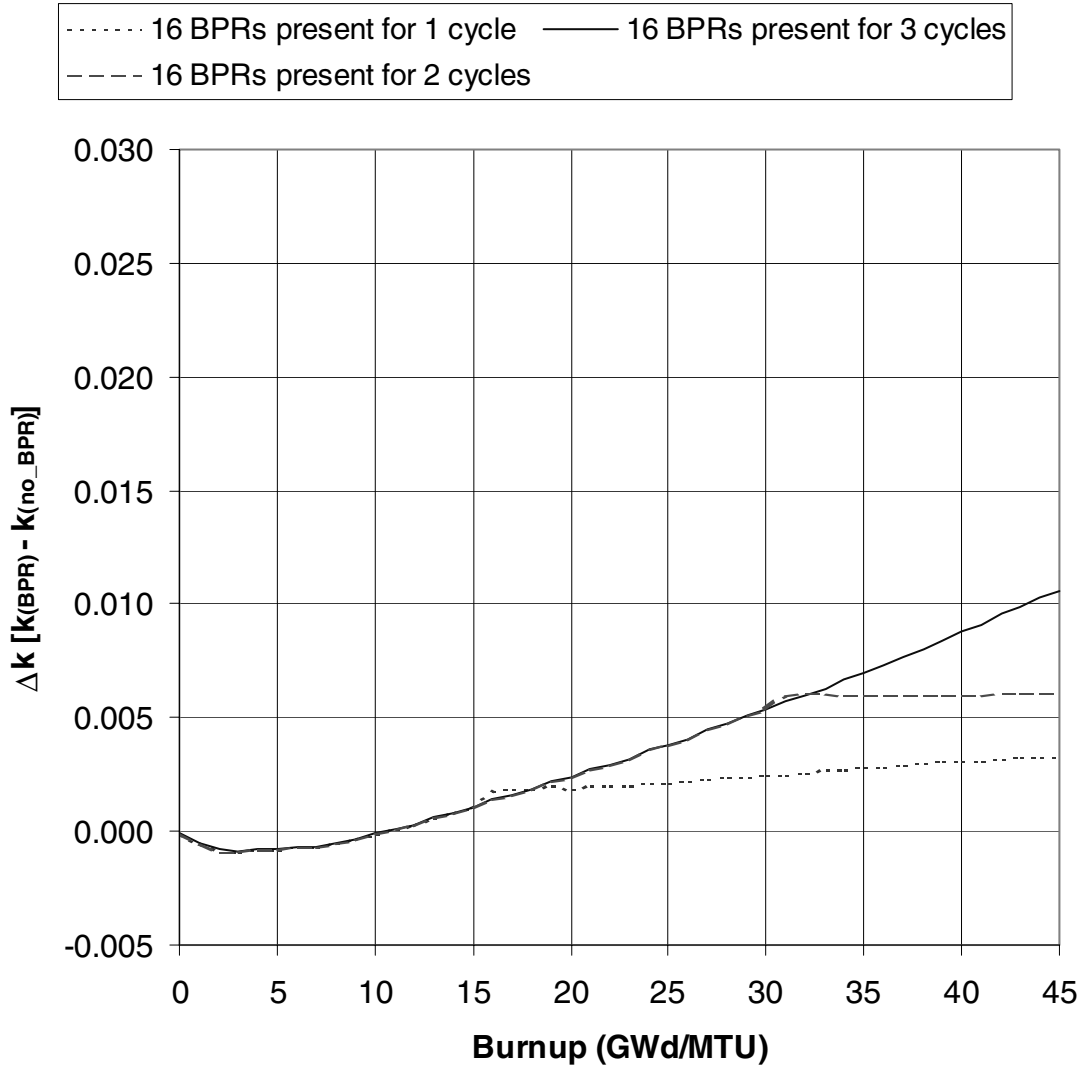


Figure 25 Δk values as a function of burnup for B&W 15×15 fuel with 5.0 wt % ^{235}U initial enrichment that has been exposed to B&W (2.0 wt % B_4C) BPRs (3 cycles of 15 GWd/MTU per cycle were assumed)

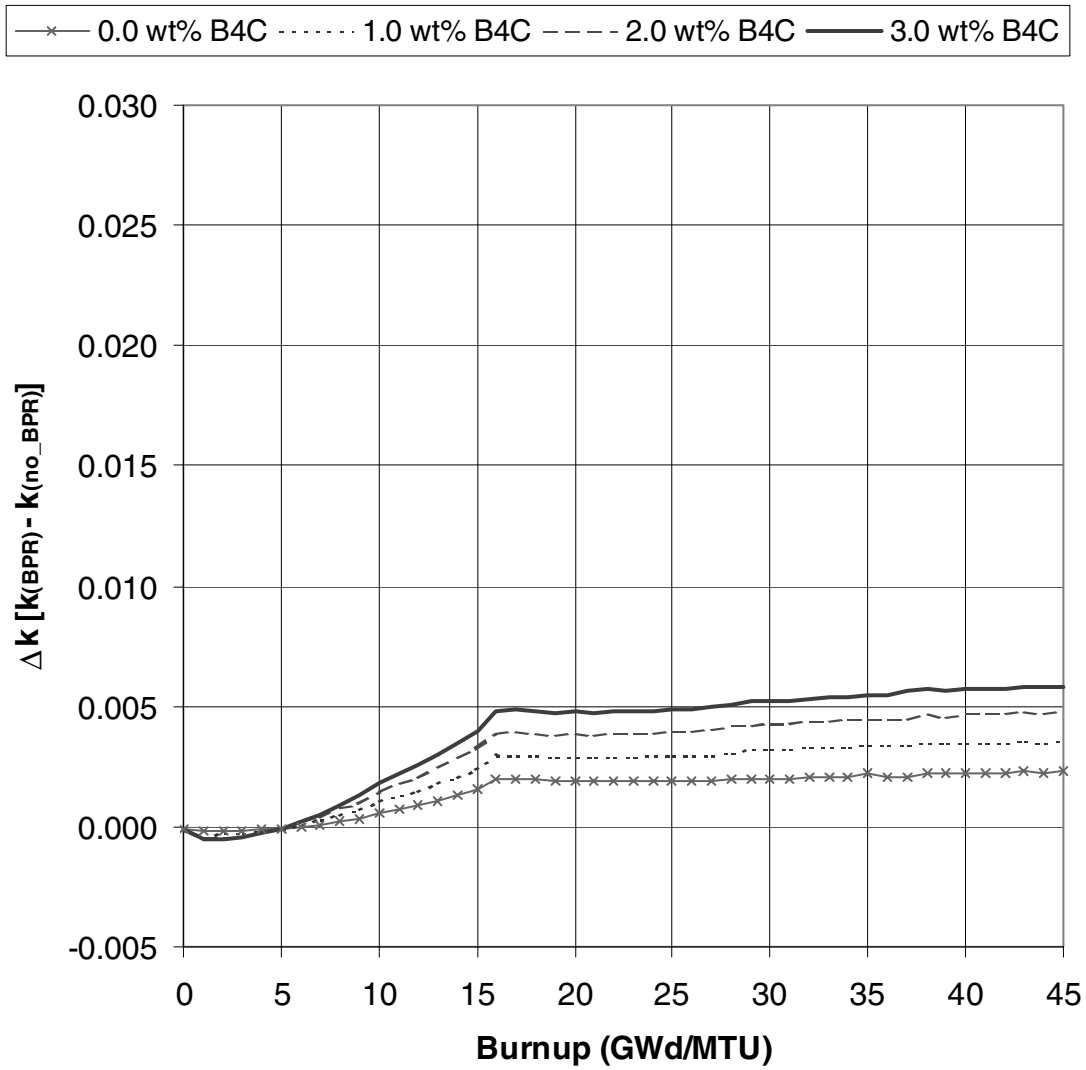


Figure 26 Δk values as a function of burnup for B&W 15×15 fuel with 4.0 wt % ^{235}U initial enrichment that has been exposed to B&W BPRs with varying B_4C weight percents for the first 15 GWd/MTU of burnup (3 cycles of 15 GWd/MTU per cycle were assumed)

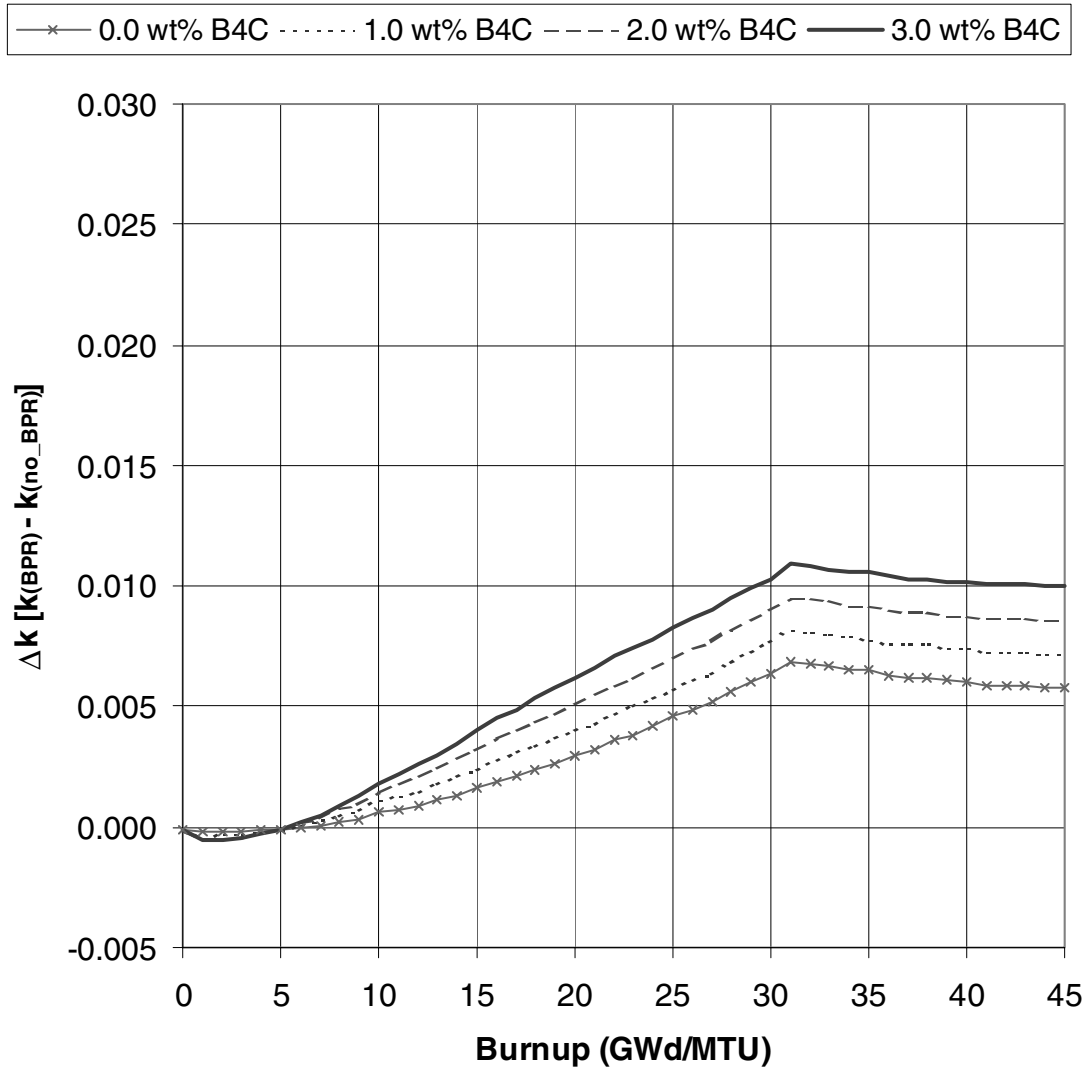


Figure 27 Δk values as a function of burnup for B&W 15×15 fuel with 4.0 wt % ^{235}U initial enrichment that has been exposed to B&W BPRs with varying B_4C weight percents for the first 30 GWd/MTU of burnup (3 cycles of 15 GWd/MTU per cycle were assumed)

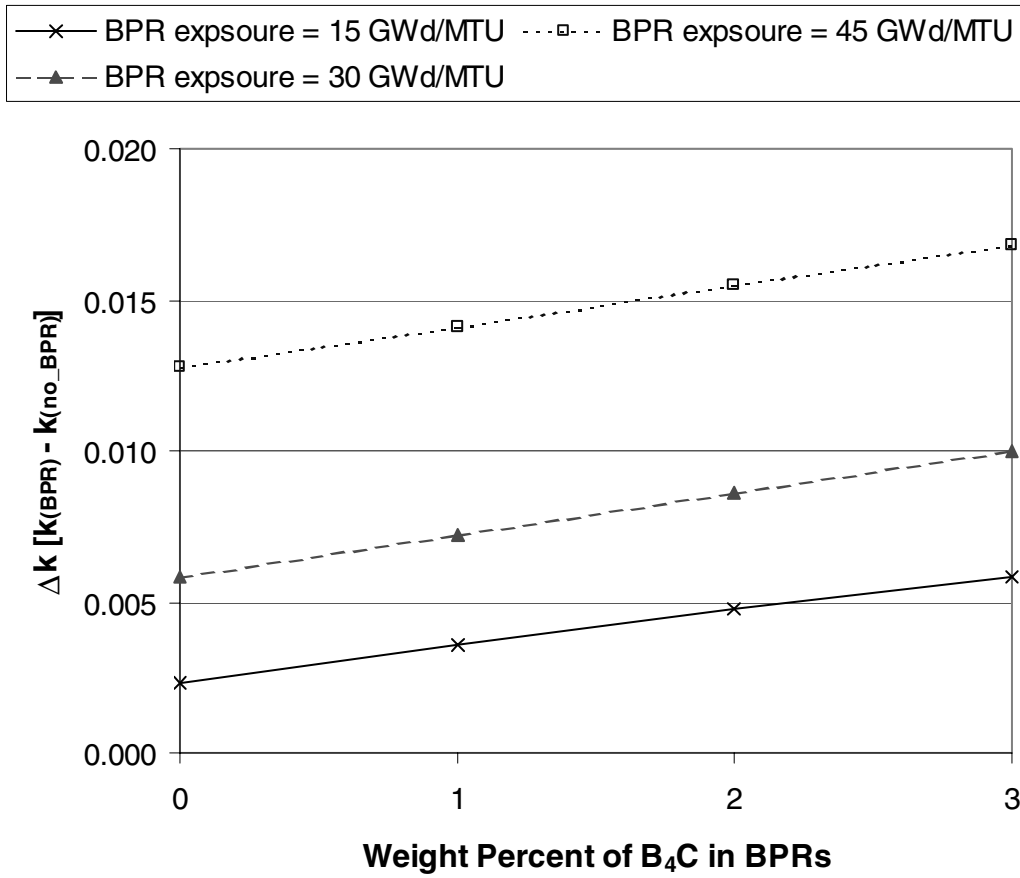


Figure 28 Δk values for B&W 15×15 fuel with 4.0 wt % ^{235}U initial enrichment and a total burnup of 45 GWd/MTU that has been exposed to BPRs with varying poison loading and burnup exposures

5.3 INFINITE PIN-CELL CALCULATIONS WITH SAS2H-CSAS1X

The calculations presented and discussed in this section correspond to infinite arrays of spent fuel rods from a Westinghouse 17×17 OFA assembly design. The actual criticality calculational model is a 1-D fuel pin-cell in out-of-reactor conditions (i.e., unborated water at 20°C). Consistent with the majority of the HELIOS calculations described in the previous section, the calculations presented in this section all correspond to zero cooling. The criticality calculations were performed with the CSAS1X sequence of SCALE, which uses the XSDRNPM 1-D discrete ordinates code.⁵ The calculational details are provided in Section 4. Isotopics for each burnup of interest were extracted from SAS2H output for use in CSAS1X calculations.

In the evolution of this study, the parametric studies were originally performed with the SAS2H-depletion and CSAS-criticality sequences of the SCALE code package,⁵ and HELIOS was employed to assess the adequacy of the SAS2H modeling for assemblies with BPRs present. The SCALE depletion (SAS2H) and criticality (CSAS) sequences have been extensively used and validated in studies of the burnup credit phenomenon. The SAS2H-CSAS1X results presented in this section chronologically precede the HELIOS results discussed in the previous section. However, once the effort of HELIOS model development was expended, it became simpler to perform many of the analysis variations (that were discussed in the previous section) with HELIOS. The SAS2H-depletion and CSAS-criticality results are included in this section with and without fission products present to investigate the reactivity effect of BPRs within the limitations of actinide-only burnup credit. Also, depletion results from HELIOS and SAS2H are compared to assess the agreement in results from independent codes/methods and cross-section libraries.

For each BPR design considered, spent fuel isotopics were calculated assuming the maximum possible number of BPRs present. In addition, for the Westinghouse BPR designs, isotopics were calculated assuming one half of the maximum number of BPRs present. For both cases, depletion calculations were performed assuming the BPRs were present during (1) the first cycle of irradiation, (2) the first two cycles of irradiation, and (3) the entire irradiation period (i.e., all three cycles). For the purpose of the depletion calculations, 3 cycles of 15 GWd/MTU per cycle were assumed. For comparison purposes, isotopics were also calculated assuming no BPRs present. These four sets of isotopics were then used in individual CSAS1X calculations to determine the reactivity effect of each BPR design as a function of burnup.

The reactivity differences (Δk values relative to the no BPR condition) as a function of burnup for various WABA exposures with and without fission products present are shown in Figures 29 and 30, respectively. The k_{inf} values were calculated for out-of-reactor conditions at burnup steps of 1 GWd/MTU and zero cooling time. The isotopics used in the criticality calculations correspond to spent fuel with 4.0 wt % ^{235}U initial enrichment that has been exposed to Westinghouse WABA rods during depletion. These figures confirm the reactivity behavior shown in the previous section with HELIOS. In addition, comparison of the two figures shows that the reactivity behavior with fission products present is very similar to that shown for the actinide-only condition. Note, however, the initial (low burnup) negative reactivity effect associated with the presence of fission products in Figure 29. This behavior is consistent with the HELIOS results shown in the previous section and can be attributed to an initial increased buildup of a few fission products (primarily ^{149}Sm) in the cases with BPRs present, as compared to the cases without BPRs present. The negative reactivity associated with the increased buildup of a few of the fission products is partially offset by the increased concentrations of fissile actinides, and thus increases with increasing initial ^{235}U enrichment. This behavior is more clearly shown in Figure 10.

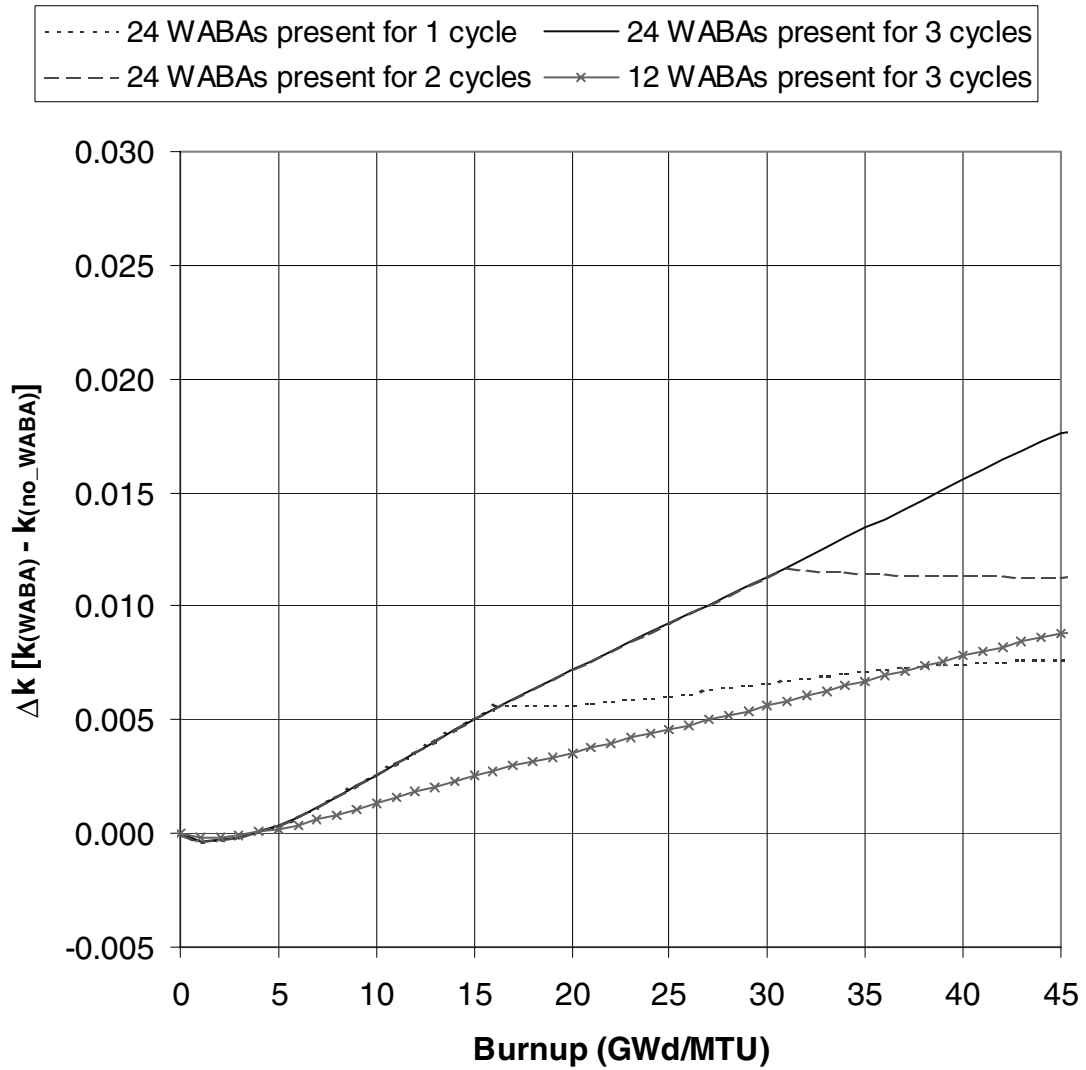


Figure 29 Δk values as a function of burnup for Westinghouse 17×17 fuel with 4.0 wt % ^{235}U initial enrichment that has been exposed to Westinghouse WABA rods (3 cycles of 15 GWd/MTU per cycle were assumed). The results are based on SAS2H-depletion and CSAS1X-criticality calculations with “actinide + fission product” nuclides (See Table 8 for specific nuclides).

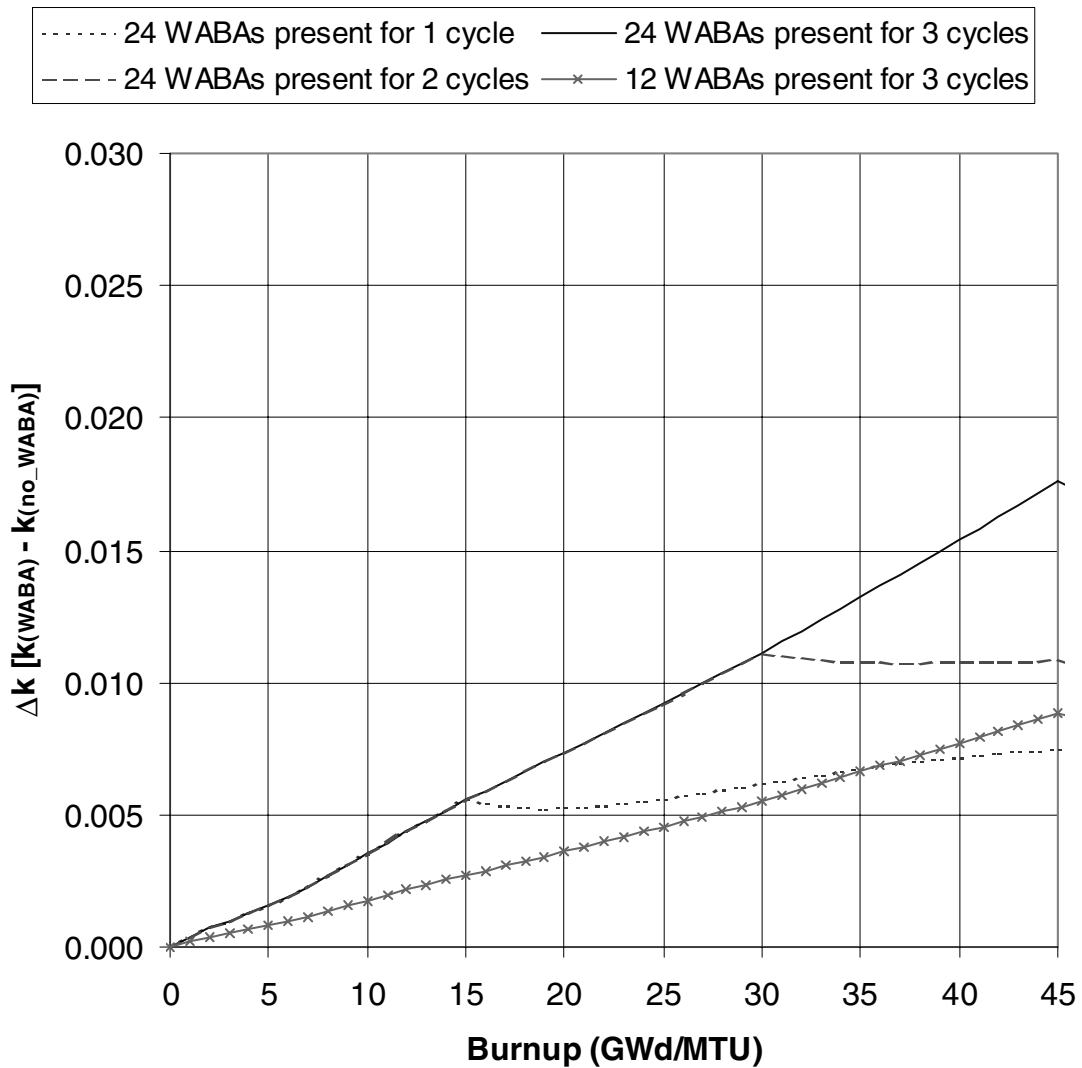


Figure 30 Δk values as a function of burnup for Westinghouse 17×17 fuel with 4.0 wt % ^{235}U initial enrichment that has been exposed to Westinghouse WABA rods (3 cycles of 15 GWd/MTU per cycle were assumed). The results are based on SAS2H-depletion and CSAS1X-criticality calculations with “actinide-only” nuclides (See Table 8 for specific nuclides).

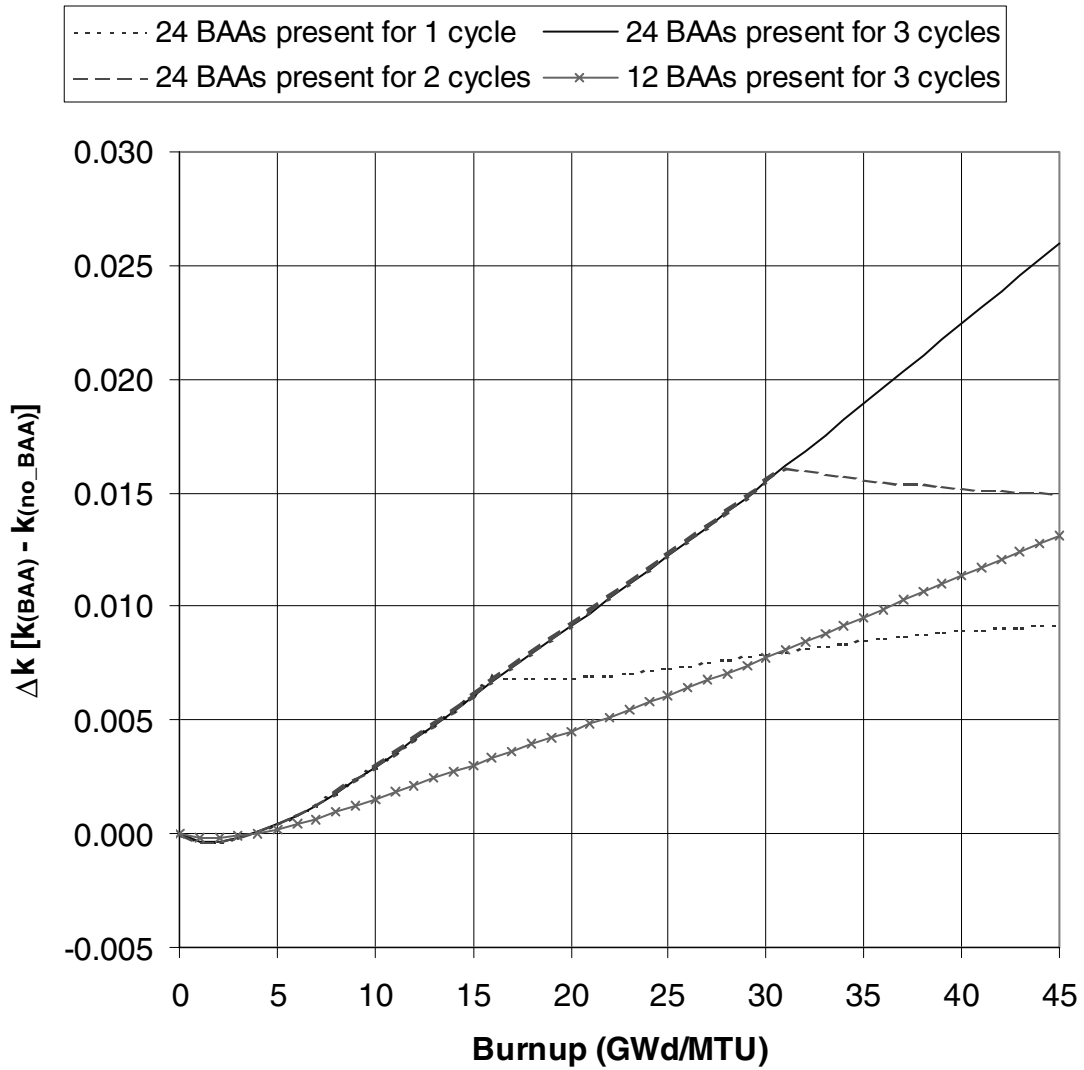


Figure 31 Δk values as a function of burnup for Westinghouse 17×17 fuel with 4.0 wt % ^{235}U initial enrichment that has been exposed to Westinghouse BAA rods (3 cycles of 15 GWd/MTU per cycle were assumed). The results are based on SAS2H-depletion and CSAS1X-criticality calculations with “actinide + fission product” nuclides (See Table 8 for specific nuclides).

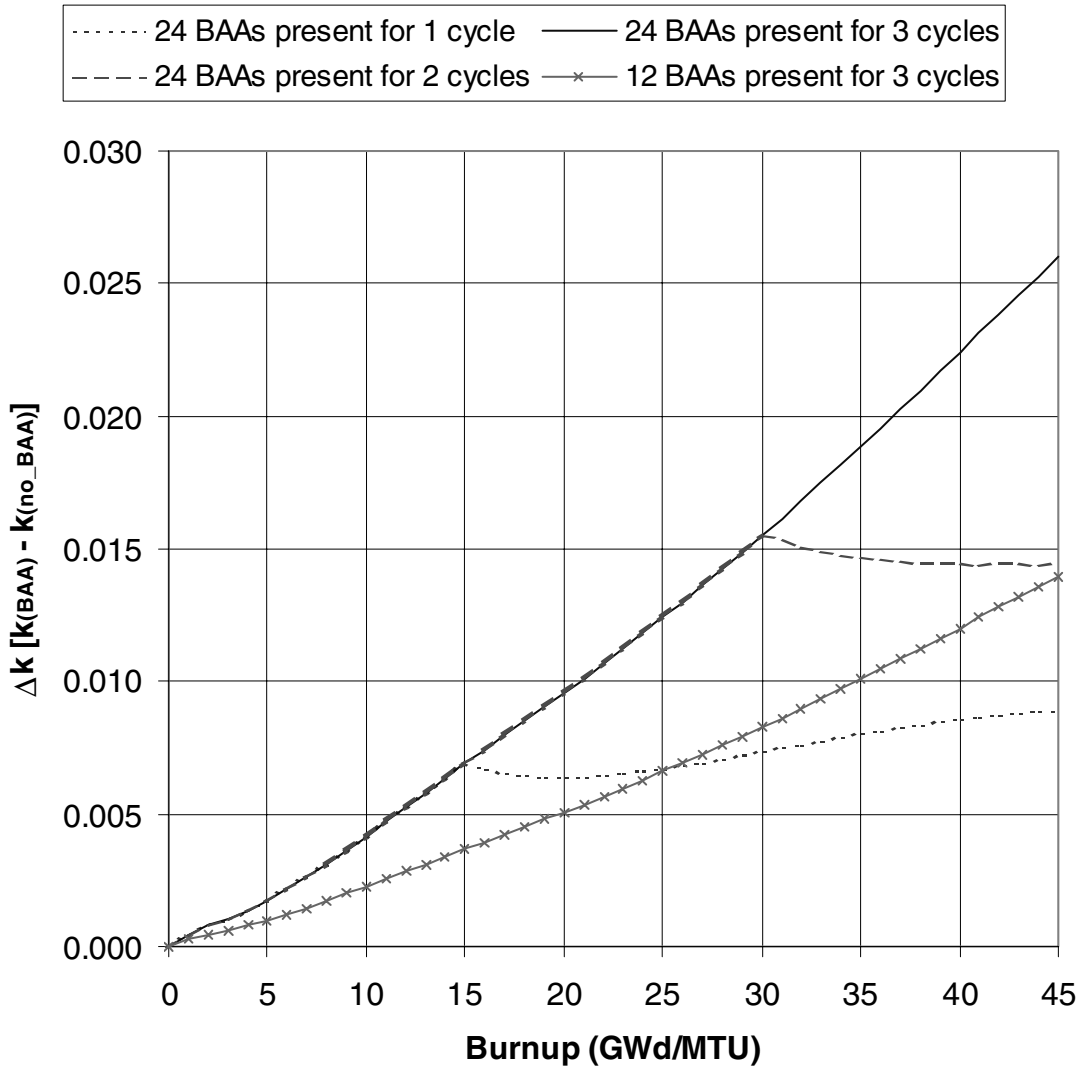


Figure 32 Δk values as a function of burnup for Westinghouse 17×17 fuel with 4.0 wt % ^{235}U initial enrichment that has been exposed to Westinghouse BAA rods (3 cycles of 15 GWd/MTU per cycle were assumed). The results are based on SAS2H-depletion and CSAS1X-criticality calculations with “actinide-only” nuclides (See Table 8 for specific nuclides).

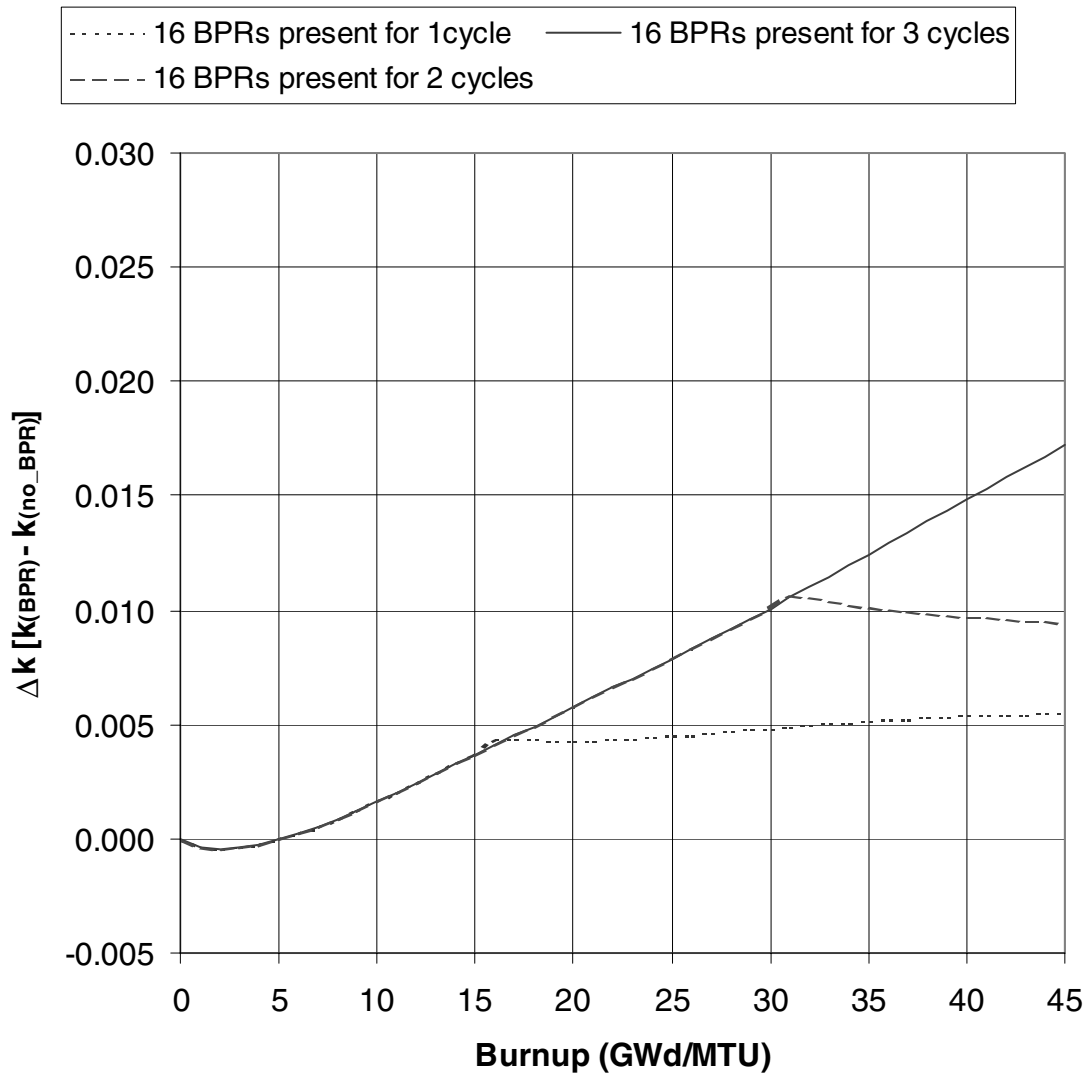


Figure 33 Δk values as a function of burnup for B&W 15×15 fuel with 4.0 wt % ^{235}U initial enrichment that has been exposed to B&W (2.0 wt % B_4C) BPRs (3 cycles of 15 GWd/MTU per cycle were assumed). The results are based on SAS2H-depletion and CSAS1X-criticality calculations with “actinide + fission product” nuclides (See Table 8 for specific nuclides).

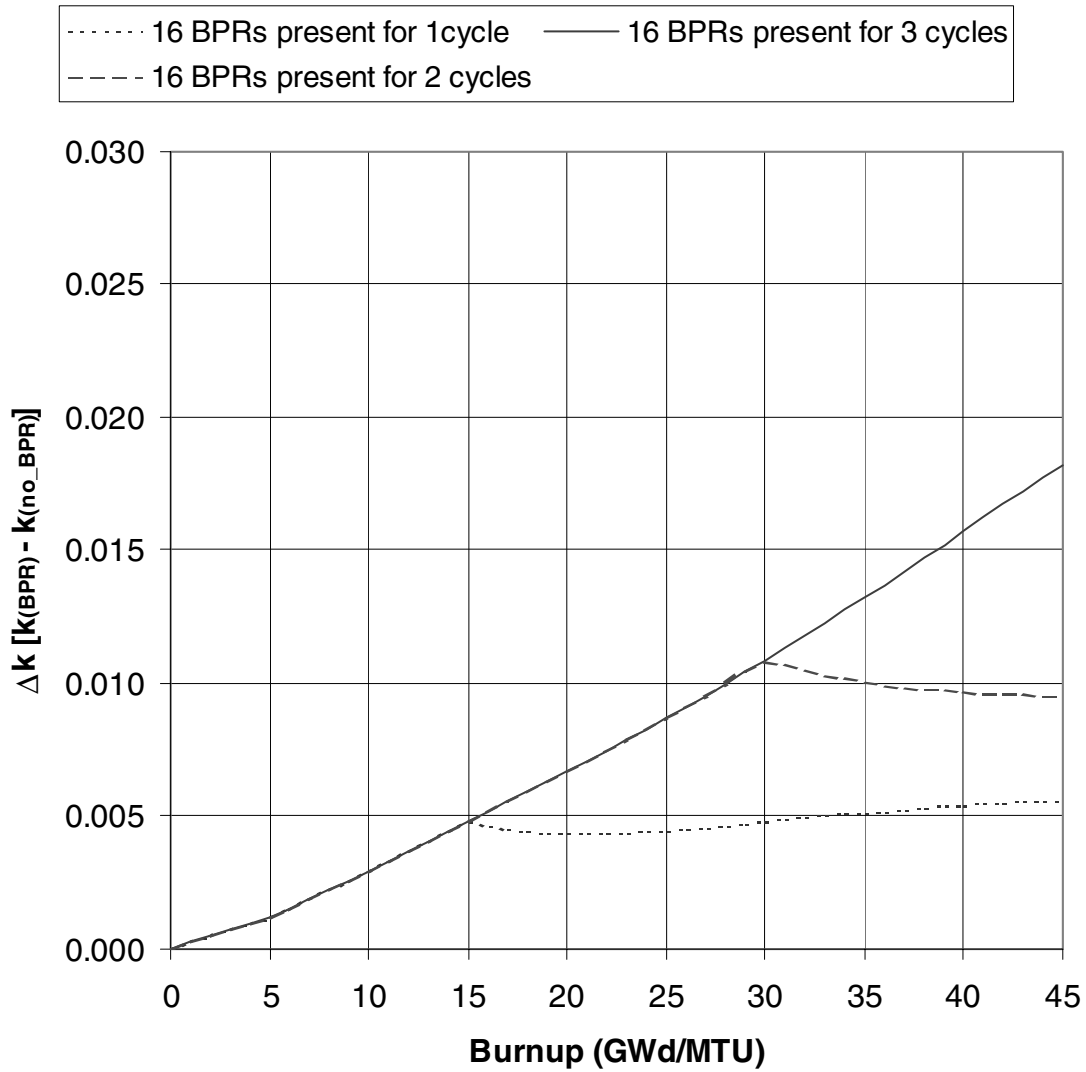


Figure 34 Δk values as a function of burnup for B&W 15×15 fuel with 4.0 wt % ^{235}U initial enrichment that has been exposed to B&W (2.0 wt % B_4C) BPRs (3 cycles of 15 GWd/MTU per cycle were assumed). The results are based on SAS2H-depletion and CSAS1X-criticality calculations with “actinide-only” nuclides (See Table 8 for specific nuclides).

For comparison of the effect of the various BPR designs, Figures 31–34 show the reactivity differences as a function of burnup for the Westinghouse BAA rods and the B&W BPR rods. For the B&W BPRs, the poison loading was assumed to be 2.0 wt % B₄C. In all cases, the 1-D SAS2H-CSAS1X Δk results show the same trends as those shown in the previous section with HELIOS. Also, note that the 1-D SAS2H-CSAS1X calculations predict slightly larger Δk values for all of the BPR designs, as compared to the 2-D HELIOS calculations.

5.3.1 Comparison of SAS2H and HELIOS Results

The SCALE depletion sequence, SAS2H, has been extensively used (e.g., Refs. 17, 18, 20–22) and validated (e.g., Refs. 23–25) in studies of the burnup credit phenomenon. Nevertheless, the HELIOS code was selected as the primary depletion tool for this analysis because of its capability to explicitly model the relatively complicated, heterogeneous assembly lattices associated with the fixed absorbers. Consequently, it is desirable to compare results from these two codes. As validation of isotopic predictions for assemblies with fixed absorbers is hindered by a paucity of applicable measured isotopic data, results of HELIOS and SAS2H calculations were compared for a selected number of cases. Although a code-to-code comparison lacks the rigor of a direct comparison to measured SNF data, such a comparison does enable an assessment of the relative behavior of the two codes.

A SAS2H fuel assembly model is limited to a 1-D radial model with a single smeared fuel region. Geometric modeling approximations are made in an effort to achieve a reasonable assembly-averaged neutron energy spectrum during the depletion process. The presence of BPRs challenges the SAS2H modeling capabilities. Therefore, for a select number of cases, isotopics were compared to those calculated with the HELIOS code to assess the agreement. Note, however, that the two codes are using different cross-section data (ENDF/B-V for SAS2H, ENDF/B-IV for HELIOS), and thus any observed differences would not be solely due to modeling differences.

To enable a consistent comparison of the depletion isotopics on reactivity, isotopics were extracted from HELIOS output for use in CSAS1X criticality calculations. The nuclide subsets used in the HELIOS-CSAS1X calculations are defined in Table 8 and are consistent with those used in the SAS2H-CSAS1X calculations. All isotopic compositions in these comparisons correspond to zero cooling time. The results of the HELIOS-CSAS1X calculations are compared to the SAS2H-CSAS1X results to gain insight into the impact of the differences in calculated isotopics on reactivity. Figure 35 compares the Δk values (relative to the no BPR condition) as a function of burnup based on isotopic compositions calculated by SAS2H and HELIOS. The results correspond to fuel with 4.0 wt % ²³⁵U initial enrichment that has been exposed to either 12 or 24 Westinghouse WABA rods while accumulating a burnup of 45 GWd/MTU.

Figure 35 shows that the differences in the Δk values increase with BPR exposure (up to 0.0025 Δk), with isotopic compositions from SAS2H resulting in larger Δk values. Despite the fact that the two depletion codes use different cross sections (ENDF/B-V for SAS2H, ENDF/B-VI for HELIOS) to calculate the isotopic compositions, good agreement is shown for the calculated Δk values. Further, good agreement between calculated k_{inf} values based on isotopics from SAS2H and HELIOS was achieved.

Figures 36 and 37 compare the reactivity differences (Δk values) based on isotopic compositions from SAS2H and HELIOS depletion calculations for the Westinghouse BAA BPRs and B&W BPRs, respectively. The SAS2H and HELIOS isotopics are generally yielding good agreement in terms of the Δk values, with the isotopic compositions from SAS2H resulting in larger Δk values than those from HELIOS.

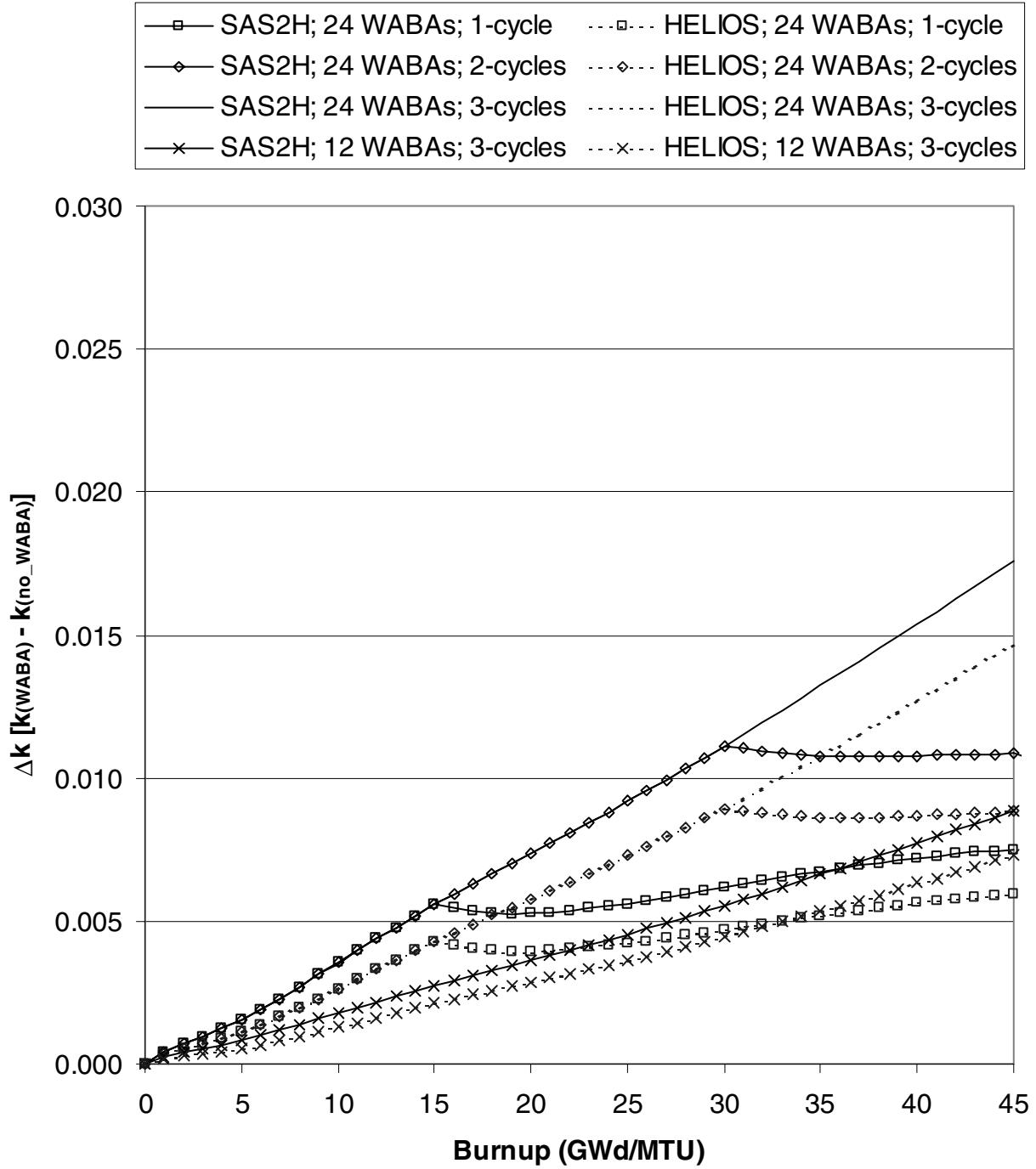


Figure 35 Comparison of reactivity differences (Δk values relative to the no BPR condition) as calculated with CSAS1X based on isotopics calculated with SAS2H and HELIOS for actinide-only burnup credit. The results correspond to fuel with 4.0 wt % ^{235}U initial enrichment that has been exposed to either 12 or 24 WABAs.

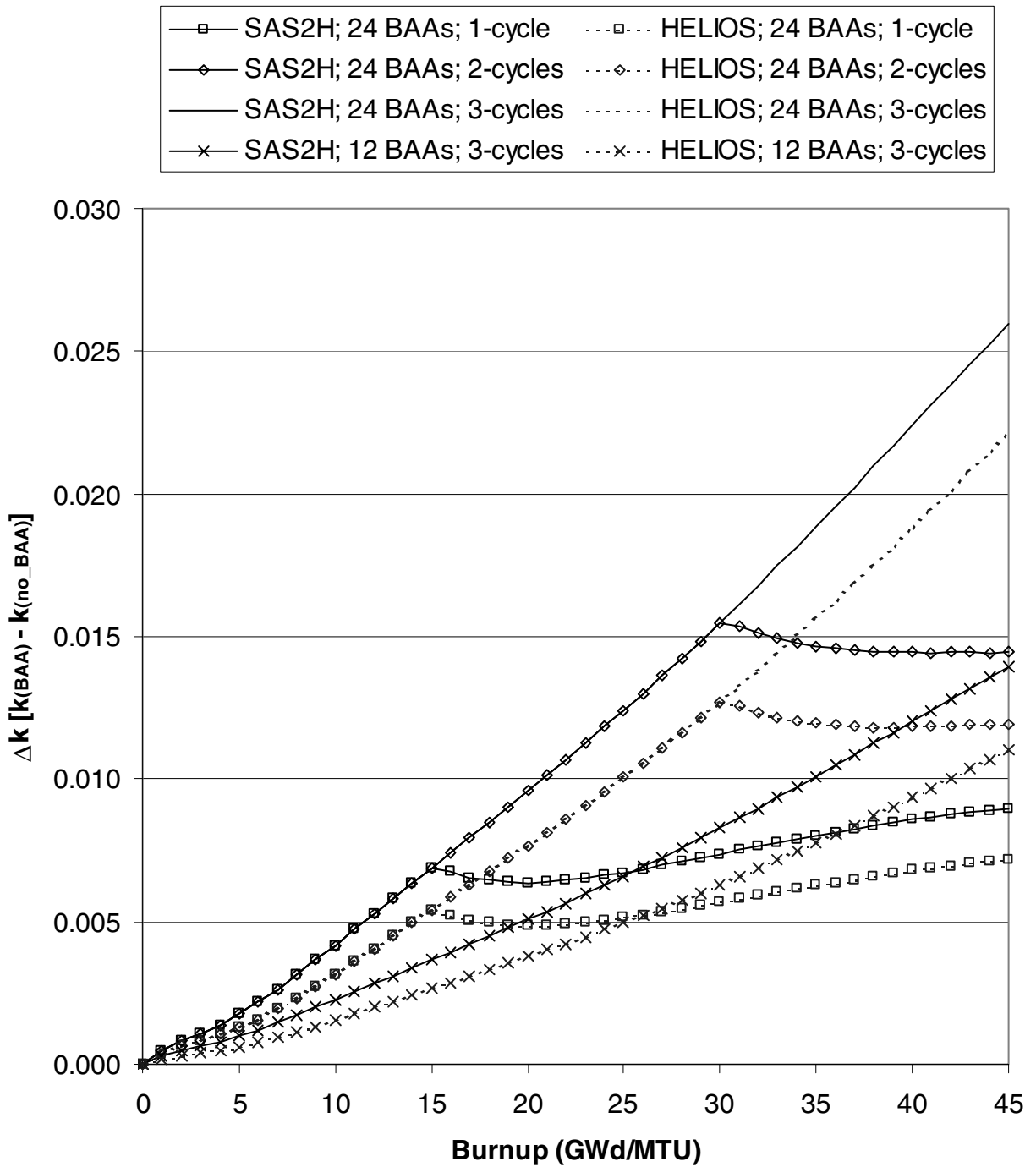


Figure 36 Comparison of reactivity differences (Δk values relative to the no BPR condition) as calculated with CSAS1X based on isotopics calculated with SAS2H and HELIOS for actinide-only burnup credit. The results correspond to fuel with 4.0 wt % ^{235}U initial enrichment that has been exposed to either 12 or 24 BAAs.

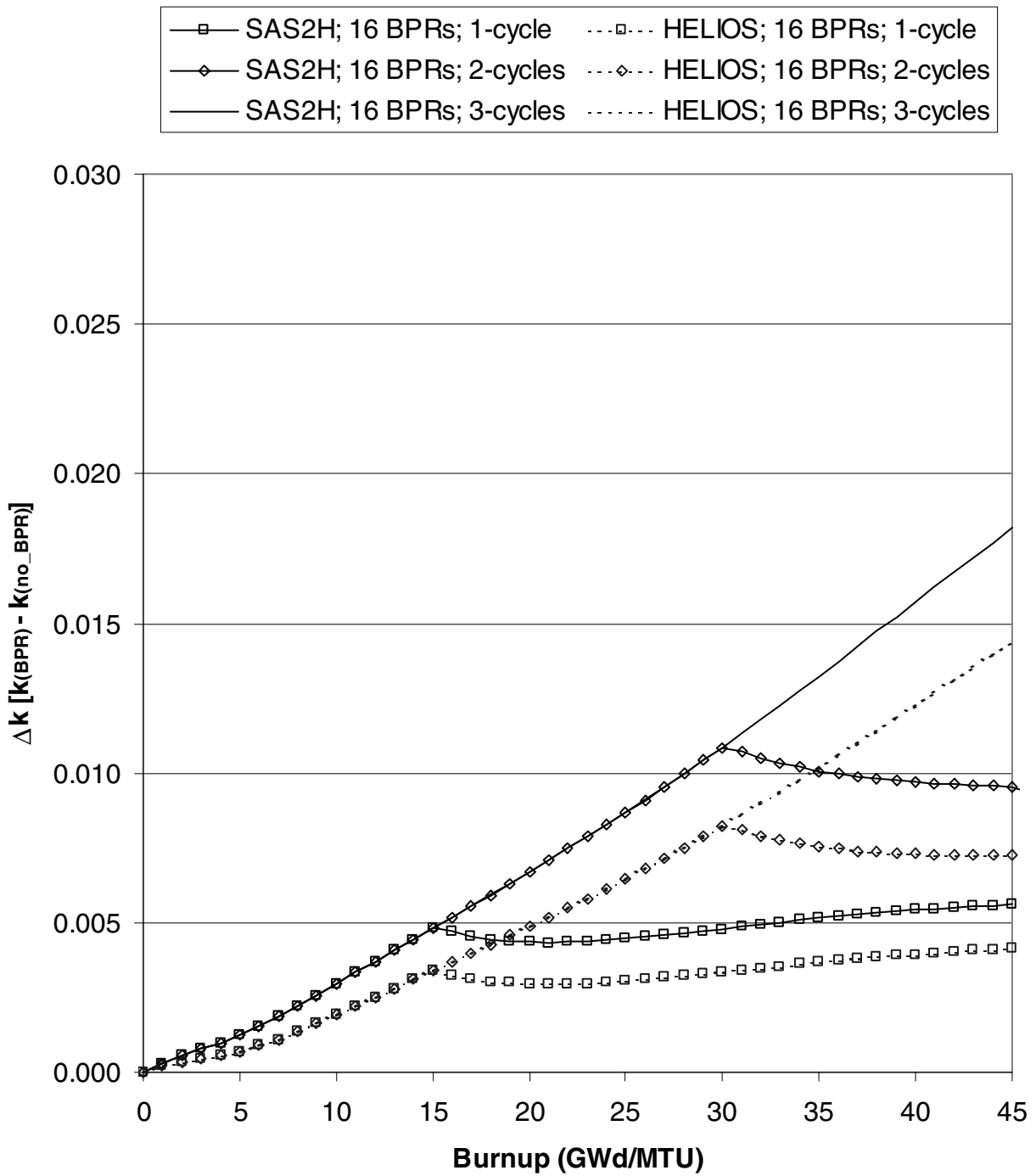


Figure 37 Comparison of reactivity differences (Δk values relative to the no BPR condition) as calculated with CSAS1X based on isotopics calculated with SAS2H and HELIOS for actinide-only burnup credit. The results correspond to B&W 15×15 fuel with 4.0 wt % ^{235}U initial enrichment that has been exposed to 16 B&W BPRs.

5.4 BURNUP CREDIT CASK CALCULATIONS

The results in the previous sections provide a basic understanding of the effect of BPR exposure on the reactivity of SNF for a number of relevant parameter variations. The results were based on out-of-reactor criticality models of infinite pin-cell arrays and infinite radial assembly arrays. However, it is known that the presence of fixed absorbers panels (e.g., Boral), which are commonly used in SNF cask storage cells, impact the neutron spectrum, and thus their presence can be an important consideration in burnup credit analyses. Therefore, calculations are presented in this section to evaluate the effect of BPR exposure on SNF stored in a realistic high-capacity rail-type cask.

For this analysis, the generic 32 PWR-assembly burnup credit (GBC-32) cask¹⁸ was used. A cross-sectional view of the computer model is shown in Figure 4. The GBC-32 design was developed to provide a reference cask configuration that is representative of typical high-capacity rail casks being considered by industry. The boron loading in the Boral panels in the GBC-32 cask is 0.0225 g ¹⁰B/cm²; detailed specifications for the GBC-32 cask are available in Ref. 18.

5.4.1 Effect of BPRs with Uniform Axial Burnup

For this study, 3-D criticality calculations were performed with the KENO V.a Monte Carlo code. Unless explicitly stated otherwise, the criticality calculations are using spent-fuel isotopic compositions from SAS2H depletion calculations.

The k_{eff} values for actinide-only and actinide + fission product burnup credit nuclides (see Table 8 for nuclide classifications) in the GBC-32 cask, assuming uniform axial burnup, for various WABA BPR exposures are listed in Tables 9 and 10, respectively. The results correspond to spent fuel with 4.0 wt % ²³⁵U initial enrichment that has been exposed to Westinghouse WABA rods while accumulating a burnup of 45 GWd/MTU. The results correspond to 5-year cooling time. For the purpose of the depletion calculations, 3 cycles of 15 GWd/MTU per cycle are assumed. The relative behavior is the same as that exhibited in the previous sections for infinite arrays of assemblies and pin cells at zero cooling time. For comparison purposes, k_{inf} values from 1-D SAS2H-CSAS1X infinite pin-cell calculations for actinide-only and actinide + fission product burnup credit for the same WABA BPR exposures and 5-year cooling are listed in Tables 11 and 12, respectively. Good agreement between the Δk values determined via 3-D cask criticality calculations and those determined via infinite pin-cell criticality calculations is observed; indicating that the Δk results are not very sensitive to the presence of fixed absorbers panels in the criticality models. Also, note that the Δk values based on cases with and without fission products present are not significantly different, indicating that the Δk results are not very sensitive to the presence of fission products. Finally, the Δk values in the GBC-32 cask associated with isotopic compositions from both SAS2H and HELIOS depletion calculations are compared in Figure 38 for 5-year cooling time and various burnup exposures. The nuclides included in the criticality calculations are limited to the actinide-only and actinide + fission product burnup credit nuclides listed in Table 8. Once again, despite the fact that HELIOS and SAS2H are using different cross-section data, the Δk values are shown to be within a few tenths of a percent, with SAS2H isotopic compositions yielding larger Δk values.

The k_{eff} values for actinide-only and actinide + fission product burnup credit nuclides (see Table 8 for nuclide classifications) in the GBC-32 cask, assuming uniform axial burnup, for the BAA BPRs are given in Tables 13 and 14, respectively. Consistent with the results shown for infinite arrays of assemblies and pin cells at zero cooling time, the Westinghouse BAA BPRs yield the largest increase in reactivity for SNF. The Δk values in the GBC-32 cask associated with isotopic compositions from both SAS2H and HELIOS depletion calculations are compared in Figure 39 for 5-year cooling time and various burnup exposures.

Finally, the k_{eff} values for actinide-only and actinide + fission product burnup credit nuclides (see Table 8 for nuclide classifications) in the GBC-32 cask, assuming uniform axial burnup, for the B&W BPRs are given in Tables 15 and 16, respectively. The Δk values in the GBC-32 cask associated with isotopics from both SAS2H and HELIOS are compared in Figure 40 for 5-year cooling time and various burnup exposures. Once again, the Δk values are shown to be within a few tenths of a percent, and the SAS2H isotopics yield larger Δk values in all cases.

5.4.1.1 Effect of Cooling Time

Although the HELIOS results in Subsection 5.2.1.1.4 demonstrated that the reactivity effect of BPRs was not strongly dependent on cooling time (within the timeframe of interest to storage and transportation), a number of calculations were repeated in the GBC-32 cask to confirm the applicability of that conclusion in a burnup credit cask environment. The Δk values for actinide-only and actinide + fission product burnup credit nuclides (see Table 8 for nuclide classifications) in the GBC-32 cask, assuming uniform axial burnup, for various cooling times between 0 and 40 years are listed in Tables 17 and 18, respectively. The results correspond to spent fuel with 4.0 wt % ^{235}U initial enrichment that has been exposed to Westinghouse WABA rods while accumulating a burnup of 45 GWd/MTU. The results show a minor decrease in the Δk values with cooling time, which is consistent with the HELIOS results shown previously. For the cases with fission products included (Table 18), the Δk values are shown to vary less than 0.1% within the 0-to-40 year timeframe, confirming the low sensitivity to cooling time. For the cases with actinides only (Table 17), the decrease in the Δk values with cooling time is somewhat more pronounced, which is attributed to the increased ^{241}Pu concentration (and subsequent decay) in the cases with BPR exposure.

5.4.2 Effect of BPRs with Consideration of the Axial Burnup Distribution

To demonstrate the impact of incorporating the axial burnup distribution, the k_{eff} values for actinide-only and actinide + fission product burnup credit in the GBC-32 cask, including the axial burnup distribution, for various BPR exposures are listed in Table 19. The axial burnup distribution used in the analysis corresponds to the bounding profile suggested in Ref. 20 for PWR fuel with burnup greater than 30 GWd/MTU. Comparing these results to those listed in Tables 9 and 10 for the uniform axial burnup assumption reveals that the inclusion of the axial burnup distribution lessens the reactivity increase associated with BPR exposure. This is due to the fact that, with the axial burnup distribution included, the lower burnup regions near the ends that dominate the reactivity of the spent fuel²⁸ have less burnup exposure to the BPRs (than the assembly average).

For simplicity, the results shown in Table 19 correspond to BPR exposure during the entire depletion. Performing calculations with consideration of the axial burnup distribution for less than full BPR exposure (e.g., 1-cycle exposure), increases the complexity of the analysis by requiring cycle-wise axial burnup distributions. For example, to accurately calculate the reactivity effect for one-cycle BPR exposure, the axial burnup distribution at the end of the first cycle must be known (or assumed) in order to know how much burnup was accumulated in each axial region with the BPRs present. The one-cycle burnup in the axial regions near the fuel ends will be less than the assembly-average one-cycle burnup. Consequently, assuming BPR exposure in all axial regions based on the assembly-average one-cycle burnup will result in greater than actual BPR exposure in the end regions that control the reactivity of the SNF, and may slightly over-estimate the effect. However, the simplicity associated with this modeling approach (i.e., assuming constant BPR exposure in all axial regions based on the assembly-average one-cycle burnup) is desirable.

5.4.3 Consideration of Risk-Based Approaches

The analyses in the previous sections provide a technical understanding of the effect of BPR exposure on the reactivity of SNF and demonstrate that assuming the maximum BPR exposure during depletion would be a simple, conservative approach to facilitate allowance of assemblies exposed to BPRs. Considering that BPRs are typically used during the first-cycle only, assuming maximum (three-cycle) BPR exposure is not consistent with actual reactor operating practice. However, consideration of only one-cycle exposure in a safety evaluation would likely require justification of the one-cycle assumption or specific limitations on cask loading (i.e., exclusion of assemblies exposed to BPRs for more than one cycle).

Therefore, an additional analysis has been performed with the GBC-32 cask to assess the impact of loading one or more assemblies into a burnup credit cask that have BPR exposure that is not bounded by the one-cycle assumption. The analysis was performed for a uniform axial burnup of 45 GWd/MTU and 5-year cooling using isotopic composition from SAS2H depletion calculations. The “more reactive” assemblies were assumed to have three-cycle exposure to WABA BPRs, and the calculations assumed that the “more reactive” assemblies were loaded from the center outward. The remaining assemblies were assumed to have one-cycle exposure to WABA BPRs. The results are shown in Figure 41 for actinide-only burnup credit and confirm the relatively small reactivity consequence associated with loading a small number of assemblies with significantly greater BPR exposure (i.e., three-cycle). Note that 3-cycle BPR exposure exceeds any known operational practice. Results are shown in Figure 41 for multiple loadings of assemblies with “more reactive” BPR exposure to demonstrate the associated impact on k_{eff} . The reactivity consequence of loading a single assembly with three-cycle exposure, as compared to the one-cycle exposure, is shown to be $\sim 0.001 \Delta k$. Further, it is shown that ~ 5 three-cycle exposure assemblies are required to raise the k_{eff} of the cask by $0.005 \Delta k$. Note that if the analysis had been performed assuming the “more reactive” assemblies received only two-cycle BPR exposure, the reactivity consequence would be smaller.

The reactivity consequence of loading an assembly with greater BPR exposure will depend on the total burnup and the “reference” BPR exposure assumed for the remaining assemblies. Considering the likelihood of the existence of assemblies with three-cycle BPR exposure and the relatively small impact on the cask k_{eff} , it is anticipated that the use of an adequate one-cycle exposure could be justified. Note, however, that it is necessary to determine an appropriate assembly-average burnup for the one-cycle exposure assumption (e.g., 15 GWd/MTU is likely too low to bound one-cycle exposure in actual discharged SNF).

Table 9 Reactivity effect of various BPR exposures for actinide-only burnup credit (See Table 8 for specific nuclides) in the GBC-32 cask using isotopic compositions from SAS2H depletion calculations (45 GWd/MTU, 5-year cooling). The results correspond to Westinghouse 17×17 fuel with 4.0 wt % ^{235}U exposed to Westinghouse WABA rods.

Number of WABA rods present	Number of cycles of exposure [†]	KENO V.a k_{eff}	Standard deviation	Difference from no BPRs $[k_{(BPRs)} - k_{(no_BPRs)}]$	Standard deviation in difference
0	3	0.89376	0.00053	Reference	---
12	1	0.89698	0.00049	0.00322	0.00072
12	2	0.89921	0.00063	0.00545	0.00082
12	3	0.90281	0.00049	0.00905	0.00072
24	1	0.90130	0.00053	0.00754	0.00075
24	2	0.90546	0.00053	0.01170	0.00075
24	3	0.91177	0.00052	0.01801	0.00074

Table 10 Reactivity effect of various BPR exposures for actinide + fission product burnup credit (See Table 8 for specific nuclides) in the GBC-32 cask using isotopic compositions from SAS2H depletion calculations (45 GWd/MTU, 5-year cooling). The results correspond to Westinghouse 17×17 fuel with 4.0 wt % ^{235}U exposed to Westinghouse WABA rods.

Number of WABA rods present	Number of cycles of exposure [†]	KENO V.a k_{eff}	Standard deviation	Difference from no BPRs $[k_{(BPRs)} - k_{(no_BPRs)}]$	Standard deviation in difference
0	3	0.79825	0.00043	Reference	---
12	1	0.80174	0.00048	0.00349	0.00064
12	2	0.80437	0.00046	0.00612	0.00063
12	3	0.80782	0.00041	0.00957	0.00059
24	1	0.80577	0.00051	0.00752	0.00067
24	2	0.80938	0.00053	0.01113	0.00068
24	3	0.81618	0.00050	0.01793	0.00066

[†] One exposure cycle corresponds to a burnup of 15 GWd/MTU.

Table 11 Reactivity effect of various BPR exposures for actinide-only burnup credit (See Table 8 for specific nuclides) in an infinite pin-cell array using isotopic compositions from SAS2H depletion calculations (45 GWd/MTU, 5-year cooling). The results correspond to Westinghouse 17 × 17 fuel with 4.0 wt % ²³⁵U exposed to Westinghouse WABA rods.

Number of WABA rods present	Number of cycles of exposure [†]	CSAS1X k_{inf}	Difference from no BPRs $[k_{(BPRs)} - k_{(no_BPRs)}]$
0	3	1.1549	Reference
12	1	1.1586	0.0037
12	2	1.1601	0.0052
12	3	1.1634	0.0085
24	1	1.1621	0.0072
24	2	1.1653	0.0104
24	3	1.1718	0.0169

Table 12 Reactivity effect of various BPR exposures for actinide + fission product burnup credit (See Table 8 for specific nuclides) in an infinite pin-cell array using isotopic compositions from SAS2H depletion calculations (45 GWd/MTU, 5-year cooling). The results correspond to Westinghouse 17 × 17 fuel with 4.0 wt % ²³⁵U exposed to Westinghouse WABA rods.

Number of WABA rods present	Number of cycles of exposure	CSAS1X k_{inf}	Difference from no BPRs $[k_{(BPRs)} - k_{(no_BPRs)}]$
0	3	1.0148	Reference
12	1	1.0187	0.0040
12	2	1.0205	0.0057
12	3	1.0237	0.0090
24	1	1.02226	0.0078
24	2	1.0262	0.0114
24	3	1.0326	0.0179

[†] One exposure cycle corresponds to a burnup of 15 GWd/MTU.

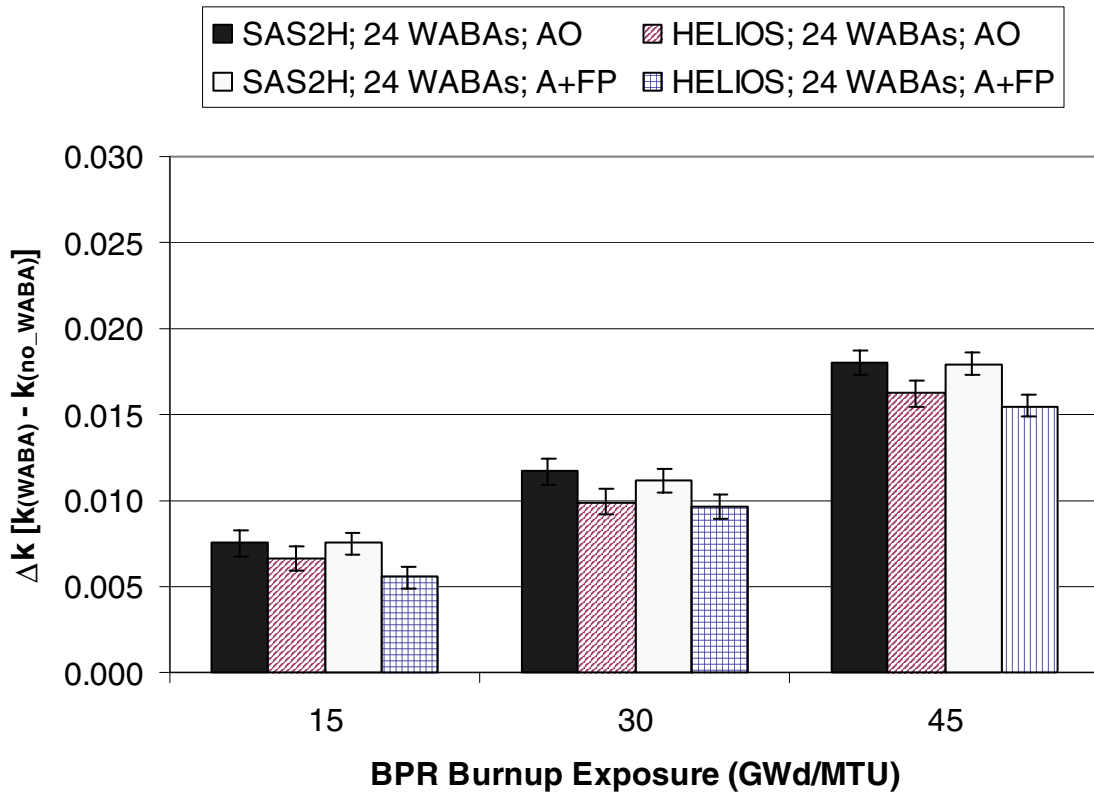


Figure 38 Comparison of reactivity differences (Δk values relative to the no BPR condition) in the GBC-32 cask (45 GWd/MTU, 5-year cooling) as calculated with KENO V.a for actinide-only (AO) and actinide + fission product (A + FP) burnup credit, based on isotopic compositions from SAS2H and HELIOS depletion calculations. The results correspond to fuel with 4.0 wt % ^{235}U initial enrichment that has been exposed to 24 WABA BPRs for various burnups.

Table 13 Reactivity effect of various BPR exposures for actinide-only burnup credit (See Table 8 for specific nuclides) in the GBC-32 cask using isotopic compositions from SAS2H depletion calculations (45 GWd/MTU, 5-year cooling). The results correspond to Westinghouse 17 × 17 fuel with 4.0 wt % ²³⁵U exposed to Westinghouse BAA rods.

Number of BAA rods present	Number of cycles of exposure [†]	KENO V.a k_{eff}	Standard deviation	Difference from no BPRs [$k_{(BPRs)} - k_{(no_BPRs)}$]	Standard deviation in difference
0	3	0.89376	0.00053	Reference	---
12	1	0.89836	0.00046	0.00460	0.00070
12	2	0.90220	0.00059	0.00844	0.00079
12	3	0.90729	0.00049	0.01353	0.00072
24	1	0.90362	0.00050	0.00986	0.00073
24	2	0.90968	0.00052	0.01592	0.00074
24	3	0.92021	0.00055	0.02645	0.00076

Table 14 Reactivity effect of various BPR exposures for actinide + fission product burnup credit (See Table 8 for specific nuclides) in the GBC-32 cask using isotopic compositions from SAS2H depletion calculations (45 GWd/MTU, 5-year cooling). The results correspond to Westinghouse 17 × 17 fuel with 4.0 wt % ²³⁵U exposed to Westinghouse BAA rods.

Number of BAA rods present	Number of cycles of exposure [†]	KENO V.a k_{eff}	Standard deviation	Difference from no BPRs [$k_{(BPRs)} - k_{(no_BPRs)}$]	Standard deviation in difference
0	3	0.79825	0.00043	Reference	---
12	1	0.80310	0.00049	0.00485	0.00065
12	2	0.80573	0.00047	0.00748	0.00064
12	3	0.81159	0.00048	0.01334	0.00064
24	1	0.80757	0.00040	0.00932	0.00059
24	2	0.81353	0.00052	0.01528	0.00067
24	3	0.82517	0.00047	0.02692	0.00064

[†] One exposure cycle corresponds to a burnup of 15 GWd/MTU.

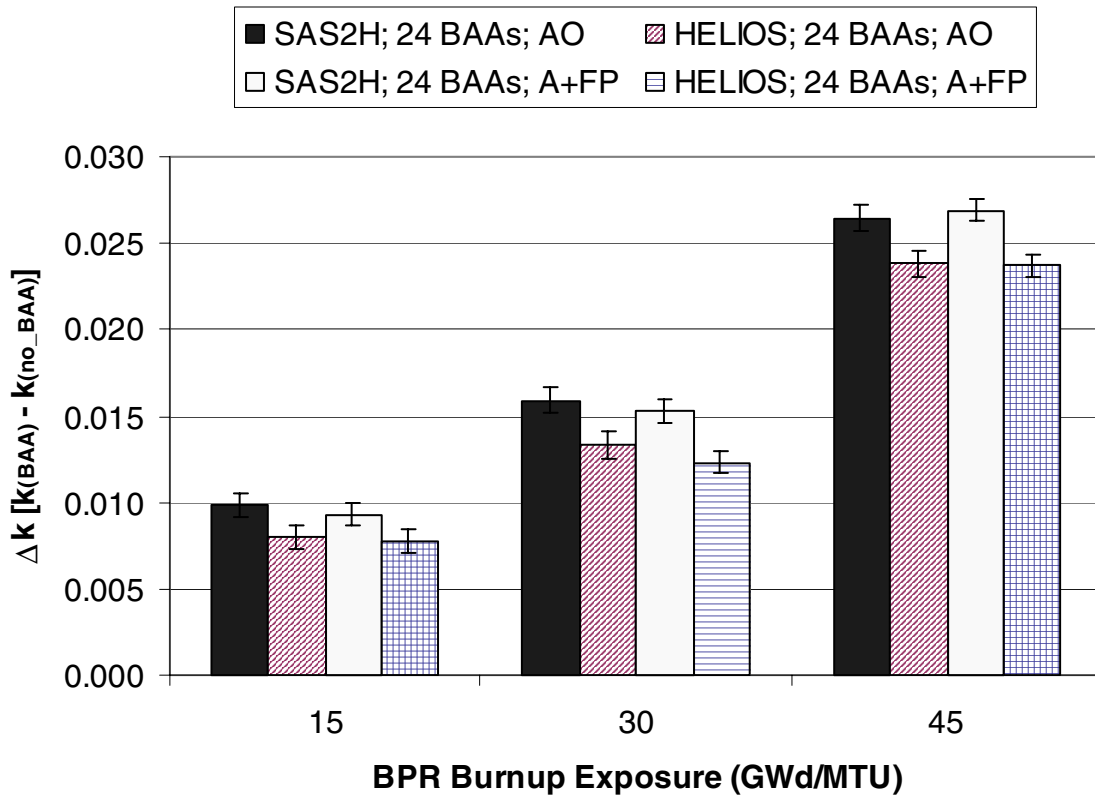


Figure 39 Comparison of reactivity differences (Δk values relative to the no BPR condition) in the GBC-32 cask (45 GWd/MTU, 5-year cooling) as calculated with KENO V.a for actinide-only (AO) and actinide + fission product (A + FP) burnup credit, based on isotopic compositions from SAS2H and HELIOS depletion calculations. The results correspond to fuel with 4.0 wt % ^{235}U initial enrichment that has been exposed to 24 BAA BPRs for various burnups.

Table 15 Reactivity effect of various BPR exposures for actinide-only burnup credit (See Table 8 for specific nuclides) in the GBC-32 cask using isotopic compositions from SAS2H depletion calculations (45 GWd/MTU, 5-year cooling). The results correspond to B&W 15 × 15 fuel with 4.0 wt % ²³⁵U exposed to B&W BPRs (2.0 wt % B₄C).

Number of BPRs present	Number of cycles of exposure [†]	KENO V.a k_{eff}	Standard deviation	Difference from no BPRs [k _(BPRs) – k _(no_BPRs)]	Standard deviation in difference
0	3	0.92334	0.00048	Reference	---
16	1	0.93019	0.00046	0.00685	0.00066
16	2	0.93429	0.0006	0.01095	0.00077
16	3	0.94407	0.00054	0.02073	0.00072

Table 16 Reactivity effect of various BPR exposures for actinide + fission product burnup credit (See Table 8 for specific nuclides) in the GBC-32 cask using isotopic compositions from SAS2H depletion calculations (45 GWd/MTU, 5-year cooling). The results correspond to B&W 15 × 15 fuel with 4.0 wt % ²³⁵U exposed to B&W BPRs (2.0 wt % B₄C).

Number of BPRs present	Number of cycles of exposure [†]	KENO V.a k_{eff}	Standard deviation	Difference from no BPRs [k _(BPRs) – k _(no_BPRs)]	Standard deviation in difference
0	3	0.82606	0.00048	Reference	---
16	1	0.83216	0.00043	0.00610	0.00064
16	2	0.83654	0.00049	0.01048	0.00069
16	3	0.84425	0.00049	0.01819	0.00069

[†] One exposure cycle corresponds to a burnup of 15 GWd/MTU.

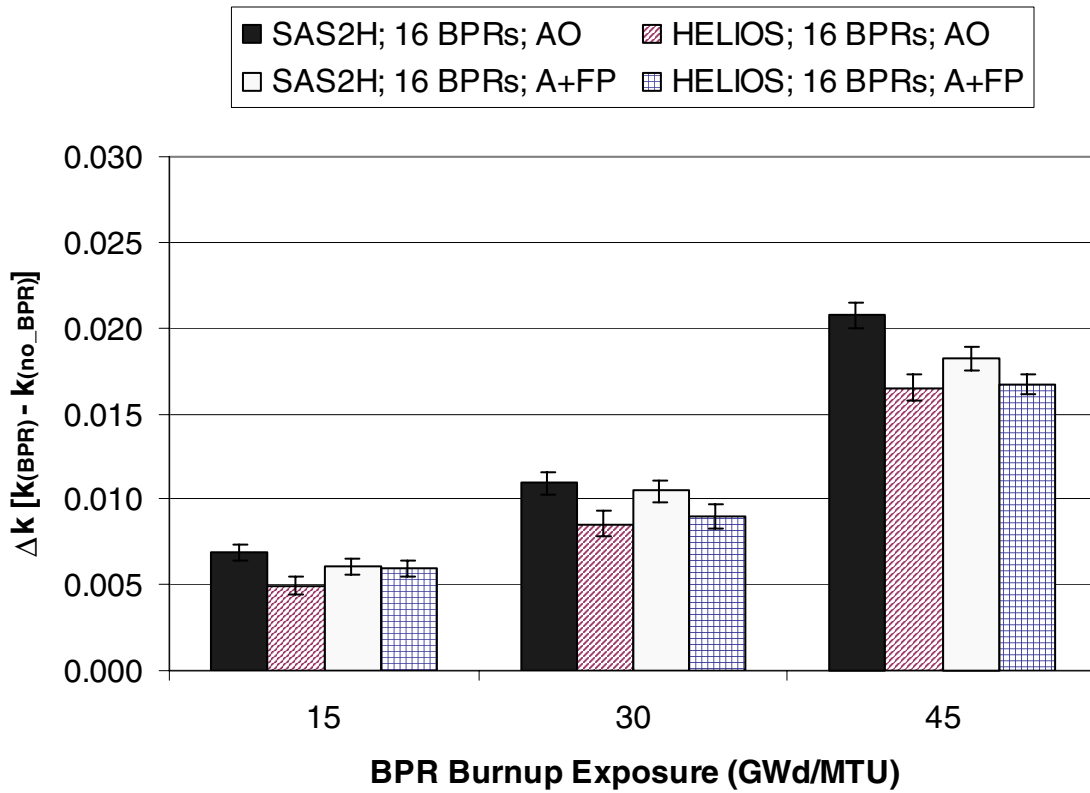


Figure 40 Comparison of reactivity differences (Δk values relative to the no BPR condition) in the GBC-32 cask (45 GWd/MTU, 5-year cooling) as calculated with KENO V.a for actinide-only (AO) and actinide + fission product (A + FP) burnup credit, based on isotopic compositions from SAS2H and HELIOS depletion calculations. The results correspond to fuel with 4.0 wt % ^{235}U initial enrichment that has been exposed to 24 B&W (2 wt % B_4C) BPRs for various burnups.

Table 17 Δk values as a function of cooling time for actinide-only burnup credit (See Table 8 for specific nuclides) in the GBC-32 cask using isotopic compositions from SAS2H depletion calculations. The results correspond to Westinghouse 17×17 fuel with 4.0 wt % burned to 45 GWd/MTU.

Cooling Time (years)	12 WABA BPRs for 3 cycles		24 WABA BPRs for 3 cycles	
	Difference from no BPRs	Standard deviation in difference	Difference from no BPRs	Standard deviation in difference
	$[k_{(BPRs)} - k_{(no_BPRs)}]$		$[k_{(BPRs)} - k_{(no_BPRs)}]$	
0	0.01045	0.00074	0.01971	0.00076
5	0.00905	0.00072	0.01801	0.00074
10	0.00959	0.00074	0.01787	0.00068
20	0.00808	0.00069	0.01721	0.00067
40	0.00882	0.00067	0.01564	0.00065

Table 18 Δk values as a function of cooling time for actinide + fission product burnup credit (See Table 8 for specific nuclides) in the GBC-32 cask using isotopic compositions from SAS2H depletion calculations. The results correspond to Westinghouse 17×17 fuel with 4.0 wt % burned to 45 GWd/MTU.

Cooling Time (years)	12 WABA BPRs for 3 cycles		24 WABA BPRs for 3 cycles	
	Difference from no BPRs	Standard deviation in difference	Difference from no BPRs	Standard deviation in difference
	$[k_{(BPRs)} - k_{(no_BPRs)}]$		$[k_{(BPRs)} - k_{(no_BPRs)}]$	
0	0.00946	0.00065	0.01824	0.00069
5	0.00957	0.00059	0.01793	0.00066
10	0.00805	0.00067	0.01750	0.00065
20	0.00881	0.00060	0.01770	0.00060
40	0.00958	0.00057	0.01756	0.00061

Table 19 Reactivity effect of various BPR exposures in the GBC-32 cask with the axial burnup distribution included, using isotopic compositions from SAS2H depletion calculations (45 GWd/MTU, 5-year cooling). The results correspond to Westinghouse 17×17 fuel with 4.0 wt % ^{235}U exposed to Westinghouse WABA rods.

Number of WABAs present	Number of cycles of exposure [†]	KENO V.a k_{eff}	Standard deviation	Difference from no BPRs [$k_{(BPRs)} - k_{(no_BPRs)}$]	Standard deviation in difference
Actinide-only burnup credit					
0	3	0.92020	0.00053	Reference	---
12	3	0.92659	0.00066	0.00639	0.00085
24	3	0.93311	0.00058	0.01291	0.00079
Actinide + fission product burnup credit					
0	3	0.84746	0.00055	Reference	---
12	3	0.85509	0.00046	0.00763	0.00072
24	3	0.86010	0.00052	0.01264	0.00076

[†] One exposure cycle corresponds to a burnup of 15 GWd/MTU.

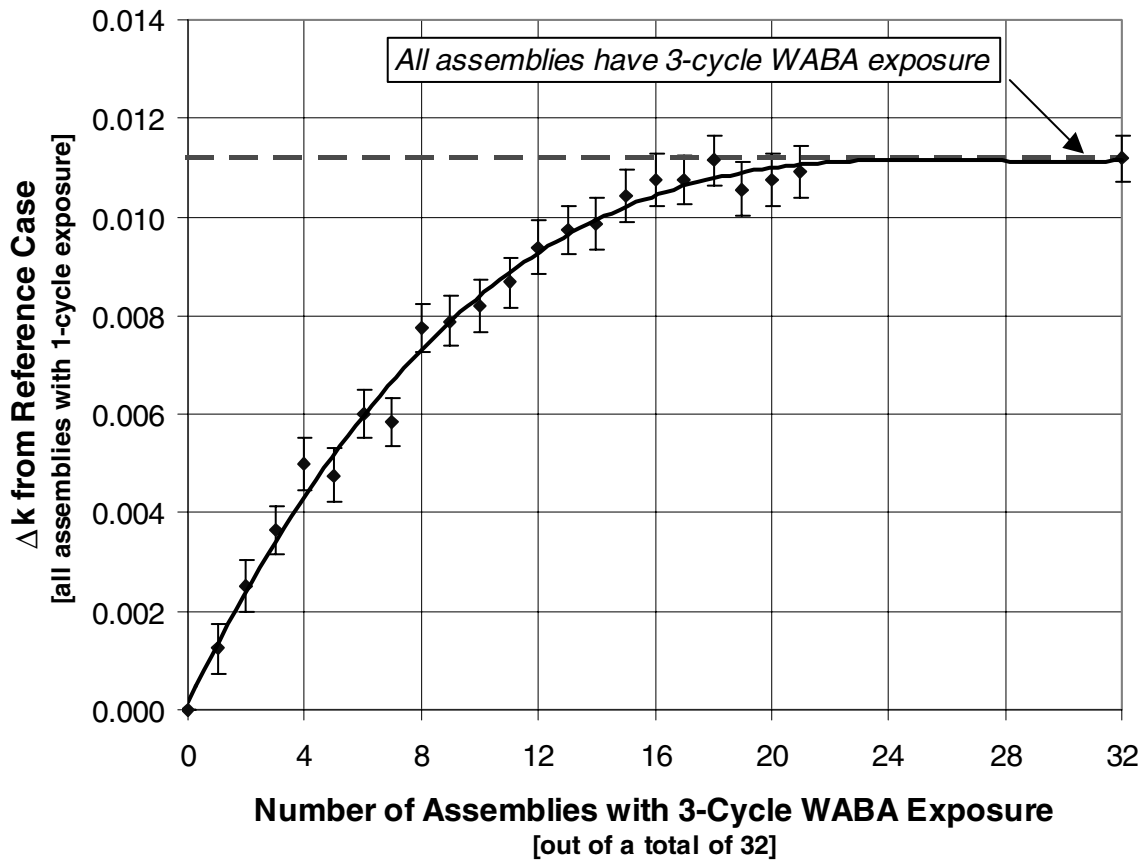


Figure 41 Increase in k_{eff} due to loading assemblies with 3-cycle BPR exposure into a GBC-32 cask in which the remaining assemblies have 1-cycle BPR exposure. The results correspond to Westinghouse 17×17 fuel with 4.0 wt % ^{235}U , Westinghouse WABA rods, actinide-only nuclides, and spent-fuel isotopic compositions from SAS2H depletion calculations.

6 DISCUSSION AND IMPLICATIONS

The results presented in this report demonstrate that the reactivity effect due to BPRs increases nearly linearly with burnup and is dependent upon the number and poison loading of the BPRs and the initial fuel enrichment. For a fixed burnup, the reactivity difference due to BPR exposure increases with decreasing initial enrichment and with increasing poison loading (either number of BPR rods or ^{10}B wt %). Although variations are observed for the different BPR designs, maximum reactivity increases have been found to be within 1 to 3% Δk , depending on initial fuel enrichment and BPR design, when maximum BPR loading and exposure time are assumed. Expected typical reactivity increases, based on one-cycle exposure, were found to be less than 1% Δk . Of the BPR designs considered, the Westinghouse BAA BPR design yielded the largest positive reactivity effect. Although BPR poisons are effectively depleted during the first cycle of exposure, a significant portion of the reactivity difference is shown to be due to the displacement of moderator.

Although most BPRAs do not have the maximum number of BPRs or the maximum possible poison loading, BPRAs that do have the maximum number of BPRs or poison loading are used. A direct relationship exists between the reactivity worth of the BPRAs and their effect on discharge reactivity — higher reactivity worth BPRAs result in larger effects on discharge reactivity. Therefore, analyses that utilize less than the maximum number of BPRs or less than the maximum poison loading may not be bounding. Figures in Section 5 show that the reactivity effect is linearly related to the number of BPRs present and the BPR poison loading. Although observed to be relatively minor, variations in the reactivity effect of BPRs due to BPR design variations necessitate that analyses consider the most bounding BPR design. Alternatively, administrative restrictions could be employed to assure that assemblies exposed to BPR designs other than those considered in the licensing evaluation are deemed unacceptable for loading. However, knowledge of assembly exposure to specific BPR designs may not be available.

While it is known that BPRs are typically inserted into an assembly during its first cycle of operation and subsequently withdrawn, exceptions to this practice do exist. If analyses were accompanied by administrative restrictions to ensure that assemblies with greater than one cycle of BPR exposure were not accepted for loading, analyses could be performed based on only a single cycle of BPR exposure. Such an approach would require the maximum single cycle exposure to be defined such that all (or most) single cycle BPR exposures are bounded. A complication associated with this approach is the necessity of plant data specifying assembly BPR exposure. Considering the large degree of conservatism (2–3% Δk) associated with assuming the BPRs are present throughout the entire irradiation, the additional complexities of such administrative controls may be considered acceptable by burnup credit applicants. Alternatively, it may be possible to credit the conservatism associated with the maximum exposure approach to account for the effects of temporary control rod insertions. BPRs and control rods both cause localized spectral hardening, and thus result in similar reactivity effects. An analysis² of the effect of control rod insertions on the reactivity of SNF suggests that the effect of control rod insertions is less than the effect associated with second- and third-cycle BPR exposure. Because it is not physically possible for a BPR and a control rod assembly to be inserted into a fuel assembly at the same time, the BPR modeling assumption may be used to bound realistic combinations of BPR and control rod exposures.

7 RECOMMENDATIONS

The analyses presented in this report provide a technical basis for revising the current ISG (Ref. 3) to allow burnup credit for assemblies that have used BPRs. Although the analyses do not address the issue of validation of depletion methods for assembly designs with BPRs, they do demonstrate that the effect of the BPRs is generally well behaved and that independent codes and cross-section libraries predict similar results. Therefore, it is concluded that the effect of the various BPR types may be adequately calculated and that the current recommendation for restricting assemblies that have used BPRs should be eliminated.

Guidance should require safety analyses to include the effect of BPRs for assemblies that are classified as acceptable contents for the particular cask. For example, safety analyses for casks that are to be loaded with assemblies that contained BPRs during irradiation should account for the limiting realistic BPR irradiation justified by the applicant's operations and design information and/or verified during cask loading. Assuming maximum BPR exposure during depletion would be a simple, conservative approach to bound the reactivity effect of BPRs, where maximum BPR exposure may be defined as the maximum possible number of BPRs with the most bounding BPR design (i.e., most bounding geometric design and maximum possible poison loading) for the entire burnup. More realistic approaches based on typical operating conditions and/or loading restriction(s) would need supporting justification (e.g., loading verification, analyses of statistically representative plant operating data, consideration of the impact on reactivity associated with loading assemblies that have greater than assumed BPR exposure, etc.).

8 REFERENCES

1. C. E. Sanders and J. C. Wagner, *Study of the Effect of Integral Burnable Absorbers for PWR Burnup Credit*, NUREG/CR-6760 (ORNL/TM-2000/321), U.S. Nuclear Regulatory Commission, Oak Ridge National Laboratory, 2002.
2. C. E. Sanders and J. C. Wagner, *Parametric Study of the Effect of Control Rods for PWR Burnup Credit*, NUREG/CR-6759 (ORNL/TM-2001/69), U.S. Nuclear Regulatory Commission, Oak Ridge National Laboratory, 2002.
3. Spent Fuel Project Office Interim Staff Guidance – 8, Rev. 1 – Limited Burnup Credit, U.S. Nuclear Regulatory Commission, July 30, 1999.
4. D. E. Carlson, C. J. Withee and C. V. Parks, “Spent Fuel Burnup Credit in Casks: An NRC Perspective,” U.S. Nuclear Regulatory Commission, pp. 419–436 in *Proc. Twenty-Seventh Water Reactor Safety Information Meeting*, October 25–27, 1999, Bethesda, Maryland, NUREG/CP-0169, March 2000.
5. *SCALE: A Modular Code System for Performing Standardized Computer Analyses for Licensing Evaluation*, NUREG/CR-0200, Rev. 6 (ORNL/NUREG/CSD-2/R6), Vols. I, II, III, May 2000. Available from Radiation Safety Information Computational Center at Oak Ridge National Laboratory as CCC-545.
6. J. J. Casal, R. J. J. Stamm'ler, E. A. Villarino, and A. A. Ferri, “HELIOS: Geometric capabilities of a new fuel-assembly program,” Vol. 2, p. 10.2.1 113, in *Proc. Intl Topical Meeting on Advances in Mathematics, Computations, and Reactor Physics*, April 28–May 2, 1991, Pittsburgh, Pennsylvania.
7. L. M. Petrie and N. F. Landers, “KENO V.a: An Improved Monte Carlo Criticality Program With Supergrouping,” Vol. II, Sect. F11 of *SCALE: A Modular Code System for Performing Standardized Computer Analyses for Licensing Evaluation*, NUREG/CR-0200, Rev. 6 (ORNL/NUREG/CSD-2/R6), Vols. I, II, and III, May 2000. Available from Radiation Safety Information Computational Center at Oak Ridge National Laboratory as CCC-545.
8. *Characteristics of Spent Fuel, High-Level Waste, and Other Radioactive Wastes Which May Require Long-Term Isolation*, DOE/RW-0184, Volume 1, December 1987.
9. *Characteristics of Potential Repository Wastes*, DOE/RW-0184-R1, Volume 1, July 1992.
10. S. M. Bowman, O. W. Hermann and M. C. Brady, *SCALE-4 Analysis of Pressurized Water Reactor Critical Configurations: Volume 2 – Sequoyah Unit 2 Cycle 3*, ORNL/TM-12294, Vol. 2, Martin Marietta Energy Systems, Inc., Oak Ridge National Laboratory, March 1995.
11. *CRWMS M&O 1998 Summary Report of Commercial Reactor Criticality Data for Sequoyah Unit 2*, B00000000-01717-5705-00064 Rev. 01, Las Vegas, Nevada: CRWMS M&O. MOL.19980716.0015.
12. *CRWMS M&O 1998 Summary Report of Commercial Reactor Criticality Data for Crystal River Unit 3*, B00000000-01717-5705-00060 Rev. 01, Las Vegas, Nevada: CRWMS M&O. MOL.19980728.0189.

13. S. M. Bowman and O. W. Hermann, *SCALE-4 Analysis of Pressurized Water Reactor Critical Configurations: Volume 3 – Surry Unit 1 Cycle 2*, ORNL/TM-12294, Vol. 3, Martin Marietta Energy Systems, Inc., Oak Ridge National Laboratory, March 1995.
14. S. M. Bowman and T. Suto, *SCALE-4 Analysis of Pressurized Water Reactor Critical Configurations: Volume 5 – North Anna Unit 1 Cycle 5*, ORNL/TM-12294, Vol. 5, Martin Marietta Energy Systems, Inc., Oak Ridge National Laboratory, October 1996.
15. B. H. Wakeman and S. A. Ahmed, *Evaluation of Burnup Credit for Dry Storage Casks*, EPRI NP-6494, Electric Power Research Institute (August 1989).
16. M. D. DeHart, *SCALE-4 Analysis of Pressurized Water Reactor Critical Configurations: Volume 4 – Three Mile Island Unit 1 Cycle 5*, ORNL/TM-12294, Vol. 4, Martin Marietta Energy Systems, Inc., Oak Ridge National Laboratory, March 1995.
17. M. D. DeHart, *Sensitivity and Parametric Evaluations of Significant Aspects of Burnup Credit for PWR Spent Fuel Packages*, ORNL/TM-12973, Lockheed Martin Energy Research Corp., Oak Ridge National Laboratory, May 1996.
18. J. C. Wagner, *Computational Benchmark for Estimation of Reactivity Margin from Fission Products and Minor Actinides in PWR Burnup Credit*, NUREG/CR-6747 (ORNL/TM-2000/306), U.S. Nuclear Regulatory Commission, Oak Ridge National Laboratory, September 2001.
19. O. W. Hermann and C. V. Parks, “SAS2H: A Coupled One-Dimensional Depletion and Shielding Analysis Module,” Vol. I, Sect. S2 of *SCALE: A Modular Code System for Performing Standardized Computer Analyses for Licensing Evaluation*, NUREG/CR-0200, Rev. 6 (ORNL/NUREG/CSD-2/R6), Vols. I, II, and III, May 2000. Available from Radiation Safety Information Computational Center at Oak Ridge National Laboratory as CCC-545.
20. *Topical Report on Actinide-Only Burnup Credit for PWR Spent Nuclear Fuel Packages*, DOE/RW-0472, Rev. 2, U.S. Department of Energy, Office of Civilian Radioactive Waste Management, September 1998.
21. T. L. Sanders and R. M. Westfall, “Feasibility and Incentives for Burnup Credit in Spent Fuel Transport Casks,” *Nucl. Sci. Eng.* **104** (1990).
22. *Disposal Criticality Analysis Methodology Technical Report*, Document No. B00000000-01717-5705-00020, Rev. 00, Department of Energy, Office of Civilian Radioactive Waste Management (OCRWM), August 1996.
23. O. W. Hermann, S. M. Bowman, M. C. Brady, and C. V. Parks, *Validation of the SCALE System for PWR Spent Fuel Isotopic Composition Analyses*, ORNL/TM-12667, Martin Marietta Energy Systems, Inc., Oak Ridge National Laboratory, March 1995.
24. M. D. DeHart and O. W. Hermann, *An Extension of the Validation of SCALE (SAS2H) Isotopic Predictions for PWR Spent Fuel*, ORNL/TM-13317, Lockheed Martin Energy Research Corp., Oak Ridge National Laboratory, September 1996.
25. M. Rahimi, E. Fuentes, and D. Lancaster, *Isotopic and Criticality Validation for PWR Actinide-Only Burnup Credit*, DOE/RW-0497, U.S. Department of Energy, May 1997.

26. C. V. Parks, M. D. DeHart and J. C. Wagner, *Review and Prioritization of Technical Issues Related to Burnup Credit for LWR Fuel*, NUREG/CR-6665 (ORNL/TM-1999/303), U.S. Nuclear Regulatory Commission, Oak Ridge National Laboratory, February 2000.
27. C. V. Parks, I. C. Gauld, J. C. Wagner, B. L. Broadhead, M. D. DeHart, and D. D. Ebert, "Research Supporting Implementation of Burnup Credit in the Criticality Safety Assessment of Transport and Storage Casks," pp. 139–161, in *U.S. Nuclear Regulatory Commission Proceedings of the Twenty-Eighth Water Reactor Safety Information Meeting*, NUREG/CP-0172, October 23–25, 2000, Bethesda, Maryland (May 2001).
28. J. C. Wagner and M. D. DeHart, *Review of Axial Burnup Distribution Considerations for Burnup Credit Calculations*, ORNL/TM-1999/246, Lockheed Martin Energy Research Corp., Oak Ridge National Laboratory, February 2000.

APPENDIX A
SELECTED HELIOS INPUT FILES

HELIOS input file for Westinghouse 17 × 17 OFA assembly without BPRs present

```

+HEL
'w17_waba_00_e40_45' =
  CASE('/fmdp/helios-1.6/babel-1.6/aix/sample-11/hy045n18g16a.dat'/
    'w17_waba_00_e40_45.hrf'/ 'Reference W17x17 assembly model')

! Westinghouse 17x17 OFA Assembly !
! No BPRs present !

! Fuel !
$rp2 = PAR("0.3922")
$rair = PAR("0.4001")
$rcan = PAR("0.4572")
! Guide tube !
$rcool = PAR("0.5613")
$rbow = PAR("0.6020")

$rgap = PAR("0.04352") ! for assembly pitch of 21.50364 cm !
$pitch = PAR("1.2598")
$ps2 = PAR("$pitch/2")
$psq2 = PAR("$rcan/2**0.5")
$psqh2 = PAR("$rbow/2**0.5")
$pgap2 = PAR("$rgap/2")
$scoup = PAR(3)

! Materials !
! 650ppm Boron in moderator !
'H2O-1' = MAT(NB/.670/1001,11.183; 8016,88.752; 5010,0.012; 5011,0.053)
! Unborated moderator !
'H2O-2' = MAT(NB/1.0/1001,11.19; 8016,88.81)
! Cladding !
Zy2 = MAT(NB/6.56/40002,100.0)
! Fuel !
'UO2-1' = MAT(10.5216/ 92234,3.4729E-02; 92235,4.0000; 92236,1.8400E-02;
  92238,95.947; 8016,0)
'air' = MAT(0/ 7014,5.000E-05)

! Geometry !
Pin = CCS($rp2,$rair,$rcan//fuel,gap,clad)
Whole = CCS($rcool,$rbow//water,clad)

$cell = PAR(("-$ps2", "-$ps2") ("-$ps2", $ps2) ($ps2, $ps2) ($ps2, "-$ps2") !nodes 1-4!
(0, "-$ps2") ("-$ps2", 0) (0, $ps2) ($ps2, 0) ($rcan, 0) (0, "-$rcan") ("-$rcan", 0)
(0, $rcan) ($psq2, $psq2) ($psq2, "-$psq2") ("-$psq2", "-$psq2") ("-$psq2", $psq2)
/4, cool/Pin(0,0)/ 1,6,11,15,cool; 6,2,16,11,cool; 2,7,12,16,cool;
7,3,13,12,cool; 3,8,9,13,cool; 8,4,14,9,cool; 4,5,10,14,cool)

$wcell = PAR(("-$ps2", "-$ps2") ("-$ps2", $ps2) ($ps2, $ps2) ($ps2, "-$ps2") !nodes 1-4!
(0, "-$ps2") ("-$ps2", 0) (0, $ps2) ($ps2, 0) ($rbow, 0) (0, "-$rbow") ("-$rbow", 0)
(0, $rbow) ($psqh2, $psqh2) ($psqh2, "-$psqh2") ("-$psqh2", "-$psqh2")
("-$psqh2", $psqh2)/4, cool/Whole(0,0)/ 1,6,11,15,cool; 6,2,16,11,cool;
2,7,12,16,cool; 7,3,13,12,cool; 3,8,9,13,cool; 8,4,14,9,cool; 4,5,10,14,cool)

$wgap = PAR(("-$pgap2", "-$ps2") ("-$pgap2", $ps2) ($pgap2, $ps2) ($pgap2, "-$ps2")
/4, cool//)

$cell2 = PAR(("-$ps2", "-$ps2") ("-$ps2", 0) ($ps2, 0) ($ps2, "-$ps2")
(0, "-$ps2") ($rcan, 0) (0, "-$rcan") ("-$rcan", 0) ($psq2, "-$psq2")
("-$psq2", "-$psq2") /4, cool/Pin(0,0) 3/ 3,4,9,6,cool; 4,5,7,9,cool;
5,1,10,7,cool)

$wcell2 = PAR(("-$ps2", "-$ps2") ("-$ps2", 0) ($ps2, 0) ($ps2, "-$ps2")
(0, "-$ps2") ($rbow, 0) (0, "-$rbow") ("-$rbow", 0) ($psqh2, "-$psqh2")
("-$psqh2", "-$psqh2") /4, cool/Whole(0,0) 2/3, 4,9,6,cool; 4,5,7,9,cool;
5,1,10,7,cool)

$wgap2 = PAR(("-$pgap2", "-$ps2") ("-$pgap2", 0) ($pgap2, 0) ($pgap2, "-$ps2")
/4, cool//)

```

```

$wcell14 = PAR((0,"-$p2") (0,0) ($p2,0) ($p2,"-$p2")
($rbox,0) (0,"-$rbox") ($psqh2,"-$psqh2")
/4,cool/Whole(0,0) 2/4,1,6,7,cool)

$wgap4 = PAR(("-$pgap2","-$pgap2") ("-$pgap2",$pgap2) ($pgap2,$pgap2 )
($pgap2,"-$pgap2") /4,cool/)

'1.0' = STR($cell)
'3.0' = STR($wcell)
'5.0' = STR($cell2)
'7.0' = STR($wcell2)
'9.0' = STR($wcell4)
'10.0' = STR($wgap)
'11.0' = STR($wgap2)
'12.0' = STR($wgap4)

White = ALB(1/1/1)

$corder =PAR((1,3,4)$coup(2,2,1)/
(2,3,4)$coup(3,2,1)/(3,3,4)$coup(4,2,1)/
(4,3,4)$coup(5,2,1)/(5,3,4)$coup(6,2,1)/
(6,3,4)$coup(7,2,1)/(7,3,4)$coup(8,2,1)/
(8,3,4)$coup(9,2,1)/(9,3,4)$coup(10,2,1))
$corder1 =PAR((1,4,1)$coup(2,2,1)/
(2,3,4)$coup(3,2,1)/(3,3,4)$coup(4,2,1)/
(4,3,4)$coup(5,2,1)/(5,3,4)$coup(6,2,1)/
(6,3,4)$coup(7,2,1)/(7,3,4)$coup(8,2,1)/
(8,3,4)$coup(9,2,1)/(9,3,4)$coup(10,2,1))
$corder2 =PAR((1,4,1)$coup(2,3,2)/
(2,4,1)$coup(3,3,2)/(3,4,1)$coup(4,3,2)/
(4,4,1)$coup(5,3,2)/(5,4,1)$coup(6,3,2)/
(6,4,1)$coup(7,3,2)/(7,4,1)$coup(8,3,2)/
(8,4,1)$coup(9,3,2)/(9,4,1)$coup(10,3,2))

Row1=CNX('9.0','5.0','5.0','7.0','5.0','5.0','7.0','5.0','5.0','11.0'/$corder)
Row2=CNX('5.0','1.0','1.0','1.0','1.0','1.0','1.0','1.0','1.0','10.0'/$corder1)
Row3=CNX('5.0','1.0','1.0','1.0','1.0','1.0','1.0','1.0','1.0','10.0'/$corder1)
Row4=CNX('7.0','1.0','1.0','3.0','1.0','1.0','3.0','1.0','1.0','10.0'/$corder1)
Row5=CNX('5.0','1.0','1.0','1.0','1.0','1.0','1.0','1.0','1.0','10.0'/$corder1)
Row6=CNX('5.0','1.0','1.0','1.0','1.0','3.0','1.0','1.0','1.0','10.0'/$corder1)
Row7=CNX('7.0','1.0','1.0','3.0','1.0','1.0','1.0','1.0','1.0','10.0'/$corder1)
Row8=CNX('5.0','1.0','1.0','1.0','1.0','1.0','1.0','1.0','1.0','10.0'/$corder1)
Row9=CNX('5.0','1.0','1.0','1.0','1.0','1.0','1.0','1.0','1.0','10.0'/$corder1)
Row10=CNX('11.0','10.0','10.0','10.0','10.0','10.0','10.0','10.0','10.0','10.0',
'12.0'/$corder2)

System =CNX(Row1,Row2,Row3,Row4,Row5,Row6,Row7,Row8,Row9,Row10/
(1-2,4,1)$coup(2-2,3,2)/
(2-2,4,1)$coup(3-2,3,2)/(3-2,4,1)$coup(4-2,3,2)/
(4-2,4,1)$coup(5-2,3,2)/(5-2,4,1)$coup(6-2,3,2)/
(6-2,4,1)$coup(7-2,3,2)/(7-2,4,1)$coup(8-2,3,2)/
(8-2,4,1)$coup(9-2,3,2)/(9-2,4,1)$coup(10-2,4,3))

System = BDRY((1-10,3) (10-1,2)$coup(0)/(1-1,2) (1-10,3)$coup(1-1,2) (10-1,2))

! Overlays !
AllMat = OVLN('H2O-1' /*-*** / Zy2 / *-*-*clad /
'air' /*-***-gap /
'UO2-1' /*-***-fuel)

All1 = OVLN(1.0 /*-***)
AllT = OVLN(600. /*-*** / 1000. /*-***-fuel / 620. /*-***-clad)
mos = OVSM(AllMat)
dos = OVSD(All1)
tos = OVST(AllT)

! Low temperature !
LofT = OVLN(293.00 /*-***)
LofM = OVLN('H2O-2' /*-***-water, *-*-*0-cool)
tLfes = OVST(tos/LofT)
mLfes = OVSM(mos/LofM)

```

```

! Burnup !
st      = STAT(mos,dos,tos,60.00)
stloF   = STAT(mLfos,dos,tLfos,60.00)
BU      = PATH(/NC,(st),45000/45,(1826.25/5))
COLD    = TREE(BU/(stloF)/0,45000/45)

! Output !
G1      = GROUP(N/ 0)
G2      = GROUP(N/ 0.625, 0)
Gpins   = AREA(*-*--<water>,*-*--<fuel>)
Apins   = AREA(<*-*--fuel>)
Aall    = AREA(<*-*-->)
Asol    = AREA(<*-*--water,*--0-cool>)

ND      = MICRO(G1, Apins / 92234, 92235, 92236, 92238, 93237,
                94238, 94239, 94240, 94241, 94242, 95241,
                95242, 95243,
                42595, 43599, 44601, 45603, 47609, 55633,
                62647, 62649, 62650, 62651, 62652, 60643,
                60645, 63651, 63653, 64655, 8016 /)

NDA     = MICRO(G1, Apins / / )

! Corners !
NE      = FACE((1-10,2,4))
SE      = FACE((10-10,4,2))
SW      = FACE((10-1,1,3))
NW      = FACE((1-1,1,3))

! Interior face !
Interior = FACE((1-1,2,1) (2-1,3,2) (3-1,3,2) (4-1,3,2)
                (5-1,3,2) (6-1,3,2) (7-1,3,2) (8-1,3,2)
                (9-1,3,2) (10-1,3,2))

! Exterior face !
Exterior = FACE((10-1,2,1) (10-2,2,1) (10-3,2,1) (10-4,2,1)
                (10-5,2,1) (10-6,2,1) (10-7,2,1) (10-8,2,1)
                (10-9,2,1) (10-10,2,1))

CurCorner = CUR(G2,NW,SW,SE,NE)
CurSide   = CUR(G2,Interior,Exterior)

'w17_waba_00_e40_45' = RUN()

```

HELIOS input file for Westinghouse 17 × 17 OFA assembly with 12 WABA BPRs present during the first 15 GWD/t of burnup

```

+HEL
'w17_waba_12_e40_15' =
  CASE('/fmdp/helios-1.6/babel-1.6/aix/sample-11/hy045n18g16a.dat'/
    'w17_waba_12_e40_15.hrf'/ '12 WABA BPR W17x17 assembly model')

! Westinghouse 17x17 OFA Assembly           !
! 12 WABA BPRs present during first 15 GWD/t burnup !
! 00 WABA BPRs during cold calcs           !

! Fuel !
$rpe = PAR("0.3922")
$rair = PAR("0.4001")
$rcan = PAR("0.4572")
! Guide tube !
$rcool = PAR("0.5613")
$rbox = PAR("0.6020")
! Burnable Poison Rod (WABA) !
$rwco = PAR("0.2858")
$rwbox = PAR("0.3391")
$rwair = PAR("0.3531")
$rwaba = PAR("0.4039")
$rwabair = PAR("0.4179")
$rcro = PAR("0.4839")

$rgap = PAR("0.04352") ! for assembly pitch of 21.50364 cm !
$pitch = PAR("1.2598")
$p2 = PAR("$pitch/2")
$psq2 = PAR("$rcan/2**0.5")
$psqh2 = PAR("$rbox/2**0.5")
$pgap2 = PAR("$rgap/2")
$coup = PAR(3)

! Materials !
! 650ppm Boron in moderator !
'H2O-1' = MAT(NB/.670/1001,11.183; 8016,88.752; 5010,0.012; 5011,0.053)
! Unborated moderator !
'H2O-2' = MAT(NB/1.0/1001,11.19; 8016,88.81)
! Cladding !
Zy2 = MAT(NB/6.56/40002,100.0)
'Zy2-1' = MAT(NB/6.56/40002,100.0)
! Fuel !
'UO2-1' = MAT(10.5216/ 92234,3.4729E-02; 92235,4.0000; 92236,1.8400E-02;
  92238,95.947; 8016,0)

! BPR poison (WABA) !
'boron1' = MAT(0/ 8016,3.9506E-02 ;6000,3.9521E-03 ;13027,2.6344E-02;
  5010,3.0697E-03; 5011,1.2753E-02)
'boron2' = MAT(0/ 8016,3.9506E-02 ;6000,3.9521E-03 ;13027,2.6344E-02;
  5010,3.0697E-03; 5011,1.2753E-02)
'air' = MAT(0/ 7014,5.000E-05)

! Geometry !
Pin = CCS($rpe,$rair,$rcan//fuel,gap,clad)
Whole = CCS($rcool,$rbox//water,clad)
Bpin = CCS($rwco,$rwbox,$rwair,$rwaba,$rwabair,$rcro,
  $rcool,$rbox//water,clad1,gap,crod,gap,clad1,water,clad)

$cell = PAR(("-$p2", "-$p2") ("-$p2", $p2) ($p2, $p2) ($p2, "-$p2") !nodes 1-4!
(0, "-$p2") ("-$p2", 0) (0, $p2) ($p2, 0) ($rcan, 0) (0, "-$rcan") ("-$rcan", 0)
(0, $rcan) ($psq2, $psq2) ($psq2, "-$psq2") ("-$psq2", "-$psq2") ("-$psq2", $psq2)
/4, cool/Pin(0,0)/ 1,6,11,15,cool; 6,2,16,11,cool; 2,7,12,16,cool;
7,3,13,12,cool; 3,8,9,13,cool; 8,4,14,9,cool; 4,5,10,14,cool)

$wcell = PAR(("-$p2", "-$p2") ("-$p2", $p2) ($p2, $p2) ($p2, "-$p2") !nodes 1-4!
(0, "-$p2") ("-$p2", 0) (0, $p2) ($p2, 0) ($rbox, 0) (0, "-$rbox") ("-$rbox", 0)
(0, $rbox) ($psqh2, $psqh2) ($psqh2, "-$psqh2") ("-$psqh2", "-$psqh2")
("-$psqh2", $psqh2)/4, cool/Whole(0,0)/ 1,6,11,15,cool; 6,2,16,11,cool;
2,7,12,16,cool; 7,3,13,12,cool; 3,8,9,13,cool; 8,4,14,9,cool; 4,5,10,14,cool)

```

```

$bc11 = PAR("-$p2", "$p2") ("-$p2", $p2) ($p2, $p2) ($p2, "$p2") !nodes 1-4!
(0, "$p2") ("-$p2", 0) (0, $p2) ($p2, 0) ($rbox, 0) (0, "$rbox") ("-$rbox", 0)
(0, $rbox) ($psqh2, $psqh2) ($psqh2, "$psqh2") ("-$psqh2", "$psqh2")
("$psqh2", $psqh2)/4, cool/Bpin(0,0)/ 1, 6, 11, 15, cool; 6, 2, 16, 11, cool;
2, 7, 12, 16, cool; 7, 3, 13, 12, cool; 3, 8, 9, 13, cool; 8, 4, 14, 9, cool; 4, 5, 10, 14, cool)
$wgap = PAR("-$pgap2", "$p2") ("-$pgap2", $p2) ($pgap2, $p2) ($pgap2, "$p2")
/4, cool//)

$cell2 = PAR("-$p2", "$p2") ("-$p2", 0) ($p2, 0) ($p2, "$p2")
(0, "$p2") ($rcan, 0) (0, "$rcan") ("-$rcan", 0) ($psq2, "$psq2")
("$psq2", "$psq2") /4, cool/Pin(0,0) 3/ 3, 4, 9, 6, cool; 4, 5, 7, 9, cool;
5, 1, 10, 7, cool)

$wcell2 = PAR("-$p2", "$p2") ("-$p2", 0) ($p2, 0) ($p2, "$p2")
(0, "$p2") ($rbox, 0) (0, "$rbox") ("-$rbox", 0) ($psqh2, "$psqh2")
("$psqh2", "$psqh2") /4, cool/Whole(0,0) 2/3, 4, 9, 6, cool; 4, 5, 7, 9, cool;
5, 1, 10, 7, cool)

$bc112 = PAR("-$p2", "$p2") ("-$p2", 0) ($p2, 0) ($p2, "$p2")
(0, "$p2") ($rbox, 0) (0, "$rbox") ("-$rbox", 0) ($psqh2, "$psqh2")
("$psqh2", "$psqh2") /4, cool/Bpin(0,0) 8/3, 4, 9, 6, cool; 4, 5, 7, 9, cool;
5, 1, 10, 7, cool)

$wgap2 = PAR("-$pgap2", "$p2") ("-$pgap2", 0) ($pgap2, 0) ($pgap2, "$p2")
/4, cool//)

$wcell4 = PAR((0, "$p2") (0,0) ($p2, 0) ($p2, "$p2")
($rbox, 0) (0, "$rbox") ($psqh2, "$psqh2")
/4, cool/Whole(0,0) 2/4, 1, 6, 7, cool)

$wgap4 = PAR("-$pgap2", "$pgap2") ("-$pgap2", $pgap2) ($pgap2, $pgap2 )
($pgap2, "$pgap2") /4, cool//)

'1.0' = STR($cell)
'3.0' = STR($wcell)
'4.0' = STR($bc11)
'5.0' = STR($cell2)
'7.0' = STR($wcell2)
'8.0' = STR($bc112)
'9.0' = STR($wcell4)
'10.0' = STR($wgap)
'11.0' = STR($wgap2)
'12.0' = STR($wgap4)

White = ALB(1/1/1)

$corder = PAR((1, 3, 4) $coup(2, 2, 1) /
(2, 3, 4) $coup(3, 2, 1) / (3, 3, 4) $coup(4, 2, 1) /
(4, 3, 4) $coup(5, 2, 1) / (5, 3, 4) $coup(6, 2, 1) /
(6, 3, 4) $coup(7, 2, 1) / (7, 3, 4) $coup(8, 2, 1) /
(8, 3, 4) $coup(9, 2, 1) / (9, 3, 4) $coup(10, 2, 1))
$corder1 = PAR((1, 4, 1) $coup(2, 2, 1) /
(2, 3, 4) $coup(3, 2, 1) / (3, 3, 4) $coup(4, 2, 1) /
(4, 3, 4) $coup(5, 2, 1) / (5, 3, 4) $coup(6, 2, 1) /
(6, 3, 4) $coup(7, 2, 1) / (7, 3, 4) $coup(8, 2, 1) /
(8, 3, 4) $coup(9, 2, 1) / (9, 3, 4) $coup(10, 2, 1))
$corder2 = PAR((1, 4, 1) $coup(2, 3, 2) /
(2, 4, 1) $coup(3, 3, 2) / (3, 4, 1) $coup(4, 3, 2) /
(4, 4, 1) $coup(5, 3, 2) / (5, 4, 1) $coup(6, 3, 2) /
(6, 4, 1) $coup(7, 3, 2) / (7, 4, 1) $coup(8, 3, 2) /
(8, 4, 1) $coup(9, 3, 2) / (9, 4, 1) $coup(10, 3, 2))

Row1=CNX('9.0', '5.0', '5.0', '8.0', '5.0', '5.0', '7.0', '5.0', '5.0', '11.0'/$corder)
Row2=CNX('5.0', '1.0', '1.0', '1.0', '1.0', '1.0', '1.0', '1.0', '1.0', '10.0'/$corder1)
Row3=CNX('5.0', '1.0', '1.0', '1.0', '1.0', '1.0', '1.0', '1.0', '1.0', '10.0'/$corder1)
Row4=CNX('8.0', '1.0', '1.0', '3.0', '1.0', '1.0', '4.0', '1.0', '1.0', '10.0'/$corder1)
Row5=CNX('5.0', '1.0', '1.0', '1.0', '1.0', '1.0', '1.0', '1.0', '1.0', '10.0'/$corder1)
Row6=CNX('5.0', '1.0', '1.0', '1.0', '1.0', '3.0', '1.0', '1.0', '1.0', '10.0'/$corder1)
Row7=CNX('7.0', '1.0', '1.0', '4.0', '1.0', '1.0', '1.0', '1.0', '1.0', '10.0'/$corder1)
Row8=CNX('5.0', '1.0', '1.0', '1.0', '1.0', '1.0', '1.0', '1.0', '1.0', '10.0'/$corder1)
Row9=CNX('5.0', '1.0', '1.0', '1.0', '1.0', '1.0', '1.0', '1.0', '1.0', '10.0'/$corder1)
Row10=CNX('11.0', '10.0', '10.0', '10.0', '10.0', '10.0', '10.0', '10.0', '10.0', '10.0',

```

```

'12.0'/$corder2)

System =CNX (Row1,Row2,Row3,Row4,Row5,Row6,Row7,Row8,Row9,Row10/
(1-2,4,1)$coup(2-2,3,2)/
(2-2,4,1)$coup(3-2,3,2)/(3-2,4,1)$coup(4-2,3,2)/
(4-2,4,1)$coup(5-2,3,2)/(5-2,4,1)$coup(6-2,3,2)/
(6-2,4,1)$coup(7-2,3,2)/(7-2,4,1)$coup(8-2,3,2)/
(8-2,4,1)$coup(9-2,3,2)/(9-2,4,1)$coup(10-2,4,3))

System = BDRY((1-10,3)(10-1,2)$coup(0)/(1-1,2)(1-10,3)$coup(1-1,2)(10-1,2))

! Overlays !
AllMat = OVLN('H2O-1' /*-**-*/ Zy2 / /*-**-clad /
              'Zy2-1' /*-**-clad1 /
              'air' /*-**-gap /
              'UO2-1' /*-**-fuel /
              'boron1' /*-'4.0'-**-crod /
              'boron2' /*-'8.0'-**-crod)

All1 = OVLN(1.0 /*-**-**)
AllT = OVLN(600. /*-**-*/ 1000. /*-**-fuel / 620. /*-**-clad)
mos = OVSM(AllMat)
dos = OVSD(All1)
tos = OVST(AllT)

! Removal of BPRs for cold conditions !
CROMat = OVLN('H2O-1' /*-'4.0'-**-crod,*-'8.0'-**-crod,
              *-'4.0'-**-clad1,*-'8.0'-**-clad1,
              *-'4.0'-**-gap,*-'8.0'-**-gap)
moscr = OVSM(mos/CROMat)

! Low temperature !
LofT = OVLN(293.00 /*-**-**)
LofM = OVLN('H2O-2' /*-**-water, *--0-cool,
              *-'4.0'-**-crod,*-'8.0'-**-crod,
              *-'4.0'-**-clad1,*-'8.0'-**-clad1,
              *-'4.0'-**-gap,*-'8.0'-**-gap)
tLfes = OVST(tos/LofT)
mLfes = OVSM(moscr/LofM)

! Burnup !
st = STAT(mos,dos,tos,60.00)
stccr = STAT(moscr,dos,tos,60.00)
stloF = STAT(mLfes,dos,tLfes,60.00)
BU1 = PATH(/NC,(st),15000/15)
BU2 = PATH(BU1:15000/NC,(stccr),30000/30,(1826.25/5))
COLD1 = TREE(BU1/(stloF)/0,15000/15)
COLD2 = TREE(BU2/(stloF)/0,30000/30)

! Output !
G1 = GROUP(N/ 0)
G2 = GROUP(N/ 0.625, 0)
Gpins = AREA(*-**-water>,*-**-<fuel>)
Apins = AREA(<*-**-fuel>)
Aall = AREA(<*-**->)
Asol = AREA(<*-**-water,*--0-cool>)
Abur = AREA(<*-**-crod>)

ND = MICRO(G1, Apins / 92234, 92235, 92236, 92238, 93237,
           94238, 94239, 94240, 94241, 94242, 95241,
           95242, 95243,
           42595, 43599, 44601, 45603, 47609, 55633,
           62647, 62649, 62650, 62651, 62652, 60643,
           60645, 63651, 63653, 64655, 8016 /)

NDA = MICRO(G1, Apins / / )
NDB = MICRO(G1, Abur / 5010/ )

! Corners !
NE = FACE((1-10,2,4))
SE = FACE((10-10,4,2))
SW = FACE((10-1,1,3))
NW = FACE((1-1,1,3))

```



```
! Interior face !
Interior = FACE((1-1,2,1) (2-1,3,2) (3-1,3,2) (4-1,3,2)
               (5-1,3,2) (6-1,3,2) (7-1,3,2) (8-1,3,2)
               (9-1,3,2) (10-1,3,2))

! Exterior face !
Exterior = FACE((10-1,2,1) (10-2,2,1) (10-3,2,1) (10-4,2,1)
                (10-5,2,1) (10-6,2,1) (10-7,2,1) (10-8,2,1)
                (10-9,2,1) (10-10,2,1))

CurCorner = CUR(G2,NW,SW,SE,NE)
CurSide   = CUR(G2,Interior,Exterior)

'w17_waba_12_e40_15' = RUN()
```

HELIOS input file for Westinghouse 17 × 17 OFA assembly with 24 WABA BPRs present during the first 15 GWD/t of burnup

```

+HEL
'w17_waba_24_e40_15' =
  CASE('/fmdp/helios-1.6/babel-1.6/aix/sample-11/hy045n18g16a.dat'/
    'w17_waba_24_e40_15.hrf'/ '24 WABA BPR W17x17 assembly model')

! Westinghouse 17x17 OFA Assembly           !
! 24 WABA BPRs present during first 15 GWD/t burnup !
! 00 WABA BPRs during cold calcs           !

! Fuel !
$rpe = PAR("0.3922")
$rair = PAR("0.4001")
$rcan = PAR("0.4572")
! Guide tube !
$rcool = PAR("0.5613")
$rbox = PAR("0.6020")
! Burnable Poison Rod (WABA) !
$rwco = PAR("0.2858")
$rwbox = PAR("0.3391")
$rwair = PAR("0.3531")
$rwaba = PAR("0.4039")
$rwabair= PAR("0.4179")
$rcro = PAR("0.4839")

$rgap = PAR("0.04352") ! for assembly pitch of 21.50364 cm !
$pitch = PAR("1.2598")
$p2 = PAR("$pitch/2")
$psq2 = PAR("$rcan/2**0.5")
$psqh2 = PAR("$rbox/2**0.5")
$pgap2 = PAR("$rgap/2")
$coup = PAR(3)

! Materials !
! 650ppm Boron in moderator !
'H2O-1' = MAT(NB/.670/1001,11.183; 8016,88.752; 5010,0.012; 5011,0.053)
! Unborated moderator !
'H2O-2' = MAT(NB/1.0/1001,11.19; 8016,88.81)
! Cladding !
Zy2 = MAT(NB/6.56/40002,100.0)
'Zy2-1' = MAT(NB/6.56/40002,100.0)
! Fuel !
'UO2-1' = MAT(10.5216/ 92234,3.4729E-02; 92235,4.0000; 92236,1.8400E-02;
  92238,95.947; 8016,0)
! BPR poison (WABA) !
'boron1' = MAT(0/ 8016,3.9506E-02 ;6000,3.9521E-03 ;13027,2.6344E-02;
  5010,3.0697E-03; 5011,1.2753E-02)
'boron2' = MAT(0/ 8016,3.9506E-02 ;6000,3.9521E-03 ;13027,2.6344E-02;
  5010,3.0697E-03; 5011,1.2753E-02)
'air' = MAT(0/ 7014,5.000E-05)

! Geometry !
Pin = CCS($rpe,$rair,$rcan//fuel,gap,clad)
Whole = CCS($rcool,$rbox//water,clad)
Bpin = CCS($rwco,$rwbox,$rwair,$rwaba,$rwabair,$rcro,
  $rcool,$rbox//water,clad1,gap,crod,gap,clad1,water,clad)

$cell = PAR(("-$p2","-$p2") ("-$p2",$p2) ($p2,$p2) ($p2,"-$p2") !nodes 1-4!
(0,"-$p2") ("-$p2",0) (0,$p2) ($p2,0) ($rcan,0) (0,"-$rcan") ("-$rcan",0)
(0,$rcan) ($psq2,$psq2) ($psq2,"-$psq2") ("-$psq2","-$psq2") ("-$psq2",$psq2)
/4,cool/Pin(0,0)/ 1,6,11,15,cool; 6,2,16,11,cool; 2,7,12,16,cool;
7,3,13,12,cool; 3,8,9,13,cool; 8,4,14,9,cool; 4,5,10,14,cool)

$wcell = PAR(("-$p2","-$p2") ("-$p2",$p2) ($p2,$p2) ($p2,"-$p2") !nodes 1-4!
(0,"-$p2") ("-$p2",0) (0,$p2) ($p2,0) ($rbox,0) (0,"-$rbox") ("-$rbox",0)
(0,$rbox) ($psqh2,$psqh2) ($psqh2,"-$psqh2") ("-$psqh2","-$psqh2")
("-$psqh2",$psqh2)/4,cool/Whole(0,0)/ 1,6,11,15,cool; 6,2,16,11,cool;
2,7,12,16,cool;7,3,13,12,cool; 3,8,9,13,cool; 8,4,14,9,cool; 4,5,10,14,cool)

```

```

$bcell = PAR(("-$p2", "-$p2") ("-$p2", $p2) ($p2, $p2) ($p2, "-$p2") !nodes 1-4!
(0, "-$p2") ("-$p2", 0) (0, $p2) ($p2, 0) ($rbox, 0) (0, "-$rbox") ("-$rbox", 0)
(0, $rbox) ($psqh2, $psqh2) ($psqh2, "-$psqh2") ("-$psqh2", "-$psqh2")
("-$psqh2", $psqh2)/4, cool/Bpin(0, 0)/ 1, 6, 11, 15, cool; 6, 2, 16, 11, cool;
2, 7, 12, 16, cool; 7, 3, 13, 12, cool; 3, 8, 9, 13, cool; 8, 4, 14, 9, cool; 4, 5, 10, 14, cool)

$wgap = PAR(("-$pgap2", "-$p2") ("-$pgap2", $p2) ($pgap2, $p2) ($pgap2, "-$p2")
/4, cool//)

$cell2 = PAR(("-$p2", "-$p2") ("-$p2", 0) ($p2, 0) ($p2, "-$p2")
(0, "-$p2") ($rcan, 0) (0, "-$rcan") ("-$rcan", 0) ($psq2, "-$psq2")
("-$psq2", "-$psq2") /4, cool/Pin(0, 0) 3/ 3, 4, 9, 6, cool; 4, 5, 7, 9, cool;
5, 1, 10, 7, cool)

$wcell2 = PAR(("-$p2", "-$p2") ("-$p2", 0) ($p2, 0) ($p2, "-$p2")
(0, "-$p2") ($rbox, 0) (0, "-$rbox") ("-$rbox", 0) ($psqh2, "-$psqh2")
("-$psqh2", "-$psqh2") /4, cool/Whole(0, 0) 2/3, 4, 9, 6, cool; 4, 5, 7, 9, cool;
5, 1, 10, 7, cool)

$bcell2 = PAR(("-$p2", "-$p2") ("-$p2", 0) ($p2, 0) ($p2, "-$p2")
(0, "-$p2") ($rbox, 0) (0, "-$rbox") ("-$rbox", 0) ($psqh2, "-$psqh2")
("-$psqh2", "-$psqh2") /4, cool/Bpin(0, 0) 8/3, 4, 9, 6, cool; 4, 5, 7, 9, cool;
5, 1, 10, 7, cool)

$wgap2 = PAR(("-$pgap2", "-$p2") ("-$pgap2", 0) ($pgap2, 0) ($pgap2, "-$p2")
/4, cool//)

$wcell4 = PAR((0, "-$p2") (0, 0) ($p2, 0) ($p2, "-$p2")
($rbox, 0) (0, "-$rbox") ($psqh2, "-$psqh2")
/4, cool/Whole(0, 0) 2/4, 1, 6, 7, cool)

$wgap4 = PAR(("-$pgap2", "-$pgap2") ("-$pgap2", $pgap2) ($pgap2, $pgap2 )
($pgap2, "-$pgap2") /4, cool//)

'1.0' = STR($cell)
'3.0' = STR($wcell)
'4.0' = STR($bcell)
'5.0' = STR($cell2)
'7.0' = STR($wcell2)
'8.0' = STR($bcell2)
'9.0' = STR($wcell4)
'10.0' = STR($wgap)
'11.0' = STR($wgap2)
'12.0' = STR($wgap4)

White = ALB(1/1/1)

$corder = PAR((1, 3, 4) $coup(2, 2, 1) /
(2, 3, 4) $coup(3, 2, 1) / (3, 3, 4) $coup(4, 2, 1) /
(4, 3, 4) $coup(5, 2, 1) / (5, 3, 4) $coup(6, 2, 1) /
(6, 3, 4) $coup(7, 2, 1) / (7, 3, 4) $coup(8, 2, 1) /
(8, 3, 4) $coup(9, 2, 1) / (9, 3, 4) $coup(10, 2, 1))
$corder1 = PAR((1, 4, 1) $coup(2, 2, 1) /
(2, 3, 4) $coup(3, 2, 1) / (3, 3, 4) $coup(4, 2, 1) /
(4, 3, 4) $coup(5, 2, 1) / (5, 3, 4) $coup(6, 2, 1) /
(6, 3, 4) $coup(7, 2, 1) / (7, 3, 4) $coup(8, 2, 1) /
(8, 3, 4) $coup(9, 2, 1) / (9, 3, 4) $coup(10, 2, 1))
$corder2 = PAR((1, 4, 1) $coup(2, 3, 2) /
(2, 4, 1) $coup(3, 3, 2) / (3, 4, 1) $coup(4, 3, 2) /
(4, 4, 1) $coup(5, 3, 2) / (5, 4, 1) $coup(6, 3, 2) /
(6, 4, 1) $coup(7, 3, 2) / (7, 4, 1) $coup(8, 3, 2) /
(8, 4, 1) $coup(9, 3, 2) / (9, 4, 1) $coup(10, 3, 2))

Row1=CNX('9.0', '5.0', '5.0', '8.0', '5.0', '5.0', '8.0', '5.0', '5.0', '11.0'/$corder)
Row2=CNX('5.0', '1.0', '1.0', '1.0', '1.0', '1.0', '1.0', '1.0', '1.0', '10.0'/$corder1)
Row3=CNX('5.0', '1.0', '1.0', '1.0', '1.0', '1.0', '1.0', '1.0', '1.0', '10.0'/$corder1)
Row4=CNX('8.0', '1.0', '1.0', '4.0', '1.0', '1.0', '4.0', '1.0', '1.0', '10.0'/$corder1)
Row5=CNX('5.0', '1.0', '1.0', '1.0', '1.0', '1.0', '1.0', '1.0', '1.0', '10.0'/$corder1)
Row6=CNX('5.0', '1.0', '1.0', '1.0', '1.0', '4.0', '1.0', '1.0', '1.0', '10.0'/$corder1)
Row7=CNX('8.0', '1.0', '1.0', '4.0', '1.0', '1.0', '1.0', '1.0', '1.0', '10.0'/$corder1)
Row8=CNX('5.0', '1.0', '1.0', '1.0', '1.0', '1.0', '1.0', '1.0', '1.0', '10.0'/$corder1)
Row9=CNX('5.0', '1.0', '1.0', '1.0', '1.0', '1.0', '1.0', '1.0', '1.0', '10.0'/$corder1)

```

```

Row10=CNX('11.0','10.0','10.0','10.0','10.0','10.0','10.0','10.0','10.0',
'12.0'/$corder2)

System =CNX(Row1,Row2,Row3,Row4,Row5,Row6,Row7,Row8,Row9,Row10/
(1-2,4,1)$coup(2-2,3,2)/
(2-2,4,1)$coup(3-2,3,2)/(3-2,4,1)$coup(4-2,3,2)/
(4-2,4,1)$coup(5-2,3,2)/(5-2,4,1)$coup(6-2,3,2)/
(6-2,4,1)$coup(7-2,3,2)/(7-2,4,1)$coup(8-2,3,2)/
(8-2,4,1)$coup(9-2,3,2)/(9-2,4,1)$coup(10-2,4,3))

System = BDRY((1-10,3)(10-1,2)$coup(0)/(1-1,2)(1-10,3)$coup(1-1,2)(10-1,2))

! Overlays !
AllMat = OVLM('H2O-1' /*-**-*/ Zy2 / *-**-clad /
'Zy2-1' /*-**-clad1 /
'air' /*-**-gap /
'UO2-1' /*-**-fuel /
'boron1' /*-4.0'-*-crod /
'boron2' /*-8.0'-*-crod)

All1 = OVLD(1.0 /*-**-**)
AllT = OVLT(600. /*-**-*/ 1000. /*-**-fuel / 620. /*-**-clad)
mos = OVSM(AllMat)
dos = OVSD(All1)
tos = OVST(AllT)

! Removal of BPRs for cold conditions !
CROMat = OVLM('H2O-1' /*-4.0'-*-crod,*-8.0'-*-crod,
*-4.0'-*-clad1,*-8.0'-*-clad1,
*-4.0'-*-gap,*-8.0'-*-gap)
moscr = OVSM(mos/CROMat)

! Low temperature !
LoFT = OVLT(293.00 /*-**-**)
LoFM = OVLM('H2O-2' /*-**-water, *-**-0-cool,
*-4.0'-*-crod,*-8.0'-*-crod,
*-4.0'-*-clad1,*-8.0'-*-clad1,
*-4.0'-*-gap,*-8.0'-*-gap)
tLfes = OVST(tos/LoFT)
mLfes = OVSM(moscr/LoFM)

! Burnup !
st = STAT(mos,dos,tos,60.00)
stccr = STAT(moscr,dos,tos,60.00)
stloF = STAT(mLfes,dos,tLfes,60.00)
BU1 = PATH(/NC,(st),15000/15)
BU2 = PATH(BU1:15000/NC,(stccr),30000/30,(1826.25/5))
COLD1 = TREE(BU1/(stloF)/0,15000/15)
COLD2 = TREE(BU2/(stloF)/0,30000/30)

! Output !
G1 = GROUP(N/ 0)
G2 = GROUP(N/ 0.625, 0)
Gpins = AREA(*-**-<water>,*-**-<fuel>)
Apins = AREA(<*-**-fuel>)
Aall = AREA(<*-**-**)
Asol = AREA(<*-**-water,*-**-0-cool>)
Abur = AREA(<*-**-crod>)

ND = MICRO(G1, Apins / 92234, 92235, 92236, 92238, 93237,
94238, 94239, 94240, 94241, 94242, 95241,
95242, 95243,
42595, 43599, 44601, 45603, 47609, 55633,
62647, 62649, 62650, 62651, 62652, 60643,
60645, 63651, 63653, 64655, 8016 /)

NDA = MICRO(G1, Apins / / )
NDB = MICRO(G1, Abur / 5010/ )

! Corners !
NE = FACE((1-10,2,4))
SE = FACE((10-10,4,2))
SW = FACE((10-1,1,3))

```

```
NW = FACE((1-1,1,3))

! Interior face !
Interior = FACE((1-1,2,1) (2-1,3,2) (3-1,3,2) (4-1,3,2)
               (5-1,3,2) (6-1,3,2) (7-1,3,2) (8-1,3,2)
               (9-1,3,2) (10-1,3,2))

! Exterior face !
Exterior = FACE((10-1,2,1) (10-2,2,1) (10-3,2,1) (10-4,2,1)
                (10-5,2,1) (10-6,2,1) (10-7,2,1) (10-8,2,1)
                (10-9,2,1) (10-10,2,1))

CurCorner = CUR(G2,NW,SW,SE,NE)
CurSide   = CUR(G2,Interior,Exterior)

'w17_waba_24_e40_15' = RUN()
```

HELIOS input file for Westinghouse 17 × 17 OFA assembly with 12 BAA BPRs present during the first 15 Gwd/t of burnup

```

+HEL
'w17_baa_12_e40_15' =
  CASE('/fmdp/helios-1.6/babel-1.6/aix/sample-11/hy045n18g16a.dat'/
    'w17_baa_12_e40_15.hrf'/ '12 BAA BPR W17x17 assembly model')

! Westinghouse 17x17 OFA Assembly           !
! 12 BAA BPRs present during first 15 Gwd/t burnup !
! 00 BAA BPRs during cold calcs           !

! Fuel !
$rpe = PAR("0.3922")
$rair = PAR("0.4001")
$rscan = PAR("0.4572")
! Guide tube !
$rcool = PAR("0.5613")
$rbox = PAR("0.6020")
! Burnable Poison Rod (BAA) !
$rwco = PAR("0.21400")
$rwbox = PAR("0.23051")
$rwair = PAR("0.24130")
$rbaa = PAR("0.42672")
$rbaair = PAR("0.43688")
$rcro = PAR("0.48387")

$rgap = PAR("0.04352") ! for assembly pitch of 21.50364 cm !
$pitch = PAR("1.2598")
$p2 = PAR("$pitch/2")
$psq2 = PAR("$rscan/2**0.5")
$psq2h = PAR("$rbox/2**0.5")
$pgap2 = PAR("$rgap/2")
$coup = PAR(3)

! Materials !
! 650ppm Boron in moderator !
'H2O-1' = MAT(NB/.670/1001,11.183; 8016,88.752; 5010,0.012; 5011,0.053)
! Unborated moderator !
'H2O-2' = MAT(NB/1.0/1001,11.19; 8016,88.81)
! Cladding !
Zy2 = MAT(NB/6.56/40002,100.0)
! BPR Cladding (BAA) !
'SS304' = MAT(7.94/ 6000, 0.080; 14000, 1.000; 15031, 0.045;
  24000, 19.000; 25055, 2.000; 26000, 68.375;
  28000, 9.500)

! Fuel !
'UO2-1' = MAT(10.5216/ 92234,3.4729E-02; 92235,4.0000; 92236,1.8400E-02;
  92238,95.947; 8016,0)

! BPR poison (BAA) !
'boron1' = MAT(0/ 8016,0.04497; 11023,0.00165; 13027,0.00058;
  14000,0.01799; 19000,0.00011; 5010,9.595E-04;
  5011,3.863E-03)
'boron2' = MAT(0/ 8016,0.04497; 11023,0.00165; 13027,0.00058;
  14000,0.01799; 19000,0.00011; 5010,9.595E-04;
  5011,3.863E-03)
'air' = MAT(0/ 7014,5.000E-05)

! Geometry !
Pin = CCS($rpe,$rair,$rscan//fuel,gap,clad)
Whole = CCS($rcool,$rbox//water,clad)
Bpin = CCS($rwco,$rwbox,$rwair,$rbaa,$rbaair,$rcro,
  $rcool,$rbox//gap,clad1,gap,crod,gap,clad1,water,clad)

$cell = PAR(("-$p2", "-$p2") ("-$p2", $p2) ($p2, $p2) ($p2, "-$p2") !nodes 1-4!
(0, "-$p2") ("-$p2", 0) (0, $p2) ($p2, 0) ($rscan, 0) (0, "-$rscan") ("-$rscan", 0)
(0, $rscan) ($psq2, $psq2) ($psq2, "-$psq2") ("-$psq2", "-$psq2") ("-$psq2", $psq2)
/4,cool/Pin(0,0)/ 1,6,11,15,cool; 6,2,16,11,cool; 2,7,12,16,cool;
7,3,13,12,cool; 3,8,9,13,cool; 8,4,14,9,cool; 4,5,10,14,cool)

```

```

$wcell = PAR(("-$p2", "-$p2") ("-$p2", $p2) ($p2, $p2) ($p2, "-$p2") !nodes 1-4!
(0, "-$p2") ("-$p2", 0) (0, $p2) ($p2, 0) ($rbox, 0) (0, "-$rbox") ("-$rbox", 0)
(0, $rbox) ($psqh2, $psqh2) ($psqh2, "-$psqh2") ("-$psqh2", "-$psqh2")
("-$psqh2", $psqh2)/4, cool/Whole(0, 0) / 1, 6, 11, 15, cool; 6, 2, 16, 11, cool;
2, 7, 12, 16, cool; 7, 3, 13, 12, cool; 3, 8, 9, 13, cool; 8, 4, 14, 9, cool; 4, 5, 10, 14, cool)

$bcell = PAR(("-$p2", "-$p2") ("-$p2", $p2) ($p2, $p2) ($p2, "-$p2") !nodes 1-4!
(0, "-$p2") ("-$p2", 0) (0, $p2) ($p2, 0) ($rbox, 0) (0, "-$rbox") ("-$rbox", 0)
(0, $rbox) ($psqh2, $psqh2) ($psqh2, "-$psqh2") ("-$psqh2", "-$psqh2")
("-$psqh2", $psqh2)/4, cool/Bpin(0, 0) / 1, 6, 11, 15, cool; 6, 2, 16, 11, cool;
2, 7, 12, 16, cool; 7, 3, 13, 12, cool; 3, 8, 9, 13, cool; 8, 4, 14, 9, cool; 4, 5, 10, 14, cool)

$wgap = PAR(("-$pgap2", "-$p2") ("-$pgap2", $p2) ($pgap2, $p2) ($pgap2, "-$p2")
/4, cool//)

$cell2 = PAR(("-$p2", "-$p2") ("-$p2", 0) ($p2, 0) ($p2, "-$p2")
(0, "-$p2") ($rcan, 0) (0, "-$rcan") ("-$rcan", 0) ($psq2, "-$psq2")
("-$psq2", "-$psq2") /4, cool/Pin(0, 0) 3/ 3, 4, 9, 6, cool; 4, 5, 7, 9, cool;
5, 1, 10, 7, cool)

$wcell2 = PAR(("-$p2", "-$p2") ("-$p2", 0) ($p2, 0) ($p2, "-$p2")
(0, "-$p2") ($rbox, 0) (0, "-$rbox") ("-$rbox", 0) ($psqh2, "-$psqh2")
("-$psqh2", "-$psqh2")/4, cool/Whole(0, 0) 2/3, 4, 9, 6, cool; 4, 5, 7, 9, cool;
5, 1, 10, 7, cool)

$bcell2 = PAR(("-$p2", "-$p2") ("-$p2", 0) ($p2, 0) ($p2, "-$p2")
(0, "-$p2") ($rbox, 0) (0, "-$rbox") ("-$rbox", 0) ($psqh2, "-$psqh2")
("-$psqh2", "-$psqh2")/4, cool/Bpin(0, 0) 8/3, 4, 9, 6, cool; 4, 5, 7, 9, cool;
5, 1, 10, 7, cool)

$wgap2 = PAR(("-$pgap2", "-$p2") ("-$pgap2", 0) ($pgap2, 0) ($pgap2, "-$p2")
/4, cool//)

$wcell4 = PAR((0, "-$p2") (0, 0) ($p2, 0) ($p2, "-$p2")
($rbox, 0) (0, "-$rbox") ($psqh2, "-$psqh2")
/4, cool/Whole(0, 0) 2/4, 1, 6, 7, cool)

$wgap4 = PAR(("-$pgap2", "-$pgap2") ("-$pgap2", $pgap2) ($pgap2, $pgap2 )
($pgap2, "-$pgap2") /4, cool//)

'1.0' = STR($cell)
'3.0' = STR($wcell)
'4.0' = STR($bcell)
'5.0' = STR($cell2)
'7.0' = STR($wcell2)
'8.0' = STR($bcell2)
'9.0' = STR($wcell4)
'10.0' = STR($wgap)
'11.0' = STR($wgap2)
'12.0' = STR($wgap4)

White = ALB(1/1/1)

$corder = PAR((1, 3, 4) $coup(2, 2, 1) /
(2, 3, 4) $coup(3, 2, 1) / (3, 3, 4) $coup(4, 2, 1) /
(4, 3, 4) $coup(5, 2, 1) / (5, 3, 4) $coup(6, 2, 1) /
(6, 3, 4) $coup(7, 2, 1) / (7, 3, 4) $coup(8, 2, 1) /
(8, 3, 4) $coup(9, 2, 1) / (9, 3, 4) $coup(10, 2, 1))
$corder1 = PAR((1, 4, 1) $coup(2, 2, 1) /
(2, 3, 4) $coup(3, 2, 1) / (3, 3, 4) $coup(4, 2, 1) /
(4, 3, 4) $coup(5, 2, 1) / (5, 3, 4) $coup(6, 2, 1) /
(6, 3, 4) $coup(7, 2, 1) / (7, 3, 4) $coup(8, 2, 1) /
(8, 3, 4) $coup(9, 2, 1) / (9, 3, 4) $coup(10, 2, 1))
$corder2 = PAR((1, 4, 1) $coup(2, 3, 2) /
(2, 4, 1) $coup(3, 3, 2) / (3, 4, 1) $coup(4, 3, 2) /
(4, 4, 1) $coup(5, 3, 2) / (5, 4, 1) $coup(6, 3, 2) /
(6, 4, 1) $coup(7, 3, 2) / (7, 4, 1) $coup(8, 3, 2) /
(8, 4, 1) $coup(9, 3, 2) / (9, 4, 1) $coup(10, 3, 2))

Row1=CNX('9.0', '5.0', '5.0', '8.0', '5.0', '5.0', '7.0', '5.0', '5.0', '11.0'/$corder)
Row2=CNX('5.0', '1.0', '1.0', '1.0', '1.0', '1.0', '1.0', '1.0', '1.0', '10.0'/$corder1)
Row3=CNX('5.0', '1.0', '1.0', '1.0', '1.0', '1.0', '1.0', '1.0', '1.0', '10.0'/$corder1)

```

```

Row4=CNX('8.0','1.0','1.0','3.0','1.0','1.0','4.0','1.0','1.0','10.0'/$corder1)
Row5=CNX('5.0','1.0','1.0','1.0','1.0','1.0','1.0','1.0','1.0','10.0'/$corder1)
Row6=CNX('5.0','1.0','1.0','1.0','1.0','1.0','3.0','1.0','1.0','10.0'/$corder1)
Row7=CNX('7.0','1.0','1.0','4.0','1.0','1.0','1.0','1.0','1.0','10.0'/$corder1)
Row8=CNX('5.0','1.0','1.0','1.0','1.0','1.0','1.0','1.0','1.0','10.0'/$corder1)
Row9=CNX('5.0','1.0','1.0','1.0','1.0','1.0','1.0','1.0','1.0','10.0'/$corder1)
Row10=CNX('11.0','10.0','10.0','10.0','10.0','10.0','10.0','10.0','10.0','10.0',
'12.0'/$corder2)

System =CNX(Row1,Row2,Row3,Row4,Row5,Row6,Row7,Row8,Row9,Row10/
(1-2,4,1)$coup(2-2,3,2)/
(2-2,4,1)$coup(3-2,3,2)/(3-2,4,1)$coup(4-2,3,2)/
(4-2,4,1)$coup(5-2,3,2)/(5-2,4,1)$coup(6-2,3,2)/
(6-2,4,1)$coup(7-2,3,2)/(7-2,4,1)$coup(8-2,3,2)/
(8-2,4,1)$coup(9-2,3,2)/(9-2,4,1)$coup(10-2,4,3))

System = BDRY((1-10,3)(10-1,2)$coup(0)/(1-1,2)(1-10,3)$coup(1-1,2)(10-1,2))

! Overlays !
AllMat = OVLM('H2O-1' /*-**-*/ Zy2 / *-**-clad /
'SS304' /*-**-clad1 /
'air' /*-**-gap /
'UO2-1' /*-**-fuel /
'boron1' /*-4.0'-*-crod /
'boron2' /*-8.0'-*-crod)

All1 = OVLD(1.0 /*-**-**)
AllT = OVLT(600. /*-**-*/ 1000. /*-**-fuel / 620. /*-**-clad)
mos = OVSM(AllMat)
dos = OVSD(All1)
tos = OVST(AllT)

! Removal of BPRs for cold conditions !
CROMat = OVLM('H2O-1' /*-4.0'-*-crod,*-8.0'-*-crod,
*-4.0'-*-clad1,*-8.0'-*-clad1,
*-4.0'-*-gap,*-8.0'-*-gap)
moscr = OVSM(mos/CROMat)

! Low temperature !
LofT = OVLT(293.00 /*-**-**)
LofM = OVLM('H2O-2' /*-**-water, *-**-0-cool,
*-4.0'-*-crod,*-8.0'-*-crod,
*-4.0'-*-clad1,*-8.0'-*-clad1,
*-4.0'-*-gap,*-8.0'-*-gap)
tLfes = OVST(tos/LofT)
mLfes = OVSM(moscr/LofM)

! Burnup !
st = STAT(mos,dos,tos,60.00)
stccr = STAT(moscr,dos,tos,60.00)
stloF = STAT(mLfes,dos,tLfes,60.00)
BU1 = PATH(/NC,(st),15000/15)
BU2 = PATH(BU1:15000/NC,(stccr),30000/30,(1826.25/5))
COLD1 = TREE(BU1/(stloF)/0,15000/15)
COLD2 = TREE(BU2/(stloF)/0,30000/30)

! Output !
G1 = GROUP(N/ 0)
G2 = GROUP(N/ 0.625, 0)
Gpins = AREA(*-**-<water>,*-**-<fuel>)
Apins = AREA(<*-**-fuel>)
Aall = AREA(<*-**-**>)
Asol = AREA(<*-**-water,*-**-0-cool>)
Abur = AREA(<*-**-crod>)

ND = MICRO(G1, Apins / 92234, 92235, 92236, 92238, 93237,
94238, 94239, 94240, 94241, 94242, 95241,
95242, 95243,
42595, 43599, 44601, 45603, 47609, 55633,
62647, 62649, 62650, 62651, 62652, 60643,
60645, 63651, 63653, 64655, 8016 /)

```



```
NDA = MICRO(G1, Apins / / )
NDB = MICRO(G1, Abur / 5010/ )

! Corners !
NE = FACE((1-10,2,4))
SE = FACE((10-10,4,2))
SW = FACE((10-1,1,3))
NW = FACE((1-1,1,3))

! Interior face !
Interior = FACE((1-1,2,1) (2-1,3,2) (3-1,3,2) (4-1,3,2)
                (5-1,3,2) (6-1,3,2) (7-1,3,2) (8-1,3,2)
                (9-1,3,2) (10-1,3,2))

! Exterior face !
Exterior = FACE((10-1,2,1) (10-2,2,1) (10-3,2,1) (10-4,2,1)
                (10-5,2,1) (10-6,2,1) (10-7,2,1) (10-8,2,1)
                (10-9,2,1) (10-10,2,1))

CurCorner = CUR(G2,NW,SW,SE,NE)
CurSide   = CUR(G2,Interior,Exterior)

'w17_baa_12_e40_15' = RUN()
```

HELIOS input file for Westinghouse 17 × 17 OFA assembly with 24 BAA BPRs present during the first 15 Gwd/t of burnup

```

+HEL
'w17_baa_24_e40_15' =
  CASE('/fmdp/helios-1.6/babel-1.6/aix/sample-11/hy045n18g16a.dat'/
    'w17_baa_24_e40_15.hrf'/ '24 BAA BPR W17x17 assembly model')

! Westinghouse 17x17 OFA Assembly           !
! 24 BAA BPRs present during first 15 Gwd/t burnup !
! 00 BAA BPRs during cold calcs           !

! Fuel !
$rpe = PAR("0.3922")
$rair = PAR("0.4001")
$rscan = PAR("0.4572")
! Guide tube !
$rcool = PAR("0.5613")
$rbox = PAR("0.6020")
! Burnable Poison Rod (BAA) !
$rwco = PAR("0.21400")
$rwbox = PAR("0.23051")
$rwair = PAR("0.24130")
$rbaa = PAR("0.42672")
$rbaair = PAR("0.43688")
$rcro = PAR("0.48387")

$rgap = PAR("0.04352") ! for assembly pitch of 21.50364 cm !
$pitch = PAR("1.2598")
$p2 = PAR("$pitch/2")
$psq2 = PAR("$rscan/2**0.5")
$psq2h = PAR("$rbox/2**0.5")
$pgap2 = PAR("$rgap/2")
$coupl = PAR(3)

! Materials !
! 650ppm Boron in moderator !
'H2O-1' = MAT(NB/.670/1001,11.183; 8016,88.752; 5010,0.012; 5011,0.053)
! Unborated moderator !
'H2O-2' = MAT(NB/1.0/1001,11.19; 8016,88.81)
! Cladding !
Zy2 = MAT(NB/6.56/40002,100.0)
! BPR Cladding (BAA) !
'SS304' = MAT(7.94/ 6000, 0.080; 14000, 1.000; 15031, 0.045;
  24000, 19.000; 25055, 2.000; 26000, 68.375;
  28000, 9.500)

! Fuel !
'UO2-1' = MAT(10.5216/ 92234,3.4729E-02; 92235,4.0000; 92236,1.8400E-02;
  92238,95.947; 8016,0)

! BPR poison (BAA) !
'boron1' = MAT(0/ 8016,0.04497; 11023,0.00165; 13027,0.00058;
  14000,0.01799; 19000,0.00011; 5010,9.595E-04;
  5011,3.863E-03)
'boron2' = MAT(0/ 8016,0.04497; 11023,0.00165; 13027,0.00058;
  14000,0.01799; 19000,0.00011; 5010,9.595E-04;
  5011,3.863E-03)
'air' = MAT(0/ 7014,5.000E-05)

! Geometry !
Pin = CCS($rpe,$rair,$rscan//fuel,gap,clad)
Whole = CCS($rcool,$rbox//water,clad)
Bpin = CCS($rwco,$rwbox,$rwair,$rbaa,$rbaair,$rcro,
  $rcool,$rbox//gap,clad1,gap,crod,gap,clad1,water,clad)

$cell = PAR(("-$p2", "-$p2") ("-$p2", $p2) ($p2, $p2) ($p2, "-$p2") !nodes 1-4!
(0, "-$p2") ("-$p2", 0) (0, $p2) ($p2, 0) ($rscan, 0) (0, "-$rscan") ("-$rscan", 0)
(0, $rscan) ($psq2, $psq2) ($psq2, "-$psq2") ("-$psq2", "-$psq2") ("-$psq2", $psq2)
/4,cool/Pin(0,0)/ 1,6,11,15,cool; 6,2,16,11,cool; 2,7,12,16,cool;
7,3,13,12,cool; 3,8,9,13,cool; 8,4,14,9,cool; 4,5,10,14,cool)

```

```

$wcell = PAR(("-$p2", "-$p2") ("-$p2", $p2) ($p2, $p2) ($p2, "-$p2") !nodes 1-4!
(0, "-$p2") ("-$p2", 0) (0, $p2) ($p2, 0) ($rbox, 0) (0, "-$rbox") ("-$rbox", 0)
(0, $rbox) ($psqh2, $psqh2) ($psqh2, "-$psqh2") ("-$psqh2", "-$psqh2")
("-$psqh2", $psqh2)/4, cool/Whole(0, 0) / 1, 6, 11, 15, cool; 6, 2, 16, 11, cool;
2, 7, 12, 16, cool; 7, 3, 13, 12, cool; 3, 8, 9, 13, cool; 8, 4, 14, 9, cool; 4, 5, 10, 14, cool)

$bcell = PAR(("-$p2", "-$p2") ("-$p2", $p2) ($p2, $p2) ($p2, "-$p2") !nodes 1-4!
(0, "-$p2") ("-$p2", 0) (0, $p2) ($p2, 0) ($rbox, 0) (0, "-$rbox") ("-$rbox", 0)
(0, $rbox) ($psqh2, $psqh2) ($psqh2, "-$psqh2") ("-$psqh2", "-$psqh2")
("-$psqh2", $psqh2)/4, cool/Bpin(0, 0) / 1, 6, 11, 15, cool; 6, 2, 16, 11, cool;
2, 7, 12, 16, cool; 7, 3, 13, 12, cool; 3, 8, 9, 13, cool; 8, 4, 14, 9, cool; 4, 5, 10, 14, cool)

$wgap = PAR(("-$pgap2", "-$p2") ("-$pgap2", $p2) ($pgap2, $p2) ($pgap2, "-$p2")
/4, cool//)

$cell2 = PAR(("-$p2", "-$p2") ("-$p2", 0) ($p2, 0) ($p2, "-$p2")
(0, "-$p2") ($rcan, 0) (0, "-$rcan") ("-$rcan", 0) ($psq2, "-$psq2")
("-$psq2", "-$psq2") /4, cool/Pin(0, 0) 3/ 3, 4, 9, 6, cool; 4, 5, 7, 9, cool;
5, 1, 10, 7, cool)

$wcell2 = PAR(("-$p2", "-$p2") ("-$p2", 0) ($p2, 0) ($p2, "-$p2")
(0, "-$p2") ($rbox, 0) (0, "-$rbox") ("-$rbox", 0) ($psqh2, "-$psqh2")
("-$psqh2", "-$psqh2")/4, cool/Whole(0, 0) 2/3, 4, 9, 6, cool; 4, 5, 7, 9, cool;
5, 1, 10, 7, cool)

$bcell2 = PAR(("-$p2", "-$p2") ("-$p2", 0) ($p2, 0) ($p2, "-$p2")
(0, "-$p2") ($rbox, 0) (0, "-$rbox") ("-$rbox", 0) ($psqh2, "-$psqh2")
("-$psqh2", "-$psqh2")/4, cool/Bpin(0, 0) 8/3, 4, 9, 6, cool; 4, 5, 7, 9, cool;
5, 1, 10, 7, cool)

$wgap2 = PAR(("-$pgap2", "-$p2") ("-$pgap2", 0) ($pgap2, 0) ($pgap2, "-$p2")
/4, cool//)

$wcell4 = PAR((0, "-$p2") (0, 0) ($p2, 0) ($p2, "-$p2")
($rbox, 0) (0, "-$rbox") ($psqh2, "-$psqh2")
/4, cool/Whole(0, 0) 2/4, 1, 6, 7, cool)

$wgap4 = PAR(("-$pgap2", "-$pgap2") ("-$pgap2", $pgap2) ($pgap2, $pgap2 )
($pgap2, "-$pgap2") /4, cool//)

'1.0' = STR($cell)
'3.0' = STR($wcell)
'4.0' = STR($bcell)
'5.0' = STR($cell2)
'7.0' = STR($wcell2)
'8.0' = STR($bcell2)
'9.0' = STR($wcell4)
'10.0' = STR($wgap)
'11.0' = STR($wgap2)
'12.0' = STR($wgap4)

White = ALB(1/1/1)

$corder = PAR((1, 3, 4) $coup(2, 2, 1) /
(2, 3, 4) $coup(3, 2, 1) / (3, 3, 4) $coup(4, 2, 1) /
(4, 3, 4) $coup(5, 2, 1) / (5, 3, 4) $coup(6, 2, 1) /
(6, 3, 4) $coup(7, 2, 1) / (7, 3, 4) $coup(8, 2, 1) /
(8, 3, 4) $coup(9, 2, 1) / (9, 3, 4) $coup(10, 2, 1))
$corder1 = PAR((1, 4, 1) $coup(2, 2, 1) /
(2, 3, 4) $coup(3, 2, 1) / (3, 3, 4) $coup(4, 2, 1) /
(4, 3, 4) $coup(5, 2, 1) / (5, 3, 4) $coup(6, 2, 1) /
(6, 3, 4) $coup(7, 2, 1) / (7, 3, 4) $coup(8, 2, 1) /
(8, 3, 4) $coup(9, 2, 1) / (9, 3, 4) $coup(10, 2, 1))
$corder2 = PAR((1, 4, 1) $coup(2, 3, 2) /
(2, 4, 1) $coup(3, 3, 2) / (3, 4, 1) $coup(4, 3, 2) /
(4, 4, 1) $coup(5, 3, 2) / (5, 4, 1) $coup(6, 3, 2) /
(6, 4, 1) $coup(7, 3, 2) / (7, 4, 1) $coup(8, 3, 2) /
(8, 4, 1) $coup(9, 3, 2) / (9, 4, 1) $coup(10, 3, 2))

Row1=CNX('9.0', '5.0', '5.0', '8.0', '5.0', '5.0', '8.0', '5.0', '5.0', '11.0'/$corder)
Row2=CNX('5.0', '1.0', '1.0', '1.0', '1.0', '1.0', '1.0', '1.0', '1.0', '10.0'/$corder1)
Row3=CNX('5.0', '1.0', '1.0', '1.0', '1.0', '1.0', '1.0', '1.0', '1.0', '10.0'/$corder1)
Row4=CNX('8.0', '1.0', '1.0', '4.0', '1.0', '1.0', '4.0', '1.0', '1.0', '10.0'/$corder1)

```

```

Row5=CNX('5.0','1.0','1.0','1.0','1.0','1.0','1.0','1.0','1.0','1.0','10.0'/$corder1)
Row6=CNX('5.0','1.0','1.0','1.0','1.0','4.0','1.0','1.0','1.0','1.0','10.0'/$corder1)
Row7=CNX('8.0','1.0','1.0','4.0','1.0','1.0','1.0','1.0','1.0','1.0','10.0'/$corder1)
Row8=CNX('5.0','1.0','1.0','1.0','1.0','1.0','1.0','1.0','1.0','1.0','10.0'/$corder1)
Row9=CNX('5.0','1.0','1.0','1.0','1.0','1.0','1.0','1.0','1.0','1.0','10.0'/$corder1)
Row10=CNX('11.0','10.0','10.0','10.0','10.0','10.0','10.0','10.0','10.0','10.0',
'12.0'/$corder2)

System =CNX(Row1,Row2,Row3,Row4,Row5,Row6,Row7,Row8,Row9,Row10/
(1-2,4,1)$coup(2-2,3,2)/
(2-2,4,1)$coup(3-2,3,2)/(3-2,4,1)$coup(4-2,3,2)/
(4-2,4,1)$coup(5-2,3,2)/(5-2,4,1)$coup(6-2,3,2)/
(6-2,4,1)$coup(7-2,3,2)/(7-2,4,1)$coup(8-2,3,2)/
(8-2,4,1)$coup(9-2,3,2)/(9-2,4,1)$coup(10-2,4,3))

System = BDRY((1-10,3)(10-1,2)$coup(0)/(1-1,2)(1-10,3)$coup(1-1,2)(10-1,2))

! Overlays !
AllMat = OVLM('H2O-1' /*-**-*/ Zy2 / /*-**-clad /
'SS304' /*-**-clad1 /
'air' /*-**-gap /
'UO2-1' /*-**-fuel /
'boron1' /*-4.0'**-crod /
'boron2' /*-8.0'**-crod)

All1 = OVLD(1.0 /*-**-**)
AllT = OVLT(600. /*-**-*/ 1000. /*-**-fuel / 620. /*-**-clad)
mos = OVSM(AllMat)
dos = OVSD(All1)
tos = OVST(AllT)

! Removal of BPRs for cold conditions !
CROMat = OVLM('H2O-1' /*-4.0'**-crod,*-8.0'**-crod,
*-4.0'**-clad1,*-8.0'**-clad1,
*-4.0'**-gap,*-8.0'**-gap)
moscr = OVSM(mos/CROMat)

! Low temperature !
LofT = OVLT(293.00 /*-**-**)
LofM = OVLM('H2O-2' /*-**-water, *-**-0-cool,
*-4.0'**-crod,*-8.0'**-crod,
*-4.0'**-clad1,*-8.0'**-clad1,
*-4.0'**-gap,*-8.0'**-gap)

tLfes = OVST(tos/LofT)
mLfes = OVSM(moscr/LofM)

! Burnup !
st = STAT(mos,dos,tos,60.00)
stccr = STAT(moscr,dos,tos,60.00)
stloF = STAT(mLfes,dos,tLfes,60.00)
BU1 = PATH(/NC,(st),15000/15)
BU2 = PATH(BU1:15000/NC,(stccr),30000/30,(1826.25/5))
COLD1 = TREE(BU1/(stloF)/0,15000/15)
COLD2 = TREE(BU2/(stloF)/0,30000/30)

! Output !
G1 = GROUP(N/ 0)
G2 = GROUP(N/ 0.625, 0)
Gpins = AREA(*-**-<water>,*-**-<fuel>)
Apins = AREA(<*-**-fuel>)
Aall = AREA(<*-**->)
Asol = AREA(<*-**-water,*-**-0-cool>)
Abur = AREA(<*-**-crod>)

ND = MICRO(G1, Apins / 92234, 92235, 92236, 92238, 93237,
94238, 94239, 94240, 94241, 94242, 95241,
95242, 95243,
42595, 43599, 44601, 45603, 47609, 55633,
62647, 62649, 62650, 62651, 62652, 60643,
60645, 63651, 63653, 64655, 8016 /)

NDA = MICRO(G1, Apins / / )
NDB = MICRO(G1, Abur / 5010/ )

```

```
! Corners !
NE = FACE((1-10,2,4))
SE = FACE((10-10,4,2))
SW = FACE((10-1,1,3))
NW = FACE((1-1,1,3))

! Interior face !
Interior = FACE((1-1,2,1) (2-1,3,2) (3-1,3,2) (4-1,3,2)
               (5-1,3,2) (6-1,3,2) (7-1,3,2) (8-1,3,2)
               (9-1,3,2) (10-1,3,2))

! Exterior face !
Exterior = FACE((10-1,2,1) (10-2,2,1) (10-3,2,1) (10-4,2,1)
               (10-5,2,1) (10-6,2,1) (10-7,2,1) (10-8,2,1)
               (10-9,2,1) (10-10,2,1))

CurCorner = CUR(G2,NW,SW,SE,NE)
CurSide   = CUR(G2,Interior,Exterior)

'w17_baa_24_e40_15' = RUN()
```

HELIOS input file for B&W 15 × 15 assembly without BPRs present

```

+HEL
'bw15_0_00_e40_45' =
  CASE('/fmdp/helios-1.6/babel-1.6/aix/sample-11/hy045n18g16a.dat'/
    'bw15_0_00_e40_45.hrf'/ 'Reference BW15x15 assembly model')

! BW 15x15 Assembly !
! No BPRs present !

! Fuel !
$rpe = PAR("0.47525")
$rair = PAR("0.48515")
$rcan = PAR("0.54355")
! Guide tube !
$rcool = PAR("0.6350")
$rbox = PAR("0.67055")

$rgap = PAR("0.07975") ! for assembly pitch of 21.811 cm !
$pitch = PAR("1.4427")
$p2 = PAR("$pitch/2")
$psq2 = PAR("$rcan/2**0.5")
$psqh2 = PAR("$rbox/2**0.5")
$pgap2 = PAR("$rgap/2")
$couple = PAR(3)

! Materials !
! 650ppm Boron in moderator !
'H2O-1' = MAT(NB/.670/1001,11.183; 8016,88.752; 5010,0.012; 5011,0.053)
! Unborated moderator !
'H2O-2' = MAT(NB/1.0/1001,11.19; 8016,88.81)
! Cladding !
$Zy2 = MAT(NB/6.56/40002,100.0)
! Fuel !
'UO2-1' = MAT(10.5216/ 92234,3.4729E-02; 92235,4.0000; 92236,1.8400E-02;
  92238,95.947; 8016,0)
'air' = MAT(0/ 7014,5.000E-05)

! Geometry !
Pin = CCS($rpe,$rair,$rcan//fuel,gap,clad)
Whole = CCS($rcool,$rbox//water,clad)

$cell = PAR(("-$p2", "-$p2") ("-$p2", $p2) ($p2, $p2) ($p2, "-$p2") !nodes 1-4!
(0, "-$p2") ("-$p2", 0) (0, $p2) ($p2, 0) ($rcan, 0) (0, "-$rcan") ("-$rcan", 0)
(0, $rcan) ($psq2, $psq2) ($psq2, "-$psq2") ("-$psq2", "-$psq2") ("-$psq2", $psq2)
/4, cool/Pin(0,0)/ 1,6,11,15,cool; 6,2,16,11,cool; 2,7,12,16,cool;
7,3,13,12,cool; 3,8,9,13,cool; 8,4,14,9,cool; 4,5,10,14,cool)

$wcell = PAR(("-$p2", "-$p2") ("-$p2", $p2) ($p2, $p2) ($p2, "-$p2") !nodes 1-4!
(0, "-$p2") ("-$p2", 0) (0, $p2) ($p2, 0) ($rbox, 0) (0, "-$rbox") ("-$rbox", 0)
(0, $rbox) ($psqh2, $psqh2) ($psqh2, "-$psqh2") ("-$psqh2", "-$psqh2")
("-$psqh2", $psqh2)/4, cool/Whole(0,0)/ 1,6,11,15,cool; 6,2,16,11,cool;
2,7,12,16,cool; 7,3,13,12,cool; 3,8,9,13,cool; 8,4,14,9,cool; 4,5,10,14,cool)

$wgap = PAR(("-$pgap2", "-$p2") ("-$pgap2", $p2) ($pgap2, $p2) ($pgap2, "-$p2")
/4, cool//)

$cell2 = PAR(("-$p2", "-$p2") ("-$p2", 0) ($p2, 0) ($p2, "-$p2")
(0, "-$p2") ($rcan, 0) (0, "-$rcan") ("-$rcan", 0) ($psq2, "-$psq2")
("-$psq2", "-$psq2") /4, cool/Pin(0,0) 3/ 3,4,9,6,cool; 4,5,7,9,cool;
5,1,10,7,cool)

$wgap2 = PAR(("-$pgap2", "-$p2") ("-$pgap2", 0) ($pgap2, 0) ($pgap2, "-$p2")
/4, cool//)

$wcell4 = PAR((0, "-$p2") (0,0) ($p2, 0) ($p2, "-$p2")
($rbox, 0) (0, "-$rbox") ($psqh2, "-$psqh2")
/4, cool/Whole(0,0) 2/4, 1,6,7,cool)

$wgap4 = PAR(("-$pgap2", "-$pgap2") ("-$pgap2", $pgap2) ($pgap2, $pgap2)
($pgap2, "-$pgap2") /4, cool//)

```

```

'1.0' = STR($cell)
'3.0' = STR($wcell)
'5.0' = STR($cell2)
'9.0' = STR($wcell4)
'10.0' = STR($wgap)
'11.0' = STR($wgap2)
'12.0' = STR($wgap4)

White = ALB(1/1/1)

$corder =PAR((1,3,4)$coup(2,2,1)/
(2,3,4)$coup(3,2,1)/
(3,3,4)$coup(4,2,1)/
(4,3,4)$coup(5,2,1)/
(5,3,4)$coup(6,2,1)/
(6,3,4)$coup(7,2,1)/
(7,3,4)$coup(8,2,1)/
(8,3,4)$coup(9,2,1))

$corder1 =PAR((1,4,1)$coup(2,2,1)/
(2,3,4)$coup(3,2,1)/
(3,3,4)$coup(4,2,1)/
(4,3,4)$coup(5,2,1)/
(5,3,4)$coup(6,2,1)/
(6,3,4)$coup(7,2,1)/
(7,3,4)$coup(8,2,1)/
(8,3,4)$coup(9,2,1))

$corder2 =PAR((1,4,1)$coup(2,3,2)/
(2,4,1)$coup(3,3,2)/
(3,4,1)$coup(4,3,2)/
(4,4,1)$coup(5,3,2)/
(5,4,1)$coup(6,3,2)/
(6,4,1)$coup(7,3,2)/
(7,4,1)$coup(8,3,2)/
(8,4,1)$coup(9,3,2))

Row1=CNX('9.0','5.0','5.0','5.0','5.0','5.0','5.0','5.0','11.0'/$corder)
Row2=CNX('5.0','1.0','1.0','1.0','1.0','1.0','1.0','1.0','1.0'/$corder1)
Row3=CNX('5.0','1.0','3.0','1.0','1.0','3.0','1.0','1.0','10.0'/$corder1)
Row4=CNX('5.0','1.0','1.0','1.0','1.0','1.0','1.0','1.0','10.0'/$corder1)
Row5=CNX('5.0','1.0','1.0','1.0','3.0','1.0','1.0','1.0','10.0'/$corder1)
Row6=CNX('5.0','1.0','3.0','1.0','1.0','1.0','1.0','1.0','10.0'/$corder1)
Row7=CNX('5.0','1.0','1.0','1.0','1.0','1.0','1.0','1.0','10.0'/$corder1)
Row8=CNX('5.0','1.0','1.0','1.0','1.0','1.0','1.0','1.0','10.0'/$corder1)
Row10=CNX('11.0','10.0','10.0','10.0','10.0','10.0','10.0','10.0',
'12.0'/$corder2)

System =CNX(Row1,Row2,Row3,Row4,Row5,Row6,Row7,Row8,Row10/
(1-2,4,1)$coup(2-2,3,2)/
(2-2,4,1)$coup(3-2,3,2)/
(3-2,4,1)$coup(4-2,3,2)/
(4-2,4,1)$coup(5-2,3,2)/
(5-2,4,1)$coup(6-2,3,2)/
(6-2,4,1)$coup(7-2,3,2)/
(7-2,4,1)$coup(8-2,3,2)/
(8-2,4,1)$coup(9-2,4,3))

System = BDRY((1-1,2,2)$coup(0))

! Overlays !
AllMat = OVLN('H2O-1' /*-**-*/ Zy2 / *-**-clad /
'air' / *-**-gap /
'UO2-1' / *-**-fuel)

All1 = OVLN(1.0 /*-**-*/)
AllT = OVLN(600. /*-**-*/ 1000. /*-**-fuel / 620. /*-**-clad)
mos = OVSM(AllMat)
dos = OVSD(All1)
tos = OVST(AllT)

! Low temperature !

```

```

LoFT    = OVL(293.00 /*-**-*)
LoFM    = OVLM('H2O-2' /*-**-*-water,      *--0-cool)
tLfos   = OVST(tos/LoFT)
mLfos   = OVSM(mos/LoFM)

! Burnup !
st      = STAT(mos,dos,tos,60.00)
stloF   = STAT(mLfos,dos,tLfos,60.00)
BU      = PATH(/NC,(st),45000/45,(1826.25/5))
COLD    = TREE(BU/(stloF)/0,45000/45)

! Output !
G1      = GROUP(N/ 0)
G2      = GROUP(N/ 0.625, 0)
Gpins   = AREA(*-**-*-<water>,*-**-*-<fuel>)
Apins   = AREA(<*-**-*-fuel>)
Aall    = AREA(<*-**-*->)
Asol    = AREA(<*-**-*-water,*-**-0-cool>)

ND      = MICRO(G1, Apins / 92234, 92235, 92236, 92238, 93237,
                94238, 94239, 94240, 94241, 94242, 95241,
                95242, 95243,
                42595, 43599, 44601, 45603, 47609, 55633,
                62647, 62649, 62650, 62651, 62652, 60643,
                60645, 63651, 63653, 64655, 8016 /)

NDA     = MICRO(G1, Apins / / )

! Corners !
NE      = FACE((1-9,2,4))
SE      = FACE((9-9,4,2))
SW      = FACE((9-1,1,3))
NW      = FACE((1-1,1,3))

! Interior face !
Interior = FACE((1-1,2,1) (2-1,3,2) (3-1,3,2) (4-1,3,2)
                (5-1,3,2) (6-1,3,2) (7-1,3,2) (8-1,3,2)
                (9-1,3,2) )

! Exterior face !
Exterior = FACE((9-1,2,1) (9-2,2,1) (9-3,2,1) (9-4,2,1)
                (9-5,2,1) (9-6,2,1) (9-7,2,1) (9-8,2,1)
                (9-9,2,1) )

CurCorner = CUR(G2,NW,SW,SE,NE)
CurSide   = CUR(G2,Interior,Exterior)

'bw15_0_00_e40_45' = RUN()

```


HELIOS input file for B&W 15 × 15 assembly with 16 BPRs (2 wt % B₄C) present during the first 15 GWd/t of burnup

```

+HEL
'bw15_2_16_e40_15' =
CASE('/fmdp/helios-1.6/babel-1.6/aix/sample-11/hy045n18g16a.dat'/
      'bw15_2_16_e40_15.hrf'/ '16 2wt% B4C BPR BW15x15 assembly model')

! BW 15x15 Assembly           !
! 16 BPRs present during first 15 GWd/t burnup !
! 00 BPRs present during cold calcs           !

! Fuel !
$rpe = PAR("0.47525")
$rair = PAR("0.48515")
$rcan = PAR("0.54355")
! Guide tube !
$rcool = PAR("0.6350")
$rbox = PAR("0.67055")
! Burnable Poison Rod !
$rbpr = PAR("0.4318")
$rbpri = PAR("0.4572")
$rbpro = PAR("0.5461")

$rgap = PAR("0.07975") ! for assembly pitch of 21.811 cm !
$pitch = PAR("1.4427")
$p2 = PAR("$pitch/2")
$psq2 = PAR("$rcan/2**0.5")
$psqh2 = PAR("$rbox/2**0.5")
$pgap2 = PAR("$rgap/2")
$scoup = PAR(3)

! Materials !
! 650ppm Boron in moderator !
'H2O-1' = MAT(NB/.670/1001,11.183; 8016,88.752; 5010,0.012; 5011,0.053)
! Unborated moderator !
'H2O-2' = MAT(NB/1.0/1001,11.19; 8016,88.81)
! Cladding !
Zy2 = MAT(NB/6.56/40002,100.0)
'Zy2-1' = MAT(NB/6.56/40002,100.0)
! Fuel !
'UO2-1' = MAT(10.5216/ 92234,3.4729E-02; 92235,4.0000; 92236,1.8400E-02;
              92238,95.947; 8016,0)
! BPR poison - 2wt% B4C !
'boron1' = MAT(0/ 8016,6.4247E-02 ;6000,8.0649E-04 ;13027,4.2831E-02;
               5010,6.2696E-04; 5011,2.5976E-03)
'air' = MAT(0/ 7014,5.000E-05)

! Geometry !
Pin = CCS($rpe,$rair,$rcan//fuel,gap,clad)
Whole = CCS($rcool,$rbox//water,clad)
Bpin = CCS($rbpr,$rbpri,$rbpro,
           $rcool,$rbox//crod,gap,clad1,water,clad)

$cell = PAR(("-$p2", "-$p2") ("-$p2", $p2) ($p2, $p2) ($p2, "-$p2") !nodes 1-4!
(0, "-$p2") ("-$p2", 0) (0, $p2) ($p2, 0) ($rcan, 0) (0, "-$rcan") ("-$rcan", 0)
(0, $rcan) ($psq2, $psq2) ($psq2, "-$psq2") ("-$psq2", "-$psq2") ("-$psq2", $psq2)
/4, cool/Pin(0,0)/ 1,6,11,15, cool; 6,2,16,11, cool; 2,7,12,16, cool;
7,3,13,12, cool; 3,8,9,13, cool; 8,4,14,9, cool; 4,5,10,14, cool)

$wcell = PAR(("-$p2", "-$p2") ("-$p2", $p2) ($p2, $p2) ($p2, "-$p2") !nodes 1-4!
(0, "-$p2") ("-$p2", 0) (0, $p2) ($p2, 0) ($rbox, 0) (0, "-$rbox") ("-$rbox", 0)
(0, $rbox) ($psqh2, $psqh2) ($psqh2, "-$psqh2") ("-$psqh2", "-$psqh2")
("-$psqh2", $psqh2)/4, cool/Whole(0,0)/ 1,6,11,15, cool; 6,2,16,11, cool;
2,7,12,16, cool; 7,3,13,12, cool; 3,8,9,13, cool; 8,4,14,9, cool; 4,5,10,14, cool)

$bcell = PAR(("-$p2", "-$p2") ("-$p2", $p2) ($p2, $p2) ($p2, "-$p2") !nodes 1-4!
(0, "-$p2") ("-$p2", 0) (0, $p2) ($p2, 0) ($rbox, 0) (0, "-$rbox") ("-$rbox", 0)
(0, $rbox) ($psqh2, $psqh2) ($psqh2, "-$psqh2") ("-$psqh2", "-$psqh2")
("-$psqh2", $psqh2)/4, cool/Bpin(0,0)/ 1,6,11,15, cool; 6,2,16,11, cool;

```

```

2,7,12,16,cool;7,3,13,12,cool; 3,8,9,13,cool; 8,4,14,9,cool; 4,5,10,14,cool)

$wgap   = PAR(("-$pgap2", "-$p2") ("-$pgap2", $p2) ($pgap2, $p2) ($pgap2, "-$p2")
/4, cool//)
$cell12 = PAR(("-$p2", "-$p2") ("-$p2", 0) ($p2, 0) ($p2, "-$p2")
(0, "-$p2") ($rcan, 0) (0, "-$rcan") ("-$rcan", 0) ($psq2, "-$psq2")
("-$psq2", "-$psq2") /4, cool/Pin(0,0) 3/ 3,4,9,6,cool; 4,5,7,9,cool;
5,1,10,7,cool)

$wgap2  = PAR(("-$pgap2", "-$p2") ("-$pgap2", 0) ($pgap2, 0) ($pgap2, "-$p2")
/4, cool//)

$wcell14 = PAR((0, "-$p2") (0, 0) ($p2, 0) ($p2, "-$p2")
($rbox, 0) (0, "-$rbox") ($psqh2, "-$psqh2")
/4, cool/Whole(0,0) 2/4,1,6,7,cool)

$wgap4  = PAR(("-$pgap2", "-$pgap2") ("-$pgap2", $pgap2) ($pgap2, $pgap2 )
($pgap2, "-$pgap2") /4, cool//)

'1.0'   = STR($cell)
'3.0'   = STR($wcell)
'4.0'   = STR($bcell)
'5.0'   = STR($cell12)
'9.0'   = STR($wcell14)
'10.0'  = STR($wgap)
'11.0'  = STR($wgap2)
'12.0'  = STR($wgap4)

White   = ALB(1/1/1)

$corder =PAR((1,3,4)$coup(2,2,1)/
(2,3,4)$coup(3,2,1)/
(3,3,4)$coup(4,2,1)/
(4,3,4)$coup(5,2,1)/
(5,3,4)$coup(6,2,1)/
(6,3,4)$coup(7,2,1)/
(7,3,4)$coup(8,2,1)/
(8,3,4)$coup(9,2,1))

$corder1 =PAR((1,4,1)$coup(2,2,1)/
(2,3,4)$coup(3,2,1)/
(3,3,4)$coup(4,2,1)/
(4,3,4)$coup(5,2,1)/
(5,3,4)$coup(6,2,1)/
(6,3,4)$coup(7,2,1)/
(7,3,4)$coup(8,2,1)/
(8,3,4)$coup(9,2,1))

$corder2 =PAR((1,4,1)$coup(2,3,2)/
(2,4,1)$coup(3,3,2)/
(3,4,1)$coup(4,3,2)/
(4,4,1)$coup(5,3,2)/
(5,4,1)$coup(6,3,2)/
(6,4,1)$coup(7,3,2)/
(7,4,1)$coup(8,3,2)/
(8,4,1)$coup(9,3,2))

Row1=CNX('9.0','5.0','5.0','5.0','5.0','5.0','5.0','5.0','11.0'/$corder)
Row2=CNX('5.0','1.0','1.0','1.0','1.0','1.0','1.0','1.0','10.0'/$corder1)
Row3=CNX('5.0','1.0','4.0','1.0','1.0','4.0','1.0','1.0','10.0'/$corder1)
Row4=CNX('5.0','1.0','1.0','1.0','1.0','1.0','1.0','1.0','10.0'/$corder1)
Row5=CNX('5.0','1.0','1.0','1.0','4.0','1.0','1.0','1.0','10.0'/$corder1)
Row6=CNX('5.0','1.0','4.0','1.0','1.0','1.0','1.0','1.0','10.0'/$corder1)
Row7=CNX('5.0','1.0','1.0','1.0','1.0','1.0','1.0','1.0','10.0'/$corder1)
Row8=CNX('5.0','1.0','1.0','1.0','1.0','1.0','1.0','1.0','10.0'/$corder1)
Row10=CNX('11.0','10.0','10.0','10.0','10.0','10.0','10.0','10.0',
'12.0'/$corder2)

System =CNX(Row1,Row2,Row3,Row4,Row5,Row6,Row7,Row8,Row10/
(1-2,4,1)$coup(2-2,3,2)/
(2-2,4,1)$coup(3-2,3,2)/
(3-2,4,1)$coup(4-2,3,2)/
(4-2,4,1)$coup(5-2,3,2)/

```

```

(5-2,4,1)$coup(6-2,3,2)/
(6-2,4,1)$coup(7-2,3,2)/
(7-2,4,1)$coup(8-2,3,2)/
(8-2,4,1)$coup(9-2,4,3))

System = BDRY((1-1,2,2)$coup(0))

! Overlays !
AllMat = OVLM('H2O-1' /*-**-*/ Zy2 / *-**-clad /
              'Zy2-1' / *-**-clad1 /
              'air' / *-**-gap /
              'UO2-1' / *-**-fuel /
              'boron1' / *- '4.0'-**-crod)

All1 = OVLD(1.0 /*-**-**)
AllT = OVLT(600. /*-**-*/ 1000. /*-**-fuel / 620. /*-**-clad)
mos = OVSM(AllMat)
dos = OVSD(All1)
tos = OVST(AllT)

! Removal of BPRs for cold conditions !
CROMat = OVLM('H2O-1' /*- '4.0'-**-crod,
              *- '4.0'-**-clad1,
              *- '4.0'-**-gap)
moscr = OVSM(mos/CROMat)

! Low temperature !
LoFT = OVLT(293.00 /*-**-**)
LoFM = OVLM('H2O-2' /*-**-water, *- -0-cool,
            *- '4.0'-**-crod,
            *- '4.0'-**-clad1,
            *- '4.0'-**-gap)

tLfes = OVST(tos/LoFT)
mLfes = OVSM(moscr/LoFM)

! Burnup !
st = STAT(mos,dos,tos,60.00)
stccr = STAT(moscr,dos,tos,60.00)
stloF = STAT(mLfes,dos,tLfes,60.00)
BU1 = PATH(/NC,(st),15000/15)
BU2 = PATH(BU1:15000/NC,(stccr),30000/30,(1826.25/5))
COLD1 = TREE(BU1/(stloF)/0,15000/15)
COLD2 = TREE(BU2/(stloF)/0,30000/30)

! Output !
G1 = GROUP(N/ 0)
G2 = GROUP(N/ 0.625, 0)
Gpins = AREA(*-**-<water>,*-**-<fuel>)
Apins = AREA(<*-**-fuel>)
Aall = AREA(<*-**-**>)
Asol = AREA(<*-**-water,*- -0-cool>)
Abur = AREA(<*-**-crod>)

ND = MICRO(G1, Apins / 92234, 92235, 92236, 92238, 93237,
           94238, 94239, 94240, 94241, 94242, 95241,
           95242, 95243,
           42595, 43599, 44601, 45603, 47609, 55633,
           62647, 62649, 62650, 62651, 62652, 60643,
           60645, 63651, 63653, 64655, 8016 /)

NDA = MICRO(G1, Apins / / )
NDB = MICRO(G1, Abur / 5010 / )

! Corners !
NE = FACE((1-9,2,4))
SE = FACE((9-9,4,2))
SW = FACE((9-1,1,3))
NW = FACE((1-1,1,3))

! Interior face !
Interior = FACE((1-1,2,1) (2-1,3,2) (3-1,3,2) (4-1,3,2)

```

```
(5-1,3,2) (6-1,3,2) (7-1,3,2) (8-1,3,2)
(9-1,3,2) )

! Exterior face !
Exterior = FACE((9-1,2,1) (9-2,2,1) (9-3,2,1) (9-4,2,1)
(9-5,2,1) (9-6,2,1) (9-7,2,1) (9-8,2,1)
(9-9,2,1) )

CurCorner = CUR(G2,NW,SW,SE,NE)
CurSide   = CUR(G2,Interior,Exterior)

'bw15_2_16_e40_15' = RUN()
```

APPENDIX B
SELECTED SAS2H INPUT FILES

SAS2H input file for Westinghouse 17 × 17 OFA assembly without BPRs present

```

=sas2h      parm=skipshipdata
001_00baa_01.in, Case 001, 00 BAAs present, 01=constant presence
44groupndf5      latticecell
'
'   - Westinghouse 17x17 OFA assembly design
'   - continuous burnup to 45 gwd/mtu
'   - initial enrichment of 4.0 wt% U-235
'   - moderator temperature = 600K
'   - fuel temperature = 1000K
'   - soluble boron concentration = 650ppm, constant
'   - specific power = 60 MW/MTU
'   - 45 libraries during burnup (1 library per gwd/mtu)
'   - 00 Burnable Absorber Assemblies (BAAs) present
'
'
'   Mixtures of fuel-pin-unit-cell
'   U-234, U-236, & U-238 isotopics calculated based on relations
'   in NUREG/CR-5625 (ORNL-6698)
uo2  1 den=10.5216 1 1000.0 92234 3.4729E-02
      92235 4.0000
      92236 1.8400E-02
      92238 95.947   end
'   Important nuclides from Table 1 of ORNL/TM-12294/V1
kr-83  1 0 1-21 1000.0 end
kr-85  1 0 1-21 1000.0 end
sr-90  1 0 1-21 1000.0 end
y-89   1 0 1-21 1000.0 end
mo-95  1 0 1-21 1000.0 end
zr-93  1 0 1-21 1000.0 end
zr-94  1 0 1-21 1000.0 end
zr-95  1 0 1-21 1000.0 end
nb-94  1 0 1-21 1000.0 end
tc-99  1 0 1-21 1000.0 end
ru-101 1 0 1-21 1000.0 end
ru-106 1 0 1-21 1000.0 end
rh-103 1 0 1-21 1000.0 end
rh-105 1 0 1-21 1000.0 end
pd-105 1 0 1-21 1000.0 end
pd-108 1 0 1-21 1000.0 end
ag-109 1 0 1-21 1000.0 end
sb-124 1 0 1-21 1000.0 end
xe-131 1 0 1-21 1000.0 end
xe-132 1 0 1-21 1000.0 end
xe-136 1 0 1-21 1000.0 end
cs-134 1 0 1-21 1000.0 end
cs-135 1 0 1-21 1000.0 end
cs-137 1 0 1-21 1000.0 end
ba-136 1 0 1-21 1000.0 end
la-139 1 0 1-21 1000.0 end
ce-144 1 0 1-21 1000.0 end
pr-141 1 0 1-21 1000.0 end
pr-143 1 0 1-21 1000.0 end
nd-143 1 0 1-21 1000.0 end
nd-145 1 0 1-21 1000.0 end
nd-147 1 0 1-21 1000.0 end
pm-147 1 0 1-21 1000.0 end
pm-148 1 0 1-21 1000.0 end
sm-147 1 0 1-21 1000.0 end
sm-149 1 0 1-21 1000.0 end
sm-150 1 0 1-21 1000.0 end
sm-151 1 0 1-21 1000.0 end
sm-152 1 0 1-21 1000.0 end
eu-153 1 0 1-21 1000.0 end
eu-154 1 0 1-21 1000.0 end
eu-155 1 0 1-21 1000.0 end
gd-155 1 0 1-21 1000.0 end
'
zirc2  2 1 620.0 end
'

```



```
power=60.0 burn=16.6667 down=0.0 end
power=60.0 burn=16.6667 down=0.0 end
power=60.0 burn=16.6667 down=0.0 end
power=60.0 burn=16.6667 down=0.0 end
power=60.0 burn=16.6667 down=0.0 end
power=60.0 burn=16.6667 down=0.0 end
power=60.0 burn=16.6667 down=0.0 end
power=60.0 burn=16.6667 down=0.0 end
power=60.0 burn=16.6667 down=0.0 end
power=60.0 burn=16.6667 down=1826.25 end
'
' Light-elements taken from SAS2H input listing in
' ORNL/TM-12294/V5 Appendix B, not verified to be accurate
o 135 cr 5.9 mn 0.33
fe 12.9 co 0.075 ni 9.9
zr 221 nb 0.71 sn 3.60
'
end
```

SAS2H input file for Westinghouse 17 × 17 OFA assembly with 12 WABA BPRs present during the first 15 GWd/t of burnup

```
=sas2h      parm=skipshipdata
001_12waba_02.in, Case 001, 12 WABAs present, 02=BPRs present for first 15 GWd/MTU
44groupndf5      latticecell
'
'   - Westinghouse 17x17 OFA assembly design
'   - continuous burnup to 45 gwd/mtu
'   - initial enrichment of 4.0 wt% U-235
'   - moderator temperature = 600K
'   - fuel temperature = 1000K
'   - soluble boron concentration = 650ppm, constant
'   - specific power = 60 MW/MTU
'   - 45 libraries during burnup (1 library per gwd/mtu)
'   - 12 Wet Annular Burnable Absorber (WABAs) present
'
'
'   Mixtures of fuel-pin-unit-cell
'   U-234, U-236, & U-238 isotopics calculated based on relations
'   in NUREG/CR-5625 (ORNL-6698)
uo2  1 den=10.5216 1 1000.0 92234 3.4729E-02
      92235 4.0000
      92236 1.8400E-02
      92238 95.947      end
'   Important nuclides from Table 1 of ORNL/TM-12294/V1
kr-83  1 0 1-21 1000.0 end
kr-85  1 0 1-21 1000.0 end
sr-90  1 0 1-21 1000.0 end
y-89   1 0 1-21 1000.0 end
mo-95  1 0 1-21 1000.0 end
zr-93  1 0 1-21 1000.0 end
zr-94  1 0 1-21 1000.0 end
zr-95  1 0 1-21 1000.0 end
nb-94  1 0 1-21 1000.0 end
tc-99  1 0 1-21 1000.0 end
ru-101 1 0 1-21 1000.0 end
ru-106 1 0 1-21 1000.0 end
rh-103 1 0 1-21 1000.0 end
rh-105 1 0 1-21 1000.0 end
pd-105 1 0 1-21 1000.0 end
pd-108 1 0 1-21 1000.0 end
ag-109 1 0 1-21 1000.0 end
sb-124 1 0 1-21 1000.0 end
xe-131 1 0 1-21 1000.0 end
xe-132 1 0 1-21 1000.0 end
xe-136 1 0 1-21 1000.0 end
cs-134 1 0 1-21 1000.0 end
cs-135 1 0 1-21 1000.0 end
cs-137 1 0 1-21 1000.0 end
ba-136 1 0 1-21 1000.0 end
la-139 1 0 1-21 1000.0 end
ce-144 1 0 1-21 1000.0 end
pr-141 1 0 1-21 1000.0 end
pr-143 1 0 1-21 1000.0 end
nd-143 1 0 1-21 1000.0 end
nd-145 1 0 1-21 1000.0 end
nd-147 1 0 1-21 1000.0 end
pm-147 1 0 1-21 1000.0 end
pm-148 1 0 1-21 1000.0 end
sm-147 1 0 1-21 1000.0 end
sm-149 1 0 1-21 1000.0 end
sm-150 1 0 1-21 1000.0 end
sm-151 1 0 1-21 1000.0 end
sm-152 1 0 1-21 1000.0 end
eu-153 1 0 1-21 1000.0 end
eu-154 1 0 1-21 1000.0 end
eu-155 1 0 1-21 1000.0 end
gd-155 1 0 1-21 1000.0 end
'
```

```

zirc2  2  1          620.0 end
'
h2o    3 den=0.670 1 600.0 end
arbm-bormod 0.670 1 1 0 0 5000 100 3 650.0E-06 600.0 end
'
'   Input materials for BPRs
zirc4  4  1          600.0 end
'
'   Al2O3-B4C
b-10   5  0  3.0697E-3  600.0 end
b-11   5  0  1.2753E-2  600.0 end
c       5  0  3.9521E-3  600.0 end
al      5  0  2.6344E-2  600.0 end
o       5  0  3.9506E-2  600.0 end
'
n       6  0  5.000E-5   600.0 end
end comp
'
'   Base reactor lattice specification
squarepitch 1.2598 0.7844 1 3 0.9144 2 0.8001 3 end
more data szf=0.50 end
'
'   Assembly and cycle parameters
npin/assembly=264 fuelngth=845.0 ncycles=45 nlib/cyc=1
printlevel=2 lightel=9 inplevel=2
numztotal=11 mxrepeats=0
facmesh=0.50 end
'
1
3 0.20206 4 0.23978 6 0.24964 5 0.28557 6 0.29546 4 0.34215
3 0.56134 2 0.60198 3 0.71079 500 2.41668 3 2.42643
'
2
3 0.20206 4 0.23978 6 0.24964 5 0.28557 6 0.29546 4 0.34215
3 0.56134 2 0.60198 3 0.71079 500 2.41668 3 2.42643
'
3
3 0.20206 4 0.23978 6 0.24964 5 0.28557 6 0.29546 4 0.34215
3 0.56134 2 0.60198 3 0.71079 500 2.41668 3 2.42643
'
4
3 0.20206 4 0.23978 6 0.24964 5 0.28557 6 0.29546 4 0.34215
3 0.56134 2 0.60198 3 0.71079 500 2.41668 3 2.42643
'
5
3 0.20206 4 0.23978 6 0.24964 5 0.28557 6 0.29546 4 0.34215
3 0.56134 2 0.60198 3 0.71079 500 2.41668 3 2.42643
'
6
3 0.20206 4 0.23978 6 0.24964 5 0.28557 6 0.29546 4 0.34215
3 0.56134 2 0.60198 3 0.71079 500 2.41668 3 2.42643
'
7
3 0.20206 4 0.23978 6 0.24964 5 0.28557 6 0.29546 4 0.34215
3 0.56134 2 0.60198 3 0.71079 500 2.41668 3 2.42643
'
8
3 0.20206 4 0.23978 6 0.24964 5 0.28557 6 0.29546 4 0.34215
3 0.56134 2 0.60198 3 0.71079 500 2.41668 3 2.42643
'
9
3 0.20206 4 0.23978 6 0.24964 5 0.28557 6 0.29546 4 0.34215
3 0.56134 2 0.60198 3 0.71079 500 2.41668 3 2.42643
'
10
3 0.20206 4 0.23978 6 0.24964 5 0.28557 6 0.29546 4 0.34215
3 0.56134 2 0.60198 3 0.71079 500 2.41668 3 2.42643
'
11
3 0.20206 4 0.23978 6 0.24964 5 0.28557 6 0.29546 4 0.34215
3 0.56134 2 0.60198 3 0.71079 500 2.41668 3 2.42643
'
12
3 0.20206 4 0.23978 6 0.24964 5 0.28557 6 0.29546 4 0.34215
3 0.56134 2 0.60198 3 0.71079 500 2.41668 3 2.42643
'
13
3 0.20206 4 0.23978 6 0.24964 5 0.28557 6 0.29546 4 0.34215
3 0.56134 2 0.60198 3 0.71079 500 2.41668 3 2.42643
'
14
3 0.20206 4 0.23978 6 0.24964 5 0.28557 6 0.29546 4 0.34215
3 0.56134 2 0.60198 3 0.71079 500 2.41668 3 2.42643
'
15
3 0.20206 4 0.23978 6 0.24964 5 0.28557 6 0.29546 4 0.34215
3 0.56134 2 0.60198 3 0.71079 500 2.41668 3 2.42643
'

```



```

'      40
3 0.20206 3 0.23978 3 0.24964 3 0.28557 3 0.29546 3 0.34215
3 0.56134 2 0.60198 3 0.71079 500 2.41668 3 2.42643
'      41
3 0.20206 3 0.23978 3 0.24964 3 0.28557 3 0.29546 3 0.34215
3 0.56134 2 0.60198 3 0.71079 500 2.41668 3 2.42643
'      42
3 0.20206 3 0.23978 3 0.24964 3 0.28557 3 0.29546 3 0.34215
3 0.56134 2 0.60198 3 0.71079 500 2.41668 3 2.42643
'      43
3 0.20206 3 0.23978 3 0.24964 3 0.28557 3 0.29546 3 0.34215
3 0.56134 2 0.60198 3 0.71079 500 2.41668 3 2.42643
'      44
3 0.20206 3 0.23978 3 0.24964 3 0.28557 3 0.29546 3 0.34215
3 0.56134 2 0.60198 3 0.71079 500 2.41668 3 2.42643
'      45
3 0.20206 3 0.23978 3 0.24964 3 0.28557 3 0.29546 3 0.34215
3 0.56134 2 0.60198 3 0.71079 500 2.41668 3 2.42643
'
'      Assembly depletion/decay parameters
power=60.0 burn=16.6667 down=0.0 end
power=60.0 burn=16.6667 down=0.0 end
power=60.0 burn=16.6667 down=0.0 end
power=60.0 burn=16.6667 down=0.0 end
power=60.0 burn=16.6667 down=0.0 end
power=60.0 burn=16.6667 down=0.0 end
power=60.0 burn=16.6667 down=0.0 end
power=60.0 burn=16.6667 down=0.0 end
power=60.0 burn=16.6667 down=0.0 end
power=60.0 burn=16.6667 down=0.0 end
power=60.0 burn=16.6667 down=0.0 end
power=60.0 burn=16.6667 down=0.0 end
power=60.0 burn=16.6667 down=0.0 end
power=60.0 burn=16.6667 down=0.0 end
power=60.0 burn=16.6667 down=0.0 end
power=60.0 burn=16.6667 down=0.0 end
power=60.0 burn=16.6667 down=0.0 end
power=60.0 burn=16.6667 down=0.0 end
power=60.0 burn=16.6667 down=0.0 end
power=60.0 burn=16.6667 down=0.0 end
power=60.0 burn=16.6667 down=0.0 end
power=60.0 burn=16.6667 down=0.0 end
power=60.0 burn=16.6667 down=0.0 end
power=60.0 burn=16.6667 down=0.0 end
power=60.0 burn=16.6667 down=0.0 end
power=60.0 burn=16.6667 down=0.0 end
power=60.0 burn=16.6667 down=0.0 end
power=60.0 burn=16.6667 down=0.0 end
power=60.0 burn=16.6667 down=0.0 end
power=60.0 burn=16.6667 down=0.0 end
power=60.0 burn=16.6667 down=0.0 end
power=60.0 burn=16.6667 down=0.0 end
power=60.0 burn=16.6667 down=0.0 end
power=60.0 burn=16.6667 down=0.0 end
power=60.0 burn=16.6667 down=0.0 end
power=60.0 burn=16.6667 down=0.0 end
power=60.0 burn=16.6667 down=0.0 end
power=60.0 burn=16.6667 down=0.0 end
power=60.0 burn=16.6667 down=0.0 end
power=60.0 burn=16.6667 down=0.0 end
power=60.0 burn=16.6667 down=0.0 end
power=60.0 burn=16.6667 down=0.0 end
power=60.0 burn=16.6667 down=0.0 end
power=60.0 burn=16.6667 down=0.0 end
power=60.0 burn=16.6667 down=1826.25 end
'
'      Light-elements taken from SAS2H input listing in
'      ORNL/TM-12294/V5 Appendix B, not verified to be accurate
o 135 cr 5.9 mn 0.33
fe 12.9 co 0.075 ni 9.9
zr 221 nb 0.71 sn 3.60
'
end

```

SAS2H input file for Westinghouse 17 × 17 OFA assembly with 24 WABA BPRs present during the first 15 GWd/t of burnup

```
=sas2h      parm=skipshipdata
001_24waba_02.in, Case 001, 24 WABAs present, 02=BPRs present for first 15 GWd/MTU
44groupndf5      latticecell
'
'   - Westinghouse 17x17 OFA assembly design
'   - continuous burnup to 45 gwd/mtu
'   - initial enrichment of 4.0 wt% U-235
'   - moderator temperature = 600K
'   - fuel temperature = 1000K
'   - soluble boron concentration = 650ppm, constant
'   - specific power = 60 MW/MTU
'   - 45 libraries during burnup (1 library per gwd/mtu)
'   - 24 Wet Annular Burnable Absorber (WABAs) present
'
'
'   Mixtures of fuel-pin-unit-cell
'   U-234, U-236, & U-238 isotopics calculated based on relations
'   in NUREG/CR-5625(ORNL-6698)
uo2  1 den=10.5216 1 1000.0 92234 3.4729E-02
      92235 4.0000
      92236 1.8400E-02
      92238 95.947      end
'   Important nuclides from Table 1 of ORNL/TM-12294/V1
kr-83  1 0 1-21 1000.0 end
kr-85  1 0 1-21 1000.0 end
sr-90  1 0 1-21 1000.0 end
y-89   1 0 1-21 1000.0 end
mo-95  1 0 1-21 1000.0 end
zr-93  1 0 1-21 1000.0 end
zr-94  1 0 1-21 1000.0 end
zr-95  1 0 1-21 1000.0 end
nb-94  1 0 1-21 1000.0 end
tc-99  1 0 1-21 1000.0 end
ru-101 1 0 1-21 1000.0 end
ru-106 1 0 1-21 1000.0 end
rh-103 1 0 1-21 1000.0 end
rh-105 1 0 1-21 1000.0 end
pd-105 1 0 1-21 1000.0 end
pd-108 1 0 1-21 1000.0 end
ag-109 1 0 1-21 1000.0 end
sb-124 1 0 1-21 1000.0 end
xe-131 1 0 1-21 1000.0 end
xe-132 1 0 1-21 1000.0 end
xe-136 1 0 1-21 1000.0 end
cs-134 1 0 1-21 1000.0 end
cs-135 1 0 1-21 1000.0 end
cs-137 1 0 1-21 1000.0 end
ba-136 1 0 1-21 1000.0 end
la-139 1 0 1-21 1000.0 end
ce-144 1 0 1-21 1000.0 end
pr-141 1 0 1-21 1000.0 end
pr-143 1 0 1-21 1000.0 end
nd-143 1 0 1-21 1000.0 end
nd-145 1 0 1-21 1000.0 end
nd-147 1 0 1-21 1000.0 end
pm-147 1 0 1-21 1000.0 end
pm-148 1 0 1-21 1000.0 end
sm-147 1 0 1-21 1000.0 end
sm-149 1 0 1-21 1000.0 end
sm-150 1 0 1-21 1000.0 end
sm-151 1 0 1-21 1000.0 end
sm-152 1 0 1-21 1000.0 end
eu-153 1 0 1-21 1000.0 end
eu-154 1 0 1-21 1000.0 end
eu-155 1 0 1-21 1000.0 end
gd-155 1 0 1-21 1000.0 end
'
```

```

zirc2  2  1          620.0 end
'
h2o    3 den=0.670 1 600.0 end
arbm-bormod 0.670 1 1 0 0 5000 100 3 650.0E-06 600.0 end
'
'   Input materials for BPRs
zirc4  4  1          600.0 end
'
'   Al2O3-B4C
b-10   5  0  3.0697E-3  600.0 end
b-11   5  0  1.2753E-2  600.0 end
c       5  0  3.9521E-3  600.0 end
al      5  0  2.6344E-2  600.0 end
o       5  0  3.9506E-2  600.0 end
'
n       6  0  5.000E-5   600.0 end
end comp
'
'   Base reactor lattice specification
squarepitch 1.2598 0.7844 1 3 0.9144 2 0.8001 3 end
more data szf=0.50 end
'
'   Assembly and cycle parameters
npin/assembly=264 fuelngth=845.0 ncycles=45 nlib/cyc=1
printlevel=2 lightel=9 inplevel=2
numztotal=11 mxrepeats=0
facmesh=0.50 end
'
1
3 0.28575 4 0.33910 6 0.35305 5 0.40385 6 0.41785 4 0.48387
3 0.56134 2 0.60198 3 0.71079 500 2.41668 3 2.42643
'
2
3 0.28575 4 0.33910 6 0.35305 5 0.40385 6 0.41785 4 0.48387
3 0.56134 2 0.60198 3 0.71079 500 2.41668 3 2.42643
'
3
3 0.28575 4 0.33910 6 0.35305 5 0.40385 6 0.41785 4 0.48387
3 0.56134 2 0.60198 3 0.71079 500 2.41668 3 2.42643
'
4
3 0.28575 4 0.33910 6 0.35305 5 0.40385 6 0.41785 4 0.48387
3 0.56134 2 0.60198 3 0.71079 500 2.41668 3 2.42643
'
5
3 0.28575 4 0.33910 6 0.35305 5 0.40385 6 0.41785 4 0.48387
3 0.56134 2 0.60198 3 0.71079 500 2.41668 3 2.42643
'
6
3 0.28575 4 0.33910 6 0.35305 5 0.40385 6 0.41785 4 0.48387
3 0.56134 2 0.60198 3 0.71079 500 2.41668 3 2.42643
'
7
3 0.28575 4 0.33910 6 0.35305 5 0.40385 6 0.41785 4 0.48387
3 0.56134 2 0.60198 3 0.71079 500 2.41668 3 2.42643
'
8
3 0.28575 4 0.33910 6 0.35305 5 0.40385 6 0.41785 4 0.48387
3 0.56134 2 0.60198 3 0.71079 500 2.41668 3 2.42643
'
9
3 0.28575 4 0.33910 6 0.35305 5 0.40385 6 0.41785 4 0.48387
3 0.56134 2 0.60198 3 0.71079 500 2.41668 3 2.42643
'
10
3 0.28575 4 0.33910 6 0.35305 5 0.40385 6 0.41785 4 0.48387
3 0.56134 2 0.60198 3 0.71079 500 2.41668 3 2.42643
'
11
3 0.28575 4 0.33910 6 0.35305 5 0.40385 6 0.41785 4 0.48387
3 0.56134 2 0.60198 3 0.71079 500 2.41668 3 2.42643
'
12
3 0.28575 4 0.33910 6 0.35305 5 0.40385 6 0.41785 4 0.48387
3 0.56134 2 0.60198 3 0.71079 500 2.41668 3 2.42643
'
13
3 0.28575 4 0.33910 6 0.35305 5 0.40385 6 0.41785 4 0.48387
3 0.56134 2 0.60198 3 0.71079 500 2.41668 3 2.42643
'
14
3 0.28575 4 0.33910 6 0.35305 5 0.40385 6 0.41785 4 0.48387
3 0.56134 2 0.60198 3 0.71079 500 2.41668 3 2.42643
'
15
3 0.28575 4 0.33910 6 0.35305 5 0.40385 6 0.41785 4 0.48387
3 0.56134 2 0.60198 3 0.71079 500 2.41668 3 2.42643
'

```



```
' 40
3 0.28575 3 0.33910 3 0.35305 3 0.40385 3 0.41785 3 0.48387
3 0.56134 2 0.60198 3 0.71079 500 2.41668 3 2.42643
' 41
3 0.28575 3 0.33910 3 0.35305 3 0.40385 3 0.41785 3 0.48387
3 0.56134 2 0.60198 3 0.71079 500 2.41668 3 2.42643
' 42
3 0.28575 3 0.33910 3 0.35305 3 0.40385 3 0.41785 3 0.48387
3 0.56134 2 0.60198 3 0.71079 500 2.41668 3 2.42643
' 43
3 0.28575 3 0.33910 3 0.35305 3 0.40385 3 0.41785 3 0.48387
3 0.56134 2 0.60198 3 0.71079 500 2.41668 3 2.42643
' 44
3 0.28575 3 0.33910 3 0.35305 3 0.40385 3 0.41785 3 0.48387
3 0.56134 2 0.60198 3 0.71079 500 2.41668 3 2.42643
' 45
3 0.28575 3 0.33910 3 0.35305 3 0.40385 3 0.41785 3 0.48387
3 0.56134 2 0.60198 3 0.71079 500 2.41668 3 2.42643
'
' Assembly depletion/decay parameters
power=60.0 burn=16.6667 down=0.0 end
power=60.0 burn=16.6667 down=0.0 end
power=60.0 burn=16.6667 down=0.0 end
power=60.0 burn=16.6667 down=0.0 end
power=60.0 burn=16.6667 down=0.0 end
power=60.0 burn=16.6667 down=0.0 end
power=60.0 burn=16.6667 down=0.0 end
power=60.0 burn=16.6667 down=0.0 end
power=60.0 burn=16.6667 down=0.0 end
power=60.0 burn=16.6667 down=0.0 end
power=60.0 burn=16.6667 down=0.0 end
power=60.0 burn=16.6667 down=0.0 end
power=60.0 burn=16.6667 down=0.0 end
power=60.0 burn=16.6667 down=0.0 end
power=60.0 burn=16.6667 down=0.0 end
power=60.0 burn=16.6667 down=0.0 end
power=60.0 burn=16.6667 down=0.0 end
power=60.0 burn=16.6667 down=0.0 end
power=60.0 burn=16.6667 down=0.0 end
power=60.0 burn=16.6667 down=0.0 end
power=60.0 burn=16.6667 down=0.0 end
power=60.0 burn=16.6667 down=0.0 end
power=60.0 burn=16.6667 down=0.0 end
power=60.0 burn=16.6667 down=0.0 end
power=60.0 burn=16.6667 down=0.0 end
power=60.0 burn=16.6667 down=0.0 end
power=60.0 burn=16.6667 down=0.0 end
power=60.0 burn=16.6667 down=0.0 end
power=60.0 burn=16.6667 down=0.0 end
power=60.0 burn=16.6667 down=0.0 end
power=60.0 burn=16.6667 down=0.0 end
power=60.0 burn=16.6667 down=0.0 end
power=60.0 burn=16.6667 down=0.0 end
power=60.0 burn=16.6667 down=0.0 end
power=60.0 burn=16.6667 down=0.0 end
power=60.0 burn=16.6667 down=0.0 end
power=60.0 burn=16.6667 down=0.0 end
power=60.0 burn=16.6667 down=0.0 end
power=60.0 burn=16.6667 down=0.0 end
power=60.0 burn=16.6667 down=0.0 end
power=60.0 burn=16.6667 down=0.0 end
power=60.0 burn=16.6667 down=0.0 end
power=60.0 burn=16.6667 down=1826.25 end
'
' Light-elements taken from SAS2H input listing in
' ORNL/TM-12294/V5 Appendix B, not verified to be accurate
o 135 cr 5.9 mn 0.33
fe 12.9 co 0.075 ni 9.9
zr 221 nb 0.71 sn 3.60
'
end
```

SAS2H input file for Westinghouse 17 × 17 OFA assembly with 12 BAA BPRs present during the first 15 Gwd/t of burnup

```
=sas2h      parm=skipshipdata
001_12baa_02.in, Case 001, 12 BAAs present, 02=BPRs present for first 15 Gwd/MTU
44groupndf5      latticecell
'
'   - Westinghouse 17x17 OFA assembly design
'   - continuous burnup to 45 gwd/mtu
'   - initial enrichment of 4.0 wt% U-235
'   - moderator temperature = 600K
'   - fuel temperature = 1000K
'   - soluble boron concentration = 650ppm, constant
'   - specific power = 60 MW/MTU
'   - 45 libraries during burnup (1 library per gwd/mtu)
'   - 12 Burnable Absorber Assemblies (BAAs) present
'
'
'   Mixtures of fuel-pin-unit-cell
'   U-234, U-236, & U-238 isotopics calculated based on relations
'   in NUREG/CR-5625 (ORNL-6698)
uo2  1 den=10.5216 1 1000.0 92234 3.4729E-02
      92235 4.0000
      92236 1.8400E-02
      92238 95.947      end
'   Important nuclides from Table 1 of ORNL/TM-12294/V1
kr-83  1 0 1-21 1000.0 end
kr-85  1 0 1-21 1000.0 end
sr-90  1 0 1-21 1000.0 end
y-89   1 0 1-21 1000.0 end
mo-95  1 0 1-21 1000.0 end
zr-93  1 0 1-21 1000.0 end
zr-94  1 0 1-21 1000.0 end
zr-95  1 0 1-21 1000.0 end
nb-94  1 0 1-21 1000.0 end
tc-99  1 0 1-21 1000.0 end
ru-101 1 0 1-21 1000.0 end
ru-106 1 0 1-21 1000.0 end
rh-103 1 0 1-21 1000.0 end
rh-105 1 0 1-21 1000.0 end
pd-105 1 0 1-21 1000.0 end
pd-108 1 0 1-21 1000.0 end
ag-109 1 0 1-21 1000.0 end
sb-124 1 0 1-21 1000.0 end
xe-131 1 0 1-21 1000.0 end
xe-132 1 0 1-21 1000.0 end
xe-136 1 0 1-21 1000.0 end
cs-134 1 0 1-21 1000.0 end
cs-135 1 0 1-21 1000.0 end
cs-137 1 0 1-21 1000.0 end
ba-136 1 0 1-21 1000.0 end
la-139 1 0 1-21 1000.0 end
ce-144 1 0 1-21 1000.0 end
pr-141 1 0 1-21 1000.0 end
pr-143 1 0 1-21 1000.0 end
nd-143 1 0 1-21 1000.0 end
nd-145 1 0 1-21 1000.0 end
nd-147 1 0 1-21 1000.0 end
pm-147 1 0 1-21 1000.0 end
pm-148 1 0 1-21 1000.0 end
sm-147 1 0 1-21 1000.0 end
sm-149 1 0 1-21 1000.0 end
sm-150 1 0 1-21 1000.0 end
sm-151 1 0 1-21 1000.0 end
sm-152 1 0 1-21 1000.0 end
eu-153 1 0 1-21 1000.0 end
eu-154 1 0 1-21 1000.0 end
eu-155 1 0 1-21 1000.0 end
gd-155 1 0 1-21 1000.0 end
'
```

```

zirc2  2  1                620.0 end
'
h2o    3  den=0.670 1 600.0 end
arbm-bormod  0.670 1 1 0 0 5000 100 3 650.0E-06 600.0 end
'
'      Input materials for BPRs
ss304  4  1                600.0 end
'
o       5  0  0.04497      600.0 end
na      5  0  0.00165      600.0 end
al      5  0  0.00058      600.0 end
si      5  0  0.01799      600.0 end
k       5  0  0.00011      600.0 end
b-10   5  0  9.595E-4      600.0 end
b-11   5  0  3.863E-3      600.0 end
'
n       6  0  5.000E-5      600.0 end
end comp
'
'      Base reactor lattice specification
squarepitch 1.2598 0.7844 1 3 0.9144 2 0.8001 3 end
more data szf=0.50 end
'
'      Assembly and cycle parameters
npin/assembly=264 fuelngth=845.0 ncycles=45 nlib/cyc=1
printlevel=2 lightel=9 inplevel=2
numzttotal=11 mxrepeats=0
facmesh=0.50 end
'
1
6 0.15132 4 0.16299 6 0.17062 5 0.30174 6 0.30892 4 0.34215
3 0.56134 2 0.60198 3 0.71079 500 2.41668 3 2.42643
'
2
6 0.15132 4 0.16299 6 0.17062 5 0.30174 6 0.30892 4 0.34215
3 0.56134 2 0.60198 3 0.71079 500 2.41668 3 2.42643
'
3
6 0.15132 4 0.16299 6 0.17062 5 0.30174 6 0.30892 4 0.34215
3 0.56134 2 0.60198 3 0.71079 500 2.41668 3 2.42643
'
4
6 0.15132 4 0.16299 6 0.17062 5 0.30174 6 0.30892 4 0.34215
3 0.56134 2 0.60198 3 0.71079 500 2.41668 3 2.42643
'
5
6 0.15132 4 0.16299 6 0.17062 5 0.30174 6 0.30892 4 0.34215
3 0.56134 2 0.60198 3 0.71079 500 2.41668 3 2.42643
'
6
6 0.15132 4 0.16299 6 0.17062 5 0.30174 6 0.30892 4 0.34215
3 0.56134 2 0.60198 3 0.71079 500 2.41668 3 2.42643
'
7
6 0.15132 4 0.16299 6 0.17062 5 0.30174 6 0.30892 4 0.34215
3 0.56134 2 0.60198 3 0.71079 500 2.41668 3 2.42643
'
8
6 0.15132 4 0.16299 6 0.17062 5 0.30174 6 0.30892 4 0.34215
3 0.56134 2 0.60198 3 0.71079 500 2.41668 3 2.42643
'
9
6 0.15132 4 0.16299 6 0.17062 5 0.30174 6 0.30892 4 0.34215
3 0.56134 2 0.60198 3 0.71079 500 2.41668 3 2.42643
'
10
6 0.15132 4 0.16299 6 0.17062 5 0.30174 6 0.30892 4 0.34215
3 0.56134 2 0.60198 3 0.71079 500 2.41668 3 2.42643
'
11
6 0.15132 4 0.16299 6 0.17062 5 0.30174 6 0.30892 4 0.34215
3 0.56134 2 0.60198 3 0.71079 500 2.41668 3 2.42643
'
12
6 0.15132 4 0.16299 6 0.17062 5 0.30174 6 0.30892 4 0.34215
3 0.56134 2 0.60198 3 0.71079 500 2.41668 3 2.42643
'
13
6 0.15132 4 0.16299 6 0.17062 5 0.30174 6 0.30892 4 0.34215
3 0.56134 2 0.60198 3 0.71079 500 2.41668 3 2.42643
'
14
6 0.15132 4 0.16299 6 0.17062 5 0.30174 6 0.30892 4 0.34215
3 0.56134 2 0.60198 3 0.71079 500 2.41668 3 2.42643
'
15
6 0.15132 4 0.16299 6 0.17062 5 0.30174 6 0.30892 4 0.34215

```



```

'      39
3 0.21400 3 0.23051 3 0.24130 3 0.42672 3 0.43688 3 0.48387
3 0.56134 2 0.60198 3 0.71079 500 2.41668 3 2.42643
'      40
3 0.21400 3 0.23051 3 0.24130 3 0.42672 3 0.43688 3 0.48387
3 0.56134 2 0.60198 3 0.71079 500 2.41668 3 2.42643
'      41
3 0.21400 3 0.23051 3 0.24130 3 0.42672 3 0.43688 3 0.48387
3 0.56134 2 0.60198 3 0.71079 500 2.41668 3 2.42643
'      42
3 0.21400 3 0.23051 3 0.24130 3 0.42672 3 0.43688 3 0.48387
3 0.56134 2 0.60198 3 0.71079 500 2.41668 3 2.42643
'      43
3 0.21400 3 0.23051 3 0.24130 3 0.42672 3 0.43688 3 0.48387
3 0.56134 2 0.60198 3 0.71079 500 2.41668 3 2.42643
'      44
3 0.21400 3 0.23051 3 0.24130 3 0.42672 3 0.43688 3 0.48387
3 0.56134 2 0.60198 3 0.71079 500 2.41668 3 2.42643
'      45
3 0.21400 3 0.23051 3 0.24130 3 0.42672 3 0.43688 3 0.48387
3 0.56134 2 0.60198 3 0.71079 500 2.41668 3 2.42643
'
'      Assembly depletion/decay parameters
power=60.0 burn=16.6667 down=0.0 end
power=60.0 burn=16.6667 down=0.0 end
power=60.0 burn=16.6667 down=0.0 end
power=60.0 burn=16.6667 down=0.0 end
power=60.0 burn=16.6667 down=0.0 end
power=60.0 burn=16.6667 down=0.0 end
power=60.0 burn=16.6667 down=0.0 end
power=60.0 burn=16.6667 down=0.0 end
power=60.0 burn=16.6667 down=0.0 end
power=60.0 burn=16.6667 down=0.0 end
power=60.0 burn=16.6667 down=0.0 end
power=60.0 burn=16.6667 down=0.0 end
power=60.0 burn=16.6667 down=0.0 end
power=60.0 burn=16.6667 down=0.0 end
power=60.0 burn=16.6667 down=0.0 end
power=60.0 burn=16.6667 down=0.0 end
power=60.0 burn=16.6667 down=0.0 end
power=60.0 burn=16.6667 down=0.0 end
power=60.0 burn=16.6667 down=0.0 end
power=60.0 burn=16.6667 down=0.0 end
power=60.0 burn=16.6667 down=0.0 end
power=60.0 burn=16.6667 down=0.0 end
power=60.0 burn=16.6667 down=0.0 end
power=60.0 burn=16.6667 down=0.0 end
power=60.0 burn=16.6667 down=0.0 end
power=60.0 burn=16.6667 down=0.0 end
power=60.0 burn=16.6667 down=0.0 end
power=60.0 burn=16.6667 down=0.0 end
power=60.0 burn=16.6667 down=0.0 end
power=60.0 burn=16.6667 down=0.0 end
power=60.0 burn=16.6667 down=0.0 end
power=60.0 burn=16.6667 down=0.0 end
power=60.0 burn=16.6667 down=0.0 end
power=60.0 burn=16.6667 down=0.0 end
power=60.0 burn=16.6667 down=0.0 end
power=60.0 burn=16.6667 down=0.0 end
power=60.0 burn=16.6667 down=0.0 end
power=60.0 burn=16.6667 down=0.0 end
power=60.0 burn=16.6667 down=0.0 end
power=60.0 burn=16.6667 down=0.0 end
power=60.0 burn=16.6667 down=0.0 end
power=60.0 burn=16.6667 down=1826.25 end
'
'      Light-elements taken from SAS2H input listing in
'      ORNL/TM-12294/V5 Appendix B, not verified to be accurate
o 135 cr 5.9 mn 0.33

```

```
fe 12.9  co 0.075  ni 9.9  
zr 221   nb 0.71   sn 3.60  
,  
end
```

SAS2H input file for Westinghouse 17 × 17 OFA assembly with 24 BAA BPRs present during the first 15 GWd/t of burnup

```
=sas2h      parm=skipshipdata
001_24baa_02.in, Case 001, 24 BAAs present, 02=BPRs present for first 15 GWd/MTU
44groupndf5      latticecell
'
'   - Westinghouse 17x17 OFA assembly design
'   - continuous burnup to 45 gwd/mtu
'   - initial enrichment of 4.0 wt% U-235
'   - moderator temperature = 600K
'   - fuel temperature = 1000K
'   - soluble boron concentration = 650ppm, constant
'   - specific power = 60 MW/MTU
'   - 45 libraries during burnup (1 library per gwd/mtu)
'   - 24 Burnable Absorber Assemblies (BAAs) present
'
'
'   Mixtures of fuel-pin-unit-cell
'   U-234, U-236, & U-238 isotopics calculated based on relations
'   in NUREG/CR-5625 (ORNL-6698)
uo2  1 den=10.5216 1 1000.0 92234 3.4729E-02
      92235 4.0000
      92236 1.8400E-02
      92238 95.947      end
'   Important nuclides from Table 1 of ORNL/TM-12294/V1
kr-83  1 0 1-21 1000.0 end
kr-85  1 0 1-21 1000.0 end
sr-90  1 0 1-21 1000.0 end
y-89   1 0 1-21 1000.0 end
mo-95  1 0 1-21 1000.0 end
zr-93  1 0 1-21 1000.0 end
zr-94  1 0 1-21 1000.0 end
zr-95  1 0 1-21 1000.0 end
nb-94  1 0 1-21 1000.0 end
tc-99  1 0 1-21 1000.0 end
ru-101 1 0 1-21 1000.0 end
ru-106 1 0 1-21 1000.0 end
rh-103 1 0 1-21 1000.0 end
rh-105 1 0 1-21 1000.0 end
pd-105 1 0 1-21 1000.0 end
pd-108 1 0 1-21 1000.0 end
ag-109 1 0 1-21 1000.0 end
sb-124 1 0 1-21 1000.0 end
xe-131 1 0 1-21 1000.0 end
xe-132 1 0 1-21 1000.0 end
xe-136 1 0 1-21 1000.0 end
cs-134 1 0 1-21 1000.0 end
cs-135 1 0 1-21 1000.0 end
cs-137 1 0 1-21 1000.0 end
ba-136 1 0 1-21 1000.0 end
la-139 1 0 1-21 1000.0 end
ce-144 1 0 1-21 1000.0 end
pr-141 1 0 1-21 1000.0 end
pr-143 1 0 1-21 1000.0 end
nd-143 1 0 1-21 1000.0 end
nd-145 1 0 1-21 1000.0 end
nd-147 1 0 1-21 1000.0 end
pm-147 1 0 1-21 1000.0 end
pm-148 1 0 1-21 1000.0 end
sm-147 1 0 1-21 1000.0 end
sm-149 1 0 1-21 1000.0 end
sm-150 1 0 1-21 1000.0 end
sm-151 1 0 1-21 1000.0 end
sm-152 1 0 1-21 1000.0 end
eu-153 1 0 1-21 1000.0 end
eu-154 1 0 1-21 1000.0 end
eu-155 1 0 1-21 1000.0 end
gd-155 1 0 1-21 1000.0 end
'
zirc2  2 1          620.0 end
'
```

```

h2o      3 den=0.670 1 600.0 end
arbm-bormod 0.670 1 1 0 0 5000 100 3 650.0E-06 600.0 end
'
'   Input materials for BPRs
ss304   4 1                600.0 end
'
o       5 0 0.04497        600.0 end
na      5 0 0.00165        600.0 end
al      5 0 0.00058        600.0 end
si      5 0 0.01799        600.0 end
k       5 0 0.00011        600.0 end
b-10   5 0 9.595E-4        600.0 end
b-11   5 0 3.863E-3        600.0 end
'
n       6 0 5.000E-5        600.0 end
end comp
'
'   Base reactor lattice specification
squarepitch 1.2598 0.7844 1 3 0.9144 2 0.8001 3 end
more data szf=0.50 end
'
'   Assembly and cycle parameters
npin/assembly=264 fuelngth=845.0 ncycles=45 nlib/cyc=1
printlevel=2 lightel=9 inplevel=2
numztotal=11 mxrepeats=0
facmesh=0.50 end
'
1
6 0.21400 4 0.23051 6 0.24130 5 0.42672 6 0.43688 4 0.48387
3 0.56134 2 0.60198 3 0.71079 500 2.41668 3 2.42643
'
2
6 0.21400 4 0.23051 6 0.24130 5 0.42672 6 0.43688 4 0.48387
3 0.56134 2 0.60198 3 0.71079 500 2.41668 3 2.42643
'
3
6 0.21400 4 0.23051 6 0.24130 5 0.42672 6 0.43688 4 0.48387
3 0.56134 2 0.60198 3 0.71079 500 2.41668 3 2.42643
'
4
6 0.21400 4 0.23051 6 0.24130 5 0.42672 6 0.43688 4 0.48387
3 0.56134 2 0.60198 3 0.71079 500 2.41668 3 2.42643
'
5
6 0.21400 4 0.23051 6 0.24130 5 0.42672 6 0.43688 4 0.48387
3 0.56134 2 0.60198 3 0.71079 500 2.41668 3 2.42643
'
6
6 0.21400 4 0.23051 6 0.24130 5 0.42672 6 0.43688 4 0.48387
3 0.56134 2 0.60198 3 0.71079 500 2.41668 3 2.42643
'
7
6 0.21400 4 0.23051 6 0.24130 5 0.42672 6 0.43688 4 0.48387
3 0.56134 2 0.60198 3 0.71079 500 2.41668 3 2.42643
'
8
6 0.21400 4 0.23051 6 0.24130 5 0.42672 6 0.43688 4 0.48387
3 0.56134 2 0.60198 3 0.71079 500 2.41668 3 2.42643
'
9
6 0.21400 4 0.23051 6 0.24130 5 0.42672 6 0.43688 4 0.48387
3 0.56134 2 0.60198 3 0.71079 500 2.41668 3 2.42643
'
10
6 0.21400 4 0.23051 6 0.24130 5 0.42672 6 0.43688 4 0.48387
3 0.56134 2 0.60198 3 0.71079 500 2.41668 3 2.42643
'
11
6 0.21400 4 0.23051 6 0.24130 5 0.42672 6 0.43688 4 0.48387
3 0.56134 2 0.60198 3 0.71079 500 2.41668 3 2.42643
'
12
6 0.21400 4 0.23051 6 0.24130 5 0.42672 6 0.43688 4 0.48387
3 0.56134 2 0.60198 3 0.71079 500 2.41668 3 2.42643
'
13
6 0.21400 4 0.23051 6 0.24130 5 0.42672 6 0.43688 4 0.48387
3 0.56134 2 0.60198 3 0.71079 500 2.41668 3 2.42643
'
14
6 0.21400 4 0.23051 6 0.24130 5 0.42672 6 0.43688 4 0.48387
3 0.56134 2 0.60198 3 0.71079 500 2.41668 3 2.42643
'
15
6 0.21400 4 0.23051 6 0.24130 5 0.42672 6 0.43688 4 0.48387
3 0.56134 2 0.60198 3 0.71079 500 2.41668 3 2.42643
'
'   Withdraw BPRs after 15 gwd/mtu
16

```



```

'      41
3 0.21400  3 0.23051  3 0.24130  3 0.42672  3 0.43688  3 0.48387
3 0.56134  2 0.60198  3 0.71079 500 2.41668  3 2.42643
'      42
3 0.21400  3 0.23051  3 0.24130  3 0.42672  3 0.43688  3 0.48387
3 0.56134  2 0.60198  3 0.71079 500 2.41668  3 2.42643
'      43
3 0.21400  3 0.23051  3 0.24130  3 0.42672  3 0.43688  3 0.48387
3 0.56134  2 0.60198  3 0.71079 500 2.41668  3 2.42643
'      44
3 0.21400  3 0.23051  3 0.24130  3 0.42672  3 0.43688  3 0.48387
3 0.56134  2 0.60198  3 0.71079 500 2.41668  3 2.42643
'      45
3 0.21400  3 0.23051  3 0.24130  3 0.42672  3 0.43688  3 0.48387
3 0.56134  2 0.60198  3 0.71079 500 2.41668  3 2.42643
'
'      Assembly depletion/decay parameters
power=60.0  burn=16.6667  down=0.0      end
power=60.0  burn=16.6667  down=0.0      end
power=60.0  burn=16.6667  down=0.0      end
power=60.0  burn=16.6667  down=0.0      end
power=60.0  burn=16.6667  down=0.0      end
power=60.0  burn=16.6667  down=0.0      end
power=60.0  burn=16.6667  down=0.0      end
power=60.0  burn=16.6667  down=0.0      end
power=60.0  burn=16.6667  down=0.0      end
power=60.0  burn=16.6667  down=0.0      end
power=60.0  burn=16.6667  down=0.0      end
power=60.0  burn=16.6667  down=0.0      end
power=60.0  burn=16.6667  down=0.0      end
power=60.0  burn=16.6667  down=0.0      end
power=60.0  burn=16.6667  down=0.0      end
power=60.0  burn=16.6667  down=0.0      end
power=60.0  burn=16.6667  down=0.0      end
power=60.0  burn=16.6667  down=0.0      end
power=60.0  burn=16.6667  down=0.0      end
power=60.0  burn=16.6667  down=0.0      end
power=60.0  burn=16.6667  down=0.0      end
power=60.0  burn=16.6667  down=0.0      end
power=60.0  burn=16.6667  down=0.0      end
power=60.0  burn=16.6667  down=0.0      end
power=60.0  burn=16.6667  down=0.0      end
power=60.0  burn=16.6667  down=0.0      end
power=60.0  burn=16.6667  down=0.0      end
power=60.0  burn=16.6667  down=0.0      end
power=60.0  burn=16.6667  down=0.0      end
power=60.0  burn=16.6667  down=0.0      end
power=60.0  burn=16.6667  down=0.0      end
power=60.0  burn=16.6667  down=0.0      end
power=60.0  burn=16.6667  down=0.0      end
power=60.0  burn=16.6667  down=0.0      end
power=60.0  burn=16.6667  down=0.0      end
power=60.0  burn=16.6667  down=0.0      end
power=60.0  burn=16.6667  down=0.0      end
power=60.0  burn=16.6667  down=0.0      end
power=60.0  burn=16.6667  down=1826.25  end
'
'      Light-elements taken from SAS2H input listing in
'      ORNL/TM-12294/V5 Appendix B, not verified to be accurate
o 135  cr  5.9  mn  0.33
fe 12.9  co 0.075  ni  9.9
zr 221  nb  0.71  sn  3.60
'
end

```

SAS2H input file for B&W 15 × 15 assembly without BPRs present

```

=sas2h      parm=skipshipdata
001_00bw2_01.in, Case 001, 00 BPRs present, 01=constant presence
44groupndf5      latticecell
'
'   - B&W 15x15 assembly design
'   - continuous burnup to 45 gwd/mtu
'   - initial enrichment of 4.0 wt% U-235
'   - moderator temperature = 600K
'   - fuel temperature = 1000K
'   - soluble boron concentration = 650ppm, constant
'   - specific power = 60 MW/MTU
'   - 45 libraries during burnup (1 library per gwd/mtu)
'   - 00 2wt% Burnable Poison Rods (BPRs) present
'
'
'   Mixtures of fuel-pin-unit-cell
'   U-234, U-236, & U-238 isotopics calculated based on relations
'   in NUREG/CR-5625 (ORNL-6698)
uo2  1  den=10.5216  1  1000.0  92234  3.4729E-02
                                     92235  4.0000
                                     92236  1.8400E-02
                                     92238  95.947   end
'   Important nuclides from Table 1 of ORNL/TM-12294/V1
kr-83  1  0  1-21  1000.0  end
kr-85  1  0  1-21  1000.0  end
sr-90  1  0  1-21  1000.0  end
y-89   1  0  1-21  1000.0  end
mo-95  1  0  1-21  1000.0  end
zr-93  1  0  1-21  1000.0  end
zr-94  1  0  1-21  1000.0  end
zr-95  1  0  1-21  1000.0  end
nb-94  1  0  1-21  1000.0  end
tc-99  1  0  1-21  1000.0  end
ru-101 1  0  1-21  1000.0  end
ru-106 1  0  1-21  1000.0  end
rh-103 1  0  1-21  1000.0  end
rh-105 1  0  1-21  1000.0  end
pd-105 1  0  1-21  1000.0  end
pd-108 1  0  1-21  1000.0  end
ag-109 1  0  1-21  1000.0  end
sb-124 1  0  1-21  1000.0  end
xe-131 1  0  1-21  1000.0  end
xe-132 1  0  1-21  1000.0  end
xe-136 1  0  1-21  1000.0  end
cs-134 1  0  1-21  1000.0  end
cs-135 1  0  1-21  1000.0  end
cs-137 1  0  1-21  1000.0  end
ba-136 1  0  1-21  1000.0  end
la-139 1  0  1-21  1000.0  end
ce-144 1  0  1-21  1000.0  end
pr-141 1  0  1-21  1000.0  end
pr-143 1  0  1-21  1000.0  end
nd-143 1  0  1-21  1000.0  end
nd-145 1  0  1-21  1000.0  end
nd-147 1  0  1-21  1000.0  end
pm-147 1  0  1-21  1000.0  end
pm-148 1  0  1-21  1000.0  end
sm-147 1  0  1-21  1000.0  end
sm-149 1  0  1-21  1000.0  end
sm-150 1  0  1-21  1000.0  end
sm-151 1  0  1-21  1000.0  end
sm-152 1  0  1-21  1000.0  end
eu-153 1  0  1-21  1000.0  end
eu-154 1  0  1-21  1000.0  end
eu-155 1  0  1-21  1000.0  end
gd-155 1  0  1-21  1000.0  end
'
zirc2  2  1  620.0  end
'

```



```
power=60.0 burn=16.6667 down=0.0 end
power=60.0 burn=16.6667 down=0.0 end
power=60.0 burn=16.6667 down=0.0 end
power=60.0 burn=16.6667 down=0.0 end
power=60.0 burn=16.6667 down=0.0 end
power=60.0 burn=16.6667 down=1826.25 end
'
' Light-elements taken from SAS2H input listing in
' ORNL/TM-12294/V5 Appendix B, not verified to be accurate
o 135 cr 5.9 mn 0.33
fe 12.9 co 0.075 ni 9.9
zr 221 nb 0.71 sn 3.60
'
end
```

SAS2H input file for B&W 15 × 15 assembly with 16 BPRs (2 wt % B₄C) present during the first 15 GWd/t of burnup

```
=sas2h      parm=skipshipdata
001_16bw2_02.in, Case 001, 16 2wt% BPRs present, 02=BPRs present for first 15 Gwd/MTU
44groupndf5      latticecell
'
'   - B&W 15x15 assembly design
'   - continuous burnup to 45 gwd/mtu
'   - initial enrichment of 4.0 wt% U-235
'   - moderator temperature = 600K
'   - fuel temperature = 1000K
'   - soluble boron concentration = 650ppm, constant
'   - specific power = 60 MW/MTU
'   - 45 libraries during burnup (1 library per gwd/mtu)
'   - 16 2wt% Burnable Poison Rods (BPRs) present
'
'
'   Mixtures of fuel-pin-unit-cell
'   U-234, U-236, & U-238 isotopics calculated based on relations
'   in NUREG/CR-5625(ORNL-6698)
uo2  1 den=10.5216 1 1000.0 92234 3.4729E-02
      92235 4.0000
      92236 1.8400E-02
      92238 95.947      end
'   Important nuclides from Table 1 of ORNL/TM-12294/V1
kr-83  1 0 1-21 1000.0 end
kr-85  1 0 1-21 1000.0 end
sr-90  1 0 1-21 1000.0 end
y-89   1 0 1-21 1000.0 end
mo-95  1 0 1-21 1000.0 end
zr-93  1 0 1-21 1000.0 end
zr-94  1 0 1-21 1000.0 end
zr-95  1 0 1-21 1000.0 end
nb-94  1 0 1-21 1000.0 end
tc-99  1 0 1-21 1000.0 end
ru-101 1 0 1-21 1000.0 end
ru-106 1 0 1-21 1000.0 end
rh-103 1 0 1-21 1000.0 end
rh-105 1 0 1-21 1000.0 end
pd-105 1 0 1-21 1000.0 end
pd-108 1 0 1-21 1000.0 end
ag-109 1 0 1-21 1000.0 end
sb-124 1 0 1-21 1000.0 end
xe-131 1 0 1-21 1000.0 end
xe-132 1 0 1-21 1000.0 end
xe-136 1 0 1-21 1000.0 end
cs-134 1 0 1-21 1000.0 end
cs-135 1 0 1-21 1000.0 end
cs-137 1 0 1-21 1000.0 end
ba-136 1 0 1-21 1000.0 end
la-139 1 0 1-21 1000.0 end
ce-144 1 0 1-21 1000.0 end
pr-141 1 0 1-21 1000.0 end
pr-143 1 0 1-21 1000.0 end
nd-143 1 0 1-21 1000.0 end
nd-145 1 0 1-21 1000.0 end
nd-147 1 0 1-21 1000.0 end
pm-147 1 0 1-21 1000.0 end
pm-148 1 0 1-21 1000.0 end
sm-147 1 0 1-21 1000.0 end
sm-149 1 0 1-21 1000.0 end
sm-150 1 0 1-21 1000.0 end
sm-151 1 0 1-21 1000.0 end
sm-152 1 0 1-21 1000.0 end
eu-153 1 0 1-21 1000.0 end
eu-154 1 0 1-21 1000.0 end
eu-155 1 0 1-21 1000.0 end
gd-155 1 0 1-21 1000.0 end
'
```

```

zirc2 2 1          620.0 end
'
h2o    3 den=0.670 1 600.0 end
arbm-bormod 0.670 1 1 0 0 5000 100 3 650.0E-06 600.0 end
'
'   BPR materials
zirc2 4 1          600.0 end
'
'   AL2O3-B4C with 2.0 wt B4C
b-10   5 0 6.2696E-4 600.0 end
b-11   5 0 2.5976E-3 600.0 end
c       5 0 8.0649E-4 600.0 end
al      5 0 4.2831E-2 600.0 end
o       5 0 6.4247E-2 600.0 end
'
n       6 0 5.000E-5 600.0 end
end comp
'
'   Base reactor lattice specification
'           pellet      clad      clad
'           pitch      OD      OD      ID
squarepitch 1.4427 0.9505 1 3 1.0871 2 0.9703 3 end
more data szf=0.50 end
'
'   Assembly and cycle parameters
npin/assembly=208 fuelngth=731.0 ncycles=45 nlib/cyc=1
printlevel=2 lightel=9 inplevel=2
numztotal=8 mxrepeats=0
facmesh=0.50 end
'
1
5 0.43180 6 0.45720 4 0.54610 3 0.63500
2 0.67056 3 0.81397 500 2.96124 3 2.98453
'
2
5 0.43180 6 0.45720 4 0.54610 3 0.63500
2 0.67056 3 0.81397 500 2.96124 3 2.98453
'
3
5 0.43180 6 0.45720 4 0.54610 3 0.63500
2 0.67056 3 0.81397 500 2.96124 3 2.98453
'
4
5 0.43180 6 0.45720 4 0.54610 3 0.63500
2 0.67056 3 0.81397 500 2.96124 3 2.98453
'
5
5 0.43180 6 0.45720 4 0.54610 3 0.63500
2 0.67056 3 0.81397 500 2.96124 3 2.98453
'
6
5 0.43180 6 0.45720 4 0.54610 3 0.63500
2 0.67056 3 0.81397 500 2.96124 3 2.98453
'
7
5 0.43180 6 0.45720 4 0.54610 3 0.63500
2 0.67056 3 0.81397 500 2.96124 3 2.98453
'
8
5 0.43180 6 0.45720 4 0.54610 3 0.63500
2 0.67056 3 0.81397 500 2.96124 3 2.98453
'
9
5 0.43180 6 0.45720 4 0.54610 3 0.63500
2 0.67056 3 0.81397 500 2.96124 3 2.98453
'
10
5 0.43180 6 0.45720 4 0.54610 3 0.63500
2 0.67056 3 0.81397 500 2.96124 3 2.98453
'
11
5 0.43180 6 0.45720 4 0.54610 3 0.63500
2 0.67056 3 0.81397 500 2.96124 3 2.98453
'
12
5 0.43180 6 0.45720 4 0.54610 3 0.63500
2 0.67056 3 0.81397 500 2.96124 3 2.98453
'
13
5 0.43180 6 0.45720 4 0.54610 3 0.63500
2 0.67056 3 0.81397 500 2.96124 3 2.98453
'
14
5 0.43180 6 0.45720 4 0.54610 3 0.63500
2 0.67056 3 0.81397 500 2.96124 3 2.98453
'
15
5 0.43180 6 0.45720 4 0.54610 3 0.63500

```

```
2 0.67056 3 0.81397 500 2.96124 3 2.98453
'
  Withdraw BPRs after 15 gwd/mtu
  16
3 0.43180 3 0.45720 3 0.54610 3 0.63500
2 0.67056 3 0.81397 500 2.96124 3 2.98453
'
  17
3 0.43180 3 0.45720 3 0.54610 3 0.63500
2 0.67056 3 0.81397 500 2.96124 3 2.98453
'
  18
3 0.43180 3 0.45720 3 0.54610 3 0.63500
2 0.67056 3 0.81397 500 2.96124 3 2.98453
'
  19
3 0.43180 3 0.45720 3 0.54610 3 0.63500
2 0.67056 3 0.81397 500 2.96124 3 2.98453
'
  20
3 0.43180 3 0.45720 3 0.54610 3 0.63500
2 0.67056 3 0.81397 500 2.96124 3 2.98453
'
  21
3 0.43180 3 0.45720 3 0.54610 3 0.63500
2 0.67056 3 0.81397 500 2.96124 3 2.98453
'
  22
3 0.43180 3 0.45720 3 0.54610 3 0.63500
2 0.67056 3 0.81397 500 2.96124 3 2.98453
'
  23
3 0.43180 3 0.45720 3 0.54610 3 0.63500
2 0.67056 3 0.81397 500 2.96124 3 2.98453
'
  24
3 0.43180 3 0.45720 3 0.54610 3 0.63500
2 0.67056 3 0.81397 500 2.96124 3 2.98453
'
  25
3 0.43180 3 0.45720 3 0.54610 3 0.63500
2 0.67056 3 0.81397 500 2.96124 3 2.98453
'
  26
3 0.43180 3 0.45720 3 0.54610 3 0.63500
2 0.67056 3 0.81397 500 2.96124 3 2.98453
'
  27
3 0.43180 3 0.45720 3 0.54610 3 0.63500
2 0.67056 3 0.81397 500 2.96124 3 2.98453
'
  28
3 0.43180 3 0.45720 3 0.54610 3 0.63500
2 0.67056 3 0.81397 500 2.96124 3 2.98453
'
  29
3 0.43180 3 0.45720 3 0.54610 3 0.63500
2 0.67056 3 0.81397 500 2.96124 3 2.98453
'
  30
3 0.43180 3 0.45720 3 0.54610 3 0.63500
2 0.67056 3 0.81397 500 2.96124 3 2.98453
'
  31
3 0.43180 3 0.45720 3 0.54610 3 0.63500
2 0.67056 3 0.81397 500 2.96124 3 2.98453
'
  32
3 0.43180 3 0.45720 3 0.54610 3 0.63500
2 0.67056 3 0.81397 500 2.96124 3 2.98453
'
  33
3 0.43180 3 0.45720 3 0.54610 3 0.63500
2 0.67056 3 0.81397 500 2.96124 3 2.98453
'
  34
3 0.43180 3 0.45720 3 0.54610 3 0.63500
2 0.67056 3 0.81397 500 2.96124 3 2.98453
'
  35
3 0.43180 3 0.45720 3 0.54610 3 0.63500
2 0.67056 3 0.81397 500 2.96124 3 2.98453
'
  36
3 0.43180 3 0.45720 3 0.54610 3 0.63500
2 0.67056 3 0.81397 500 2.96124 3 2.98453
'
  37
3 0.43180 3 0.45720 3 0.54610 3 0.63500
2 0.67056 3 0.81397 500 2.96124 3 2.98453
'
  38
3 0.43180 3 0.45720 3 0.54610 3 0.63500
2 0.67056 3 0.81397 500 2.96124 3 2.98453
'
  39
```



```

3 0.43180 3 0.45720 3 0.54610 3 0.63500
2 0.67056 3 0.81397 500 2.96124 3 2.98453
'
40
3 0.43180 3 0.45720 3 0.54610 3 0.63500
2 0.67056 3 0.81397 500 2.96124 3 2.98453
'
41
3 0.43180 3 0.45720 3 0.54610 3 0.63500
2 0.67056 3 0.81397 500 2.96124 3 2.98453
'
42
3 0.43180 3 0.45720 3 0.54610 3 0.63500
2 0.67056 3 0.81397 500 2.96124 3 2.98453
'
43
3 0.43180 3 0.45720 3 0.54610 3 0.63500
2 0.67056 3 0.81397 500 2.96124 3 2.98453
'
44
3 0.43180 3 0.45720 3 0.54610 3 0.63500
2 0.67056 3 0.81397 500 2.96124 3 2.98453
'
45
3 0.43180 3 0.45720 3 0.54610 3 0.63500
2 0.67056 3 0.81397 500 2.96124 3 2.98453
'
' Assembly depletion/decay parameters
power=60.0 burn=16.6667 down=0.0 end
power=60.0 burn=16.6667 down=0.0 end
power=60.0 burn=16.6667 down=0.0 end
power=60.0 burn=16.6667 down=0.0 end
power=60.0 burn=16.6667 down=0.0 end
power=60.0 burn=16.6667 down=0.0 end
power=60.0 burn=16.6667 down=0.0 end
power=60.0 burn=16.6667 down=0.0 end
power=60.0 burn=16.6667 down=0.0 end
power=60.0 burn=16.6667 down=0.0 end
power=60.0 burn=16.6667 down=0.0 end
power=60.0 burn=16.6667 down=0.0 end
power=60.0 burn=16.6667 down=0.0 end
power=60.0 burn=16.6667 down=0.0 end
power=60.0 burn=16.6667 down=0.0 end
power=60.0 burn=16.6667 down=0.0 end
power=60.0 burn=16.6667 down=0.0 end
power=60.0 burn=16.6667 down=0.0 end
power=60.0 burn=16.6667 down=0.0 end
power=60.0 burn=16.6667 down=0.0 end
power=60.0 burn=16.6667 down=0.0 end
power=60.0 burn=16.6667 down=0.0 end
power=60.0 burn=16.6667 down=0.0 end
power=60.0 burn=16.6667 down=0.0 end
power=60.0 burn=16.6667 down=0.0 end
power=60.0 burn=16.6667 down=0.0 end
power=60.0 burn=16.6667 down=0.0 end
power=60.0 burn=16.6667 down=0.0 end
power=60.0 burn=16.6667 down=0.0 end
power=60.0 burn=16.6667 down=0.0 end
power=60.0 burn=16.6667 down=0.0 end
power=60.0 burn=16.6667 down=0.0 end
power=60.0 burn=16.6667 down=0.0 end
power=60.0 burn=16.6667 down=0.0 end
power=60.0 burn=16.6667 down=0.0 end
power=60.0 burn=16.6667 down=0.0 end
power=60.0 burn=16.6667 down=0.0 end
power=60.0 burn=16.6667 down=0.0 end
power=60.0 burn=16.6667 down=0.0 end
power=60.0 burn=16.6667 down=0.0 end
power=60.0 burn=16.6667 down=0.0 end
power=60.0 burn=16.6667 down=1826.25 end
'
' Light-elements taken from SAS2H input listing in
' ORNL/TM-12294/V5 Appendix B, not verified to be accurate
o 135 cr 5.9 mn 0.33
fe 12.9 co 0.075 ni 9.9
zr 221 nb 0.71 sn 3.60

```

```
'  
end
```

INTERNAL DISTRIBUTION

1. S. M. Bowman, 6011, MS-6370
2. B. L. Broadhead, 6011, MS-6370
3. W. C. Carter, 6011, MS-6370
4. M. D. DeHart, 6011, MS-6370
5. M. E. Dunn, 6011, MS-6370
6. K. R. Elam, 6011, MS-6370
7. R. J. Ellis, 6025, MS-6363
8. M. B. Emmett, 6011, MS-6370
9. I. C. Gauld, 6011, MS-6370
10. J. C. Gehin, 6025, MS-6363
11. S. Goluoglu, 6011, MS-6370
12. J. N. Herndon, 4500N, MS-6228
13. D. F. Hollenbach, 6011, MS-6370
14. C. M. Hopper, 6011, MS-6370
15. B. L. Kirk, 6025, MS-6362
16. S. B. Ludwig, NTRC, MS-6472
17. G. E. Michaels, 4500N, MS-6210
18. B. D. Murphy, 6011, MS-6370
19. C. V. Parks, 6011, MS-6370
20. L. M. Petrie, 6011, MS-6370
21. R. T. Primm, III, 6025, MS-6363
22. B. T. Rearden, 6011, MS-6370
23. J.-P. Renier, 6025, MS-6363
24. C. E. Sanders, 6011, MS-6370
25. J. J. Simpson, 4500N, MS-6210
26. J. C. Wagner, 6011, MS-6370
27. R. M. Westfall, 6011, MS-6370
28. Laboratory Records-RC
4500N, MS-6285
29. Central Research Library
4500N, MS-6191
- 30-50. Return extra ORNL copies to:
W. C. Carter, 6011, MS-6370

EXTERNAL DISTRIBUTION

51. M. L. Anderson, Bechtel SAIC Company, LLC, 1261 Town Center Drive, Las Vegas, NV 89134
52. S. Anton, Holtec International, 555 Lincoln Drive West, Marlton, NJ 08053
53. A. C. Attard, U.S. Nuclear Regulatory Commission, NRR/DSSA/SRXB, MS O10-B3, Washington, DC 20555
54. M. G. Bailey, U.S. Nuclear Regulatory Commission, NMSS/SFPO/SLID, MS O13-D13, Washington, DC 20555-0001
55. A. S. Barto, U.S. Nuclear Regulatory Commission, NMSS/SFPO/TRA, MS O13-D13, Washington, DC 20555-0001
56. C. J. Benson, Bettis Atomic Power Laboratory, PO Box 79, West Mifflin, PA 15122
57. G. H. Bidinger, NUMEC, 17016 Cashell Road, Rockville, MD 20853
58. J. Boshoven, Transnuclear West, Inc., 39300 Civic Center Drive, Suite 280, Fremont, CA 94538
59. M. C. Brady Raap, Pacific Northwest National Laboratory, 902 Battelle Boulevard, PO Box 999 / MSIN: K8-34, Richland, WA 99352
60. R. J. Cacciapouti, Duke Engineering and Services, 400 Donald Lynch Boulevard, Marlborough, MA 01752
61. D. E. Carlson, U.S. Nuclear Regulatory Commission, NMSS/SFPO/TRD, MS O13-D13, Washington, DC 20555-0001

62. J. M. Conde López, Consejo de Seguridad Nuclear, Jefe de Area de Ingeniería Nuclear, Subdirección General de Tecnología Nuclear, Justo Dorado, 11, 28040 Madrid, SPAIN
63. D. R. Conners, Bettis Atomic Power Laboratory, PO Box 79, West Mifflin, PA 15122
64. P. Cousinou, Institut de Protection et de Sûreté Nucléaire, Département de Recherches en Sécurité, CECI B.P. 6 - 92265 Fontenay-Aux-Roses, Cedex, FRANCE
65. T. W. Doering, Bechtel SAIC Company, LLC, 1261 Town Center Drive, Las Vegas, NV 89134
66. E. P. Easton, U.S. Nuclear Regulatory Commission, NMSS/SFPO/TRD, MS O13-D13, Washington, DC 20555-0001
67. F. Eltawila, U.S. Nuclear Regulatory Commission, RES/DSARE/SMSAB, MS T10-K8, Washington, DC 20555-0001
68. K. T. Erwin, U.S. Nuclear Regulatory Commission, NMSS/SFPO/TRB, MS O13-D13, Washington, DC 20555-0001
69. A. Feri, Scandpower, Inc., 101 Lakeforest Blvd., Suite 340, Gaithersburg, MD 20877
70. L. R. Foulke, Bechtel Bettis, Inc., Bettis Atomic Power Laboratory, PO Box 79, West Mifflin, PA 15122
71. A. S. Giantelli, U.S. Nuclear Regulatory Commission, NMSS/SFPO/TRA, MS O13-D13, Washington, DC 20555-0001
72. R. N. B. Gmal, Gesellschaft für Anlagen-und Reaktorsicherheit (GRS) mbH, Leiter der Gruppe Kritikalität, Forschungsgelände, 85748 Garching b. München
73. P. Grimm, Paul Scherrer Institute, CH-5232 Villigen Psi, SWITZERLAND
74. N. Gulliford, Winfrith Technology Centre, 306/A32, AEA Technology PLC, Winfrith, Dorchester, Dorset DT2 8DH, UNITED KINGDOM
75. J. Guttmann, U.S. Nuclear Regulatory Commission, NMSS/SFPO/TRD, MS O13-D13, Washington, DC 20555-0001
76. A. Haghghat, Nuclear and Radiological Engineering Department, 202 Nuclear Sciences Building University of Florida, PO Box 118300, Gainesville, FL 32611-830
77. S. Hanauer, U.S. Department of Energy, RW-22, Washington, DC 20545
78. G. Harms, Sandia National Laboratory, PO Box 5800, Mail Stop 1143, Albuquerque, NM 87185-1143
79. L. A. Hassler, Framatome ANP, 3315 Old Forest Road, PO Box 10935, Lynchburg, VA 24506-0935
80. D. Henderson, Framatome ANP, 3315 Old Forest Road, PO Box 10935, Lynchburg, VA 24506-0935
81. M. W. Hodges, U.S. Nuclear Regulatory Commission, NMSS/SFPO/TRD, MS O13-D13, Washington, DC 20555-0001
82. H. R. Hwang, Radiation Safety Analysis Group, KOPEC, 150, Duckjin Dong, Taejon, SOUTH KOREA 305-600
83. H. Kühl, Wissenschaftlich-Technische Ingenieurberatung GMBH, Karl-Heinz-Beckurts-Strasse 8, 52428 Jülich
84. W. H. Lake, Office of Civilian Radioactive Waste Management, U.S. Department of Energy, RW-46, Washington, DC 20585
85. D. B. Lancaster, Nuclear Consultants.com, 320 South Corl Street, State College, PA 16801
86. C. Lavarenne, Institut de Protection et de Sûreté Nucléaire, Department of Prevention and Studies of Accidents, Criticality Studies Division, CEA - 60-68, avenue de Général Leclerc, B.P. 6 - 92265, Fontenay - Aux - Roses, Cedex, FRANCE
- 87-91. R. Y. Lee, U.S. Nuclear Regulatory Commission, RES/DSARE/SMSAB, MS T10-K8, Washington, DC 20555-0001
92. W. J. Lee, NAC International, 655 Engineering Drive, Norcross, GA 30092

93. M. Mason, Transnuclear, Two Skyline Drive, Hawthorne, NY 10532-2120
94. A. J. Machiels, Electric Power Research Institute, Advanced Nuclear Technology, Energy Conservation Division, 3412 Hillview Ave., Palo Alto, CA 94304-1395
95. L. Markova, Ustav jaderného výzkumu Rez, Theoretical Reactor Physics, Nuclear Research Institute, Czech Republic, 25068 REZ
96. D. Marloye, Belgonucléaire, Av. Ariane 4, B-1200, Brussels, BELGIUM
97. J. R. Massari, Constellation Nuclear Services, 2200 Defense Highway, Suite 405, Crofton, MD 21114-2404
98. C. W. Mays, Framatome ANP, 3315 Old Forest Road, PO Box 10935, Lynchburg, VA 24506-0935
99. J. N. McKamy, U.S. Department of Energy, Office of Engineering Assistance and Site Interface, EH-34, 19901 Germantown Rd., Germantown, MD 20874
100. N. B. McLeod, JAI Corporation, 4103 Chain Bridge Road, Suite 200, Fairfax, VA 22030
101. D. Mennerdahl, E. Mennerdahl Systems, Starvägen 12, S-183 57 Täby, SWEDEN
102. R. L. Murray, 8701 Murray Hill Drive, Raleigh, NC 27615
103. J. A. Myers, U. S. Nuclear Regulatory Commission, NMSS/SFPO/TRD, MS O13-D13, Washington, DC 20555-0001
104. K. A. Neimer, Duke Engineering & Services, 400 S. Tyron St., WC26B, PO Box 1004, Charlotte, NC 28201-1004
105. P. Noel, Bechtel SAIC Company, LLC, 1261 Town Center Drive, Las Vegas, NV 89134
106. I. Nojiri, Japan Nuclear Cycle Development Institute, Environment and Safety Division, Tokai Works, Muramatsu Tokai-mura, Naka-gun Ibaraki-ken 319-1194, JAPAN
107. J.-C. Neuber, Framatome-ANP, Dept. NDM3, PO Box 101063, D-63010 Offenbach, GERMANY
108. A. Nouri, OECD/NEA Data Bank, Le Seine-Saint Germain, 12 Boulevard des Iles, F-92130 Issy-les-Moulineaux, FRANCE
109. Office of the Assistant Manager for Energy Research and Development, Department of Energy Oak Ridge Operations (DOE-ORO), PO Box 2008, Oak Ridge, TN 37831
110. H. Okuno, Japan Atomic Energy Research Institute, Department of Fuel Cycle, Safety Research, 2-4 Shirakata-Shirane, 319-1195 Tokai-mura, Naka-Gun, Ibaraki-ken, JAPAN
111. P. M. O’Leary, Framatome ANP, 3315 Old Forest Road, PO Box 10935, Lynchburg, VA 24506-0935
112. J. R. Massari, Constellation Nuclear Services, 2200 Defense Highway, Suite 405, Crofton, MD 21114-2404
113. N. L. Osgood, U.S. Nuclear Regulatory Commission, Office of Nuclear Materials Safety and Safeguards, MS O13-D13, Washington, DC 20555-0001
114. T. Parish, Department of Nuclear Engineering, Texas A & M University, College Station, TX 77843-3313
115. V. A. Perin, U.S. Nuclear Regulatory Commission, NMSS/DWM/HLWB, MS T7-F3, Washington, DC 20555-0001
116. B. Petrovic, Westinghouse Electric Company, Science and Technology Department, 1344 Beulah Road, Pittsburgh, PA 15235
117. J. S. Philbin, Sandia National Laboratory, PO Box 5800, Mail Stop 1143, Albuquerque, NM 87185-1143
118. M. L. Pitts, Framatome ANP, 3315 Old Forest Road, PO Box 10935, Lynchburg, VA 24506-0935
119. M. Rahimi, U.S. Nuclear Regulatory Commission, NMSS/DWM/HLWB, MS T7-F3, Washington, DC 20555-0001

120. E. L. Redmond II, Holtec International, 555 Lincoln Drive West, Marlton, NJ 08053
121. F. Reitsma, Reactor Theory, Building 1900, Pelindaba, NECSA, PO Box 582,
0001 PRETORIA, SOUTH AFRICA
122. C. Rombough, CTR Technical Services, Inc., 5619 Misty Crest Dr., Arlington, TX 76017-4147
123. J. E. Rosenthal, U.S. Nuclear Regulatory Commission, RES/DSARE/REAHFB, MS T10-E46,
Washington, DC 20555-0001
124. D. Salmon, Bechtel SAIC Company, LLC, 1261 Town Center Drive, Las Vegas, NV 89134
125. A. Santamarina, Commissariat A L'Energie Atomique, Nuclear Reactor Division, Reactor
Studies Department, Reactor and Cycle Physics Service,
CEA/CADARACHE/DRN/DER/SPRC Bat. 230, 13108 Saint-Paul-Lez-Durance, Cedex,
FRANCE
126. E. Sartori, OECD/NEA Data Bank, Le Seine-Saint Germain, 12 Boulevard des Iles, F-92130
Issy-les-Moulineaux, FRANCE
127. J. J. Sapyta, Framatome Cogema Fuels, 3315 Old Forest Road, PO Box 10935, Lynchburg, VA
24506-0935
128. J. Scaglione, Bechtel SAIC Company, LLC, 1261 Town Center Drive, Las Vegas, NV 89134
129. D. Schrire, Hot Cell Laboratory, Studsvik Nuclear, Nyköping 61182, SWEDEN
130. H. H. Schweer, Bundesamt fuer Strahlenschutz, Willi Brandt Str. 5, D-38226 SALZGITTER,
GERMANY
131. M. Smith, Virginia Power Co., PO Box 2666, Richmond, VA 23261
132. N. R. Smith, AEA Technology, A32 Winfrith, Dorchester, Dorset DT2 8DH, United Kingdom
133. R. Stamm'ler, Studsvik Scandpower AS, Gasevikveien 2, PO Box 15, NO-2027 Kjeller
NORWAY
134. J. T. Stewart, Department of Environment, Transport, and Re, RMTD, 4/18, GMH, 76
Marsham Street, London SW1P 4DR, UNITED KINGDOM
135. T. Suto, Power Reactor and Nuclear Fuel Development Corporation, Technical Service Division,
Tokai Reprocessing Plant, Tokai Works, Tokai-Mura, Naka-gun, Ibaraki-ken, JAPAN
136. H. Taniuchi, Kobe Steel, Ltd., 2-3-1 Shinhama, Arai-Cho, Takasago, 676 JAPAN
137. D. A. Thomas, Bechtel SAIC Company, LLC, 1261 Town Center Drive, Las Vegas, NV 89134
138. P. R. Thorne, British Nuclear Fuels plc (BNFL), Nuclear and Radiological Safety,
R101 Rutherford House, Risley Warrington WA3 6AS, UNITED KINGDOM
139. J. R. Thornton, Duke Engineering & Services, 230 S. Tyron St., PO Box 1004, Charlotte, NC
28201-1004
140. S. E. Turner, Holtec International, 230 Normandy Circle East, Palm Harbor, FL 34683
141. A. P. Ulses, U.S. Nuclear Regulatory Commission, NRR/DSSA/SRXB, MS O10-B3,
Washington, DC 20555-0001
142. M. E. Wangler, U.S. Department of Energy, EH-33.2, Washington, DC 20585-0002
143. M. D. Waters, U.S. Nuclear Regulatory Commission, NMSS/SFPO/SLID, MS O13-D13,
Washington, DC 20555-0001
144. A. Wells, 2846 Peachtree Walk, Duluth, GA 30136
145. S. A. Whaley, U.S. Nuclear Regulatory Commission, NMSS/SFPO/TRD, MS O13-D13,
Washington, DC 20555-0001
146. B. H. White, U.S. Nuclear Regulatory Commission, NMSS/SFPO/TRD, MS O13-D13,
Washington, DC 20555-0001
147. R. Wilson, Rocky Flats Field Office, USDOE, 10808 Highway 93, Golden, CO 80403-8200
148. C. J. Withee, U.S. Nuclear Regulatory Commission, NMSS/SFPO/TRD, MS O13-D13,
Washington, DC 20555-0001

NRC FORM 335 (2-89) NRCM 1102 3201, 3202	U.S. NUCLEAR REGULATORY COMMISSION BIBLIOGRAPHIC DATA SHEET <i>(See instructions on the reverse)</i>	1. REPORT NUMBER (Assigned by NRC, Add Vol., Supp., Rev., and Addendum Numbers, if any.) NUREG/CR-6761 ORNL/TM-2000/373				
2. TITLE AND SUBTITLE Parametric Study of the Effect of Burnable Poison Rods for PWR Burnup Credit	3. DATE REPORT PUBLISHED	<table border="1" style="width: 100%;"> <tr> <td style="text-align: center;">MONTH</td> <td style="text-align: center;">YEAR</td> </tr> <tr> <td style="text-align: center;">March</td> <td style="text-align: center;">2002</td> </tr> </table>	MONTH	YEAR	March	2002
	MONTH	YEAR				
	March	2002				
4. FIN OR GRANT NUMBER W6479						
5. AUTHOR(S) J. C. Wagner and C. V. Parks	6. TYPE OF REPORT Technical	7. PERIOD COVERED (Inclusive Dates)				
	8. PERFORMING ORGANIZATION — NAME AND ADDRESS (If NRC, provide Division, Office or Region, U.S. Nuclear Regulatory Commission, and mailing address; if contractor, provide name and mailing address.) Oak Ridge National Laboratory, Managed by UT-Battelle, LLC PO Box 2008, Bldg. 6011, MS-6370 Oak Ridge, TN 37831-6370 USA					
9. SPONSORING ORGANIZATION — NAME AND ADDRESS (If NRC, type "Same as above"; if contractor, provide NRC Division, Office or Region, U.S. Regulatory Commission, and mailing address.) Division of Systems Analysis and Regulatory Effectiveness Office of Nuclear Regulatory Research U.S. Nuclear Regulatory Commission Washington, DC 20555-0001						
10. SUPPLEMENTARY NOTES R. Y. Lee, NRC Project Manager						
11. ABSTRACT (200 words or less) The U.S. Nuclear Regulatory Commission's (NRC) Interim Staff Guidance on burnup credit (ISG-8) recommends restricting the use of burnup credit to assemblies that have not used burnable absorbers. This restriction eliminates a large portion of the currently discharged spent nuclear fuel (SNF) assemblies from cask loading, severely limiting the practical usefulness of burnup credit. In the absence of readily available information on burnable poison rod (BPR) design specifications and usage, and the subsequent reactivity effect of BPR exposure on SNF, NRC staff has indicated a need for additional information. In response, this report presents a parametric study of the effect of BPR exposure on the reactivity of SNF for various BPR designs, fuel enrichments, and exposure conditions, and documents BPR design specifications. The calculations demonstrate that the positive reactivity effect due to BPR exposure increases nearly linearly with burnup and is dependent on the number, poison loading, and design of the BPRs and the initial fuel enrichment. Reactivity increases, based on one-cycle BPR exposure, were found to be less than 1% Δk. The report concludes with recommendations for inclusion of SNF assemblies exposed to BPRs in criticality safety analyses using burnup credit for dry cask storage and transport.						
12. KEY WORDS/DESCRIPTORS (List words or phrases that will assist researchers in locating the report.) burnable poison, burnup credit, criticality safety, spent fuel, storage, transportation	13. AVAILABILITY STATEMENT unlimited	14. SECURITY CLASSIFICATION <i>(This Page)</i> unclassified				
	<i>(This Report)</i> unclassified	15. NUMBER OF PAGES				
	16. PRICE					

